CONCEPTUAL HYDROLOGICAL RESPONSE MODELS OF SELECTED ARID SOILSCAPES IN THE DOUGLAS AREA, SOUTH AFRICA

By

Martin Tinnefeld

A dissertation submitted in accordance with the requirements for the degree

Magister Scientiae Agriculturae

DEPARTMENT OF SOIL, CROP AND CLIMATE SCIENCES

Faculty of Natural and Agricultural Sciences

University of the Free State

Bloemfontein

February 2016

Supervisor: Prof. P.A.L. le Roux

Co-supervisor: Dr. J. J. Van Tol

Dedicated to the people who have noticed, discovered, questioned and persevered; and to those who will in future times to come. To all those dedicated to the people who have noticed, discovered, questioned and persevered; and to those who will in future times to come. To all those who have/will support them along their journey. Thank you. Danke Eva Tinnefeld. Danke Günter Tinnefeld.

TABLE OF CONTENTS

TABLE OF CONTENTS iii
DECLARATION vii
ABSTRACT viii
LIST OF FIGURES x
LIST OF TABLES xiv
ACKNOWLEDGEMENTS xv
LIST OF SYMBOLS AND ABBREVIATIONS xvi
INTRODUCTION 1
1.1. BACKGROUND 1
1.2. HYPOTHESIS and OJECTIVES 6
1.2.1. Hypothesis 6
CHAPTER 2 7
Literature review 7
2.1. Overview 7
2.2. Scale of study 8
2.3. Conceptual hydrological response models 9
2.4. Soil map information 11
2.5. Flowpaths and residence times 11
2.6. Morphology 13
2.7. Ancient and recent/in phase flowpath indicators 15
2.7.1. Ancient flowpaths indicators 16
2.7.2. Recent/in phase flowpath indicators 16
2.8. Soil hydraulic properties 19
2.8.1. Pore size distribution and Macroporosity 19
2.8.2. Soil hydraulic conductivity 22
2.8.3. Porosity of soil 24
2.8. Arid soils of the Orange River Basin 26
2.9. Hydrology of arid soils 29
CHAPTER 3 34
DESCRIPTION OF STUDY AREA 34
2.10. Location and extent 34

2.11. Soil distribution, parent material and topography 37
2.11.1. Land Type Ae 276 37
2.11.2. Land Type Ae 15 37
2.11.3. Land Type Ae 277 37
2.11.4. Land Type Ia 4 38
2.12. Climate and land use 38
CHAPTER 4 40
METHODOLOGY 40
4.1. Soil survey and mapping 40
4.2. Laboratory procedure 41
4.2.1. Physical methods 41
4.2.2. Chemical methods 41
4.3. Field measurements 42
4.3.1. Unsaturated hydraulic conductivity 42
4.4. Water retention curves 44
4.5. Conceptual hydrological response model 48
4.6. Soil maps and contours 50
CHAPTER 5 51
SOIL DISTRIBUTION OF THE SITES 51
5.1. Introduction 51
5.1.1. Soilscapes of Site 1 profiles – Land Type Ae276 51
5.1.2. Soilscapes of Site 2 - Land Type Ae15 55
5.1.3. Soilscapes of Site 3 - Land Type Ae266 58
5.1.4. Soilscapes of Site 4 - Land Type Ia4 61
5.2. Conclusion 65
CHAPETR 6 66
CONCEPTUAL HYDROLOGICAL RESPONSE MODELS OF ARID SOILSCAPES 66
6.1. Introduction 66
6.3. Results and Discussion 66
6.3.1. Site 1 66
6.3.2. Site 2 73
6.3.3. Site 3 78
6.3.4. Site 4 81
6.4. Conclusion 84

CHAPTER 7 86
HYDROLOGICAL PROPERTIES OF ARID SOILS 86
7.1 Results and Discussion 86
7.1.1 Site 1 86
7.1.2. Site 2 89
7.1.3. Site 3 91
7.1.4. Site 4 91
7.2. Predicting unsaturated hydraulic conductivity curves using water retention curve data 92
7.3. Conclusion 96
CHAPTER 8 98
CONCLUSIONS AND RECOMMENDATION 98
REFERENCES 100
Appendix A 113
Land Types 113
Appendix B 118
Soil profile description forms 118
Profile P1: Kimberley (*Ky*) 1100 (Taung) 118
Profile P2: Addo (*Ad*) 1211 (Spekboom) 123
Profile P3: Kimberley (*Ky*) 1100 (Taung) 128
Profile P4: Hutton (*Hu*) 3100 (Stella) 132
Profile P5: Coega (*Cg*) 1000 (Nabies) 136
Profile P6: Addo (*Ad*) 1211 (Spekboom) 140
Profile P7: Hutton (*Hu*) 3100 (Stella) 144
Profile P8: Coega (*Cg*) 2000 (Marydale) 148
Profile P9: Hutton (*Hu*) 3100 (Stella) 152
Profile P10: Hutton (*Hu*) 3100 (Stella) 156
Profile P11: Clovelly (*Cv*) 3100 (Setlagole) 160
Profile P12: Namib (*Nb*) 1200 (Beachwood) 164
Profile P13: Valsrivier (*Va*) 1112 (Luckhoff) 168
Appendix C 172
Soil observation distribution maps 172
Appendix D 176
Hydraulic properties of select arid soils 176

Appendix E 188
Figures explained in detail 188

DECLARATION

I hereby declare that this dissertation submitted for the degree of Magister Scientiae Agriculturae to the University of the Free State, is my own work and has not been submitted to any other University. Where use has been made of work of others, it is duly acknowledged in the text.

I also agree that the University of the Free State has the sole right to publication of this dissertation.

Signed: 

Martin Tinnefeld

ABSTRACT

The conceptual hydrological response model (CHRM) is a powerful tool, able to transfer hydrological information of hillslopes. Soil, a first order control of partitioning of water flow, is often the only source of information of hillslope water flowpaths and storage mechanisms. Conceptual hydrological models applied at different scales, serve as the framework to understand and structure the hydrological response of sites, hillslopes and catchments. They complement decision making and planning of natural resource allocation and delineation for land-use change in ecology, agriculture, mining and urbanisation. Soil morphology, chemistry and hydrometrics are used singularly and complimented in combination as indicators and controllers of hydrology to construct CHRMs. The more accurate the input parameters of soil morphology, chemistry and hydrometrics, the more accurate the final CHRM.

Arid soils of South Africa have been neglected to be investigated for their hydrological properties. This is due to the low rainfall, infrequent hydrological response and resulting low output of data. Where such hydrological studies have been performed under higher rainfall climatic zones, soil has been found to respond as a store and conduit of water. These are referred to as storage mechanisms and flowpaths within the soil and can be determined by studying the soils' morphology, improved by soil chemistry and are verified by application of hydrometrics.

Soil distribution patterns are not random and are influenced by hillslope hydrology. The vastness of the arid regions of South Africa, make it difficult to select singular representative hillslopes. However, by describing the soil distribution patterns of randomly distributed detailed soil maps within different land types, allowed for soil distribution trends to be identified in this study. These soil distribution trends were seen to coincide with terrain morphological units.

Representative modal profiles were selected on dominant and representative terrain morphological units of 4 different land types on criteria that they are representative soils

of the land type and sites. The soils have well developed horizons resulting in vertical pedological variation including different degrees of carbonate precipitation.

Methodology of other research, to interpret morphology in higher rainfall regions of South Africa, was used to construct a conceptual hydrological response model for the arid hillslopes and the region in general. Hydrological properties of modal profiles, were used to confirm the concepts.

A class 1 hillslope hydrological response: soil/bedrock interflow to wetland; dominates on all four sites. Individual sites and their respective soil distribution patterns showed fast pedon recharge to the soil/rock interface. Pedon interflow at higher lying topographical positions with associated steeper slope, contributed to carbonate as dominating morphological flowpath indicator lower lying in the landscape. This is primarily driven by a low rainfall/high evapotranspirative demand of arid climates. Topographically lower lying soils showed reduced infiltration due to high alluvial clay and silt deposits and/or soil matrix saturation with carbonate precipitation sufficient to reduce the permeability of the soil.

Keywords: Arid hydropedology, Conceptual Hydrological Model, Soil-Map-Hydrology, Flowpath, Storage mechanism

LIST OF FIGURES

Figure 2. 1 Scale of research in hydropedology. Scales here shown are a catchment, hillslope, and soil observation points and their horizons (Le Roux et al., 2011) from Van Tol et al., (2010 b).
…….....8
Figure 2. 2 A conceptual hydrological response model (Van Tol et al., 2010 b).
……..... 10
Figure 2. 3 Conceptual Soil hydrologic cycle (Schoeneberger & Wysocki, 2005).
…….....12
Figure 2. 4 Mean and standard error of mean the $AD_{S>0.7}$ value per diagnostic horizon group (Van Huyssteen et al., 2005).
…….....13
Figure 2. 5 Soil morphological indicators of a catena in a dry climate (Lin et al., 2005).
……..... 15
Figure 2. 6 Comparison between unsaturated hydraulic conductivity curves obtained by tension infiltrometer unsaturated hydraulic conductivity only (TI-obs), using the VGM hydraulic model with retention data only (VGM) and using VGM model fitted to tension and infiltration data of (a) Oakleaf, (b) Clovelly, (c) Griffin and (d) Oakleaf orthic A horizons (Kuenene, 2013).
…….....24
Figure 2. 7 Decrease in mean grain size (Mz), with distance from Vaal River, for the red sands. Mz values represent average of all subsurface values of each profile (Van Rooyen, 1971).
…….....28
Figure 2. 8 Schematic cross-section of clayey soils on Karroo sediments (Van Rooyen, 1971).
…….....29
Figure 2. 9 Schematic cross-section of Hutton soils on calcrete (Van Rooyen, 1971).
……..... 29
Figure 2. 10 Schematic diagram of the diagnostic morphology of the stages in the morphogenetic sequences of carbonate horizon formation in gravelly and nongravelly materials. Carbonate accumulations are indicated by black forms and shading for clarity (Gille et al, 1966).
…….....31
Figure 2. 11 Scale diagram of horizon associated with a large pipe penetrating the thick K (carbaonte) horizon of a Cacique soil on the La Mesa surface. Scale is in feet (Gille et al, 1966).
…….....32

Figure 3. 1 Location of the Study area on an aridity map of South Africa (Hoffman and Todd, 1999).
…….....34
Figure 3. 2 Location and extent of sites in red, land types in grey and nearest towns.
……..... 35

Figure 3. 3 Weather statistic for Douglas including average –rainfall, -days with rain and average -min and -max temperatures per month (SAWS, 2014).
…….....39

Figure 4. 1 Double ring infiltrations on Site 4.
…….....44
Figure 4. 2 Photos illustrating the laboratory vacuum/saturation chamber and hanging water column setup for determining water retention curves (Le Roux et al., 2015).
……..... 45

Figure 5. 1 One meter contours (left) and soil map (right) with modal profile distribution of Site 1.
…….....52
Figure 5. 2 East to west transect of site 1 soil distribution with horizonisation and modal profile location. The position in the hillslope is graphically presented in a line sketch in the top left corner.
…….....53
Figure 5. 3 North to south transect of site 1 soil distribution with horizonisation and modal profile location. The position in the hillslope is graphically presented in a line sketch in the top left corner.
…….....55
Figure 5. 4 Soil map (left) and 1 m contours (right) with master profile distribution of Site 2.
…….....56
Figure 5. 5 South to north transect of site 2 soil distribution with horizonisation and modal profile location. The position in the hillslope is graphically presented in a line sketch in the top left corner.
…….....57
Figure 5. 6 East to west transect of site 2 soil distribution with horizonisation and modal profile location. The position in the hillslope is graphically presented in a line sketch in the top left corner.
…….....58
Figure 5. 7 One meter contours (left) and soil map (right) with master profile distribution of Site 3.
…….....59
Figure 5. 8 North to south transect of site 3 soil distribution with horizonisation. The position in the hillslope is graphically presented in a line sketch in the top left corner.
…….....60
Figure 5. 9 East to west transect of site 3 soil distribution with horizonisation and modal profile location. The position in the hillslope is graphically presented in a line sketch in the top left corner
…….....61
Figure 5. 10 One meter contours (right) and soil map (left) with master profile distribution of Site 4.
…….....62

Figure 5. 11 South to north transect of site 4 soil distribution with horizonisation and modal profile location. The position in the hillslope is graphically presented in a line sketch in the top left corner. ……63
Figure 5. 12 East to west transect of site 4 soil distribution with horizonisation. The position in the hillslope is graphically presented in a line sketch in the top left corner. ……64

Figure 6. 1 Topography (left) and soil form distribution (right) of site 1. ……67
Figure 6. 2 Kimberly soil form pedon conceptual hydrology. ……70
Figure 6. 3 Conceptual hydrological response based on morphology of Addo soils. ……71
Figure 6. 4 Conceptual hydrological response based on morphology of Hutton soils. ……72
Figure 6. 5 Conceptual hydrological response based on morphology of Coega soils. ……72
Figure 6. 6 CHRM of site 1. ……73
Figure 6. 7 Soil map (left) and 1 m contours (right) with master profile distribution of Site 2. ……74
Figure 6. 8 Conceptual hydrological response based on morphology of Coega soils. ……75
Figure 6. 9 Conceptual hydrological response based on morphology of Hutton soils. ……76
Figure 6. 10 Conceptual hydrological response based on morphology of deep Coega soils. ……77
Figure 6. 11 Conceptual hydrological response based on morphology of Clovelly soils. ……77
Figure 6. 12 CHRM of site 2. ……78
Figure 6. 13 One meter contours (left) and soil map (right) with master profile distribution of Site 3. ……79
Figure 6. 14 Conceptual hydrological response based on morphology of Namib soils.. 80
Figure 6. 15 CHRM of site 3. ……81
Figure 6. 16 One meter contours (right) and soil map (left) with master profile distribution of Site 4. ……82
Figure 6. 17 Conceptual hydrological response based on morphology of Namib soils. …… 83

Figure 6. 18 CHRM of site 4.
…….....83
Figure 6. 19 CHRM of a soilscape of an arid region.
…….....85

Figure 7. 1 The relationship of the hydraulic conductivity (mm hr^{-1}) versus the predicted water content relationship of the Kimberley (a), Addo (b), Kimberley (c) and Hutton (d) soil forms and their respective horizons.
…….....93
Figure 7. 2 The relationship of the hydraulic conductivity (mm hr^{-1}) versus the predicted water content relationship of the Coega (a), Addo (b), Hutton (c) and Addo (d) soil forms and their respective horizons.
…….....94
Figure 7. 3 The relationship of the hydraulic conductivity (mm hr^{-1}) versus the predicted water content relationship of the Hutton (a), Hutton (b), Clovelly (c) and Namib (d) soil forms and their respective horizons.
…….....95
Figure 7. 4 The relationship of the hydraulic conductivity (mm hr^{-1}) versus the predicted water content relationship of the Addo soil form and its respective horizons.
…….....96

LIST OF TABLES

Table 2. 1 General characteristics of iron oxide minerals, adapted from Van Huyssteen et al., (2005), and Cornell and Schwertmann (1996) ……..14
Table 2. 2 Stages of the morphogenetic sequences and the youngest land surfaces on which the stages occur (Gile et al., 1966) ……..31

Table 3. 1 Broad soil pattern code descriptions of land types (Land type Survey Staff, 1972-2006) ……..36
Table 3. 2 Land type defined TMU areas (Land type Survey Staff, 1972-2006) ……..36

Table 4. 1 Site and profile numbers, soil forms, their location and in which Land types they are found ……..40

Table 6. 1 Morphological, topographical and chemical information of modal profiles P1 to P5 ……..69
Table 6. 2 Morphological, topographical and chemical information of modal profiles P6 to P11 ……..75
Table 6. 3 Morphological, topographical and chemical information of modal profile P12 ……..80
Table 6. 4 Morphological, topographical and chemical information of modal profile P13 ……..82
Table 7. 1 Hydrometric properties of the Addo, Hutton, Coega and Clovelly modal profiles P6 to P11 ……..89
Table 7. 2 Hydrometric properties of the Namib modal profile P12 ……..91
Table 7. 3 Hydrometric properties of the Valsrivier modal profile P13 ……..91

ACKNOWLEDGEMENTS

Prof. P.A.L Le Roux – You believed in me and guided me, not just in life, but in soil science as well. I am so very honoured to have been your M.Sc. student. Without your hard work, hydropedology, and thus humanity would be at a loss.

To my doting parents, for all their support and unconditional love.

To Franjo Soldo, my friend, my alibi, my confidant, my nemeses and the voice of reason, the beacon of light when life seems dull.

The Water Research Commission for partially funding the research (K5/2012) of which some of this study is a part.

To Digital Soils Africa, for exposing me to these sites and partially funding this research.

To Dr. Bataung Kuenene, for his expertise on hydrometrics.

To Dr. Johan Van Tol for his insight and expertise, recommendations and advice.

To my friends, colleagues and the team at the University of the Free State. Thank you George, Bata, Nancy, Darren, Tracey, Christina, Ivon and Louise. Thank you for listening, thank you for sharing.

Hannes Bruwer, thank you for all the small things that made my life great. Hannes Bruwer, Frank Lawrence, George Steytler, Wynand Human and Vickie Bruwer for making their farms available for this research.

LIST OF SYMBOLS AND ABBREVIATIONS

Horizon abbreviations according to the Soil Classification Working Group (1991)

gc	- E-horizon
gh	- G-horizon
hk	- Hardpan carbonate horizon
nc	- Neocarbonate B horizon
ob	- Overburden
ot	- Orthic A horizon
r	- Rock
re	- Red apedal B horizon
sc	- Soft carbonate horizon
so	- Saprolite horizon
uw	- Unspecified without signs of wetness
yb	- Yellow-brown apedal B horizon

Soil form abbreviations according to the Soil Classification Working Group (1991)

Ad	- Addo soil form
Ag	- Augrabies soil form
Ak	- Askham soil form
Cg	- Coega soil form
Cv	- Clovelly soil form
Fw	- Ferwood soil form
Hu	- Hutton soil form
Ka	- Katspruit soil form
Km	- Klapmuts soil form
Ky	- Kimberley soil form
Nb	- Namib soil form
Py	- Plooysburg soil form
Se	- Sepane soil form
Va	- Valsrivier soil form

Others

CEC	- Cation exchange capacity ($cmol_c\ kg^{-1}$)
CEC_{soil}	- Cation exchange capacity of the the soil ($cmol_c\ kg^{-1}$ soil)
CEC_{clay}	- Cation exchange capcity of the clay texture fraction ($cmol_c\ kg^{-1}$ clay)
CEC_{OC}	- Cation exchange capacity of Organic Carbon ($cmol_c\ kg^{-1}$ OC)
Db	- Bulk density ($mg\ m^{-3}$)
DH	- Diagnostic horizon
DUL	- Drained upper limit ($mm\ mm^{-1}$)
ET	- Evapotranspiration (mm)
K_s	- Saturated hydraulic conductivity ($cm\ s^{-1}$)
K_h	- Unsaturated hydraulic conductivity ($cm\ s^{-1}$)
K_m	- Hydraulic conductivity through macropores ($cm\ s^{-1}$)
MP	- Macropores (%)

MSL	- Mean sea level
N	- Maximum number of water conducting pores
OC	- Organic carbon content (%)
PWP	- Plant Wilting Point (mm mm^{-1})
PSD	- Particle Size Distribution (%)
S_e	- Effective saturation also reduced water content (%)
TI	- Tension infiltrometer
TLB	- Tractor-Loader-Bulldozer
TMU	- Terrain Morphological Unit
VGM	- Van Genuchten-Maulem Model
V_f	- Total pore volume (mm^3 mm^{-3})
V_W	- Water content (mm^3 mm^{-3})
g	- Gravitational force (m s^{-1})
obs	- Observation(s)
S_{index}	- Swelling index (no unit; classed as in SCWG, 1991)
S_{Grade}	- Structure grade (no unit; classed as in SCWG, 1991)
Θ	- Soil water content (mm^3 mm^{-3})
$Θ_s$	- Saturated water content (mm^3 mm^{-3})
$Θ_r$	- Residual water content (mm^3 mm^{-3})
$Θ_m$	- Water conducting macroporosity (mm^3 mm^{-3})
λ, α, n, m	- Van Genuchten parameters influencing shape of water retention curves
f	- Porosity (%)
s	- Degree of saturation (%)
K_{sp}	- Solubility product constant
a^{-1}	- Per annum
$4^{(x)}$	- 4 represents the primary terrain morphological unit (toeslope) with the superscript indicating the secondary or polymorphological terrain unit

1 cm = 10 mm
1 cm^3 = 1000 mm^3
10 mm = 0.1 kPa

CHAPTER 1

INTRODUCTION

1.1. BACKGROUND

Water resources need to be maintained sustainably (NWA, 1998), necessitating the understanding of processes controlling the flow of water through soil, the initial acceptor of rainwater (Lin, 2010). The National Water Act requires a clear understanding of key hydrological processes for effective water resource management (Act 36 of 1998, section 5(1)) (NWA)). Soil resources have been mapped and delineated (Land type Survey Staff, 1972-2006). The management and use of soil can only be done correctly if reliable indicators of the soil water regime are understood (Jacobs *et al*., 2002). In the vadose zone, this implies identification, definition and the quantification of the pathways, connectivity, thresholds, and residence times of water flow (Le Roux *et al*., 2015). This serves hydrology and in combination with pedology, serves the management of water resources.

The field of hydropedology, is currently a much researched field, aiming at understanding these processes (Van Huyssteen, 2008; Le Roux *et al*., 2011; Lin, 2012, Le Roux *et al*., 2015). Transfer of hydropedologic information is done by applying hydrological classification of soils in South Africa (Le Roux *et al*., 2011). The quantification of flow in soils by hydrometrics is expensive and tedious, however relevant to confirm rates and quantities spatially and temporally (Uhlenbrook *et al*., 2005; Wenninger *et al*., 2008). Quantifying temporal response by use of soil water drainage curves and the rates under saturated und unsaturated soil conditions, initially facilitates modellers, secondly confirms soil morphological indicators and lastly quantifies catchment hydrological response (Hensley *et al*, 2000; Schulze, 1995; Le Roux *et al*., 2011; Van Tol *et al*., 2010 a; Van Tol *et al*., 2010 b; Van Huyssteen *et al*., 2005; Kuenene *et al*., 2011; Kuenene *et al*., 2014 b). The eventual use of pedotransfer functions (PTFs) (Bouma, 2004; Van Tol *et al*., 2012) to replace such measurements, are however still limited (Kuenene *et al*., 2014 a).

The lack of hydrometric measurements on the functional response of diagnostic horizons, profiles and hillslopes of arid climates, presents a void in the understanding of pedology and application of hydropedology to these landscapes. Error due to uncertainty in hydrologic parameters, are due to lack of knowledge and in variability (Morgan and Henrion, 1990). This questions the application of indicative hydromorphic properties applied at semi-arid and humid sites, compared to arid sites of South Africa. Exemplary, carbonate precipitation as a standing flowpath indicator, may vary as an indicator of a flowpaths in arid regions. This is due to the climatic difference, influencing widespread accumulation of carbonates as horizons (Le Roux *et al*., 2013).

Hydropedology is an integrated study of the soil-water relationships (Lin, 2003). The scientific synergy of pedology, soil physics and hydrology allows for spatial and temporal scale information integration. For example, applying the science of hydropedology to existing soil survey data, could transform it to hydraulic information (Lin *et al*., 2005). Hydropedology as an applied science "has significant implications for preserving our environment, keeping arable land productive, slowing global climate change, and understanding the complex interfaces of soil and water" (Lin, 2012). It is an analytical, resource based composite, aimed at transferring information.

The morphological features defining soil horizons, are closely related to soil forming processes, in which water plays the dominant role (Fritsch & Fritzpatrick, 1994). Morphology acts as an indicator of: flowpaths (Ticehurst *et al*., 2007; Van Tol *et al*., 2010a and period of annual duration of near saturation (Van Huyssteen *et al*., 2005), water holding capacity, degree of luviation and depth of moisture penetration (Lin *et al*., 2005). Of all morphological indicators, colour (Van Huyssteen and Ellis, 1997) is the most used and conspicuous during hydropedological field observations (Ticehurst *et al*., 2007; Van Tol *et al*., 2010b; Kuenene *et al*., 2013). Hydrological responses include flow rates and thresholds. These responses are quantified by measurements facilitating the application of soil morphology in hydropedology (Le Roux *et al*., 2011; Kuenene *et al*., 2014 b).

Soil morphological indicators correlate with processes driven by water (Van Huyssteen *et al*., 2005), and is therefore less conspicuous the more arid the region. Arid soils can frequently be of binary origin of aeolian and colluvial deposition (Hensley *et al*., 2012). This has an effect on horizonisation, as with duplex soils and resulting variation in chemical and physical properties.

Water, a major driver of solute transport and chemical properties of a soil (Essington, 2004), is indicative of a soils morphology being subject to change, which is related to the stability of its hydrological environment (Lin*.,* 2003). The clear diagnostic horizonisation of South African soils (Soil Classification Working Group (SCWG), 1991; Le Roux *et al*., 2013) indicates towards a profile in equilibrium with its environment. Understanding the hydrological link between morphological, chemical equilibrium and climate, is quantified and confirmed by hydrometrics (Van Tol *et* al., 2010 b; Bouwer *et al*., 2015; Kuenene *et al*., 2014 a; Kuenene *et al*., 2014 b). Collectively, the hydrology impacts on the morphology of soil (SCWG, 1991).

Morphology aids in the classification of soils, aimed at unveiling topic-specific information of soil forming process understanding (Lin, 2003). The SCWG (1991) has established a taxonomic system to name soils of South Africa according to the vertical sequencing of horizons. This classification system (SCWG, 1991; Le Roux *et al*., 2013; Van Huyssteen *et al*., 2013 b) provides basic information for hydrological models (Schulze, 1995) and most recently, hydrological-soil types (Le Roux, et al., 2011) and hillslopes of South Africa (Van Tol *et al*., 2011 a). Classification of soils is based on a defined set of morphological properties, which distinguishes between diagnostic soil horizons (SCWG, 1991).

Diagnostic soil horizons not only form in different ways and therefore indicate differences in hydrology, but also respond hydrologically differently and therefore are the smallest functional units of conceptual hydrological response models (CHRMs) (le Roux *et al*., 2015). The hydrology of soils is based on the soil form and horizon properties (Kuenene *et al*., 2011, Van Tol *et al*., 2011b). The hydrological functionality of individual soil horizons is influenced by the morphology of underlying and overlying materials (Tani, 1997;

Ticehurst *et* al., 2007; Van Tol *et al*., 2010a), and the horizons' morphology (Hutson, 1984). Hillslope morphological distribution patterns are linked to hillslope hydrology (Le Roux *et al*., 2011). Flowpaths and storage mechanisms are hydrological processes associated with the soil distribution pattern, therefore controlling hillslope hydrology (Soulsby *et al*., 2006). A hillslopes' hydrological functionality is determined by grouping soil hydrological functional types, distributed along a hillslope catena (Van Tol *et al*., 2013b).

Morphology distribution within soils and hillslopes is not random (Webster, 2000). Hillslopes are two dimensional transects, through all the present component terrain morphological units (TMUs). The hydrology is shown in the variation in vegetation and soils, but controlled by the geology and resultant hydrological pathways and storage mechanisms in soils (Tani, 1997; Van Tol *et* al., 2010 a; Van Tol *et al*., 2011 a; Kuenene, 2013). For conceptual hydrological modelling of a catchment, the hillslope needs to be considered as the modal representation of a three dimensional soil distribution, or soilscape (Beven, 2000 and Sivapalan, 2003 b). Soilscape is defined as "The pedologic portion of a discrete stretch of terrain. To understand a soilscape topographic, geologic, hydrologic, biotic and pedologic studies are needed, as well as those of human impact on the environment" (Hole, 1978). 'Soilscape' is more commonly referred to and applied when discussing hydropedology (Le Roux *et al*., 2015; Bouwer, 2013).

CHRMs form the primary structure of many hydrological models (Freeze & Harlan, 1969). Traditionally the CHRMs for hillslopes were developed using geomorphological and other surface features (Meyer & Gee, 1999). Recently, a procedure using soil distribution patterns has been applied to semi-arid (Van Tol *et al*., 2010 b; Van Zijl *et al*., 2013 and Bouwer *et al*., 2015) and humid (Kuenene *et al*., 2014 b) hillslopes in South Africa. The procedure includes the analysis of the hydrology of soils (Le Roux *et al*., 2011) and hillslopes (Van Tol *et al*., 2013 b) following a hydropedological approach (Le Roux *et al*., 2015).

A hillslope CHRM, is a depiction of the vadose zone hydrological system and exclude surface hydrology including rivers and dams. The hydrological response of saturated flow is depicted by means of arrows, indicating the rate and direction of saturated flow. The CHRM depiction and discussion focuses on the hydrological interaction of soils and underlying fractured rock (Van Tol *et al*., 2010 a; Van Tol *et al*., 2010 b; Kuenene *et al*., 2014 b; Bouwer *et al*., 2015). The interaction is vertical as water drains from the soil to the fractured rock, and lateral as the water may return to the soil downslope. Lateral flow is influenced by factors such as ratios in hydraulic conductivity between conducting and impeding layers, slope angle and slope length (Van Tol *et al.,* 2013 a). Resistance to flow by impermeable layers such as solid rock (Tani, 1997), are controllers for ponding or lateral flow in the vadose zone (Tromp-van Meerveld and McDonnell, 2006). Soil factors influencing flow directions can be indicated by a soils' morphology (Van Tol *et al*., 2010 a; Van Tol *et al*., 2010 b; Le Roux *et al*., 2011).

Carbonate deposits and horizons have been defined as flowpath indicators in semi-arid climates (Van Tol *et al*., 2010 a). Carbonate horizons in South Africa have not been hydrometrically investigated. Their vast probability distribution and occurrence in arid soils (Le Roux *et al*., 2013), requires that these horizons be further investigated in order to quantify their control functions. Lack of flow events questions their indicative properties in a hillslopes hydrological functionality.

It is aimed to design a CHRM with indicators of conceptual flowpaths and flow rates of soil horizons for an arid zone using the soil distribution patterns of four soil maps.

1.2. HYPOTHESIS and OJECTIVES

1.2.1. Hypothesis

In the absence of hydrometric measurements and redox indicators of flowpaths and storage mechanisms in arid zones, conceptual hydrological response models can be developed for the arid regions of South Africa using indicative pedofeatures and quantifying hydrological controls.

CHAPTER 2

Literature review

2.1. Overview

South African research in hydropedology is built on three tiers: 1) conceptualization (Le Roux, 2011), 2) quantification (Van Huyssteen *et al*., 2005; Van Huyssteen *et al*., 2013; Van Huyssteen, 2013) and 3) classification (Van Tol *et al*., 2011 a; Van Tol *et al*., 2013 b; Van Huyssteen, 2013). This follows the call by Sivapalan (2003 a) to simplify, clarify and classify complex hydrological processes. Hillslopes or rather soilscapes, describing soil distribution patterns of catchments should be studied to understand and quantify hydropedology (Weiler and McDonnell, 2004; Lin et al., 2006; Sivapalan *et* al., 2003; Soulsby *et al*., 2006; Wagner *et al*., 2007) (Figure 2.1).

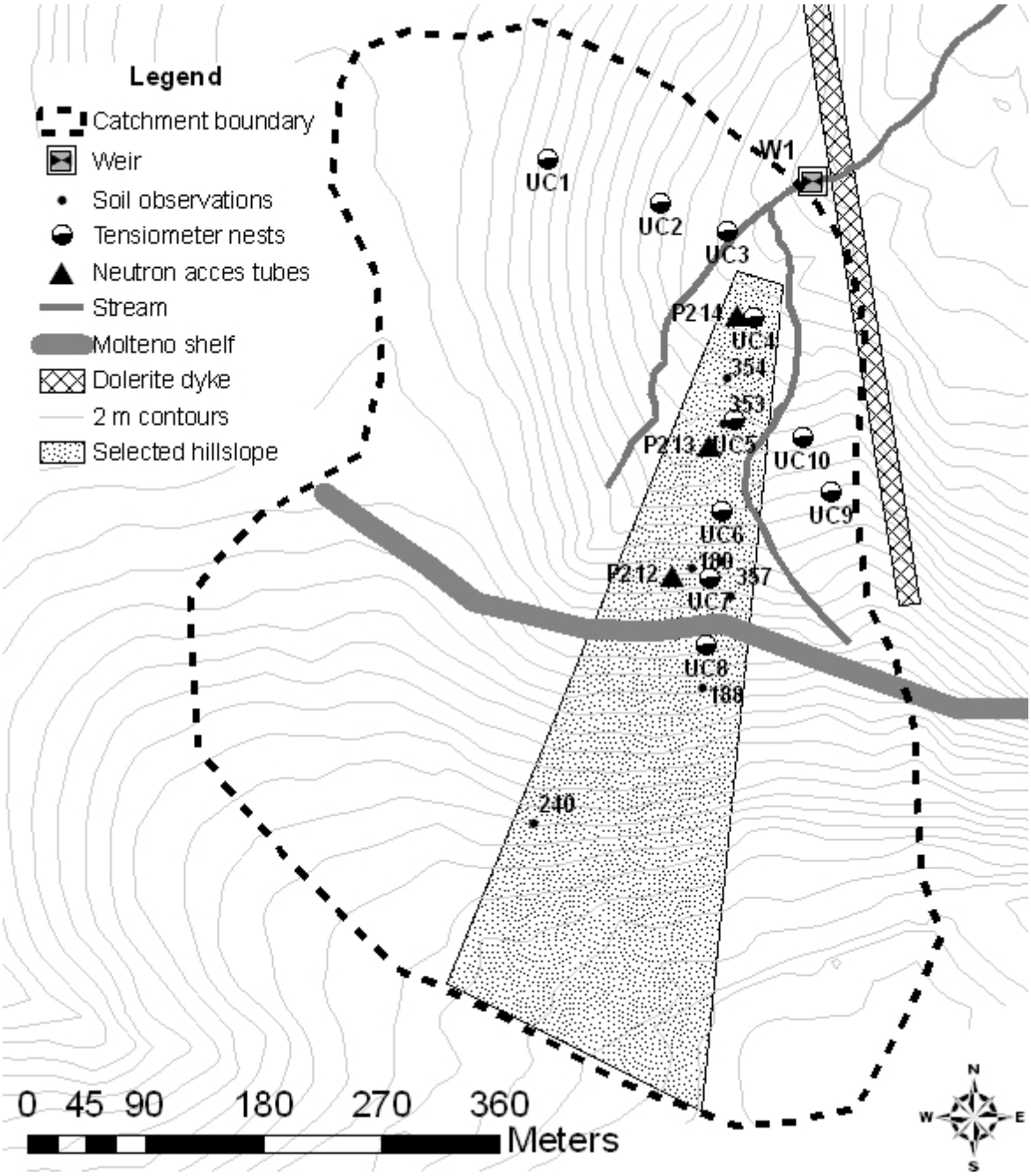

Figure 2. 1 Scale of research in hydropedology. Scales here shown are a catchment, hillslope, and soil observation points and their horizons (Le Roux et al., 2011) from Van Tol et al., (2010 b).

2.2. Scale of study

Catchments include all hydrological variables constituting a hydrological response (Wagner *et al*., 2007). McDonnell *et al*., (2006) suggest that a hillslope as a whole should

be studied instead of points, giving a better and complete understanding. This is however impossible, as it would destroy natural pathways of water flow through soil. Sivapalan *et al*., (2003) suggest the catchment hydrological response to be that of the cumulative soilscape response, making up a catchment. Four levels of pedon hydrological studies are conducted in South Africa 1) Soil forms (including horizons), 2) hillslopes, 3) soilscapes and 4) catchments (Figure 2.1) (Van Tol *et al*., 2010 b; Le Roux *et al*., 2011; Bouwer, 2013).

- Soil forms as classified according to the SCWG (1991), are subjected to morphological interpretation of flow response (Le Roux *et al*., 2011), physical hydrometric tests such as saturated hydraulic conductivity, water retention and water holding capacity (Kuenene *et al*., 2014 b), annual duration of saturation (Van Huyssteen *et al*., 2005) and chemical interpretations of flow response (Bouwer *et al*., 2015).
- Hydrological hillslopes are two dimensional segments of a catena, on which selected soil point observations are made, subjected to point or long term hydrological measurements (BEEH, 2003).
- Soilscapes are three dimensional catena segments (Figure 2.1), which allow for more interactive measurements, as with hillslopes, to be taken. These include the process of subsoil lateral flow (SLF) (Van Tol *et al*., 2013 a; Bouwer *et al*., 2015) and geomorphological surface features (Van Tol *et al*., 2010 a).
- Catchments are studied on all three previous levels, to determine the complete hydropedological cycle, including a weir to measure outflow from a catchment as in the Weatherly and Two Streams catchment sites (BEEH, 2003; Everson *et al*., 2006; Van Tol *et al*., 2010 b; Kuenene *et al*., 2014 a).

2.3. Conceptual hydrological response models

Conceptual Hydrological Response Models (CHRMs) depict the hydrological cycle in its entirety or of components thereof (Freeze & Harlan, 1969; Meyer & Gee, 1999) (Figure 2.2). CHRMs were first applied before computing abilities were able to project hydrological responses, as with modelling independent of time and space (Van Rooyen, 1971). Soil morphology, specifically distribution of calcareous horizons were used to

develop a CHRM in an arid climate (Van Rooyen, 1971). Surface geomorphological properties such as surface topography and vegetation were applied to make assumptions about porous media below soil surfaces (Van Tol *et al*., 2010 a). It is also a modern tool, used to interpret surface runoff, and making use of the catena concept, subsurface hydrological and associated morphological responses are derived from this (Van Tol *et al*., 2010 b; Kuenene *et al*., 2013; Bouwer, 2013).

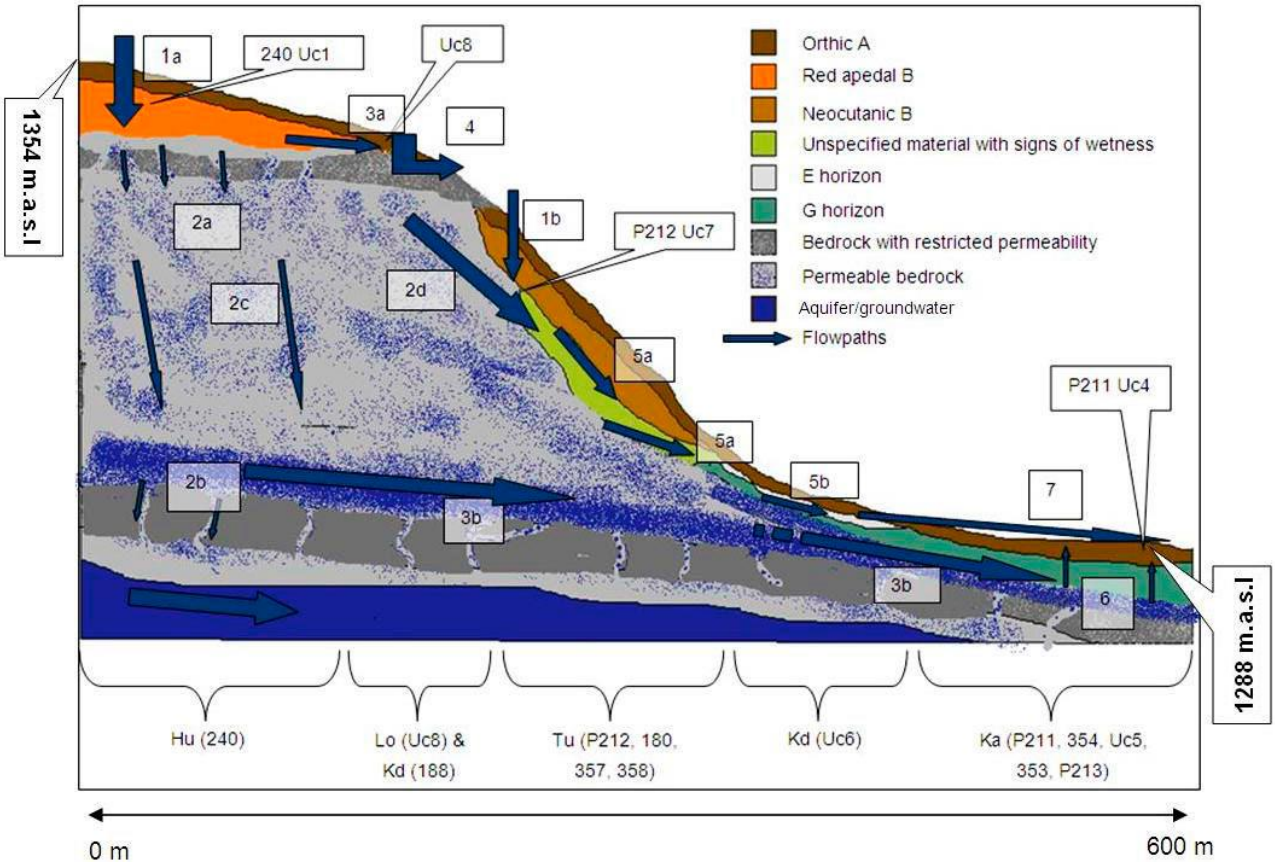

Figure 2. 2 A conceptual hydrological response model (Van Tol et al., 2010 b).

Van Zijl and Le Roux (2014) created a conceptual hydrological response map, by using morphological and chemical data of selected soils. Soil observations were chosen as per protocol for digital soil mapping (Van Zijl, 2013). By mapping the soil morphology of the Stevenson Hamilton site in the Kruger National Park, inference allowed for hydrological response characteristics of soil types and hillslopes (Van Tol *et al*., 2013 a; Van Tol *et al*., 2013 b) to be applied and mapped.

Bouwer *et al*., (2015) used the soils current chemistry of the Weatherly catchment (BEEH, 2003) to improve the existing morphological CHRM of the catchment. He applied iron, manganese, pH and base saturation as chemical indicators of flow. Of these, pH and base saturation were most indicative of hydrological response.

2.4. Soil map information

Soil maps are used to transfer information to the end user (Webster and Beckett, 1968). The end user can spatially and temporarily determine soil properties from such a map and use this for making decisions. Soil property information conveyed in soil maps include polygons of specific soil information such as soil morphology or soil chemo-physical attributes (Van der Sluijs and De Gruijter, 1985; Davidson and Lefebvre, 1993). Chemical and physical indicators of a soils hydrology are *inter alia* pH, exchangeable cations and texture (Van Huyssteen *et al*., 2005; Bouwer *et al*., 2015).

2.5. Flowpaths and residence times

The term ‘soil hydrological cycle’ (Schoeneberger and Wysocki, 2005) defines the concept of water flow through soil (Figure 2.3). The cessation of flow results in residence times and implicates soil as a storage mechanism of water (Van Huyssteen *et al*., 2005; Van Tol *et al*., 2010 a). Asano *et al*., (2002) found that with an increase in soil depth, there is an increase in residence times. McGuire and McDonnell, (2006) found that residence times can lead to information about flow pathways, storage mechanisms of the soil and the source of the water.

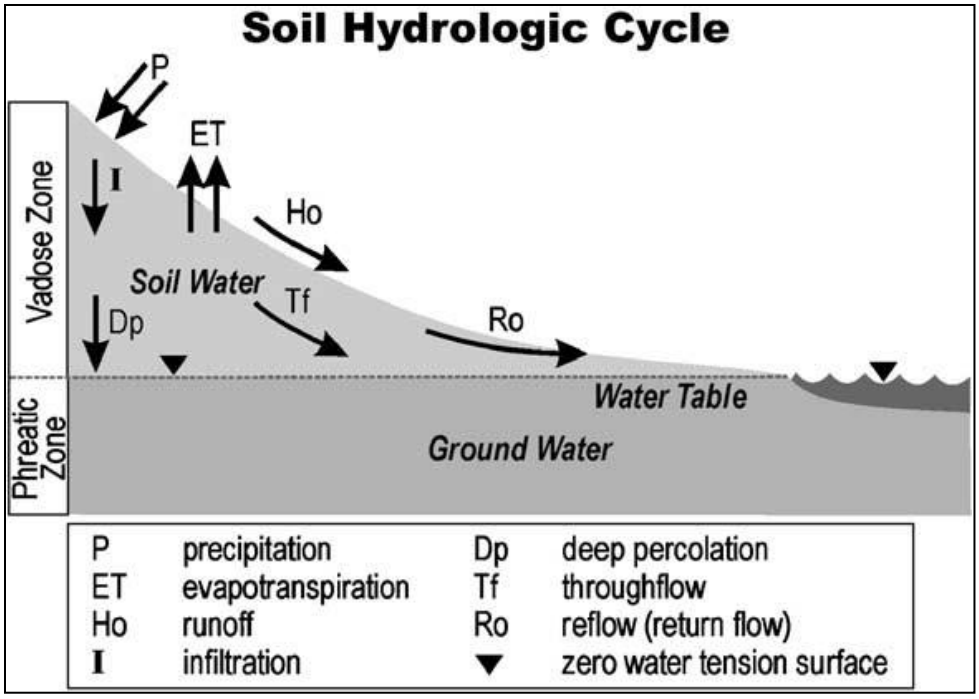

Figure 2. 3 Conceptual Soil hydrologic cycle (Schoeneberger & Wysocki, 2005).

Four soil flowpaths are categorized (Figure 2.3), namely overland flow, recharge flow, throughflow or interflow and return flow. This has led to categorization of soil types associated with these flowpaths (Le Roux *et al*., 2011). Recharge soils are typically found on crest positions in semi-arid climates and are characterized by freely drained horizons with red to yellow colour overlying permeable, fractured rocks. They are divided into shallow and deep recharge soils (Van Tol *et al*., 2011 b). Interflow soils are divided, permitting water to flow laterally as either macropore flow (Van Tol *et al*., 2012), at A/B horizon interfaces as in Estcourt soils (SCWG, 1991) or at the soil/bedrock interface. Ticehurst *et al*., (2007) identifies three lateral flow paths. These pathways are namely overland flow, subsurface A/B horizon lateral flow and bedrock interflow. Different pathways are also dominant at different soil water contents. Slope length and slope % and the combination of the two, strongly impact on soil lateral flow (SLF) rate (Van Tol *et al*., 2013 a). SLF can also impact on morphological indicators of the soft plinthic B horizon, found in the Westleigh soils (Hensley *et al*., 2012). These form under a fluctuating phreatic water table (SCWG, 1991). They are found on slopes (Hensley *et al*., 2012) and are fed by deep intermediate vadose zone lateral flow. Return flow, also known as exfiltration,

occurs where water exits the soil to resurface and continue as overland flow or pond as in wetlands. Soil types classified as responsive are Katspruit (SCWG, 1991) and other wetland soils (Le Roux *et al*., 2011).

2.6. Morphology

Soil morphology is a signature of hydrological conditions in the soil (Van Huyssteen *et al*., 2005). Red apedal B horizons have a short annual duration of near saturation (S > 0.7). The annual duration of saturation, is defined as the period of a year a soil horizon is saturated at >70% of its pores by water (Van Huyssteen *et al*., 2005). This is postulated the point where soil air exchange is significantly limited and reduction occurs. This assumes an existing oxide reducing microbial colony and sufficient organic matter as energy source for reduction reactions (D'Amore *et al*., 2004).

A uniform red soil colour is an indication of a well-drained soil, which seldom reaches saturation (Ticehurst *et al*., 2007). Van Huyssteen *et* al. (2005) reported near saturation more than 120 days of the year on the long term (Figure 2.4). This extreme is measured in the deep red apedal subsoil (1.5 m depth). A gradient in duration of conditions exist in yellow-brown, E-horizons and G-horizons (Van Huyssteen, 1995; Van Huyssteen *et al*., 2005).

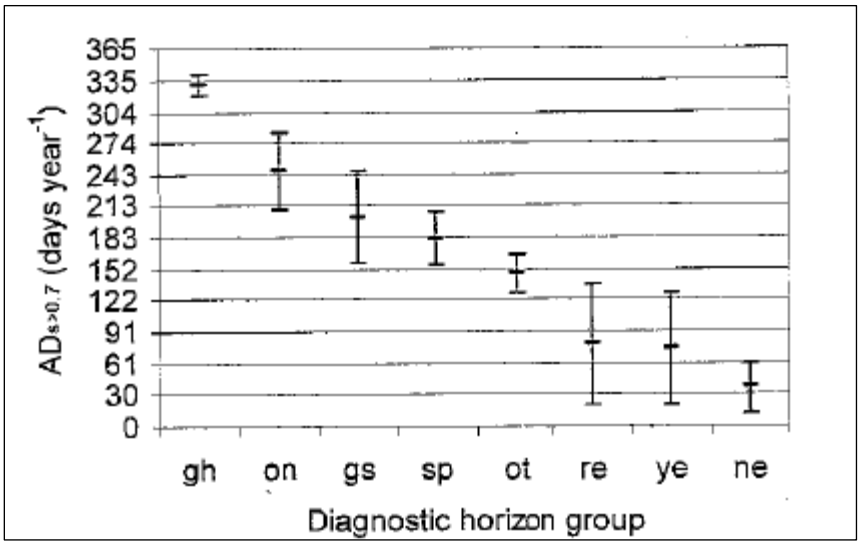

Figure 2. 4 Mean and standard error of mean the $AD_{S>0.7}$ value per diagnostic horizon group (Van Huyssteen et al., 2005).

Iron is characteristically red as in haematite or yellow as in goethite (Cornell and Schwertmann, 1996) (Table 2.1).

Table 2. 1 General characteristics of iron oxide minerals, adapted from Van Huyssteen et al., (2005), and Cornell and Schwertmann (1996)

Mineral	Haematite	Geothite	Lepidocrocite	Ferrihydrite
Composition	α-Fe_2O_3	α-FeO(OH)	γ-FeO(OH)	$(Fe^{3+})_2O_3 \bullet 0.5H_2O$ $5Fe_2O_3 \bullet 9H_2O$
Colour	Metallic grey, dull to bright red	Yellowish to reddish to dark brown or black	Ruby-red to reddish brown, light reddish to red-orange	Dark brown, yellow-brown
	5YR-2.5YR	7.5YR-2.5YR	5YR-7.5YR	5YR-7.5YR

Due to the high occurrence of iron in soil, it is a significant indicator when it is released from minerals by hydrolysis or oxidation of Fe^{2+} into the soil (Bohn, 1985). Equation 1 indicates this process:

$$\text{Fe (II)-O-Si} + H_2O \longrightarrow \text{Fe (III)} + \text{OH} + \text{Si-OH}\ e^- \qquad (1)$$

Calcium carbonate deposits in the soil matrix and horizonisation are morphological indicators of hydrological response in arid zones (Van Rooyen, 1971; Le Roux *et al*., (2011); Lin *et al*., 2005) (Figure 2.5). Biopore fillings are also known as a hydrological signature.

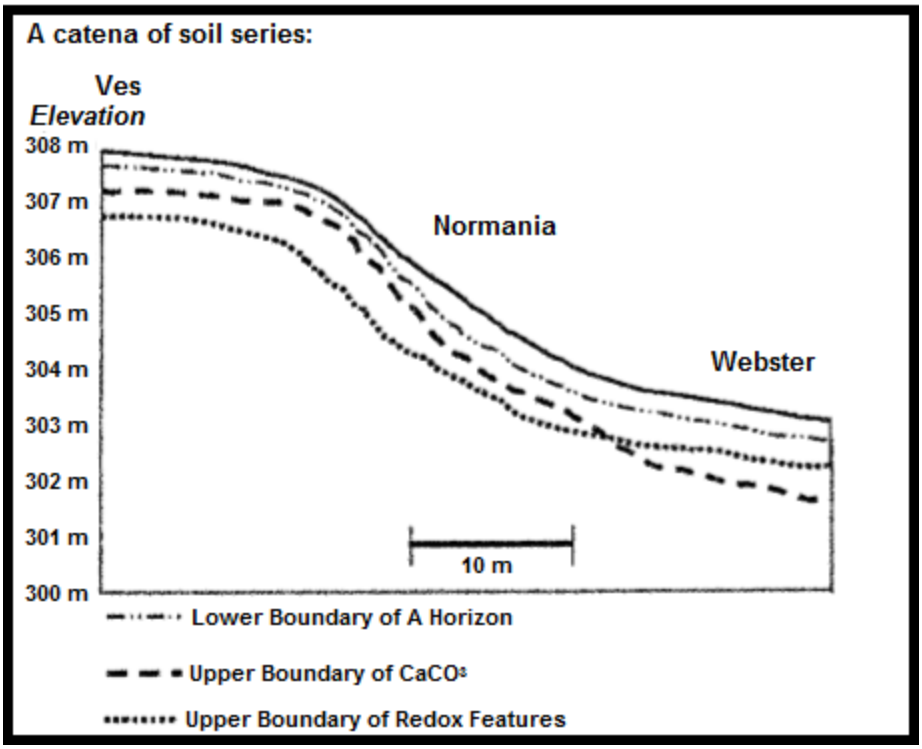

Figure 2. 5 Soil morphological indicators of a catena in a dry climate (Lin et al., 2005).

Soil horizons differ in morphological properties, both indicating and controlling soil water responses in sub-soils (Vereecken, 1992, Le Roux *et al*., 2011). Soil morphological properties of texture and structure within horizons control pore size distribution and therefore soil hydrology (Turner, 1976; Hutson, 1984). Horizons differ mainly in texture and structure, influencing hydrological response due to hydraulic conductivity, porosity and macroporosity (Hill and Sumner, 1966). The porosity and hydraulic conductivity potential of a soil changes with depth, as a response to factors such as bulk density, texture and organic matter content (Hutson, 1984; Weiler *et al*., 2005; Van Tol *et al*., 2012). The sequence of horizon hydrological character influences the pedon hydrological response (Tani, 1997; Ticehurst *et* al., 2007; Van Tol *et al*., 2013 b).

2.7. Ancient and recent/in phase flowpath indicators

Contrary to real-time water measurements which represent a finite volume of the catchment and a similar representation in time, soil morphological flowpath indicators

show where in the soil water has been flowing for a long time (Van Tol *et al*., 2010 a; Le Roux *et al*., 2011). Most morphological indicators are well buffered and stable under a variety of conditions representing long-term conditions well. They may therefore be also be relict as they respond slowly and may be inherited from different hydrological conditions. Chemical flowpath indicators respond fast and are called 'recent' (Bouwer *et al*., 2015). These indicators has a better chance to be in phase, representing the factors controlling the current flowpaths and hydrological response.

2.7.1. Ancient flowpaths indicators

Catena processes luviation and carbonate deposits are considered to be ancient flowpath indicators (Van Tol *et al*., 2010 a; Lin *et al*., 2005). These flowpath indicators were applied to refine the concept of hillslope hydrology for semi-arid climate zones in South Africa (Van Tol *et al*., 2011 b). The availability of measured and quantified hydrological properties, allows for a transfer of morphological indicators to result in plausible explanations of morphological properties, also known as pedotransfer functions (Wörsten, 1985; Bouma, 2004). It is scientifically difficult and perhaps impossible to measure and thus quantify the entire hillslope segment of a catena, as there would be too much disturbance and the natural hydrological process be nullified. This warrants placement and distribution of measurements to be selectively placed on hand of these ancient flowpath indicators, (Van Huyssteen *et al*., 2005; Van Tol *et al*., 2010 a; Kuenene *et al*., 2014 a).

2.7.2. Recent/in phase flowpath indicators

Essington (2004) states that chemical weathering in soil can only occur, if water is present. The change in soil chemistry is mediated by water. Burns *et al.,* (1998) define chemical evolution within the soil as "The changes in concentrations of chemical constituents that occur as water moves along a flow path and interacts with the biology and geology media". As example, contents of basic elements typically increases from the

summit to the valley bottom, which is attributed to the loss in bases where it is dissolved during weathering and adsorbed in the soil lower down.

Soil morphology is well buffered and accommodates a wide spectrum of chemical conditions. To refine flowpaths, soil chemistry, was applied (Bouwer *et al*., 2015) to soils and horizons. It exposed a range of conditions in base saturation and pH. They were inferred as current indicators of flowpaths (Bouwer *et al*., 2015).

An accumulation of cations are found at the oxidic (red apedal B horizons) and redox (soft plinthic / unspecified wet horizons) transition. This is ascribed to the leaching in the overlying red apedal B horizon and capillary rise from the soft plinthic B horizon (Bouwer, 2013). An increase in bases in the soil solution, caused by exchange in the reduced state is due to competition with iron and manganese for negative exchange sites. This leads to the loss of base cations to the overlying horizon when the water stagnates.

Degree of saturation was found not to have a significant effect on pH, although pH fluctuates during saturation (Smith & Van Huyssteen, 2011). Oxidation of reduction soils does not have a significant effect on pH (Phillips and Greenway, 1998). This indicates an equilibrium in base saturation and soluble cation exchange probability of saturated soils. This however does not hold true for addition of a leaching component, as the core samples of Smith & Van Huyssteen (2011) were saturated via capillary rise and sealed to inhibit percolation and evaporation.

Soils containing bicarbonate, closely associate to the carbon dioxide pressure, concentration of bicarbonate ion, and the ionic strength of the soil solution (Seatz & Peterson, 1964). This is shown by

$$pH = pK_1 - 0.5\sqrt{\mu^+}\log\frac{[HCO_3]}{[CO_2]} \qquad (2)$$

Where: pK_1 is the negative logarithm of the first dissociation constant of carbonic acid (6.26 at 24˚C) and μ the ionic strength of the soil solution. The $[CO_2]$ (moles per litre) =

$(\mathrm{P} \cdot a \cdot pCO_2 \cdot 1000)/(760 \cdot 22.400)$ where *P* equals atmospheric pressure in millimetres of mercury, a the solubility of CO_2 in millilitres per millilitre of water, and pCO_2 is the CO_2 pressure atmosphere (Bradfield, 1942).

Due to sporadic rain events of high rapidity and quantity of arid regions, sodium as hydrated ion is subject to leaching. When sodium rich clay disperses, a small portion of the sodium ions will hydrolyse, increasing the hydroxyl ion concentration of the solution. In the presence of electrolyte and the negative adsorption of anions from the negatively charged clay surfaces, both reduces the hydrolysis of disassociating sodium ions and reduce the resulting pH (Seatz & Peterson, 1964). The lack in affinity to form strong bonds with negatively charged soil particles during saturated conditions, implicates it to be readily leached compared to other cations. The exchangeable and adsorbed forms of sodium versus calcium (Gupta *et al*., 1984), influences the saturated hydraulic conductivity of sandy soils (Pupisky and Shainberg, 1979). Other salts found in limited areas which reduce the pH of soils are sulphuric acid formed through sulphide oxidation (Seatz & Peterson, 1964).

Seatz & Peterson (1964) state that 'In alkaline soils, quite different chemical situations exist when the pH is principally influenced by exchangeable calcium alone, by exchangeable calcium and an excess of calcium carbonate, or by exchangeable sodium.' This influences the evaluation of factors associated with soil pH and must be viewed with the soil constituents controlling soils pH instead of just pH *per se*.

A reduction in CO_2 pressure within the soil is partially responsible for the rise in pH of calcareous soils as the proportion of water to soil is increased (Gardner & Whitney, 1943a; Gardner & Whitney, 1943b). The hydrolysis of calcium carbonate producing hydroxyl ions is prevented by adequate carbon dioxide in the soil.

2.8. Soil hydraulic properties

In situ hydrological measurements used to quantify flow rates of conceptual hydrological response models can also be used to verify models. Hydrological measurements can be categorized into two groups: soil physical and long term hydrometrical measurements. The long term measurements include permanent instalments of: for example DFM probes, neutron meter tubes and water marks (Everson *et al*., 2006; and BEEH, 2003). Soil physical measurements include double ring infiltrometers, tension infiltrometers and permeameters. These are used in combination or singularly to quantify soil hydraulic properties and parameterise models (Kuenene *et al*., 2011; Van Tol *et al*., 2011 b). Soil hydraulic properties need to be determined in combination with the soils morphology, for intercomparison, to be of maximum value to hydropedologists (Le Roux *et al*., 2011). Although hydrological measurements are expensive, time consuming and cumbersome (Van Alphen *et al*., 2001), they are necessary for the hydrological modelling of catchments (Tomasella *et al*., 2003).

2.8.1. Pore size distribution and Macroporosity

Soil water retention is a result of each soils unique particle and pore size distribution. Removing the descriptive pedology from hydrological measurements, results in empirical characterization of soil structure which has no direct information pertaining to functional soil hydrology. This makes it imperative for descriptive pedology and hydrological measurements to co-evolve, facilitating in-field characterisations and use of pedotransfer functions (Bouma, 2004).

Every soil has a different soil water retention curve (Dexter, 2004), which indicates the volumetric water content as a function of matric suction (Dirksen, 1999). At a specific tension the water will flow in the water film. The soils' drainage characteristics, can be characterised by using a soil water retention curve (SWRC) (Hensley *et al*., 2000). This leads to determining pore size and geometry contribution controlling the hydraulic conductivity of a soil. Kuenene *et al*., (2014 a) found that on average 75% of the hydraulic

conductivity was controlled by macropores of the soils in the Two Streams catchment. Using soil water retention characteristics, the catchment water balance and response can be characterised. This information can be used in combination with a weir to determine the streamflow of a catchment (Everson et al., 1998; Van Huyssteen et al., 2009a; Van Huyssteen et al., 2009b; Van Huyssteen et al., 2010).

Pore size distribution within soils is strongly affected by the soil structure and bulk density represented by the amount of water retained at -10 kPa (Rawls *et al*., 1992). This value is often used as an arbitrary boundary, separating water controlled by the structural controlled porosity and textural controlled matric suction (Marshall, 1959; Kuitlek, 2004). Kuenene (2013) used -10 kPa as the drained upper limit (DUL) or drainable water contributing to flow within a soil, separating the structural and textural hydrologically controlled domain. The diameter of macropores is considered at greater than 0.1 mm (Luxmoore, 1981), which drain at suctions of less than -0.3 kPa (Jury, 1991).
The total effective macroporosity (MP) ($m^3\ m^{-3}$) is calculated as (Watson and Luxmore, 1986):

$$\Theta_m = N\pi r^2 \qquad (3)$$

Where N is the number of hydraulic effective macropores, r is the calculated critical pore radius:

$$r = \frac{2\gamma\cos(\vartheta)}{\rho g h} \sim \frac{0.15}{h} \qquad (4)$$

where h is the soil water suction in mm. Equation 3 is completed for tension infiltration at h = 3 mm to quantify macropores.

Van Tol *et al*., (2012) reported on this theory and applied it to construct a pedotransfer function for macroporosity derived from soil morphological properties. Van Tol *et al*., (2010 a) and Kuenene *et al*., (2014 a) applied this theory when discussing desorption characteristics of horizons to create a hydrological responses of different horizons. This

lead to a determination of catchment water balance and to quantify streamflow response of the catchment. The boundary between structural and textural domains depends on the soil's inherent and dynamic manipulated properties, and found not to be fixed for natural soils (Tuller and Or, 2002).

A convenient approach to determine the water retention curve, is the hanging water column method (Dirkensen, 1999). This is a laboratory method suitable for the determination of water release at suctions of less than -10 kPa (Dirkenson, 1999). This represents the arbitrary DUL and therefore the water subject to contribute to flow within the soil (Hensley *et al*., 2000; Kuenene *et al*., 2014 a). Use of pressure plates is made to cover the suction range from > -10 kPa to -1500 kPa (Klute, 1986; Jury *et al*., 1991; Kuenene, 2013). This -1500kPa is considered to be the permanent wilting point (PWP) or residual water content (θ_r) for models such as the Van Genuchten model (Van Genuchten, 1980).

To overcome difficulties of irregular pore geometry and discontinuity, texture and mineralogy variations, mathematical models have been developed for predicting soil water retention values (Carsel and Parish, 1988). Use is made of the power function relationship when characterizing the soil water retention curve (Brooks and Corey, 1964; van Genuchten, 1980). Parameters used in the van Genuchten model (1980):

$$S_e = ((\theta - \theta_r) / (\theta_s - \theta_r)) = [(1)/((1+(\alpha\lambda)^n)]^m \quad (5)$$

Where: S_e is the effective saturation and is dimensionless; θ_r is the residual water content ($mm^3\ mm^{-3}$) and θ_s is the saturated water content ($mm^3\ mm^{-3}$); α, n, λ and m are van Genuchten parameters influencing shape of water retention curves. The parameters S_e, α, n, θ_r and θ_s which are required for the estimation of the model. Assuming m = 1-1/n, simplifies the model (van Genuchten, 1980). θ_r is considered as the water content at -1500 kPa or air dry water content and θ_s is usually known or determined (van Genuchten et al., 1991; Kuenene, 2013). The van Genuchten and Mualem model of soil hydraulic conductivity, are used in the retention curve program (RETC) and considered a sound

basis to estimate the unsaturated hydraulic conductivity curve (van Genuchten et al., 1991; Kuenene, 2013).

2.8.2. Soil hydraulic conductivity

Soil hydraulic properties are controlled by soil physical and morphological properties. These soil physical properties influence the hydraulic gradient in soil pores (Bagarello et al., 2004; Messing, 1989). These soil properties vary horizontally and vertically in a soil profile (Kuenene et al, 2014 b).

Soil properties within soil forms, create heterogenetic hydrological responses (Van Huyssteen *et al*., 2005). Horizons account for the vertical heterogeneity and some horizontal homogeneity within the soil catena. Horizon boundaries separating soil properties within soil forms (SCWG, 1991), impact on vertical hydrological response of individual horizon units spatially (vertically) within soil forms (Kuenene *et al*., 2013). This requires at least vertically sequenced hydrological measurements to properly model pedon hydrological responses (Schulze, 1995; Kuitlek and Nielson, 1994). Kuenene *et al*. (2014 b) state that it is important to expose this heterogeneity, to improve field characterisation of soil morphological indicators in term of their flow regimes.

2.8.2.1. Saturated hydraulic conductivity

The saturated hydraulic conductivity (K_s) is determined by measuring the flow rate under a specific hydraulic gradient when all pores are filled with water. Pore properties account for the variability of K_s in different soils (Kuitlek, 2004). Continuous macropores account for fast flow in soils, whereas high macroporosity which is discontinuous, does not. This is important, as high macroporosity does not necessarily account for fast flow in soils (Bodhinayaka *et al*., 2004). As pore properties are controlled by soil physical and morphological properties, land use and variability in response to different methods of measurement affect the K_s data (Bagarello *et al*., 2004; Stockton and Warrick, 1971). To limit pore collapse, *in situ* K_s measurements are considered to be the most accurate.

Various methods including disk permeameters (Perroux and White, 1988), constant-head and Guelph permeameters (Amoozegar, 2002; Reynolds *et al*., 1983), auger hole (Van Beers, 1983) and double ring infiltrometer (Haise *et al*., 1956) are used to determine hydraulic conductivity. The simple and convenient application of the double ring infiltrometer and simple mathematical model (Lilli *et al*., 2008) make this a popular method for obtaining K_s (Chang *et al*., 2010; Van Tol *et al*., 2011 b; Kuenene *et al*., 2014 a).

2.8.2.2. Unsaturated hydraulic conductivity

As the soil water at saturation drains, the larger pores or macropores will be emptied first. As the smaller pores begin to empty, the hydraulic conductivity begins to drop rapidly (Kuenene, 2013). The unsaturated conductivity is therefore a function of matric suction. The ratio of decrease in unsaturated hydraulic conductivity to suction has been used to illustrate the desorption of horizons and characterising the hydrological response of soil horizons, soil forms, hillslopes and the contribution of soil water retention to streamflow (Kuenene *et al*., 2011; Kuenene *et al*., 2014 a).

To determine the unsaturated hydraulic conductivity in-field, tension infiltrometers are used for the very wet range from -2 to 0 mm suction (Watson and Luxmoore, 1986; Reynolds and Elrick, 1991; Van Tol *et al*., 2010 a; Kuenene *et al*., 2011; Kuenene *et al*., 2014 b). Laboratory determinations (Klute and Dirksen, 1986) are often less suitable, due to samples not representing field conditions of heterogeneity. Indirect estimation methods of hydraulic conductivity are more suitable (van Genuchten, 1980).

Use of the RETC program (van Genuchten *et al*., 1991) has been widely used to facilitate the determination of the unsaturated hydraulic conductivity from retention data (Dunn and Philip, 1991; Cameira *et al*., 2003; Kuenene *et al*., 2011; Kuenene *et al*., 2014 a). Tension infiltrometer measurements define the field saturated hydraulic conductivity of soils under near saturation (0 to -30 mm suction). Kuenene (2013) found that predicting unsaturated hydraulic conductivity (K_h) curves with the predictive van Genuchten-Mualem (VGM) model (Van Genuchten and Leij, 1992) using retention data only, incurred discrepancies

leading to unsatisfactory results. Kuenene (2013) found an only 8-fold higher simulated K value at 0.3 kPa tension using the VGM retention data than that using in-field measurements (Figure 2.10). This necessitates the use of in-field measurements when determining the water retention characteristics using the VGM model. However cumbersome these in-field measurements are, they are an accurate presentation of the near saturated flow of water, most commonly used when determining solute transport and rapid flow of water in soils (Cameira *et al*., 2003).

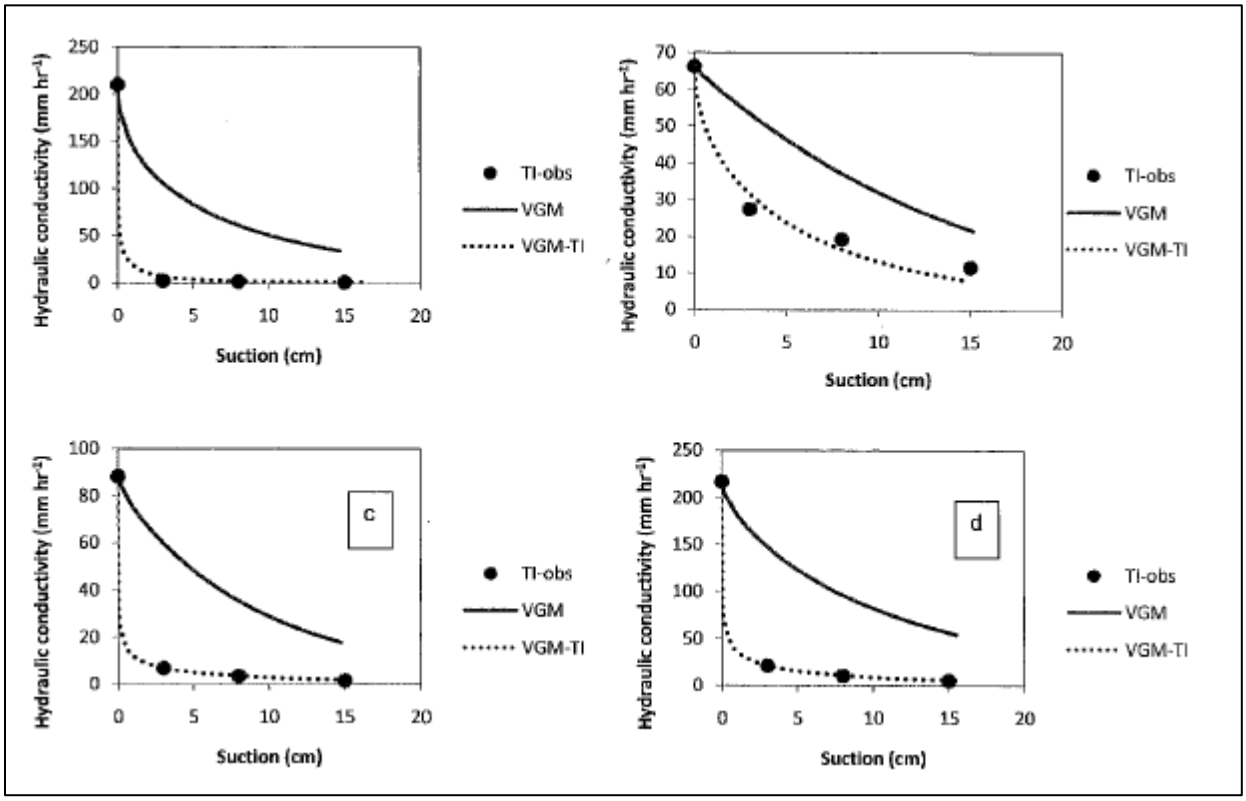

Figure 2. 6 Comparison between unsaturated hydraulic conductivity curves obtained by tension infiltrometer unsaturated hydraulic conductivity only (TI-obs), using the VGM hydraulic model with retention data only (VGM) and using VGM model fitted to tension and infiltration data of (a) Oakleaf, (b) Clovelly, (c) Griffin and (d) Oakleaf orthic A horizons (Kuenene, 2013).

2.8.3. Porosity of soil

Measurements of hydrological properties include physical properties of the soil (Hillel, 1980). To measure saturated hydraulic conductivity, three variables are noted as important. These are bulk density, pore size distribution and clay content. Pore size is

divided into three groups namely: macropores, mesopores and micropores. The macropores (MP) control the near saturated hydraulic conductivity, maximum flux rate of water under steady state conditions and most of the solute movement in soils (McDonnell, 1990; Jarvis and Messing, 1995; Bodhinayaka et al. 2004; Clothier et al. 2008). MP is defined as having a diameter of greater than 1 mm (Luxmoore, 1981). The dependency of K_s on the pore size and distribution implicates different response for every soil. MP estimations include indirect measurements under various matric potentials using the combination of double ring and tension infiltration devises (Watson and Luxmorre, 1986; Kuenene *et al*., 2011; Kuenene *et al*., 2014 b). Tension infiltrometer infiltration measurements are performed under negative water pressures with respect to the atmospheric pressure, conducting water to infiltrate the soil matrix, excluding macropores to dominate the infiltration process (Jarvis *et al*., 1987). Pedotransfer functions have been established for macroporosity (Van Tol *et al*., 2012). This is shown in the following formula:

$$S_{index} = CEC_{soil} – (OC \times 1.7241) \times 100 \quad (6)$$

Where: S_{index} is the swelling index dependent of the CEC_{soil} ($cmol_c(-)\ kg^{-1}$ soil) subtracted by the CEC_{OC} set at 100 $cmol_c(-)\ kg^{-1}$ soil and given as apedal, weak, moderate and strong ; OC is the organic carbon content (%).

$$\Theta_m = -0.126 + (0.664 \times OC) – (0.027 \times S_{index}) + [0.31\ (\text{if } S_{Grade} = \text{Apedal})] \quad (7)$$

Where: S_{Grade} is the structure grade; and Θ_m is the measured water conducting macroporosity (%).

The degree of water saturation is the volume of water relative to the porosity (f) (Hillel, 1980). Porosity can be calculated as:

$$f = 1- \rho_{b/}\rho_s \quad (8)$$

Where: f is the porosity, ρb is the bulk density of soil (mg m^{-3}) and ρ_s is the particle density (mg m^{-3}) of the soil. The degree of saturation can be calculated as:

$$s = V_W \div V_f \quad (9)$$

Where: *s* is the degree of saturation (as fraction), V_W is the water content ($mm^3\ mm^{-3}$) and V_f is the total pore volume ($mm^3\ mm^{-3}$). Complete saturation (s = 1) is seldom reached since air is usually trapped in pores by water (Hillel, 1980). The DUL i.e. the water content below which drainage due to gravity virtually ceases, is expected to be around 0.65 in most soils (Smith & Van Huyssteen, 2011).

Trapped air is an error variable of field infiltrations, yet can be eliminated in laboratory hydraulic conductivity and water retention measurements by de-airing core samples (Dirkens, 1999). This procedure has been replicated by Kuenene *et al*., (2011) and Kuenene *et al*., (2014 a).

Van Tol *et al*., (2010 a) calculated the water storage capacity of the Bedford catchment by determining the weighted mean bulk density (D_b) which was used to estimate the mean porosity of the catchment. The D_b was determined from undisturbed core samples taken during the field survey. This procedure was replicated by Kuenene *et al*., (2011) and Kuenene *et al*., (2014 a) to estimate the water storage capacity in the Two Streams catchment.

2.8. Arid soils of the Orange River Basin

Arid soils of the Orange River Basin (ORB) are the aeolian sand deposits of so–called Kalahari origin (Söhnge & Visser, 1937; Van der Merwe, 1962; Thompson, 1965; Du Toit, 1966). These sands are recent additions of the Kalahari System and derived from rocks within the Kalahari basin itself (King, 1963). Paiget (1963) postulated that the sandy soil parent material is of an eastern source where Karroo sediments dominate. The redistribution and transport system controlling the transport of these sands are westerly flowing rivers and subsequent redistribution from the river beds (Paiget, 1963). Three types of sands are recognized, as found by Harmse (1963):

- Older red sand partially consolidated and accumulated as river-border dunes during Early Middle Pleistocene;
- Aeolian-flat sand which originated in the Kalahari and was blown in , to form seif dunes with smooth-easterly trend during Late Middle to Early Upper Pleistocene; and
- Garnet-bearing sand which accumulated as river-border dunes during the Late Upper Pleistocene.

With an increase in annual rainfall (even if slight), response in vegetation to control and stabilize the redistribution of sands plays a role in the select properties of these aeolian sands. These are namely soil colour which changes from brick-red in very arid to white in high rainfall areas, as well as pH which changes from slightly alkaline to acid with an increase in rainfall (Van der Merwe, 1954). These sands are inherently low in clay (Van Rooyen, 1971).

The predominating red colour was investigated substantially in Hutton type soils (Du Toit, 1966). Harmse (1963) states that the variation in colour of these sands is not due to sedimentological differences but of *in situ* weathering under redox conditions. This indicates the removal of the iron oxide coatings responsible for the red colour with an increase in water additions to the soil (Van Rooyen, 1971).

Sands originating from the Orange River were found to have distinctly paler colours than that of the red sands (Van Rooyen, 1971). They are well drained and lack traces of hydromorphism. Where dolerite is found in the landscape adjacent to these sands, a redder tint is discernible (Van Rooyen, 1971).

Sand fractions of these arid soils dominate, increasing in finer sand fractions with distance from river, with the Orange-Vaal confluence showing a marked coarse sand fraction dominating (Van Rooyen, 1971). The mean grain size and texture fractions decrease with an increase in distance from the river, as shown in Figure 2.6.

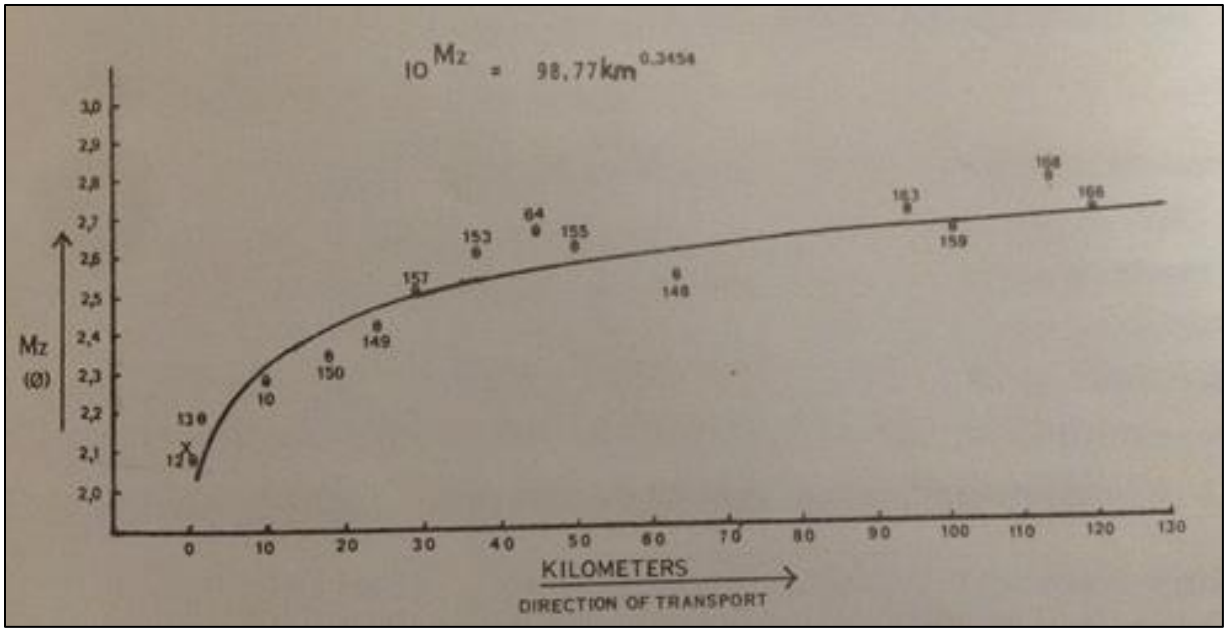

Figure 2. 7 Decrease in mean grain size (Mz), with distance from Vaal River, for the red sands. Mz values represent average of all subsurface values of each profile (Van Rooyen, 1971).

Van Rooyen (1971) found that yellow-sands have a different parent material source than those of the red coloured sands on hand of heavy mineral analysis. He further found an increase in yellow sands with a greater distance from the river bank deposits of the Vaal-Riet confluence. Localized dolerite and lava outcrops show to have an impact on localized reddening of the sands.

Soils are found to be predominantly eutrophic, with base saturation higher than 100% and a low CEC seldom higher than 10 $cmol_c$ kg^{-1} soil. Calcium and magnesium dominate the cations and pH is seldom below 7 (Van Rooyen, 1971).

Conceptual hydrological response models to illustrate impacts of irrigation with two different underlying materials (Karroo sediments and calcrete), were constructed for the ORB (Van Rooyen, 1971) (Figure 2.7 and 2.8). These were constructed primarily by analysing the soil morphology, in particular iron, with minimal input of saturated hydraulic conductivities and drainable water content measurements.

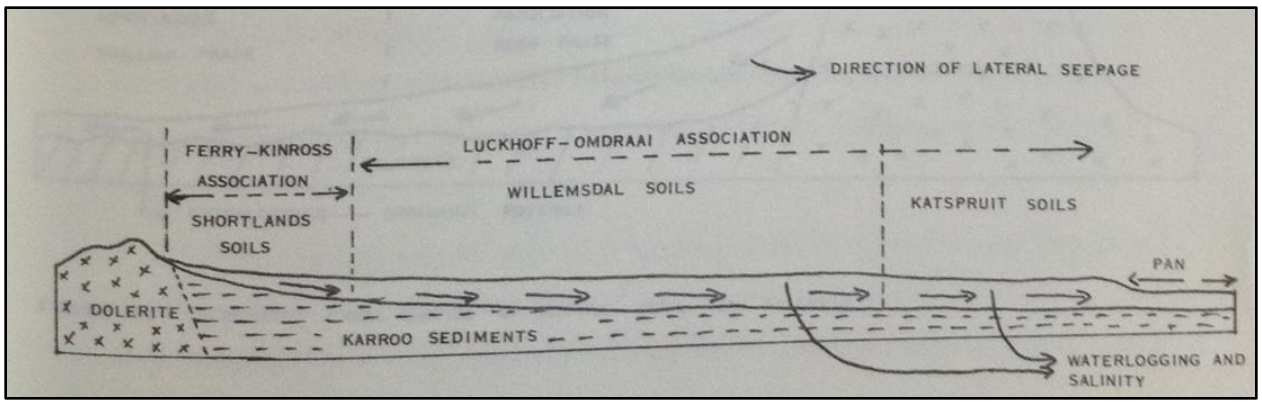

Figure 2. 8 Schematic cross-section of clayey soils on Karroo sediments (Van Rooyen, 1971).

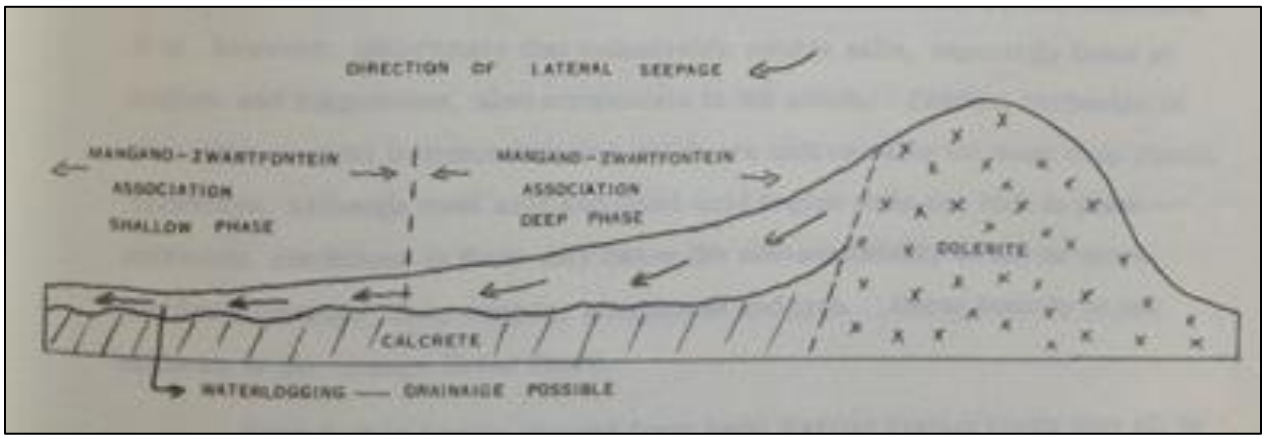

Figure 2. 9 Schematic cross-section of Hutton soils on calcrete (Van Rooyen, 1971).

2.9. Hydrology of arid soils

To study hydrological properties of soils in their natural state, the size of catchment, accessibility of the site and most importantly, a high frequency of precipitation is required. This has limited most hydropedological study sites/catchments to the east of South Africa, where more precipitation occurs, accelerating result based outcomes (Van Tol *et al*., 2012). Comparatively the western part, more so the arid part of South Africa has been subjected to very little hydropedological studies. Therefore, the diagnostic horizons of the carbonate family, namely neocarbonate B, soft carbonate B and hardpan carbonate B horizons (SCWG, 1991), which only occur in arid climates have not been studied.

Carbonate precipitation can influence hydrological functionality in soils they are found in, due to their indurated morphology (Gile *et al*., 1966). Carbonates are chemically, once precipitated, poorly soluble, especially under more arid, natural conditions:

$$CaCO_3 \leftrightarrow Ca^{2+} + CO_3^{2-} \qquad K_{sp} = 3.7 \times 10^{-10} \text{ to } 8.7 \times 10^{-9} \text{ at } 25°C. \qquad (10)$$

Carbonates originate from two sources, namely meteoric precipitation or from igneous geology (Gile, 1961; Gile et al., 1966). Meteoric deposition accumulates through evapotranspiration losses of the soil, allowing the remaining CO_3^{-3} to precipitate (Equation 11 and 12) (Jenny, 1980). The latter is released via chemical weathering of the rock, which frees the carbonates which bind mostly with Ca or lesser so with Mg. Meteoric CO_3^{-2} is delivered via rain as bicarbonate (HCO_3^-).

$$CO_3^{2-} + 2\ H_2O \rightleftharpoons HCO_3^- + H_2O + OH^- \rightleftharpoons H_2CO_3 + 2\ OH^- \qquad (11)$$

$$H_2CO_3 + 2\ H_2O \rightleftharpoons HCO_3^- + H_3O^+ + H_2O \rightleftharpoons CO_3^{2-} + 2\ H_3O^+ \qquad (12)$$

Once the CO_3^{-2} is bound to Ca^{+2}, it precipitates. This calcium carbonate indicates a flowpath (Gile et al., 1966). The high incidence of dust storms allows for illuvial deposits to contribute to carbonate deposition and precipitation (Bretz & Horberg, 1949, Gile et al., 1966).

Precipitation of carbonates occurs in two different media in which they form (Table 2.2) (Figure 2.11), namely in media with particles greater than 2 mm and smaller than 2 mm (gravely and non-gravely soils) (Gile et al., 1966). A sequence in carbonate accumulations is idealised in the schematic representation of Figure 2.12.

Table 2. 2 Stages of the morphogenetic sequences and the youngest land surfaces on which the stages occur (Gile et al., 1966)

Stage	Diagnostic carbonate morphology		Youngest Geomorphic Surface on which Stage of Horizon Occurs
	Gravelly soils	Nongravelly Soils	
I	Thin, discontinuous pebble coatings	Few filaments or faint coatings	Fillmore <2600 to 5000 years
II	Continuous pebble coatings, some interpebble fillings	Few to common nodules	Leasburg >5000 years-latest Pleistocene
III	Many interpebble fillings	Many nodules and internodular fillings	Picacho Late-Pleistocene
IV	Laminar horizon overlying plugged horizon	(increasing carbonate impregnation)	Picacho Late-Pleistocene
	(thickened laminar and plugged horizon	Laminar horizon overlying plugged horizon	Jornada Mid- to late-Pleistocene La Mesa Mid-Pleistocene

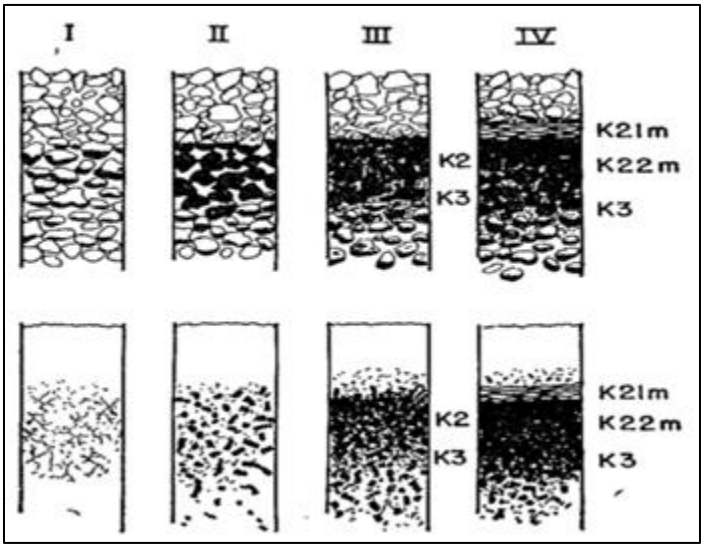

Figure 2. 10 Schematic diagram of the diagnostic morphology of the stages in the morphogenetic sequences of carbonate horizon formation in gravelly and nongravelly materials. Carbonate accumulations are indicated by black forms and shading for clarity (Gille et al, 1966).

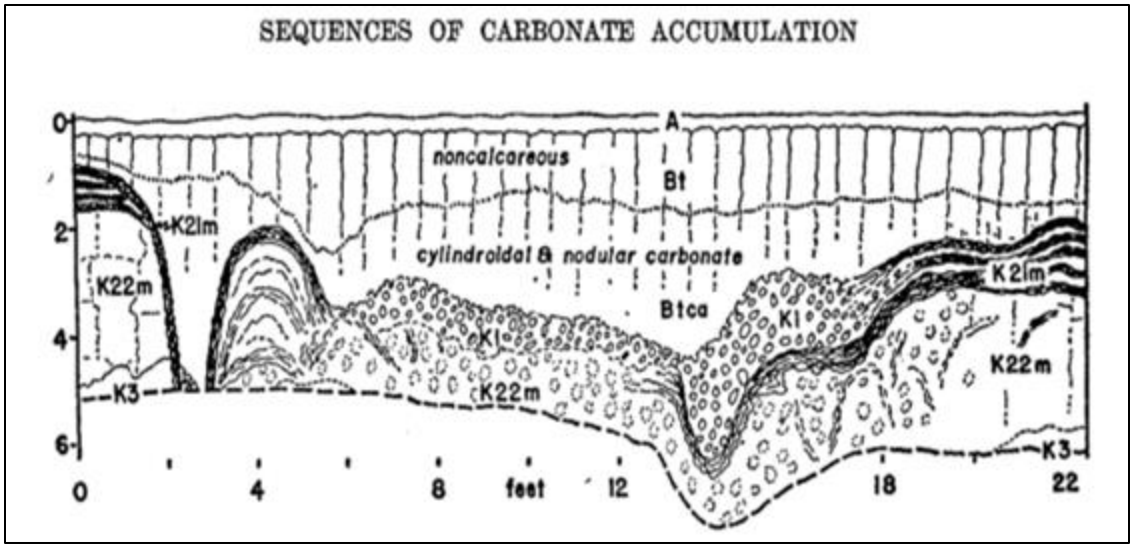

Figure 2. 11 Scale diagram of horizon associated with a large pipe penetrating the thick K (carbaonte) horizon of a Cacique soil on the La Mesa surface. Scale is in feet (Gille et al, 1966).

The chemistry of carbonates and soils containing carbonates is subject to a high pH of 7 and greater (Birekland, 1974)) (Equation 13), influencing base status and fertility of soils (Gardner & Whitney, 1943b):

$$[CaCO_3] + [H_2O] = [Ca^{2+}] + [HCO_3^-] + [OH^-]. \quad (13)$$

PiPujol & Buurman (1997) suggests that calcium carbonate reacts to water regimes of the soil. An increase to mean depth to $CaCO_3$ layer, correlates with an increase in the precipitation and leaching gradient. The depth of carbonate precipitation and soil pH have a negative correlation (Lin *et al*., 2005).

Lin *et al*., (2005) suggests that local topography is very significant in the carbonate precipitation distribution (Figure 2.5). They explain that the difference in two regions is due to more leaching in the depressions of drier areas where water accumulates and that there is water logging in wetter areas were $CaCO_3$ can accumulate. Van Tol *et al*., (2010 a) found carbonate precipitation to be a flowpath indicators in the Bedford catchment located in a semi-arid climate zone of South Africa. Kuenene (2013) found no carbonate

precipitation in the humid Cathedral Peak VI study site although calcium and magnesium rich basic parent material dominates. Local variations of the climatic regions therefore make the $CaCO_3$ subject to hydrology driven by climate.

Continuous decalcification is defined by Buol *et al*., (1997) as the eluviation of specifically carbonates and an associated process of calcification as the accumulation of carbonates. Calcium and magnesium are the primary minerals that bind with carbonates in soil.

Rainfall has a pH average of less than 7 (Carroll, 1962). This is acidic and may play a role in the dissolving and subsequent redistribution of carbonates in soils.

Summary

Literature shows an established field of hydropedology. This includes morphology, chemistry and hydrometrics as tools to identify flowpaths and their rates. Research has been based in wetter regions, limiting the confirmed application of flowpath indicators in arid regions.

CHAPTER 3

DESCRIPTION OF STUDY AREA

2.10. Location and extent

The study area is located in arid Northern Cape Province of South Africa (Figure 3.1).

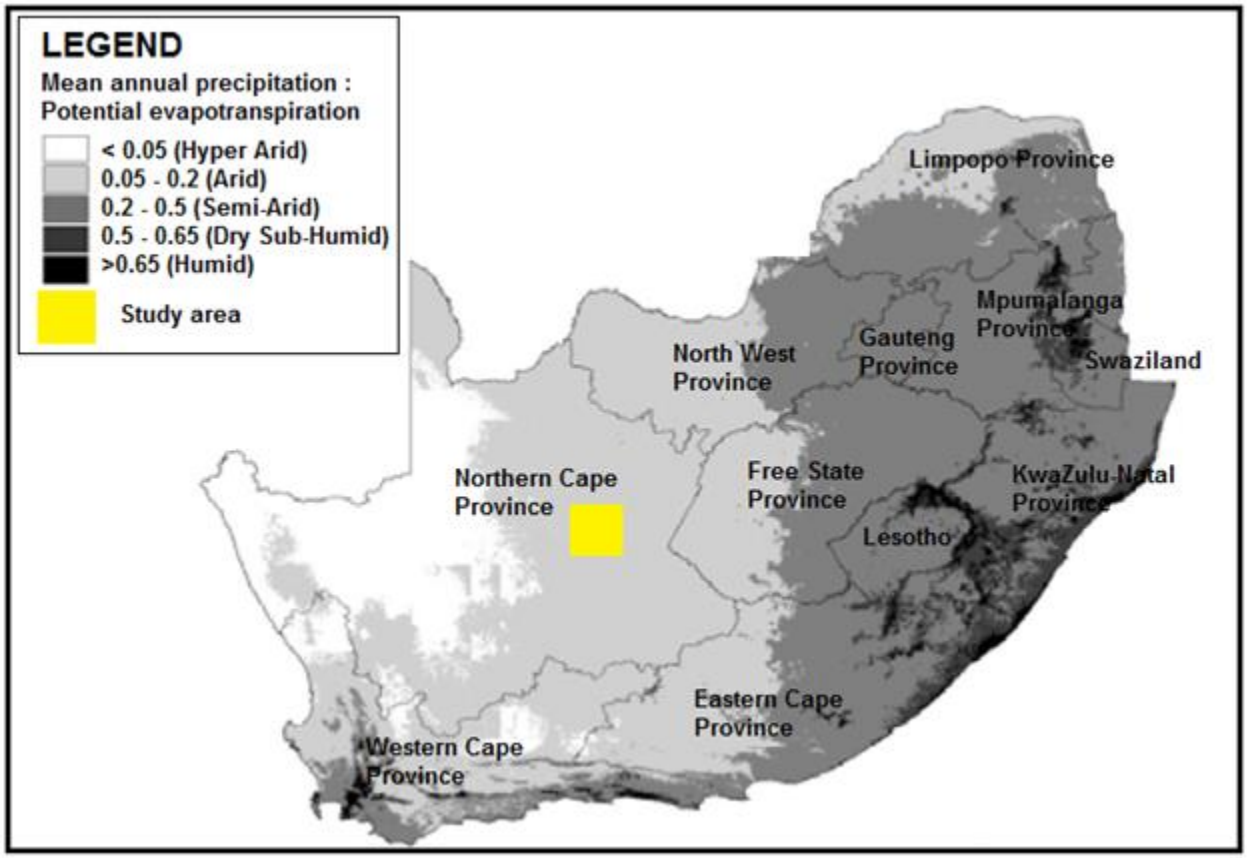

Figure 3. 1 Location of the Study area on an aridity map of South Africa (Hoffman and Todd, 1999).

Four soilscapes were selected on four sites in four different land types (Figure 3.2 and Table 3.1) (Land type Survey Staff, 1972-2006). Land types are areas of similar terrain, climate and soil distribution patterns (Hensley *et al*., 2012). These soilscapes are located close to the Orange River (Ae276), Vaal River (Ae15), Orange-Vaal confluence (Ae276) and Riet River (Ia4) within the Orange River Basin (Figure 3.2).

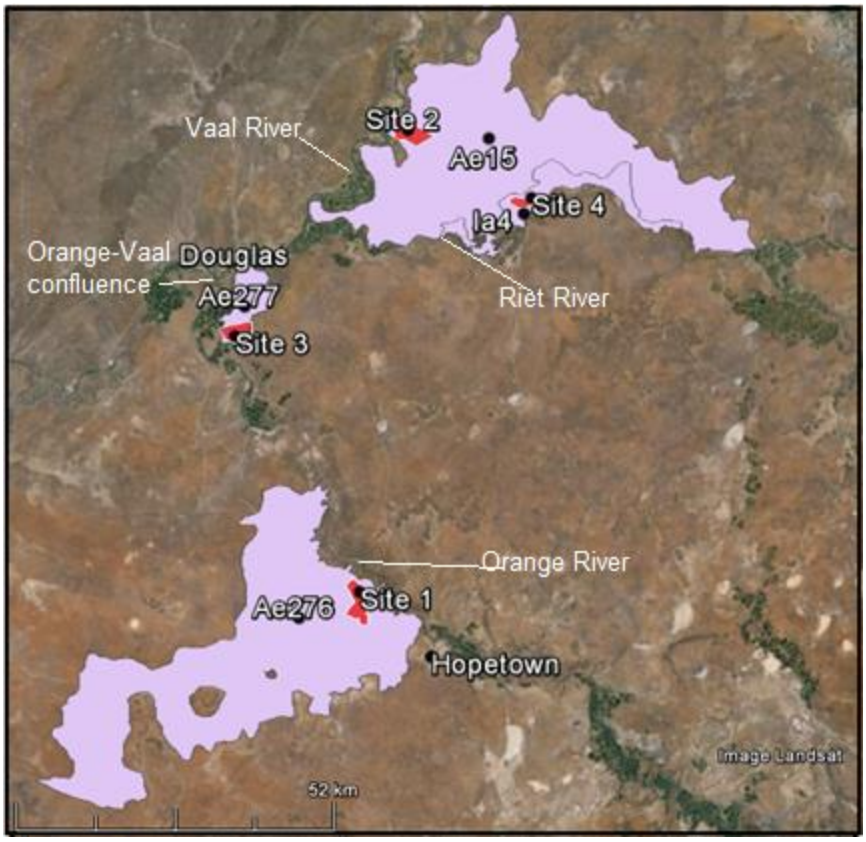

Figure 3. 2 Location and extent of sites in red, land types in grey and nearest towns.

Freely drained apedal soils dominate the Ae Land Types (Table 3.1) (Appendix A). Deep alluvial, freely drained soils dominate (> 60%) Ia Land Types, while soils with pedocutanic B horizons also occur (Table 3.1).

Table 3. 1 Broad soil pattern code descriptions of land types (Land type Survey Staff, 1972-2006)

Land type			
Map symbol	Soil pattern	Soil classes	Dominant soils
Ae	Freely drained, red, eutrophic, apedal soils comprise >40% of the land type (yellow soils comprise <10%)	Freely drained, structureless soils	Hutton Clovelly Griffin Shortlands Oakleaf
Ia	Deep alluvial soils comprise >60% of land type	Freely drained, structureless soils; Soils with a pedocutanic (blocky structured) horizon	Hutton Clovelly Griffin Shortlands Oakleaf Valsrivier Swartland

The site 1 falls into Land Type Ae276, site 2 into Land Type Ae15, site 3 into Land Type Ae277 and site 4 into Land Type Ia4 (Table 3.2). TMU 4 dominates all the land types between 75-82% (Table 3.2). Dominating soil types for land types Ae15, Ae277 and Ae276 are Hutton soils and for land type Ia4 Oakleaf soils (Table 3.2).

Table 3. 2 Land type defined TMU areas (Land type Survey Staff, 1972-2006)

Site	Land type	TMU 1 (%)		TMU 3 (%)		TMU 4 (%)		TMU 5 (%)		Dominant soils (% largest to smallest)	Coordinates
		%	Area (ha)	%	Area (ha)	%	Area (ha)	%	Area (ha)		Latitude/ longitude
1	Ae276	6	8204	16	21878	75	102555	3	4102	Hu, Ms, Va, Sw, Cv	29° 6'52.36"S 23°46'41.37"E
2	Ae15	4	32201	9	28981	82	264048	5	16100	Hu, Ms, Va, Sw, Du, Ka	28°52'18.64"S 24°11'2.60"E
3	Ae277	-	-	15	992	80	5288	5	330	Hu, Cv, Ms, Oa, R	28°57'30.07"S 24°15'16.13"E
4	Ia4	1	114	1	114	80	9136	18	2056	Oa, Va, Ms, Hu, Cv,	29°34'4.32"S 23°51'58.51"E

Hu = Hutton soil form; Ms = Mispah soil from; Va = Valsrivier soil form; Sw = Swartland soil form; Du = Dundee soil form = Ka = Katspruit soil form; Cv = Clovelly soil form; Oa = Oakleaf soil form; R = Rock.

2.11. Soil distribution, parent material and topography

2.11.1. Land Type Ae 276

TMU 4 dominates this Land type, has a concave to straight slope shape, slope length of 1000 – 4000 m and slope of <1% (Land type Survey Staff. 1972 – 2006). Soils dominating this TMU are 500-1000 mm deep Hutton soils (56%) and 100-300 mm Hutton soils (31%). To a lesser extent Mispah soils of 10-200 mm depth cover 8% of the TMU, Valsrivier and Swartland soils - 4% and Clovelly soils - only 1%. Parent material is aeolian sand, alluvium and calcrete deposits underlain by andesite (Allanridge Formation), as well as tillite and mudstone of the Dwyka Formation. Tillite and andesite outcrops occur (Land type Survey Staff. 1972 – 2006).

2.11.2. Land Type Ae 15

The dominating TMU4 has a straight slope shape, slope length stretching up to 2000 m and a small slope gradient <2% (Land type Survey Staff. 1972 – 2006). Hutton and Mispah soil forms dominate this TMU (55%), with Valsrivier and Swartland soil forms (25%) and Dundee and Katspruit soil forms (20%) occurring. The parent material is dominated by aeolian red to flesh-coloured sand of tertiary to recent age. Dolerite outcrops are found in the land scape (Land type Survey Staff. 1972 – 2006).

2.11.3. Land Type Ae 277

This land type is dominated by TMU 4, has a straight to concave slope shape, slope length of 2000 – 4000 m and a slope of <2% (Land type Survey Staff. 1972 – 2006). Hutton soil forms deeper than 600 mm dominate TMU 4 (50%), with Hutton soil forms of 100 – 300 mm (10%) and Clovelly soil forms deeper than 600 mm (24%) occurring. Other soils occurring are Mispah soil forms of 50 – 200 mm (6%), Oakleaf soil forms deeper than 1200 mm and rock (4%) distributed over this TMU. The parent material consists of alluvium, sand and calcrete deposits. These overly andesite, as well as conglomerate and sandstone belonging to the Allanridge and Bothaville Formations, respectively. These form part of the Ventersdorp Supergroup (Land type Survey Staff, 1972 – 2006).

2.11.4. Land Type Ia 4

The dominant TMU4, has a straight slope shape, slope length of 500-2000 m and a slope of 0-1% (Land type Survey Staff. 1972 – 2006). Dominating soils of this TMU 4 are 900 to 1200+ mm deep Oakleaf soils (45%), Valsrivier soils of 200-300 mm depth (17%) and others such as Mispah, Hutton and Clovelly soils forms of between 150-300 mm and 600-1200+ mm depth. The Geology is dominated by shale and mudstone of the Dwyka Formation and Ecca Group with dolerite intrusions. Basaltic and andesitic lavas of the Ventersdorp Group also occur (Land type Survey Staff. 1972 – 2006).

2.12. Climate and land use

All sites fall into the arid climate zone (Figure 3.1). Average annual rainfall is 314 mm. Rainfall period is during the summer months. Highest rainfall is in February (Figure 3.4). Average summer temperatures range from 16°C to 34°C. Average winter temperatures range from 1°C to 19 °C (Figure 3.3). Evapotranspiration is 1500-1700 mm a^{-1}. Frost days are between 15 and 45 days per year. Wind direction speed is mainly influenced by cold fronts during the winter months. Wind speeds can reach up to 40 km h^{-} for consecutive days. Windy months include August to November (Van Rooyen, 1971). Summer winds are controlled by the Kalahari high pressure system, with predominating winds from the north-west (SAWS, 2014). Boreholes distributed through the sites showed fluctuation in water levels post rain events. According to land owners the groundwater rise during irrigation seasons and drop between irrigation seasons indicating local recharge. All sites were under natural vegetation, used for extensive commercial animal and game grazing and browsing at time of field work.

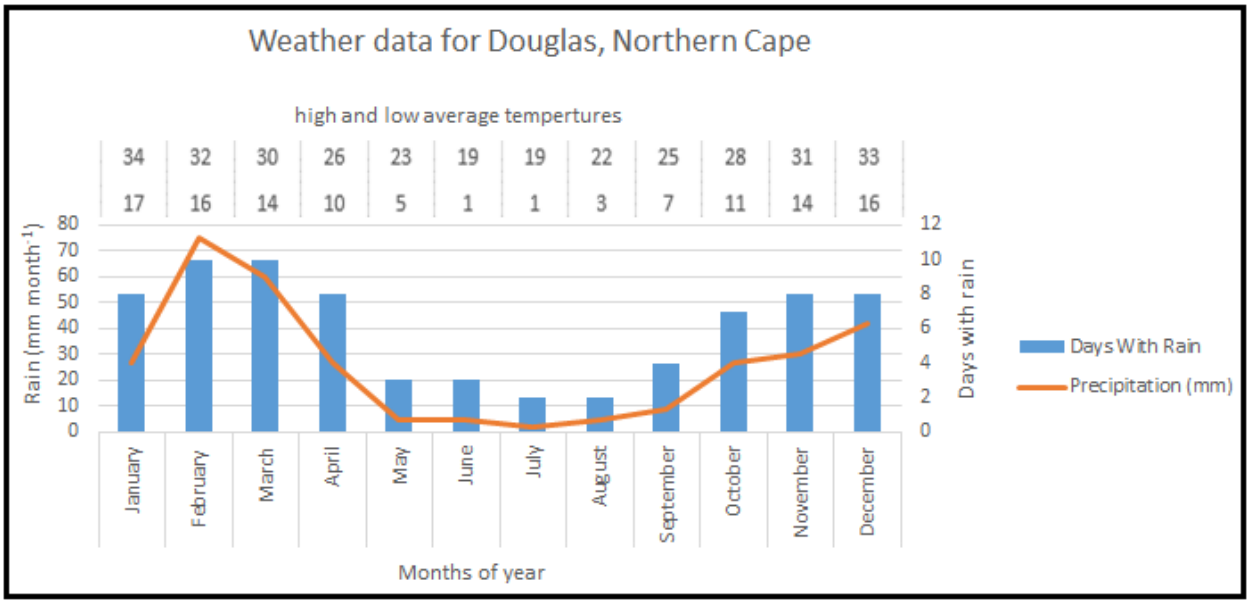

Figure 3. 3 Weather statistic for Douglas including average –rainfall, -days with rain and average -min and -max temperatures per month (SAWS, 2014).

CHAPTER 4

METHODOLOGY

4.1. Soil survey and mapping

A total of 806 soil profile observations were made with a TLB until refusal (hard rock). Soils were described (Turner, 1991) and classified in accordance with the Soil African Soil Taxonomy (SCWG, 1991; Munsell Colour Company, 1981). Thirteen profiles representing soils dominating on the sites were sampled per horizon and subjected to hydraulic measurements (Table 4.1) (Appendix A and B).

Table 4. 1 Site and profile numbers, soil forms, their location and in which Land types they are found

Land type	Site	Profile no.	Soil form	Coordinates	
				Latitude	Longitude
Ae276	1	1	Kimberley	29˚32’22.92’’S	23˚57’34.07’’E
		2	Addo	29˚31’27.73’’S	23˚57’4.72’’E
		3	Kimberley	29˚34’37.99’’S	23˚58’37.95’’E
		4	Hutton	29˚33’9.72’’S	23˚58’17.71’’E
		5	Coega	29˚34’23.05’’S	23˚58’5.30’’E
Ae15	2	6	Addo	28˚51’57.04’’S	24˚4’18.56’’E
		7	Hutton	28˚51’29.40’’S	24˚3’57.00’’E
		8	Coega	28˚50’50.44’’	24˚2’39.00’’E
		9	Hutton	28˚50’57.64’’S	24˚1’56.43E
		10	Hutton	28˚52’22.33’’S	24˚2’26.58’’E
		11	Clovelly	28˚51’58.56’’S	24˚2’15.07’’E
Ae277	3	12	Namib	29˚8’40.41’’S	23˚45’2.31’’E
Ia4	4	13	Valsrivier	29˚32’22.92’’S	23˚57’34.73’’E

4.2. Laboratory procedure

4.2.1. Physical methods

Soil samples taken from diagnostic horizons of 13 profiles were air dried at 105°C, and then sieved and analysed using methods prescribed by The Non-Affiliated Soil Analysis Work Committee (1990). Coarse fraction > 2 mm in diameter was separated by sieving and weighed. This was then captured as percentage coarse fraction by weight of total sample.

Carbonate percentage of total sample in non-precipitated form, or of nodules smaller than 2 mm in diameter, was calculated by treating a 100g sample with 10% HCl (The Non-Affiliated Soil Analysis Work Committee, 1990). The HCl was then washed out three times with distilled water and dried at 105°C. This sample was then weighed and the difference to original sample weight noted as percentage weight carbonate of total sample.

Bulk density was calculated from 1300.39 cm^3 volume cores replicated 3 times per diagnostic horizon of representative soil profiles. Porosities were determined as water-field porosities in the laboratory after saturation of the soil (Kuenene, 2013).

4.2.2. Chemical methods

Exchangeable cations, CEC and pH_{water} and pH_{KCl} were determined (The Non-Affiliated Soil Analysis Work Committee, 1990), organic carbon and nitrogen were determined by an LECO elemental analyzer for orthic A horizons (LECO, 2014).

4.3. Field measurements

Saturated hydraulic conductivity per horizon using double ring infiltrometers were measured in duplicate (Figure 3.5). The saturated hydraulic conductivity (Ks, mm h^{-1}) was obtained by the falling head method (Jury *et al*., 1991);

$$Ks=\frac{L}{t_1}\ln\frac{b_0+L}{b_1+L} \quad (1)$$

Where L is the depth of the soil layer in question (mm), b_o is the initial depth of total head above the soil column, b_1 is the depth that the falling head is not allowed to fall below (mm), t_1 is the time taken for b_o to fall to b_1 (in hours).

Orthic A horizon K_s were measured in the undisturbed and disturbed condition. Disturbing was done by scraping the surface crust or overburden away with a spade. This was done to measure the impact of surface crusts and overburdens on Ks. Undisturbed measurements were performed by installing the double rings, filling both the inner and outer ring and allowing the soil surface (crust) to dry out without removing the double rings. This allowed the surface crust, disturbed by the installation of the double rings to reform and thus reduces preferential flow along the rings edges, where surface crust was broken during installation.

Hydraulic properties of underlying rock were not investigated. Values were assumed to be constant at 0.014 mm h^{-1} as per Galfi and Kovács (1981) for conglomerate.

4.3.1. Unsaturated hydraulic conductivity

Unsaturated hydraulic conductivity at near saturation was measured using a tension infiltrometer (Ankeny *et al*,. 1991). Since tension infiltrometer measure infiltration rates at water pressures that are negative with respect to atmospheric pressure (Jarvis *et al*., 1987), it allows infiltration into the soil matrix but does not allow infiltration into larger macropores that may otherwise dominate the infiltration process (Jarvis *et al*,. 1987). After

completion of the double ring infiltrometer tests a thin layer of diatomaceous earth was applied over the measurement spot. This smoothed out any irregularities of the soil surface and ensures good contact between the soil surface and the infiltrometer membrane. Infiltration measurements were performed at tensions of -30, -80, and -150 mm. The amount of infiltration into the soil was measured by recording the water level falling in the graduated reservoir tower as a function of time. Infiltration measurements continued until a steady state was achieved. The equivalent pore radius (r) corresponding to each negative pressure is calculated from the capillary-rise equation given by;

$$r = -\frac{2\gamma \cos\alpha}{\rho g h} = \frac{-0.15}{h} \qquad (2)$$

Where r is the pore radius (μm), γ is the surface tension of water (cm^{-2}), α is the wetting angle of the water and the pore wall (assumed zero), ρ is the density of water (g cm^{-3}), g is acceleration due to gravity (cm s^{-2}), and h is the negative hydraulic pressure in the tension infiltrometer (cm). By maintaining the supply head at a range of negative pressure values, it is possible to determine the role of macropores and meso/micropores during infiltration. By subtraction, the hydrological role of the larger pores during the infiltration process can be evaluated. According to the capillary theory, infiltration at tensions of 30, 80, and 150 mm water will exclude from the flow process, pores of equivalent radius greater than 0.5, 0.20 and 0.1 mm, respectively. The maximum number of effective pores per unit area (*N*) will be calculated according to the procedure of Watson and Luxmoore (1986), using the minimum pore radius, r (cm), in each class and applying the capillary equation (2) in conjunction with the Poiseuille's equation:

$$N = \frac{8\mu K_m}{\rho_w g \pi r^4} \qquad (3)$$

Where μ is the viscosity of water (g cm^{-1} s^{-1}), ρw the density of water (g cm^{-3}), g is the acceleration due to gravity (cm s^{-2}), and Km the difference in K for two consecutive tensions. The effective water conducting porosity θ_m (m m^{-3}), will be calculated as:

$$\Theta_m = N\pi r^2 \qquad (4)$$

and defined as the portion of the soil volume corresponding to macropores with flowing water (Watson & Luxmoore, 1986).

The contribution of the macropore to Ks is estimated as;

$$\varphi(\%) = \frac{K_m}{K_s} * 100 \quad (5)$$

Where φ (%) is percent of total flux due to the macropores and Ks is the saturated hydraulic conductivity.

Figure 4. 1 Double ring infiltrations on Site 4.

4.4. Water retention curves

Undisturbed core samples were taken from diagnostic horizon of representative profiles to determine water retention characteristics. To prepare the undisturbed soil samples for retention measurements, the first step was to cover the base of the cores with filter cloth, fastened using elastic bands. This was to enable saturation of the samples from the base

upwards, as well as facilitating good contact between core sample and the appropriate extraction material on which they were placed during desorption. The next step was to saturate the soil cores using a two way vacuum saturation chamber setup. There were two of these setups in the soil hydrology laboratory, enabling 18 soil cores to be handled simultaneously (Kuenene, 2013). One setup consists of four chambers, one of them (the tall one) filled with water with a stirrer placed at the bottom of the vessel to continuous stir the water in the vessel during the de-airing process. In each of the other three vessels, three core samples were placed on a 3 mm high gauge wire-mesh platform. All the chambers, fitted with air tight lids, were de-aired together using a vacuum pump working at -70 kPa at room temperature for 24 hours.

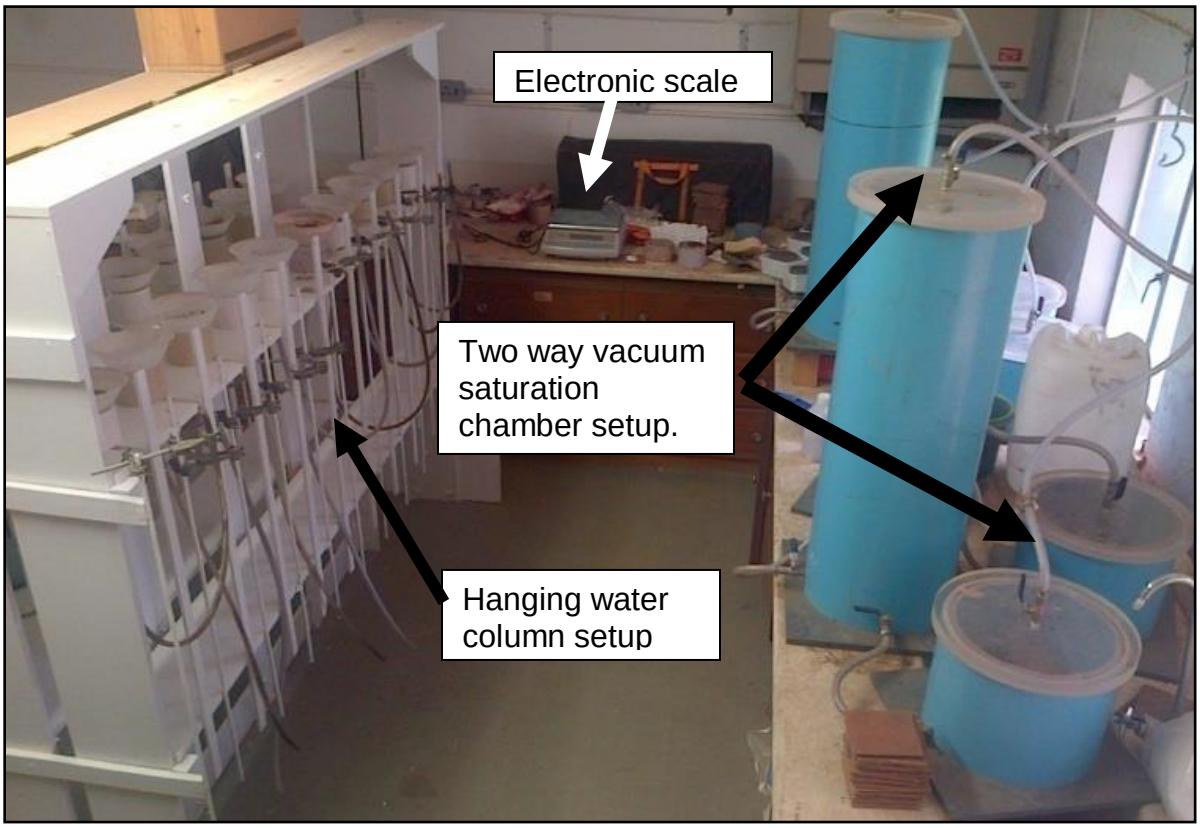

Figure 4. 2 Photos illustrating the laboratory vacuum/saturation chamber and hanging water column setup for determining water retention curves (Le Roux et al., 2015).

Thereafter the vacuum pump was turned off. Ensuring that the two-way chamber system remained air tight, the de-aired water was allowed to gradually flow into the three smaller chambers containing the de-aired core samples until the water level just below the top of

the core samples. Soil samples were then left for a further 24 hours in the chamber, to ensure that full saturation was achieved. Thereafter, each sample was carefully weighed on an electronic scale to get the saturation weight measurement. The saturated samples (18) were then immediately mounted on a hanging water column setup in accordance with the procedure of Dirksen (1999), with the soil core pressed lightly downwards to ensure a good contact between the diatomaceous earth and the sample. Sample tops were covered with aluminium foil, over which were placed and small inverted plastic flower pots fitted inside with moistened sponge to prevent evaporation from the samples. It was found necessary to check continually that all hoses from the extraction cups were filled with water free of air bubbles that would prevent water from being drained. The suction levels (*h*) were set consecutively at levels of 0, 38, 50, 100, 200, 400, 600, 800 mm read on a measuring tape mounted downwards from the extraction cup surface. The gravimetric water content was determined at each level, when equilibrium had been reached, by weighing the samples. The last step was to oven dry the samples at 105°C to obtain bulk density (ρ_b) and calculate the volumetric water content at each kPa value using the respective ρ_b values. The filter cloth and elastic band were also air dried and weighed. Soil water retention curves were drawn from the θ_v/h (means of 3 replicates) for each horizon. The θ_v/h data were then fitted to the van Genuchten (1980) equation using the non-linear curve-fitting program RETC (van Genuchten *et al*., 1991).The parametric θ-h model described by van Genuchten (1980) is written as:

$$S_e = \frac{(\theta-\theta_r)}{(\theta_s-\theta_r)} = \left[\frac{1}{1+(\alpha h)^n}\right]^m \quad (6)$$

Where S_e is effective saturation, θ is the volumetric water content ($cm^3\ cm^{-3}$), θ_r and θ_s are the residual and saturated θ_v, respectively ($cm^3\ cm^{-3}$), *h* (cm) is the suction head, α, n, and m are parameters directly dependent on the shape of the θ-*h* curve. The value of θ_s was fixed as the measured water content at saturation and θ_r was fixed as the water content at 1500 kPa suction, consistent with the suggestion of van Genuchten (1980). The RETC computer programme (van Genuchten *et al*., 1991) was then used to determine the van Genuchten parameters (α & n). In accordance with the suggestion of van Genuchten (1980), m = 1-1/n. The hydraulic conductivity curves were predicted from

the fitted water retention parameters using van Genuchten-Mualem (VGM) model (Van Genuchten, 1980).

$$K(\theta) = K_s S_e^L \left(1 - \left(1 - S_e^{1/m}\right)^m\right)^2 \quad (7)$$

Where K_s is the measured saturated hydraulic conductivity and L is a constant for which the value of 0.5 was used in accordance with van Genuchten (1980). Other parameters are as above. For hydropedological purpose, hydraulic conductivity vs degree of saturation (s) is presented to facilitate pedological interpretation. The degree of saturation (*S*), is defined as the fraction of the porosity that is occupied by water (Van Huyssteen *et al*., 2010). It is calculated as follows

$S = \theta/f$ with $f = 1 - \rho_b/\rho_s$ (8)

where ρ_s is soil particle density, generally taken as 2.65 Mg m^{-3} for all soils low in organic carbon. The degree of water saturation ranges from 0.0 in an oven dry soil to 1.0 in a completely saturated soil. However, complete saturation is seldom reached in the field conditions, since some air is nearly always trapped by water in a very wet soil (Hillel, 1981). The corresponding relationship between the unsaturated hydraulic conductivity and the pressure head is

$$K(h) = \frac{K_s \left\{1 - (\alpha h)^{n-1}\left[1 + (\alpha h)^n\right]^{-m}\right\}}{\left\{1 - (\alpha h)^n\right\}^{m/2}} \quad (9)$$

Where *h* is the pressure head. Other parameters are as above.

Measured retention values at 0, 38, 50, 100, 200, 300, 400, 600, 800 mm suctions together with Wilmots' statistical program were used to predict the Θ_r or residual water content (Willmot *et al*., 1985). This was then processed in the RETC program in combination with tension infiltration values of 0, 30, 80 and 150 mm suction. The output is then mined for values of 1000, 3000, 8000, 10000, 30000, 100000 and 150000 mm retention values. The measured and predicted suction values are combined and reprocessed in combination with the tension infiltration values. This data is then used to graphically represent the fitted retention values in water retention graphs. Measured and predicted retention values were used to visually compare fitted retention curves.

The same data output of the above mention method of measured and predicted retention values were used to predict hydraulic conductivity curves.

4.5. Conceptual hydrological response model

Four steps were used to design the verbal conceptual soilscape hydrological model (Bouwer, 2013). A fith step is included for purpose of depicting the model:
Morphology was used to infer hydrological response of the horizons and soil types;
Texture and structure: Sandy apedal soils indicate a freely drained profile whereas increase in clay (>15%) indicate a reduction in Infiltration. Compaction of surface or surface crusting indicates reduced infiltration into profile. Layers of compaction (stratifications) within the profile indicate a reduction in infiltration. Structure formation as result of increased clay of medium to hard and very hard indicate a reduced infiltration rate. Coarse fraction and stone lines indicate a preferential flowpath and reduced water holding capacity.
Transitions: abrupt transitions indicate a change in infiltration rate from one horizon to another. Diffuse transitions indicate a similar infiltration rate of two vertically sequenced horizons.
Color: Red color indicates a high iron content and a freely drainable horizon/profile. Yellow colour indicates a period where iron (red) is reduced due to a period of porespace ($S_{>0.7}$) saturation with water. This could also indicate a different source of aeolian sands (Vaal River instead of Orange River) (Van Rooyen, 1971). Grey colours indicate removal of iron from horizon or areas within a soil. Mottles and concretions of iron and manganese indicate a fluctuating water table.
Carbonate and gypsum precipitation: Free lime indicates a poorly drained profile. Lime nodules, concretions and induration of various dimensions indicate a variable moisture regime, fluctuating phreatic water table due to a lateral flowpath in the soil. This is driven by an evapotranspirative demand greater than profile available water. Accumulation of carbonates sufficient for precipitation considered as coarse fractions >2 mm and more than 10% of matrix, are considered to indicate a reduction of flow or dominant drainage

depth, dehydrated and driven to precipitation by evapotranspiration. Indurated carbonate layers indicate a prolonged and more intense process discussed above. Presence of gypsum indicates very poor drainage.

Roots and visible macropores: An increase in rooting depth and root density indicates an increase in water holding capacity and probability for microorganisms to impact on soil colour, soil chemistry, soil structure and soil chemistry (decrease in pH, decrease in base saturation, increase in carbonate precipitation). A decrease in rooting depth and accumulation of roots at a layer, indicates an increase in bulk density of underlying material. Visible macropores indicate a preferential flowpath and increase in infiltration rate.

Chemical data were interpreted to establish the relationship between morphology and pedological processes;

Ancient flowpath indicators: These include catena processes of luviation and carbonate precipitation, both sensory attainable morphological attributes of the soil. These ancient flowpath indicators require verification by means of hydrometrics. Deductions can then be made, as in both afore mentioned cases an increase in soil chemical indicators will occur due to a net accumulation of luviated chemical indicators.

Recent flowpath indicators: Associated with these are an increase in base saturation and pH at areas of ponding within soils along vertical flowpaths. This may be observed at a transition between soil layers of lower bulk density over a layer of higher bulk density affecting saturated hydraulic conductivity. Further, this indicates areas of accumulation. Iron occurs in oxidized and reduced form, indicating hydrological flow rate and is preceded by manganese precipitation as indication of scale of potential reduction periods. An apedal red soil with 1) manganese accumulation and 2) yellowing of the red matrix will thus indicate a change in profile hydrology and an increase in period of saturation.

In situ double ring saturated hydraulic infiltration and tension infiltration measured data, and calculated laboratory soil water content measurements, was used to verify the interpretations;

As discussed under 2.8.

A conceptual model is improved using more detailed morphological and hydrological observations.

The process of creating a verbal or graphical CHRM is followed in sequence as listed above. Each step following step (i) improves the interpretation of flowpaths and storage mechanisms.

Depicting a conceptual hydrological response model

A rough sketch of the terrain is drawn including all present terrain morphological units with elevation on the Y-axis and vertical distance on the X -axis.

Soil form distribution patterns and soil depth is indicated along the topography.

Underlying geology and its structural integrity is roughly indicated.

Arrows, indicating flow direction, flow speed (arrow base length) and flow volume (arrow base width) are allocated to soil forms. A rough estimate is made at indicating an aquifer. If applicable, an indication of increase in annual duration of saturation is made.

4.6. Soil maps and contours

Soil maps and contours were drawn in Google Earth (Google Inc.). Soil maps were constructed by use of the polygon function. Contours were drawn by use of the path function, where elevation changed by 1 meter on the elevation display. This was processed at an eye elevation of 1.2 km. This information was confirmed by repeated site visits and spot checks. Due to the slight change in topography, standard 20 m contours available from various sources, and the interpolation thereof were deemed insufficient to represent effect of slight changes in topography. Observation points were placed using the placemark function and GPS coordinates extracted from digital photographs taken from an iPad mini3. This accounts for a 15 meter horizontal error. Elevations were extracted from Google Earth.

CHAPTER 5

SOIL DISTRIBUTION OF THE SITES

5.1. Introduction

All the soils are of binary origin (Van Rooyen, 1971). The parent materials are aeolian sand, blown out of the Vaal, Orange and Riet Rivers and their respective confluences on Karoo sedimentary rocks, as well as Kalahari sands (Van Rooyen, 1971). Modal profile descriptions, chemical properties and images are provided in Appendix B. Point observation distribution is given in Appendix D.

5.1.1. Soilscapes of Site 1 profiles – Land Type Ae276

Site 1 has dominant Kimberley (modal profile P1 and P3) and Hutton (modal profile P4) soils on undulating topography (Appendix A) (Figure 5.1). Addo soils (modal profile P2) form on slope around shallow topographic depressions or pans at the TMU4 $^{(4)}$ (Figure 5.1). Steep topographic depressions have Coega (modal profile P5) soils on TMU4 $^{(1)}$ and Fernwood soils overlying soft carbonate horizon on steep slopes (TMU4 $^{(3)}$) (Figure 5.1, Pan). The pan is of Katspruit soils with a fluctuating water table at about 300 to 500 mm depth. Underlying wavy broken Dwyka mudstone and tillite occur as saprolite. This indicates two types of hillslopes within the TMU4 of steep and shallow slope. Above the site the upper TMU4 continues, dominated by shallow (<500 mm) Coega soil.

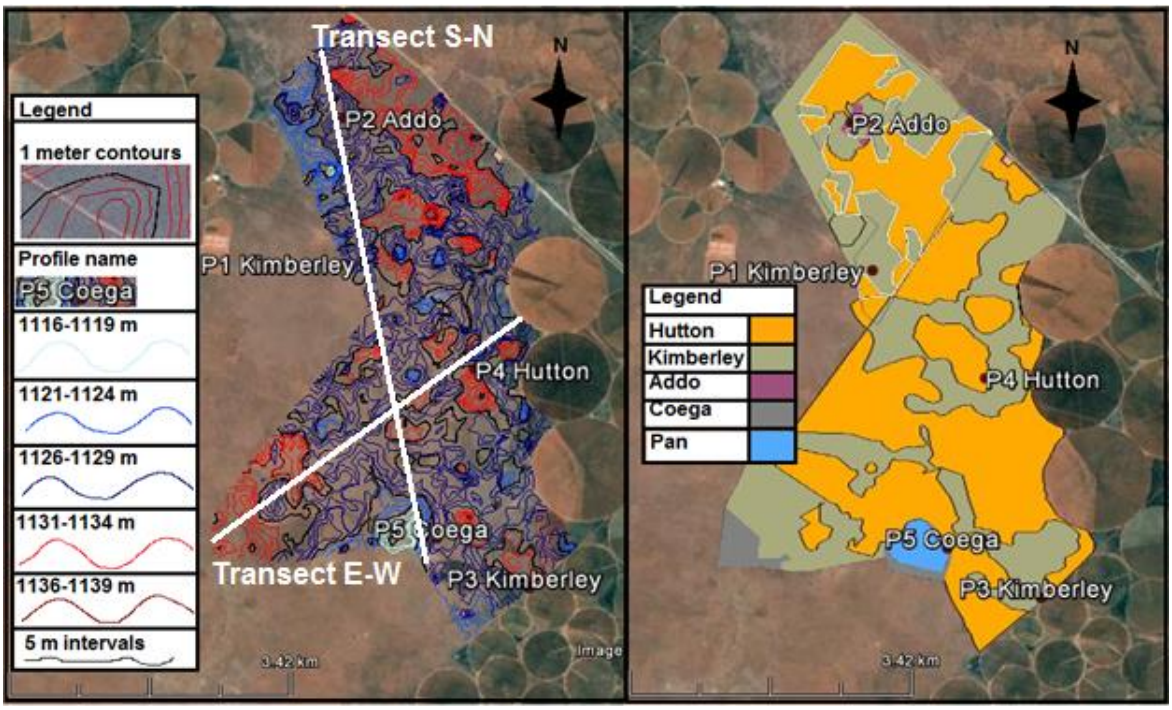

Figure 5. 1 One meter contours (left) and soil map (right) with modal profile distribution of Site 1.

5.1.1.1. East - west transect

The soil distribution (Figure 5.2), has a north-south aspect. The left of the figure represents east and the right of the figure west. The TMU is noted as midslope. Overall topography ranges from 1135 to 1126 m relative to MSL. The site is located in a dip, where the northern part continues to the Orange River, 1.2 km onwards. This topography

has a concave/straight landform. The southern side extends away from the river and towards elevated topography.

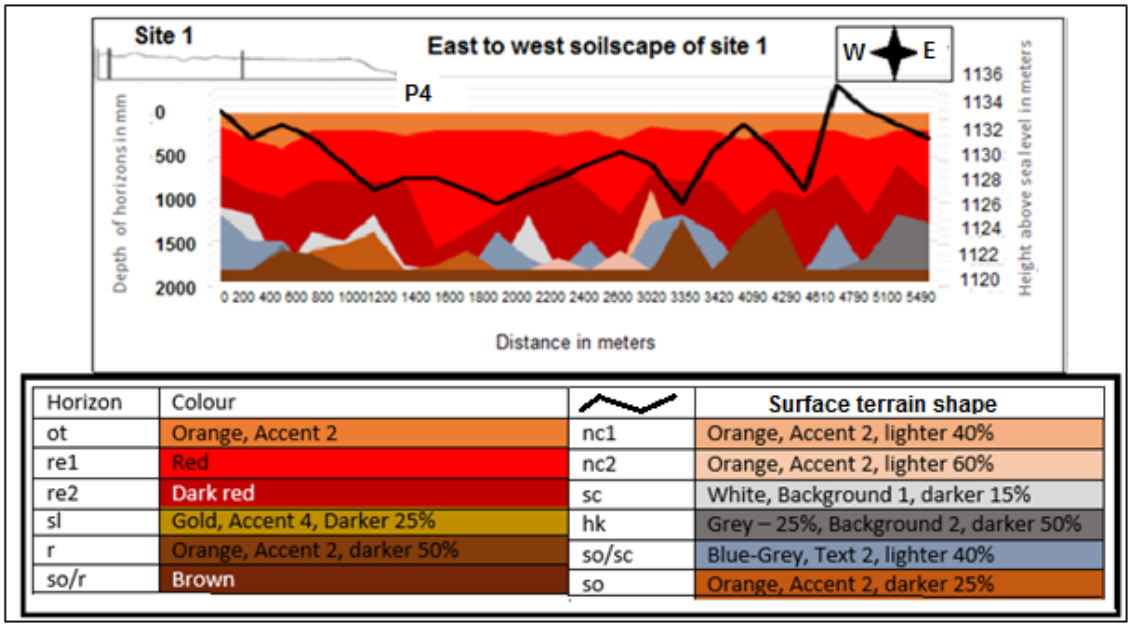

Horizon	Colour		Surface terrain shape
ot	Orange, Accent 2	nc1	Orange, Accent 2, lighter 40%
re1	Red	nc2	Orange, Accent 2, lighter 60%
re2	Dark red	sc	White, Background 1, darker 15%
sl	Gold, Accent 4, Darker 25%	hk	Grey – 25%, Background 2, darker 50%
r	Orange, Accent 2, darker 50%	so/sc	Blue-Grey, Text 2, lighter 40%
so/r	Brown	so	Orange, Accent 2, darker 25%

Figure 5. 2 East to west transect of site 1 soil distribution with horizonisation and modal profile location. The position in the hillslope is graphically presented in a line sketch in the top left corner.

Topsoil and subsoil thickness increase simultaneously where topography is steeper. Orthic A horizons average at 300 mm depth. Overall average soil depth for the site is about 1100 mm. B1 and B2 horizons are dominated by red apedal B horizons. Topographic depressions have accumulated carbonate precipitates sufficient for classification as soft carbonate horizon as third horizons. Soils in the higher topography have a hardpan carbonate horizon, as third horizon, at the eastern edge of the site. Saprolite forms at the most western and lowest point of the topography, grading into hard rock. A neocarbonate B3 horizon occurs at the bottom of a long slope within the centre of

the pan-like depression. Rock is observed to underlie all soil material and ranges in depth from 1.5 to 2.5 meters. Rock follows surface topographical trends.

5.1.1.2. South – north transect

This transect is on the midslope (Figure 5.3). The topography is flat with undulating polymorphological depressions and rises. The altitude ranges from 1129.5 to 1115.5 m relative to MSL The site has a deep depression on the eastern edge and crest-like peak following west with undulating surface. The western part slopes to the Orange River, 2.4 km onwards. Soil depth is influenced by underlying geological topography. Topsoil depth mimics topographical depressions. B horizons are dominated by red apedal B horizons. Saprolite grades to hard rock. Soft carbonate accumulation occurs in surface topographic depressions. Hardpan carbonate is found forming underlying transitional material on a TMU4 (1). Stone-lines are observed to underlie red apedal B2 horizons exclusively. A 8 meter deep depression with a diameter of 1505 meters on the eastern end exhibits E-horizons extending the entirety of both the east and west facing slopes, increasing in thickness towards the depression. They are underlain by soft carbonate horizons as third horizons. The depression floor is a Katspruit soil form. These soils had a water table of 300 mm below the soil surface during summer and 500 mm below the soil surface during winter months.

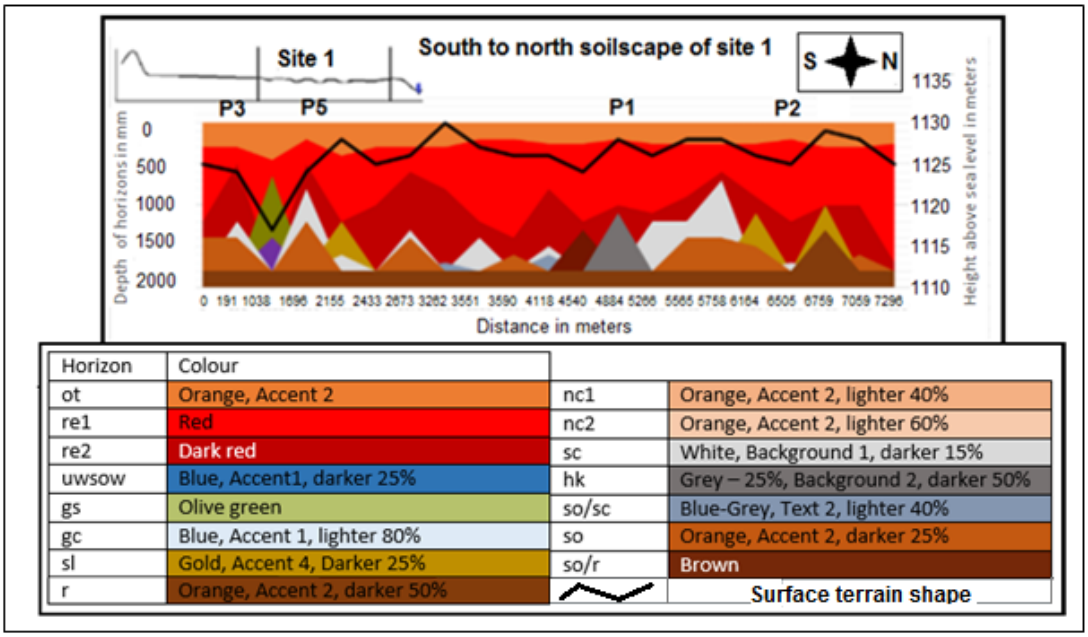

Figure 5. 3 North to south transect of site 1 soil distribution with horizonisation and modal profile location. The position in the hillslope is graphically presented in a line sketch in the top left corner.

5.1.2. Soilscapes of Site 2 - Land Type Ae15

Variation in soil form distribution (Figure 5.4 left) is observed to increase with a decrease in topography and slope (Figure 5.4 right). Altitude ranges from 1036 to 1021 m relative to MSL. The concave/straight curvature of the south-eastern edge to the north-western edge of the site, facilitates a surface topographical funnel for water into this from the higher lying topography. More carbonate precipitation is observed here.

Higher elevation and more shallow soils are observed in the south-eastern part of the site, as well as soils in the north eastern corner being even shallower. Carbonate precipitated in and on fractured and hard rock limit soil depth on these soils. With a decrease in topography, soil depth increases and carbonate precipitation changes in sequence from Coega, Augrabies, Addo to Augrabies and finally to Kimberley. Figure 5.4 (right) point ‘P6 Augrabies’ and elevation point ‘1085 m’ are the highest points in the topography with TMU5 [(3)] and TMU1, respectively.

Clovelly soils are found at the base of the TMU 3 to 4 transition. The yellow-brown colour closer to the river and Vaal-Riet confluence relates to the observations by Van Rooyen

(1971). Hutton soils of P10 are subject to colour influenced by the higher lying dolerite mesa south of its location and is redder (Van Rooyen, 1971) (Figure 5.4 left).

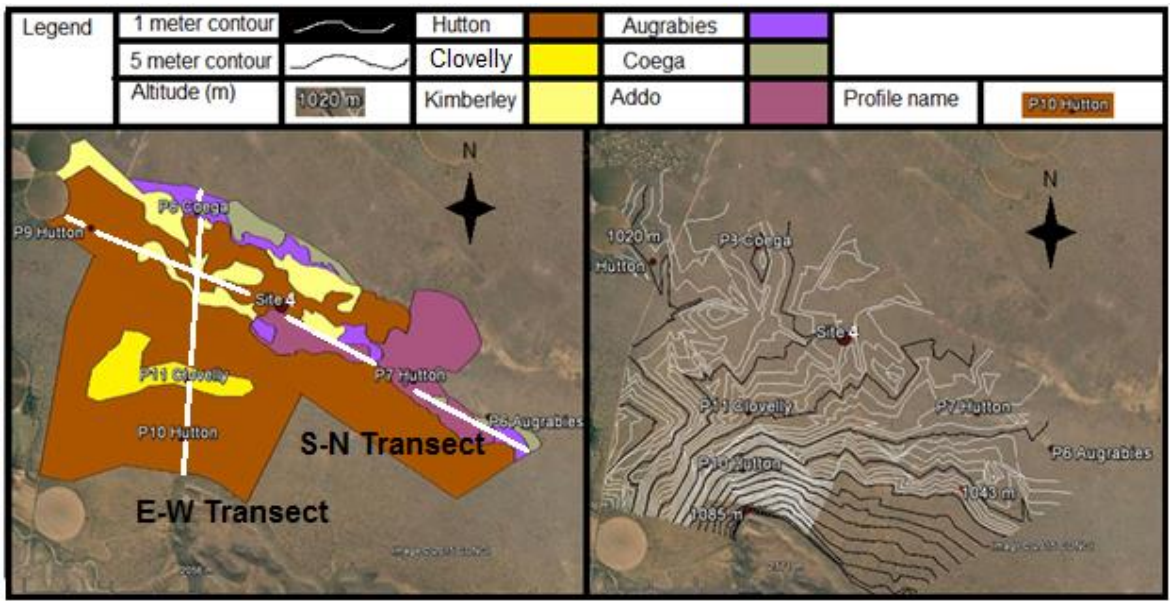

Figure 5. 4 Soil map (left) and 1 m contours (right) with master profile distribution of Site 2.

5.1.2.1. South - north transect

The soil distribution shown in Figure 5.5, has a north facing slope. The TMU is noted as midslope changing into footslope, with two backslopes forming the midslope / footslope transition. A depression is observed between these two backslopes. Overall topography ranges from 1136 to 1124 m relative to MSL. The site exhibits an average slope of 0.3%. The northern site border continues 2.4 km to the Vaal River. This is observed as a general concave profileform.

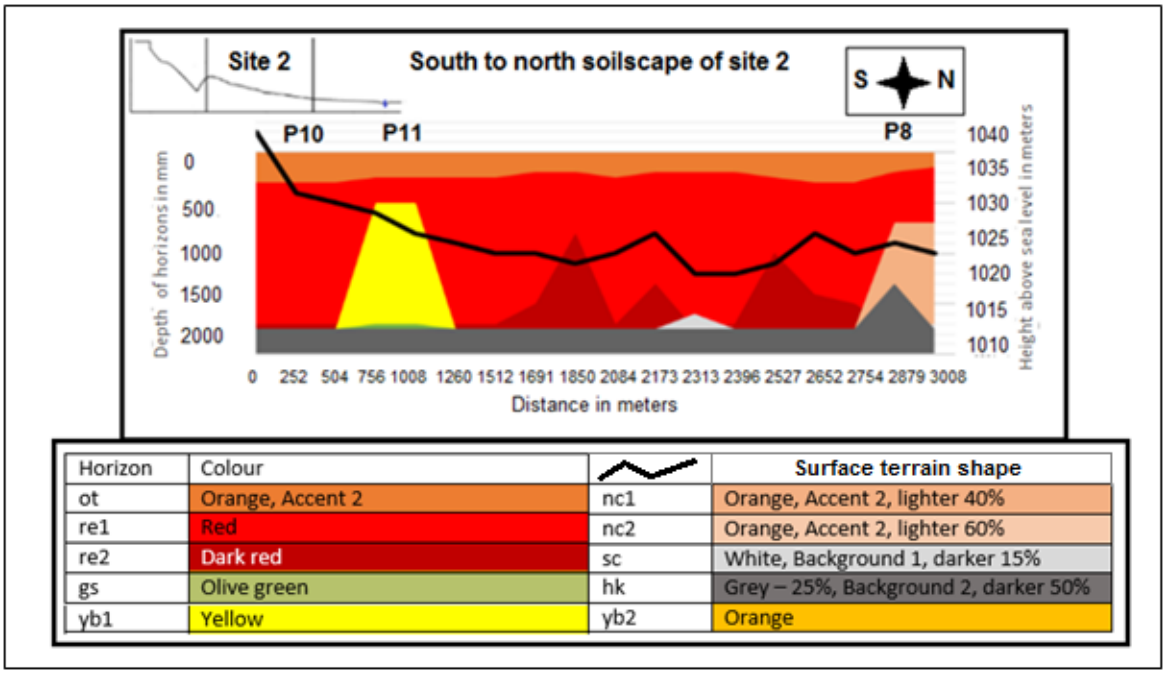

Horizon	Colour		Surface terrain shape
ot	Orange, Accent 2	nc1	Orange, Accent 2, lighter 40%
re1	Red	nc2	Orange, Accent 2, lighter 60%
re2	Dark red	sc	White, Background 1, darker 15%
gs	Olive green	hk	Grey – 25%, Background 2, darker 50%
yb1	Yellow	yb2	Orange

Figure 5. 5 South to north transect of site 2 soil distribution with horizonisation and modal profile location. The position in the hillslope is graphically presented in a line sketch in the top left corner.

Soil depth is influenced by slope %, decreasing with a reduction in slope. Topsoil depth mimics topography, with horizonisation increasing with a decrease in slope of north facing topography. Orthic A horizons average at 256 mm thickness. Red apedal B1 horizons are distributed throughout the site. At the TMU3/4 transition, yellow-brown apedal B1 horizons occur, exceeding 2000 mm in thickness. Yellow-brown apedal B2 horizon occurs as second B horizon underlying red apedal B1 horizons at 1750 mm. Neocarbonate B2 horizons are found below red apedal B1 horizons on the footslope, to depths of 2000 mm. Soft carbonate horizon is found on north facing slopes, peaking in depressions and on the footslope beneath neocarbonate B2 horizons. Hardpan carbonate horizons are found on footslope flat topography beneath neocarbonate B2 horizons.

5.1.2.2. West-east transect

The soil distribution shown in Figure 5.6, has a west facing slope. The TMU is noted as midslope changing into footslope, with slight terracing on the midslope. A depression is

observed on the flat midslope. Overall topography ranges from 1136 to 1121 m relative to MSL. The site exhibits an average slope of 3.6%. The northern part continues to the Vaal River 2.4 km. Orthic A horizon thickness decreases down slope, with an increase in depth and increase in slope. The soilscape is dominated by carbonate precipitates in the subsoil decreasing in hardness with a decrease in slope Hardpan carbonate is observed to dominate the transition to hard rock.

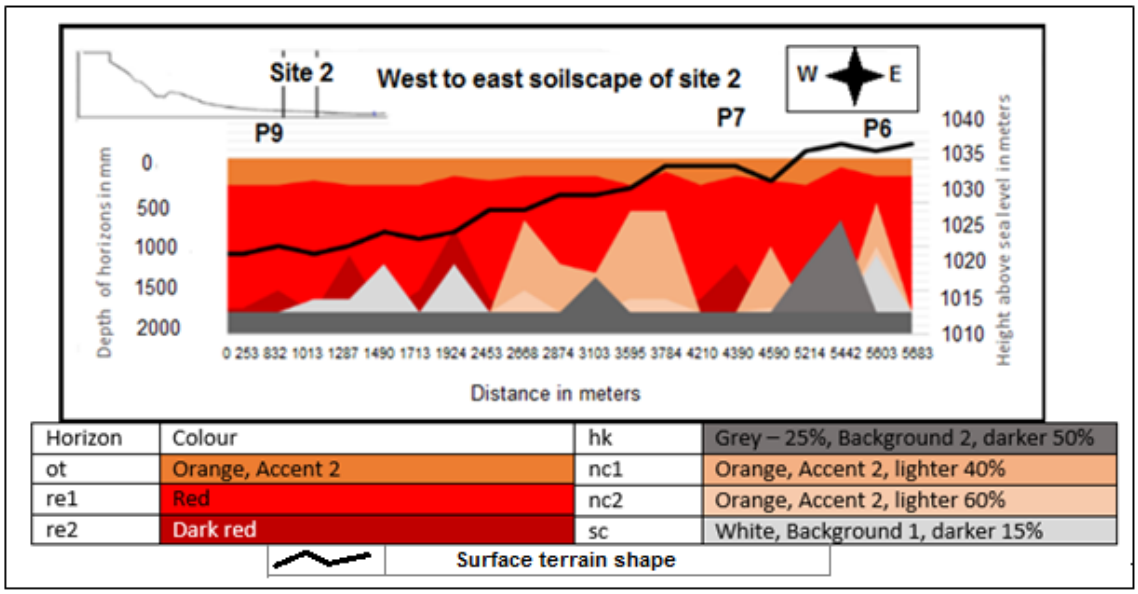

Figure 5. 6 East to west transect of site 2 soil distribution with horizonisation and modal profile location. The position in the hillslope is graphically presented in a line sketch in the top left corner.

5.1.3. Soilscapes of Site 3 - Land Type Ae266

The site consists of TMU's 3 and 4. Soil distribution patterns grade from freely-drained deep Hutton (similar to modal profile P10), Clovelly (similar to modal profile P11) and Namib (modal profile P12) soils on TMU 3 into carbonate containing shallow Namib (similar to modal profile P12), Askham (orthic A / yellow-brown apedal B / hardpan

carbonate horizons), Addo (similar to modal profile P2) and Plooysburg (orthic A / red apedal B / hard pan carbonate horizons) soil forms on TMU 4 (Figure 5.7 (left)).

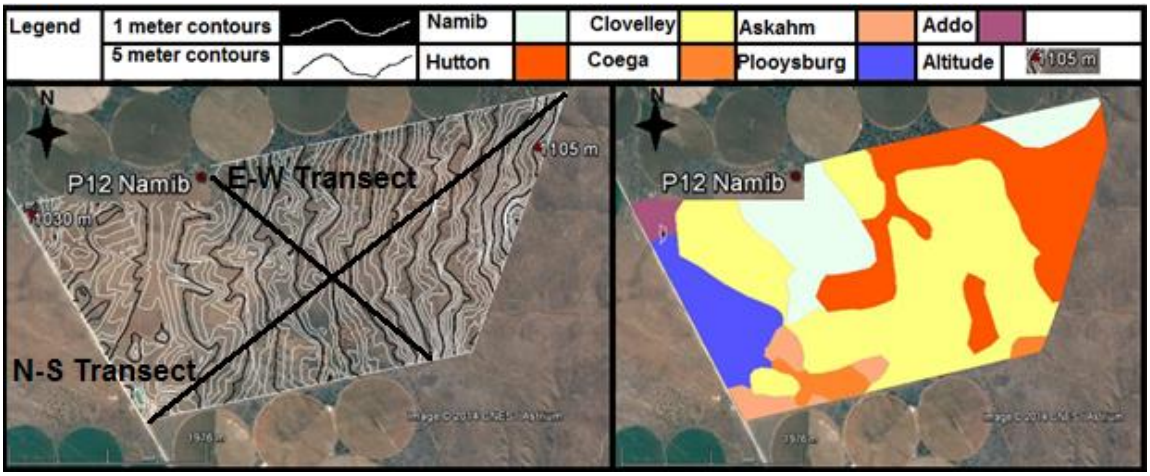

Figure 5. 7 One meter contours (left) and soil map (right) with master profile distribution of Site 3.

TMU4 is underlain by dolerite boulders on Dwyka mudstone and tillite. An increase in carbonate precipitation is observed higher up in the profiles' orthic A horizons with an levelling out of the topography. Underlying wavy broken Dwyka mudstone and tillite occur as saprolite as saprolite.

5.1.3.1. North – south and east – west transects

The soil distribution shown in Figures 5.8 and 5.9, have a south-west-facing slope. The left of Figure 5.8 represents north and the right south.

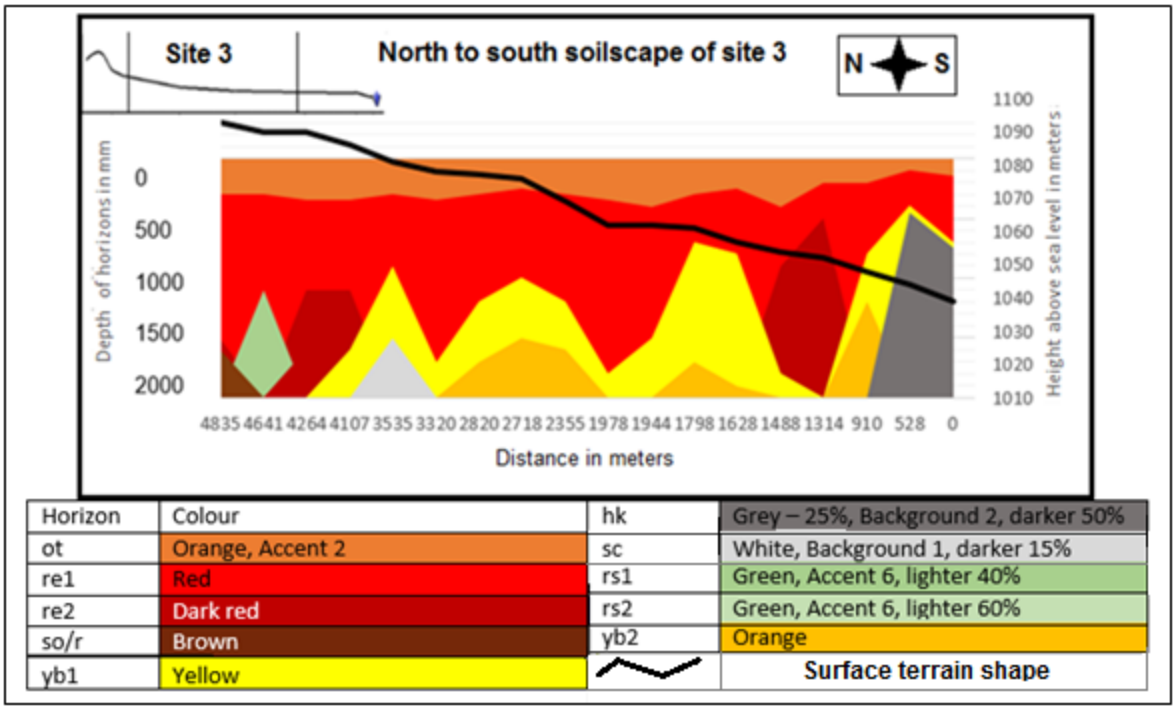

Figure 5. 8 North to south transect of site 3 soil distribution with horizonisation. The position in the hillslope is graphically presented in a line sketch in the top left corner.

The left of Figure 5.9 represents West and the right East.

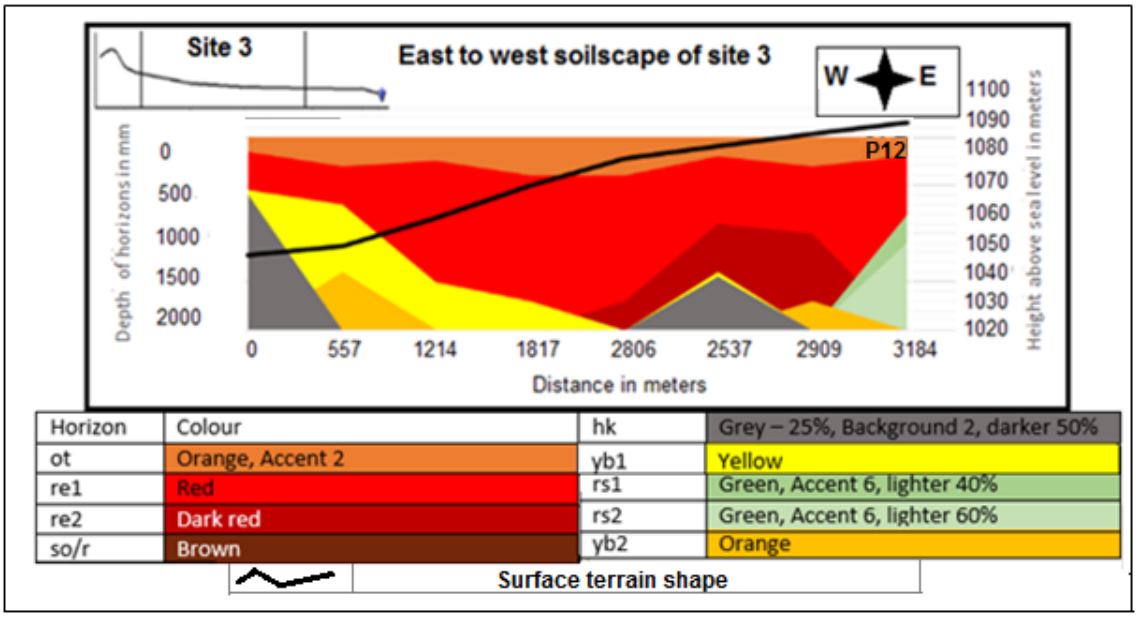

Figure 5. 9 East to west transect of site 3 soil distribution with horizonisation and modal profile location. The position in the hillslope is graphically presented in a line sketch in the top left corner

The TMU4 profile-curvature is noted as a convex and TMU3 as concave. Overall topography ranges from 1189 to 1145 MSL. The site has an average slope of 1.41%. The eastern part continues to the Orange River 2.4 km away. This is observed as a general convex planform curvature.

Soil depth is influenced by slope %, with shallow soils on flatter topography. Three segments are observed in the terrain with footslope, lower- and upper-midslope. Upper midslope has a 1% slope, lower midslope 1.7% and footslope 0.7% slope. Change in slope is from convex to concave.

Average orthic A horizon depth is 275 mm. Regic sand horizons are found on the midslope transition to footslope. Midslope is dominated by red apedal B horizons and a decrease in slope by yellow-brown apedal B horizons. The lowest point in the topography sees hard pan carbonate precipitating. Effective soil depth is reduced with a decrease in slope.

5.1.4. Soilscapes of Site 4 - Land Type Ia4

Soil distribution of site 4 indicates a change from apedal material on midslope and lower footslope underlain with saprolite of shale, Dwyka mudstone and tillite, as well as soft and hard pan carbonate forming primarily within this saprolite. The Riverside site has a footslope to toeslope transition, whereas the Aucampshope site has a footslope / floodplain transition. Soil form distribution (Riverside) is from footslope Hutton soils (orthic A / red apedal B / unspecified (saprolite) horizons) to Kimberley (orthic A / red apedal B / soft carbonate) to Coega soils (bleached orthic A horizon / hardpan carbonate) on toeslope. Toeslope to floodplain has a transitional Addo soil (bleached orthic A / neocarbonate B1 / soft carbonate horizons) grading into a Klapmuts (orthic A / E horizon / pedocutanic B horizons) on a slope of 3%. This then grades into an orthic A on pedocutanic B with gypsum once slope has changed to 0% (Figure 5.10).

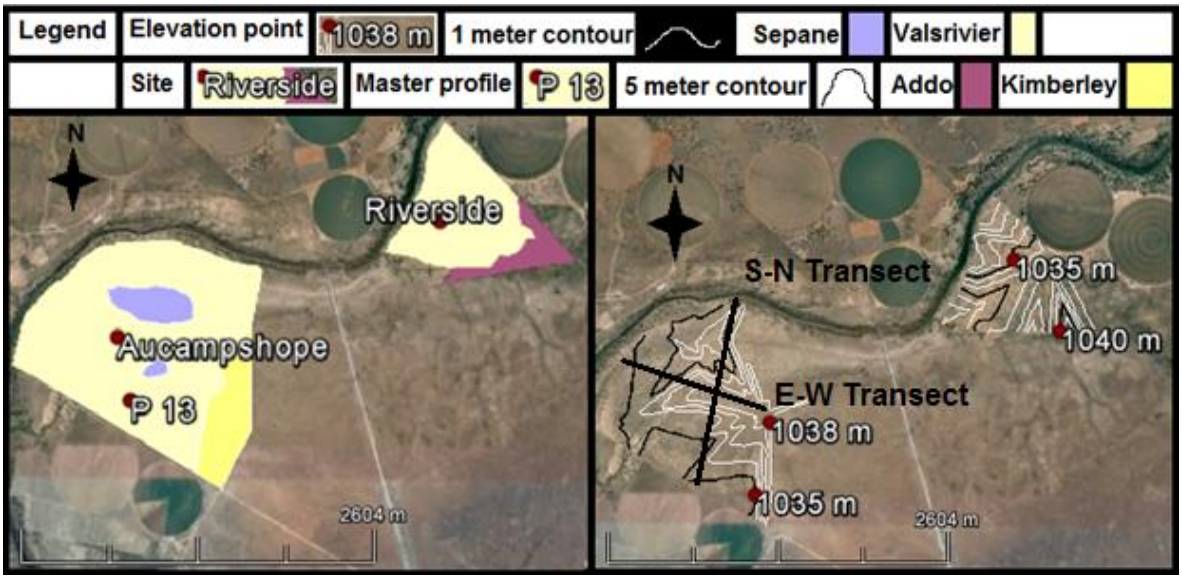

Figure 5. 10 One meter contours (right) and soil map (left) with master profile distribution of Site 4.

Footslope to floodplain transition (Aucampshope) is from orthic A to red apedal B to soft carbonate on the sloping (2% slope) transition, to orthic A underlain by pedocutanic B with gypsum. Sepane soil form occurs in convex profile and convex planform curvature positions. These depressions are not more than 1 meter in depth and from along surface drainage lines. Colluvial banks occur along the Riet River bank.

5.1.4.1. South – north transect

The soil distribution shown in Figure 5.11, have a north facing slope. The left of the figure represents south and the right of figure north.

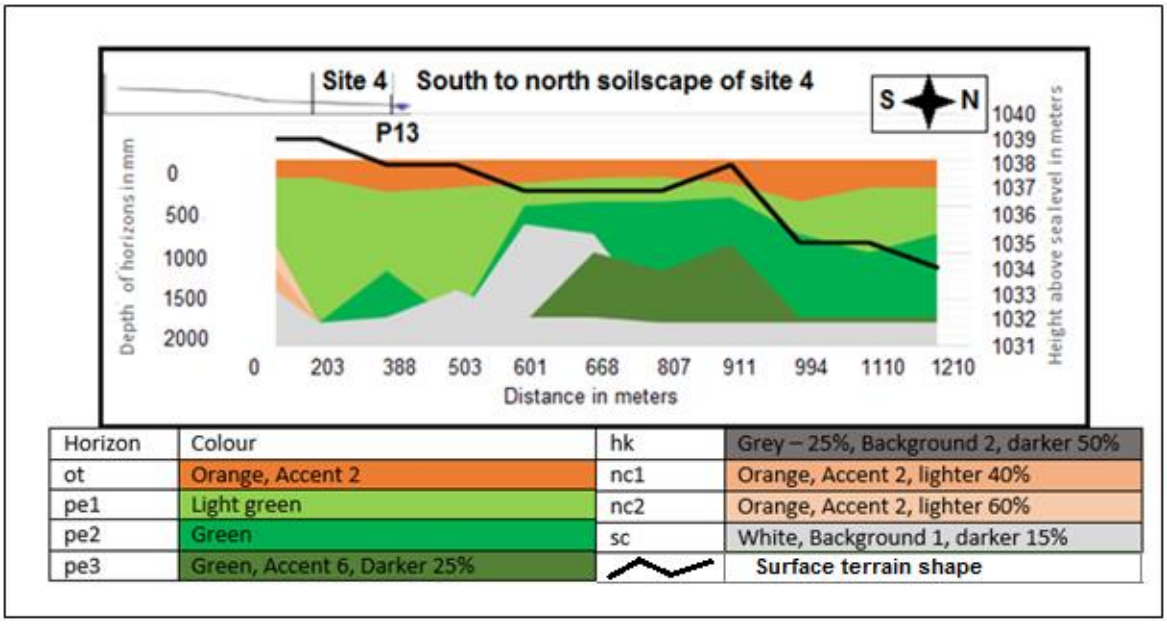

Horizon	Colour	hk	Grey – 25%, Background 2, darker 50%
ot	Orange, Accent 2	nc1	Orange, Accent 2, lighter 40%
pe1	Light green	nc2	Orange, Accent 2, lighter 60%
pe2	Green	sc	White, Background 1, darker 15%
pe3	Green, Accent 6, Darker 25%		Surface terrain shape

Figure 5. 11 South to north transect of site 4 soil distribution with horizonisation and modal profile location. The position in the hillslope is graphically presented in a line sketch in the top left corner.

The TMU is noted as transition from midslope into footslope, changing into toeslope / floodplain with slight terracing. A depression is observed on the flat midslope. The toeslope and footslope are known to flood every 20 or so years. A general concave / concave curvature is observed. Overall topography ranges from 1038.5 to 1033.5 MSL. The site exhibits an average slope of 0.4%. The northern part continues to merge into the Riet River. A depression on the lower footslope increases horizonisation. Soft carbonate and neocarbonate horizons are observed to form at the transition from higher topography. Pedocutanic B horizons are the dominant B horizons. Underlying material is soft carbonate horizon precipitated in shallow saprolitic shale and Dwyka mudstone and tillite. Average soil depth is at 1500 to 2000 mm depth.

5.1.4.2. East – west transect

The soil distribution shown in Figure 5.12, have a west facing slope. The left of the figure represents east and the right of figure west. The TMU is noted as transition from footslope to toeslope. The toeslope merges into the Riet River. Overall topography ranges from 1039.8 to 1032.8 MSL. Orthic A horizons depth varies with surface topography. A topographical depression increase horizonisation. A decrease in slope reduces horizonisation. Average soil depth is at 1500 to 200 mm.

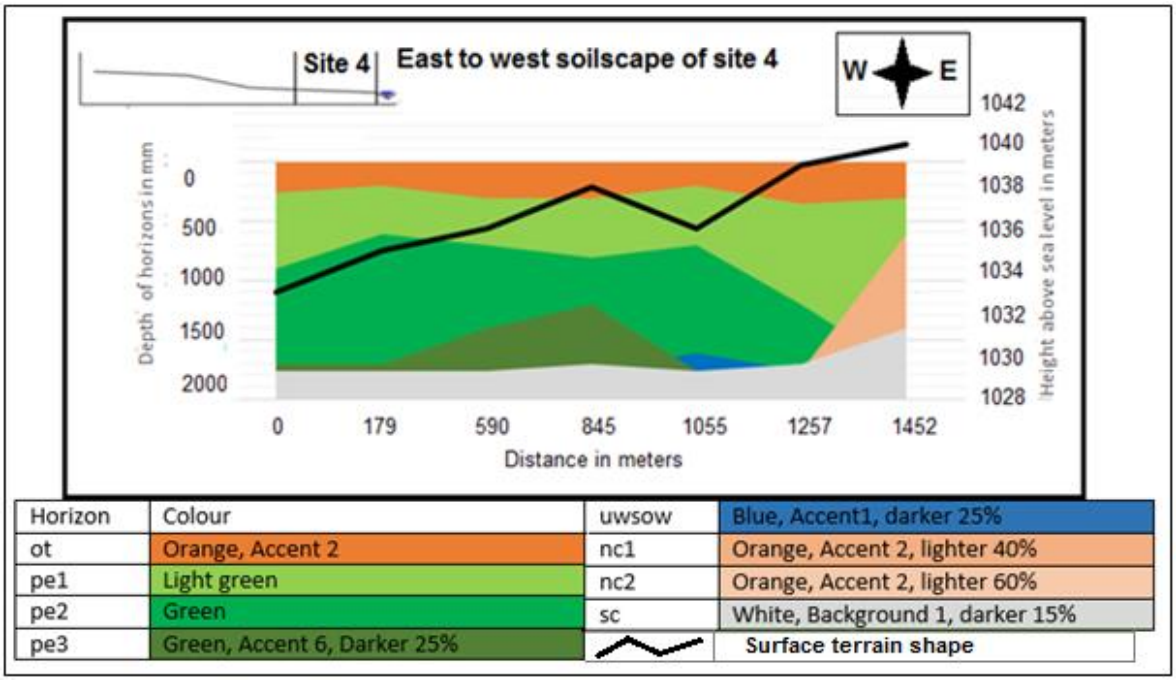

Figure 5. 12 East to west transect of site 4 soil distribution with horizonisation. The position in the hillslope is graphically presented in a line sketch in the top left corner.

5.2. Conclusion

Dominant soil horizons are orthic A horizons, red apedal B1 and B2 horizons, soft and hardpan carbonate horizons, yellow-brown apedal B horizons, neocarbonate B horizons for sites 1, 2 and 3. They are found on TMU's 3 and 4. Soil distribution analysis, shows a low variation in horizonisation for site 1 TMU4. Variation is observed to increase where slope increases and merges into pans. Shallow rock and saprolite is often found in conjunction with soft carbonate and/or hardpan carbonate horizons. Levelling out of topography on TMU 4's of sites 2 and 3 show an increase in carbonate horizons and decrease in soil depth. Site 3 TMU 3 (Figures 5.8 and 5.9) and site 2 TMU south to north transect (Figure 5.5) show yellow-brown apedal B horizons.

Dominant soil horizons on TMU5 are orthic A, pedocutanic B1, 2 and 3 and soft carbonate horizons. Heavy clay soils (Figure 5.11 and 5.12) show an increase in horizonisation with change in surface topography.

CHAPETR 6

CONCEPTUAL HYDROLOGICAL RESPONSE MODELS OF ARID SOILSCAPES

6.1. Introduction

Morphology as indicator of conceptual hydrological response in soils has been researched within South Africa (Le Roux *et al*., 2015). The soil classification system of South Africa (SCWG, 1991) incorporates flowpaths and storage mechanisms in the definition of horizons as indicators of pedogenesis using morphology. The conceptual hydrological response of soils is inferred on horizon level and combined in profile response (Le Roux *et al*., 2011; Van Tol *et al*., 2010 b; Kuenene, 2013; Bouwer, 2015). Topographical position of soils, local climate and land use are considered as integral parts of establishing a pedon conceptual hydrological response (Van Tol *et al*., 2010 b). Landscape attributes such as concavity and convexity, slope length and slope angle and underlying geological attributes relevant to above lying soils' hydrological response, are applied when connecting point pedon observations to a soilscape (Le Roux *et al*., 2011). Conspicuous morphological properties, such as colour (Van Huyssteen; 1997) and structure, are used as indicator of horizon and pedon conceptual hydrology (Van Huyssteen *et al*., 2005). Chemical indicators of pH and basic cations are good indicators of hydrological response within soils (Van Huyssteen *et al*., 2005; Bouwer *et al*., 2015.

6.2. Method and Materials

See section 4.4..

6.3. Results and Discussion

6.3.1. Site 1

The site slope in a westerly direction and is located on the TMU 4. The micro topography of the TMU has polymorphological hillock shaped terrain units with TMU's $4^{(1)}$, TMU's $4^{(3)}$, TMU's $4^{(4)}$ and TMU's $4^{(5)}$. They surround a pan wetland (a) (Figure 6.1) and grade into a pan wetland (b) located outside the site.

Kimberley, Hutton, Coega, Fernwood, Katspruit, Addo and Augrabies soil forms occur on site 1 (Figure 6.1). Soils dominating the hillocks are Hutton (P4) and Kimberley soil forms (P2 and P3). Hutton and Kimberley soil forms occur on fractured rock- Kimberley soil forms are shallower. Coega soil forms dominate the upslope area above the site. Soils of the Addo soil form (P2) occur on gentle slopes, grading into pan wetland (b) (Figure 6.1). The hillslope of the depression (a) has shallow Coega soil forms (P5) occupying the crest. Fernwood soil forms overlying a soft carbonate horizon, occur on a steep midslope, grading into a Katspruit soil form with a carbonate-rich G horizon in the valley bottom position.

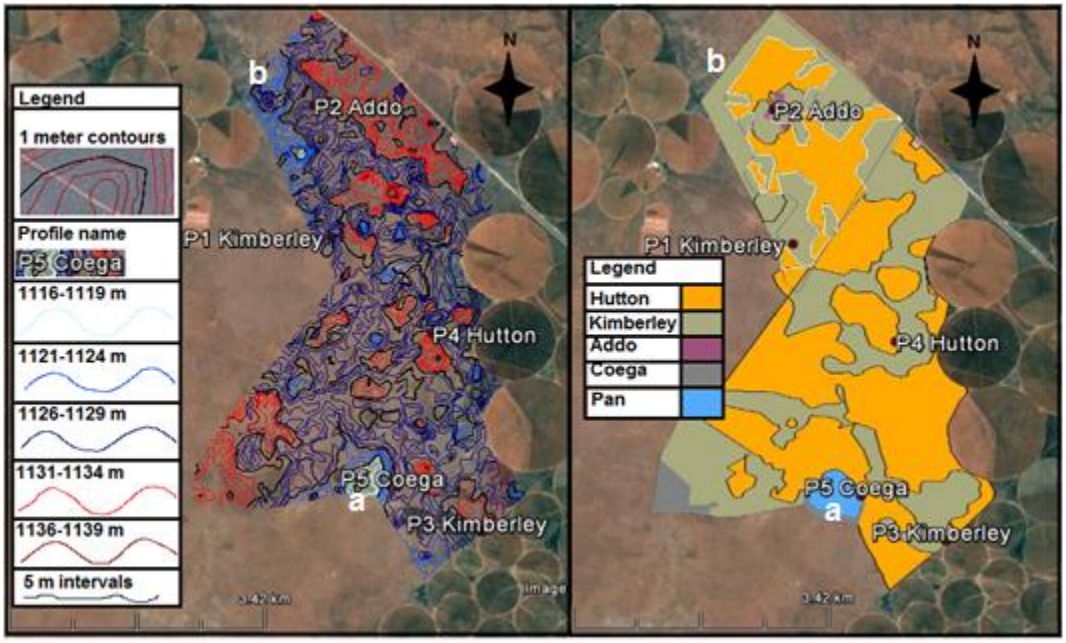

Figure 6. 1 Topography (left) and soil form distribution (right) of site 1.

6.3.1.1. Hydrological response of the soil types of site 1

6.3.1.1.1. Kimberley soils pedon hydrology – P1 and P3

The Kimberley soils lie in a convex/convex curvature position (Figure 6.1) indicating a recharge function. The orthic A and red apedal B horizons, including the stone line, morphologically indicate vertical downward flow (Figure 6.2). The saprolitic soft carbonate horizon grades into calcareous fractured rock. This morphology indicates that the carbonate precipitate originates from the fractured rock stored water. The soft carbonate

horizon is thicker in profile P3. The dolerite is a probable source of calcium. Precipitation of carbonates leaching from the orthic A and red apedal B horizons are unlikely as these horizons often occur without any carbonate precipitate in the deep subsoil. In these soft and hard carbonate horizons the carbonate precipitation is well defined and carbonate precipitation is limited to these horizons

Vertical downward flow in the red apedal B horizon probably aid to the distribution or redistribution of carbonates in these soils. The clear transition from the red apedal B horizon to the soft carbonate horizon, and an increase in hardening and layering of the soft carbonate horizon downwards indicates a contribution by vertical flow from the overlying red apedal B horizon. Munsell colour also changes downwards from orthic A horizon and orthic A horizon/red apedal B horizon transition of brown / yellowish brown (dry / wet), to brown / reddish brown in the red apedal B horizon, to strong brown / brown in bottom of the red apedal B horizon with the stone line and white/ pale yellow in the soft carbonate horizon (Table 6.1). This indicates that the carbonate horizon is a product of subdominant vertical flow through the soil and a dominant return flow from the fractured rock. Increase in carbonate precipitation as a result of return-flow from fractured rock and soil/rock interface vertical flow is expected to escalate down slope.

Table 6. 1 Morphological, topographical and chemical information of modal profiles P1 to P5

Profile	TMU	Curvature	Diagnostic horizon	Depth (mm)	Munsell colour (wet)	Sodium	Calcium	$CaCO_3$ content (% by weight)	pH (water)	Particle size distribution (%)		
						$cmol_c\ kg^{-1}$ soil				Sand	Silt	Clay
P1	4	Vv	ot	200	5YR5/6	0.002	1.69	0	6.65	88.4	5.1	4.3
			ot/re	200	5YR5/6	0.004	5.08	3.61	7.23	85.1	5.8	6.8
			re	800	5YR5/3	0.003	5.92	0	6.88	90.9	3.7	4.4
			sl	900	7.5YR4/4	0.003	3.41	0	7.71	85.3	5.6	6.7
			sc	1300	5Y7/3	0.41	20.98	9.84	8.16	92.8	4.9	2.3
P2	4	Cc	ot	250	7.5YR5/3	0.002	3.57	0	7.46	87.4	7.6	3.8
			nc1	600	7.5YR5/4	0.003	3.92	0	7.75	86	8.6	4.1
			nc2	1300	7.5YR3/4	0.002	24.06	1.15	8.25	79.8	6.8	7.9
			sl	1400	7.5YR5/2	0.002	18.34	0.87	8.3	78.1	10.9	8.8
			sc	1500	5YR6/1	0.004	18.89	0.33	8.29	75.2	13.7	8.7
P3	4	Vv	ot	175	2.5YR3/4	0.002	5.02	0	8.25	89.6	1.8	4.3
			re	550	2.5YR3/4	0.002	5.08	0.78	8.27	87.7	2.6	5.2
			sc	1600	2.5YR4/4	0.003	15.7	3.54	8.16	84.6	8.6	6.5
			on	1700	7.5YR4/6	0.003	0.81	1.26	8.51	86.2	7.3	5.2
P4	4	Sc	ot	200	7.5YR5/4	0.05	2.85	0	6.89	86	2	12
			re1	600	7.5YR5/4	0.06	4.43	0	6.53	84	4	12
			re2	1200	5YR5/4	0.07	8.53	0	7.87	59	14	27
P5	1	Vv	ot	100	10YR5/6	0.04	2.06	0.15	6.15	91.9	2.7	5.4
			ot/hk	-	-	-	-	86	8.84	-	-	-

The increase in pH_{water} and exchangeable calcium from the orthic A horizon to red apedal B horizon indicates a leaching vertical flow. The increase to the soft carbonate indicates a contribution from another source.

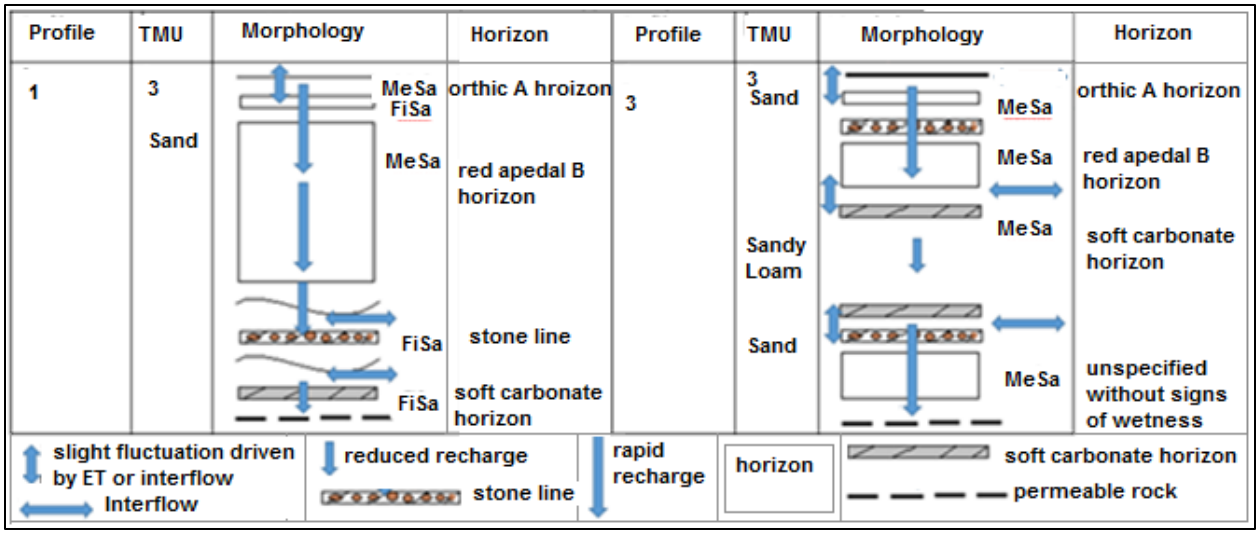

Figure 6. 2 Kimberly soil form pedon conceptual hydrology.

6.3.1.1.2. Addo soil form pedon hydrology – P2

The Addo profile P2 lies in a concave/concave curvature position (P2 in Figure 6.1). The neocarbonate horizon, soft carbonate horizon and stone line is apedal and sandy indicating a vertical flow as response to rain events (Figure 6.3). The carbonate precipitate in the soft carbonate horizon is an indication of a capillary rise of water from a very slow flow of a dominant return flowpath from fractured rock. The terrain curvature is another indicator of a flowpath as it supports the presence of a dominant interflow associated with a rock structure; for example a bedding plane, in the sedimentary rocks. This curvature is associated with a decrease in slope. Return flow is expected to be slower and can be responsible for the capillary flow redistributing carbonates from the fractured rock upwards to the saprolite, to the neocarbonate B horizon. The soil has a thin, hard surface crust, promoting surface runoff. Clay content are constant down the profile at the neocarbonate B1 horizon (3.8 and 4.1%) and increases slightly to the soft carbonate horizon (7.9 to 8.7%), suggest that vertical downward flow was active in the development, supporting an illuvial process (Table 6.1).

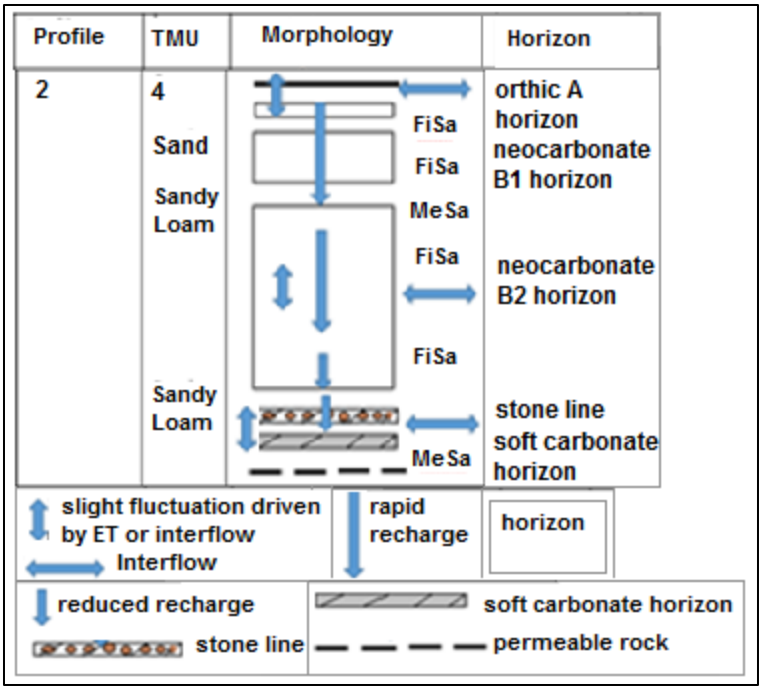

Figure 6. 3 Conceptual hydrological response based on morphology of Addo soils.

6.3.1.1.3. Hutton soil form pedon hydrology – P4

The Hutton soil form is situated in a polymorphological topographic depression at the undulating footslope/toeslope transition (Figure 6.1). The absence of carbonates in this profile (Table 6.1), indicates that interflow is in the fractured rock not affecting soil properties of these soils (Figure 6.4). Chemical indicators of exchangeable sodium, calcium and increase with depth indicates the profile horizons to recharge to the fractured rock (Table 6.1). Morphology indicates that the apedal orthic A horizon and red apedal B1 horizon drains freely to recharge the saprolite that recharges fractured rock.

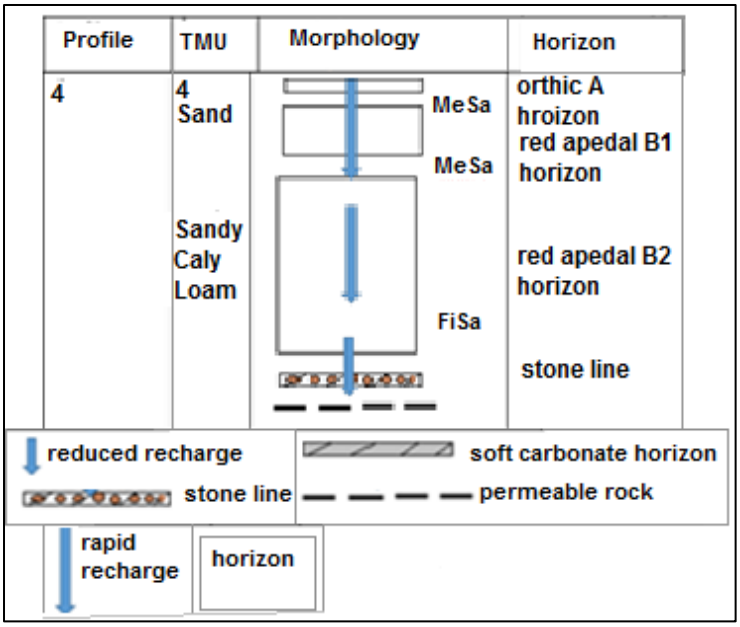

Figure 6. 4 Conceptual hydrological response based on morphology of Hutton soils.

6.3.1.1.4. Coega soil form pedon hydrology – P5

The Coega soil form is located on a ploymorphological terrain unit 1 position, descending to a pan (Figure 6.1). The abrupt transition to hardpan carbonate may be an indication that the vertical flowpath is dissolving the carbonates and redistributing it (Figure 6.5). The comparatively low pH of the orthic A horizon indicates free drainage to the hardpan carbonate horizon (Table 6.1). The hardpan carbonate horizon serve as an aquiclude creating a shallow responsive condition.

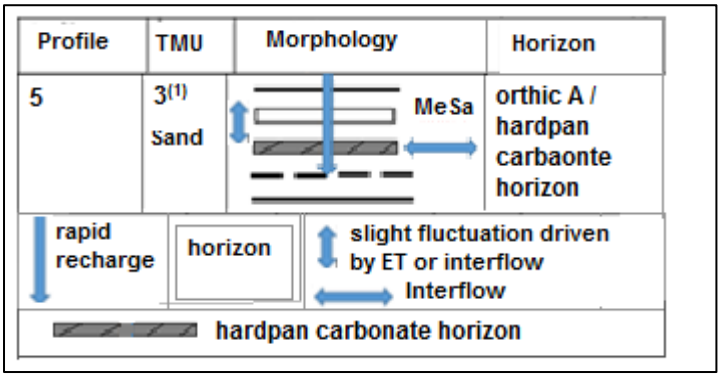

Figure 6. 5 Conceptual hydrological response based on morphology of Coega soils.

6.3.1.2. Site 1 hydrological response

Interflow in the fractured rock controls the morphology of the hillslope (Figure 6.6). The Hutton soils recharges the fractured rock during high rainfall and interflow takes it down slope to increasingly return to the deep subsoil. In the soil the evapotranspitation is higher and the carbonate in precipitated form is observed. Vertical downward action redistribute the carbonates to form hardpan carbonate horizons serving as shallow responsive soils.

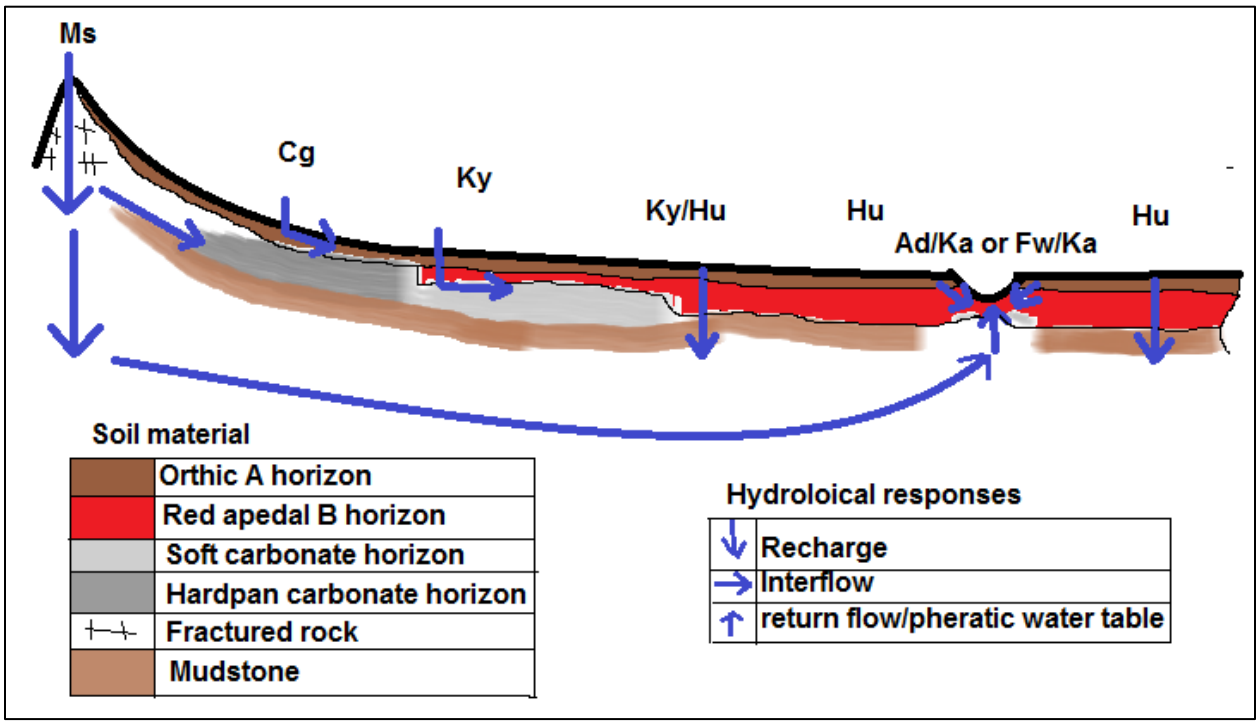

Figure 6. 6 CHRM of site 1.

6.3.2. Site 2

The site represents the south western half of a catchment, with P6 (Figure 6.7) located near the southern watershed. The line formed by observations P6, P7, Site 3 and P9 on Figure 6.7 (left), shows the TMU 5 position, decreasing towards the Vaal River. The Vaal River is located about 2 km east of the observation P9. The other half of the catchment is located to the north and east of this TMU 5 line. It has a long TMU 4 with flat topography, followed by similar TMU 3, 2 and 1 topographical and soil distributions. Terracing occurs on TMU 3.

Hutton, Kimberley, Augrabies, Addo, Coega and Clovelly soil forms dominate on site 2 (Figure 6.7). TMUs include 3, 4 and 5. Higher in the landscape, south of site 2 (Figure 6.7), a dolerite mesa includes TMUs 1, 2 and 3 of Mispah soils 100 mm thick, on dolerite. The TMU 1 position is covered by aeolian sands.

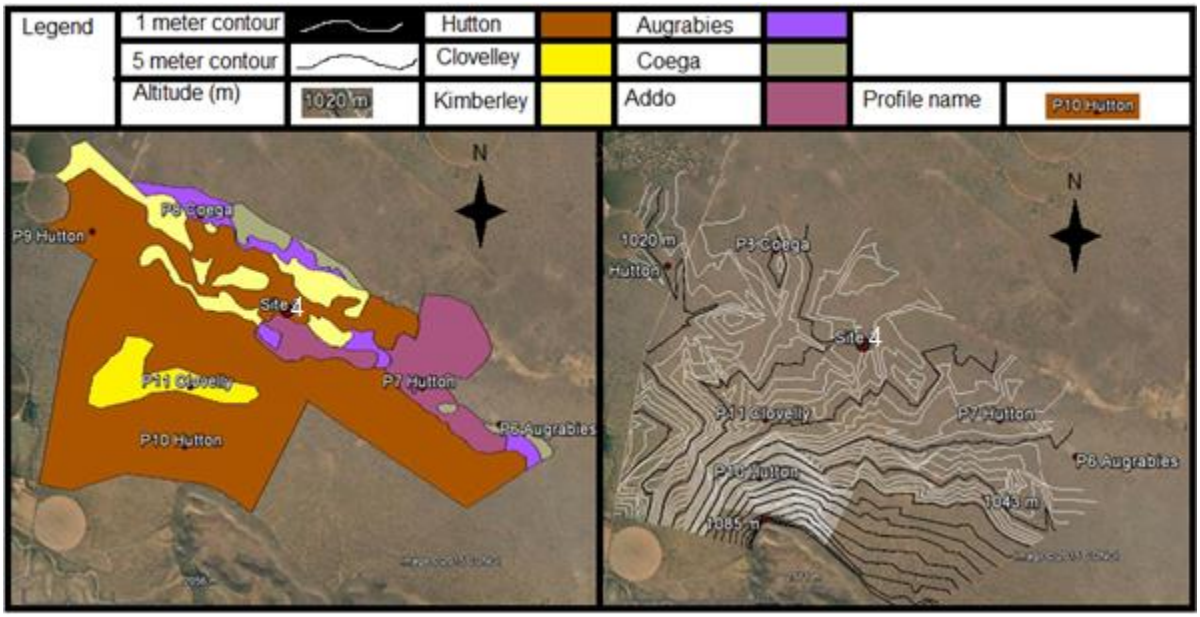

Figure 6. 7 Soil map (left) and 1 m contours (right) with master profile distribution of Site 2.

6.3.2.1. Hydrological response of the soil types of site 2

6.3.2.1.1. Addo soil form pedon hydrology – P6

This soil hydrological response is similar to P2 (Figure 6.8). It is located lower down the hillslope below a steeper slope (Figure 6.7). Dolerite rock on the crest may explain the thicker carbonate precipitation. An increase in exchangeable calcium, calcium carbonate content and clay content indicates an accumulative zone of a hillslope lateral flowpath (Table 6.2).

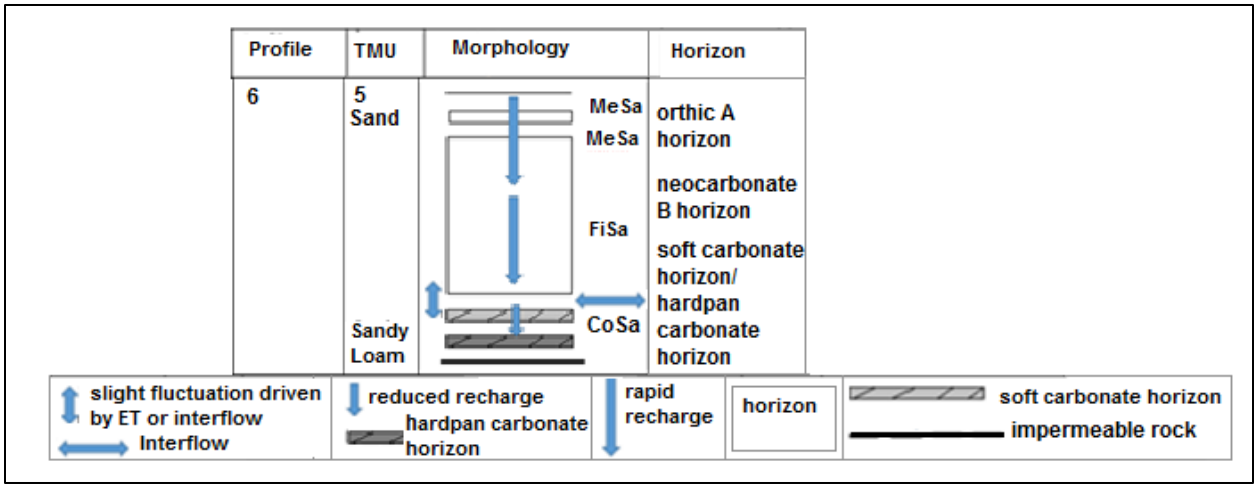

Figure 6. 8 Conceptual hydrological response based on morphology of Coega soils.

Table 6. 2 Morphological, topographical and chemical information of modal profiles P6 to P11

Profile	TMU	Curvature	Diagnostic horizon	Depth (mm)	Munsell colour (wet)	Sodium	Calcium	$CaCO_3$ content (%)	Ph (H_2O)	Particle size distribution (%)		
						$cmol_c\ kg^{-1}$ soil				Sand	Silt	Clay
P6	5	Cc	ot	300	2.5YR3/4	0.002	0.07	0	7.29	92.7	2.2	4.5
			nc1	600	2.5YR3/4	0.002	2.3	0	6.58	88.7	2.4	6.7
			sc	900	5YR4/4	0.003	1.98	5.2	8.13	77.3	6.1	15.9
P7	4	Sv	ot	300	7.5YR3/4	0.002	1.10	0	8.04	92	2.0	4.1
			re1	1400	7.5YR4/3	0.003	1.80	0.03	8.96	94.4	0.8	3.9
			re2	2000	7.5YR5/3	0.002	1.05	0.1	8.19	82.3	6.8	9.8
			so	2100	7.5YR4/6	0.003	1.5	0.19	8.89	93.1	1.6	4.4
P8	5	Ss	ot	150	5YR3/4	0.004	1.68	0	8.44	86.7	6.8	4.6
			hk	300	7.5YR3/3	0.005	1.78	3.05	8.49	87.9	7.2	4.4
			hk2	750	7.5YR5/4	-	18.69	1.06	-	-	-	-
P9	4	Cc	ot	200	5YR3/4	0.004	2.11	0	6.59	90.9	4.2	4.9
			re	1380	2.5YR3/4	0.004	2.47	0	6.92	92.8	1.2	5.9
			nc	2000	5YR4/4	0.003	15.47	0.66	6.7	89.9	2.3	6.4
P10	3	Vv	ot	300	5YR3/4	0.002	1.05	0	6.06	94.5	1.8	2.8
			re1	600	5YR4/4	0.003	0.99	0	7.04	90.5	2.7	5.5
			re2	1000	2.5YR3/6	0.003	1.67	0	8.34	91.6	1.7	6.0
			yb	2000	2.5YR4/4	0.004	0.47	0	7.62	92.8	2.7	2.4
P11	4	Sc	ot	300	5YR3/4	0.003	1.27	0	7.3	96	0.9	2.3
			yb1	850	7.5YR4/4	0.003	1.74	0	7.5	94	1.1	4.1
			yb2	2000	7.5YR4/6	0.003	1.67	0	8.01	93	1.1	5.8

6.3.2.1.2. Hutton soil form pedon hydrology – P7, P9 and P10

Similar profile hydrological response to the Hutton soil form P4, is expected from these Hutton soils namely rapid vertical recharge of the profile and underlying fractured rock (Figure 6.9). Yellowing of P10 at 2000 mm, the transition to hard rock, located on TMU3 with slope indicates short periods of saturation and returnflow (Table 6.2). The saprolite of P7 is calcareous confirming that and the neocarbonate horizon at 1380 mm depth of profile P9, both located lower down in the topography, indicate an increasing lateral flowpath.

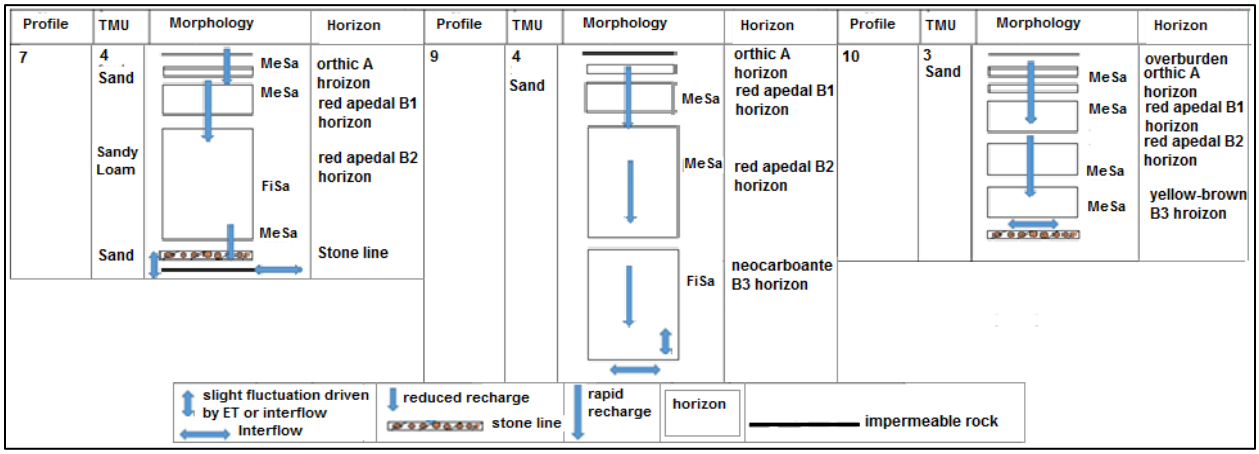

Figure 6. 9 Conceptual hydrological response based on morphology of Hutton soils.

6.3.2.1.3. Deep Coega soil form Pedon hydrology – P8

This soil is similar to P5, located on a flat TMU5. The substrate in which the carbonate of the hardpan carbonate horizon has precipitated is saprolitic in nature and extends to a depth of 750 mm. A high pH and carbonate concretions in the orthic horizon (Table 6.2), are probably precipitated by capillarity (Figure 6.10). This profile has a hydrological shallow responsive nature.

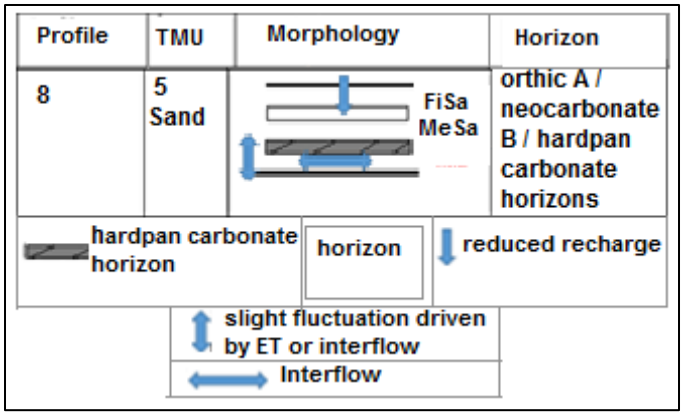

Figure 6. 10 Conceptual hydrological response based on morphology of deep Coega soils.

6.3.2.1.4. Clovelly soil form Pedon hydrology – P11

The Clovelly soil form is located at the transition from TMU3 to TMU4, with a decrease in slope. Van Rooyen (1971) found more yellow sand grains emanating from the Vaal River. However, the increase in both chroma and hue down the profile indicates the activity of a process increasing with depth (Table 6.2). This facilities interpretation of a longer period of saturation fed by hillslope water (Figure 6.11).

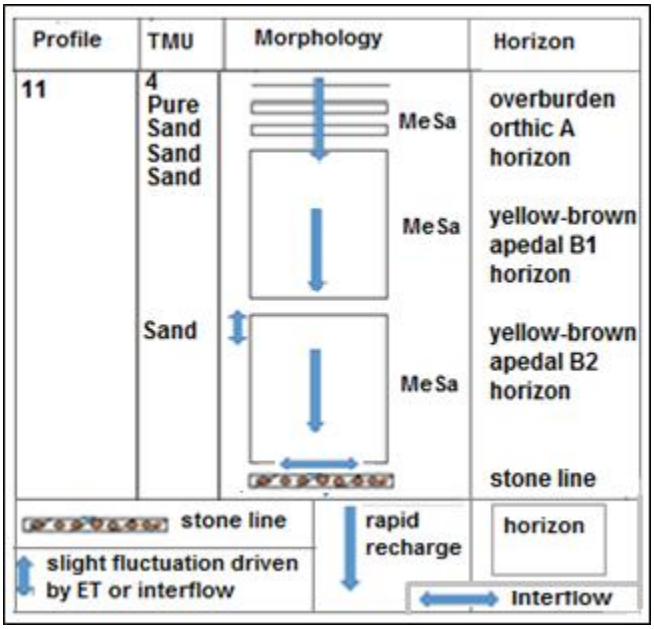

Figure 6. 11 Conceptual hydrological response based on morphology of Clovelly soils.

6.3.2.2. Hydrological response of site 2

All soil types facilitate morphological interpretation of a large interflow area in the hillslope (Figure 6.12). Again soil morphology indicates interflow in the deep subsoil and fractured rock.

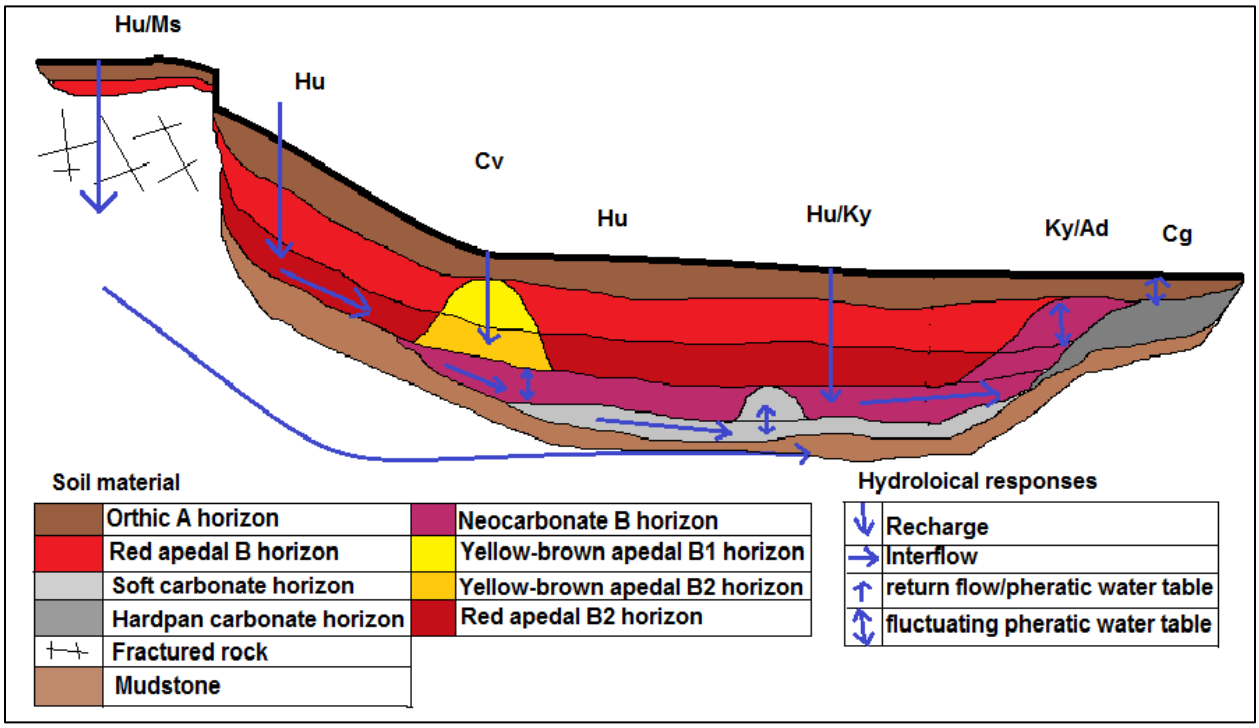

Figure 6. 12 CHRM of site 2.

6.3.3. Site 3

The site consists of TMU's 3 and 4. Soil distribution patterns grade from apedal deep Hutton, Clovelley and Namib soils on TMU 3 into shallow Namib soils with carbonaceous subsoils, Askham, Addo and Plooysburg soil forms on TMU 4 (Figure 6.13). TMU4 is underlain by dolerite boulders on Dwyka mudstone and tillite. Carbonate precipitation is higher in orthic A horizons of more level topography. Wavy broken Dwyka mudstone and tillite occur as saprolite.

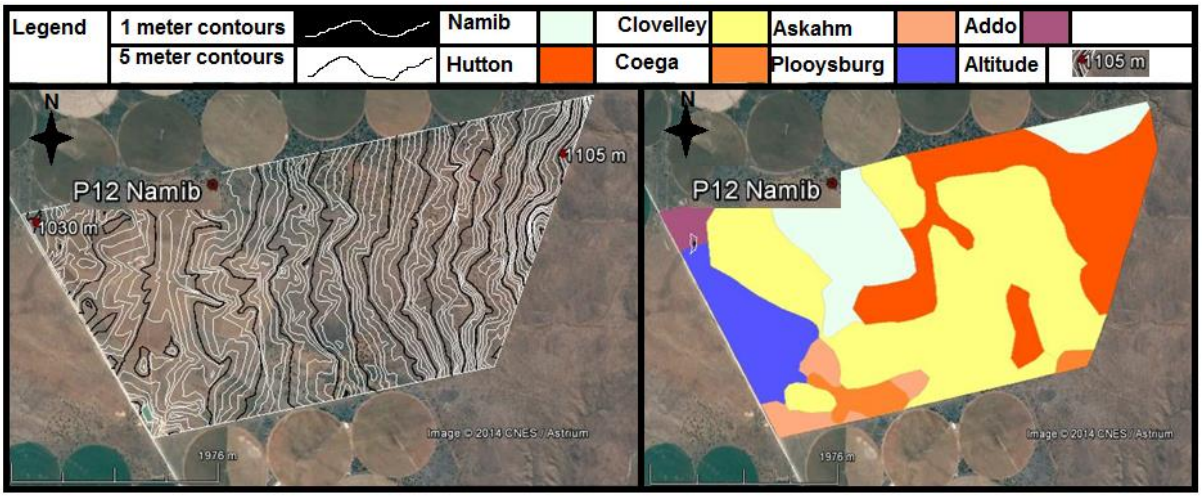

Figure 6. 13 One meter contours (left) and soil map (right) with master profile distribution of Site 3.

6.3.3.1. Hydrological response of the soil types of site 3

6.3.3.1.1. Namib soil form pedon hydrology – P12

The Namib soil form is located on the TMU 3 / 4 transition. A shallow 150 mm overburden of unconsolidated recently deposited wind-blown aeolian sand tops the profile. The profile is pure sand (Table 6.3). Carbonate occurs sporadic at aeolian stratification transitions throughout the profile. The increase in measured sodium and calcium may be due to downward leaching or upward movement by capillary rise, but probably both (Figure 6.14).

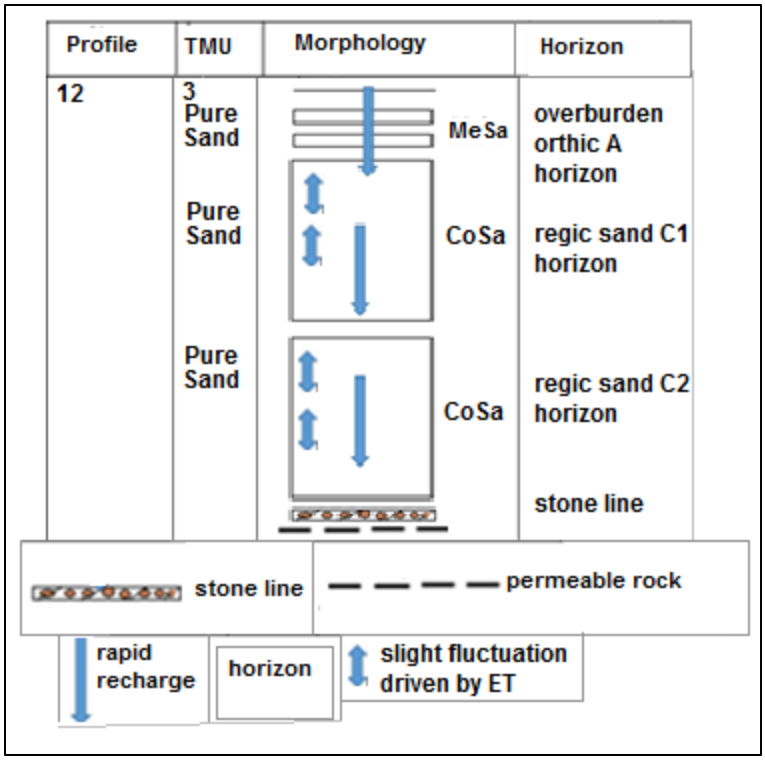

Figure 6. 14 Conceptual hydrological response based on morphology of Namib soils.

Table 6. 3 Morphological, topographical and chemical information of modal profile P12

Profile	TMU	Curvature	Diagnostic horizon	Depth (mm)	Munsell colour (wet)	Sodium	Calcium	$CaCO_3$ content (%)	pH (H_2O)	Particle size distribution (%)		
						$cmol_c\ kg^{-1}$ soil)				Sand	Silt	Clay
P12	3	Vs	ot	200	7.5YR3/3	0.003	9.3	0.09	8.24	93	2.5	3.4
			rs1	1150	7.5YR3/4	0.08	8.99	0.22	7.48	91	2.4	3.7
			rs2	2000	7.5YR3/3	0.13	13.28	0.45	7.95	92	3.2	4.5

6.3.3.2. Site 3 hydrological response

Linking the yellow-brown colour to hydropedology is uncertain as it could be linked to the source. Absence of carbonate precipitates in the Huttons and Clovellys however indicates a large recharge area and the various degrees of carbonate accumulation in the Plooysburg, Namib, Askam and Coega soils is an indication of interflow and return-flow of different degrees (Figure 6.15).

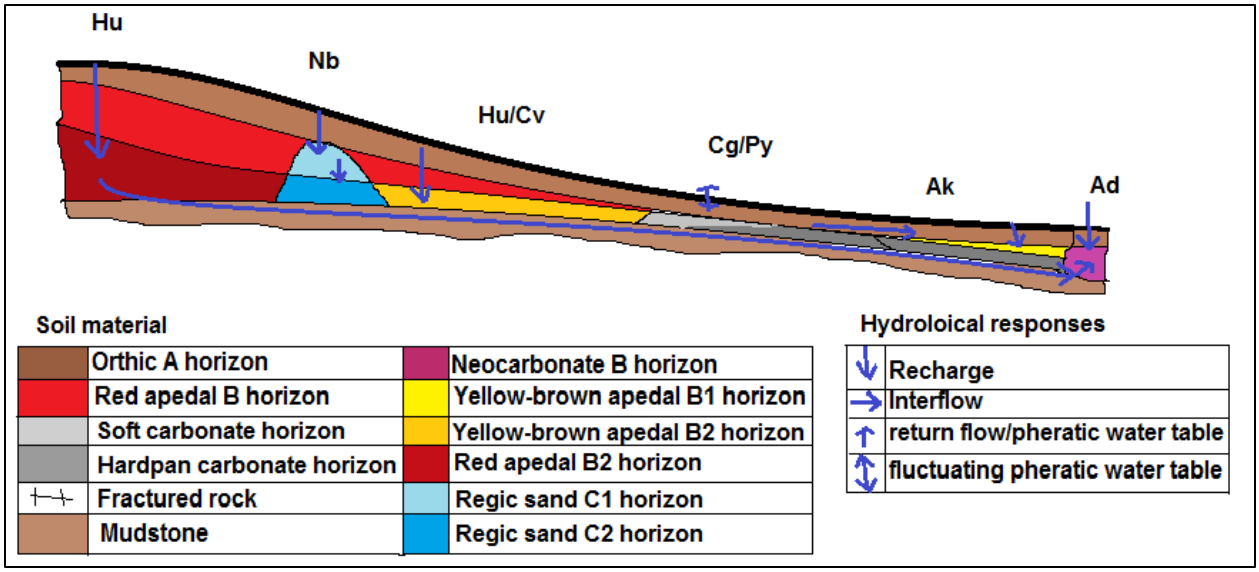

Figure 6. 15 CHRM of site 3.

6.3.4. Site 4

Site 4 has two areas namely Riverside occupying a footslope to toeslope and Aucampshope occupying a footslope to floodplain. Soil form distribution of Riverside down slope is Hutton soils on saprolite to Kimberley to Coega soils with bleached A horizons. At the Aucampshope site the distribution is Addo soil with bleached orthic A horizon grading into a Klapmuts on a slope of 1% and Valsrivier with gypsum on the flat floodplain (Figure 7.4). Sepane soil form occurs in concave concave depressions on the floodplain. The depressions are up to 1 meter in depth and occur along surface drainage lines. Saprolitic shale, Dwyka mudstone and tillite, as well as soft and hardpan carbonate are transitions to fractured rock and alluvium on the floodplain.

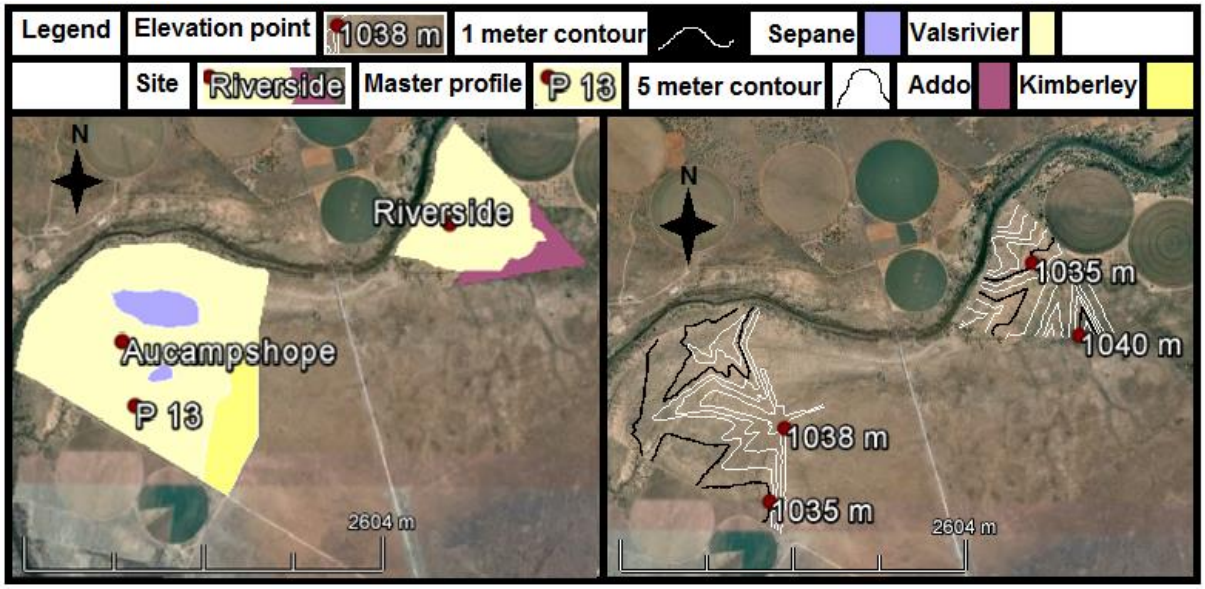

Figure 6. 16 One meter contours (right) and soil map (left) with master profile distribution of Site 4.

6.3.4.1. Hydrological response of the soil types of site 4

6.3.4.1.1. Valsirivier soil form pedon hydrology – P13

The Valsrivier soil form is located on a floodplain associated with alluvial and/or possible hillslope luviated clay and silt deposits. Increase in clay contents from the orthic A horizon to the pedocutanic B1 horizons and change in structure to fine strong angular blocky with gypsum accumulation, indicates this to be poorly drained and a shallow responsive soil (Table 6.4) (Figure 6.17). Sodium figures indicates a slow downward leaching of the A horizon only. The occurrence of gypsum supports that and the accumulation of calcareous precipitates in the deep subsoil is an indication of lateral flow in the deep subsoil.

Table 6. 4 Morphological, topographical and chemical information of modal profile P13

Profile	TMU	Curvature	Diagnostic horizon	Depth	Munsell colour (wet)	Sodium	Calcium	$CaCO_3$ content (%)	pH (H_2O)	Particle size distribution (%)		
						$cmol_c\ kg^{-1}$ soil				Sand	Silt	Clay
P13	5	Sv	ot vp1 vp2	350 700 1850	2.5YR5/6 10YR3/3 10YR3/2	0.34 5.17 9.48	4.34 4.34 16.1	0 3.61 4.96	6.65 7.23 6.88	48 29 15	30 31 47	20 40 38

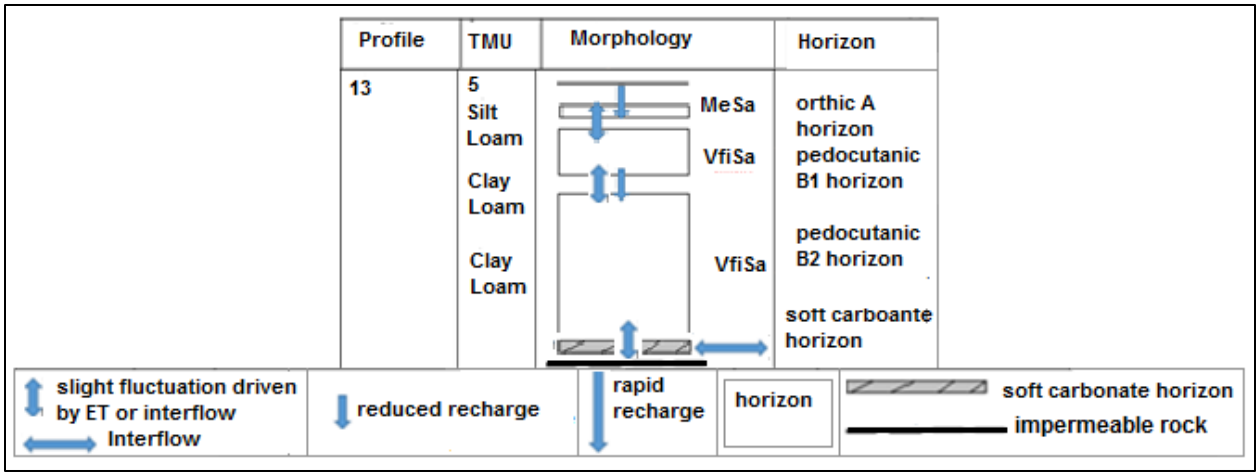

Figure 6. 17 Conceptual hydrological response based on morphology of Namib soils.

6.3.4.2. Site 4 hydrological response

The soils of this terrain position are not responsible for recharge of the lower vadose zone. Interflow is indicated by the Kimberley soils and a new flowpath in the deep subsoils of the Sepane and Valsrivier soils (Figure 6.18). This flowpath is probably linked to a flow of water in the river alluvium, probably towards the river from the hillslope but during high flows it can be affected by river flow and riparian interaction.

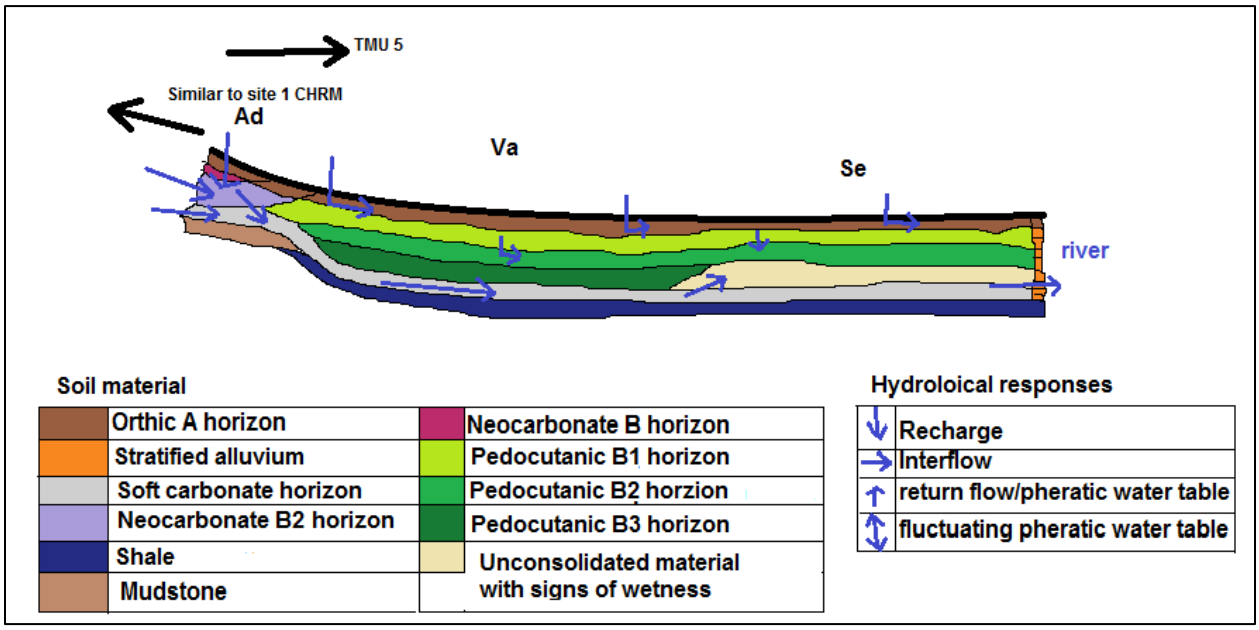

Figure 6. 18 CHRM of site 4.

6.4. Conclusion

As the crests of the landscape are not covered by the surveys, their contribution is not covered in the study. Random observations on the crests indicate that they are recharge areas of Mispah soils and shallow recharge Hutton and responsive Coega soils. The hillslopes of the area predominantly recharge (Table 3.2) through Hutton soils covering most of the area (Figure 6.5). Interflow is mainly in the fractured rock (fr, Figure 6. 19) from where it returns to the subsoils of Kimberley, Plooysburg and other soil forms. Signatures of flowpaths follow the order of calcareous free, calcareous neo-carbonate, soft and hardpan carbonate horizons with a decrease in altitude on the terrestrial area. In the riparian floodplain, interflow is in the deep subsoils. A/B horizon interflow is indicated in the Coega soils with hardpan carbonate subsoils and bleached A horizons and in the E horizon of the Klapmuts supported by the abrupt E/B transition and gypsum in the pedocutanic B horizon. The responsive area is limited to shallow responsive Coega, Klapmuts, Sepane and Valsrivier soils. This is an example of topsoil hydrological response to rain, in other words event driven that is to a large extent isolated from subsoil response which is seasonally driven as it rather responds to hillslope flows in high rainfall years only.

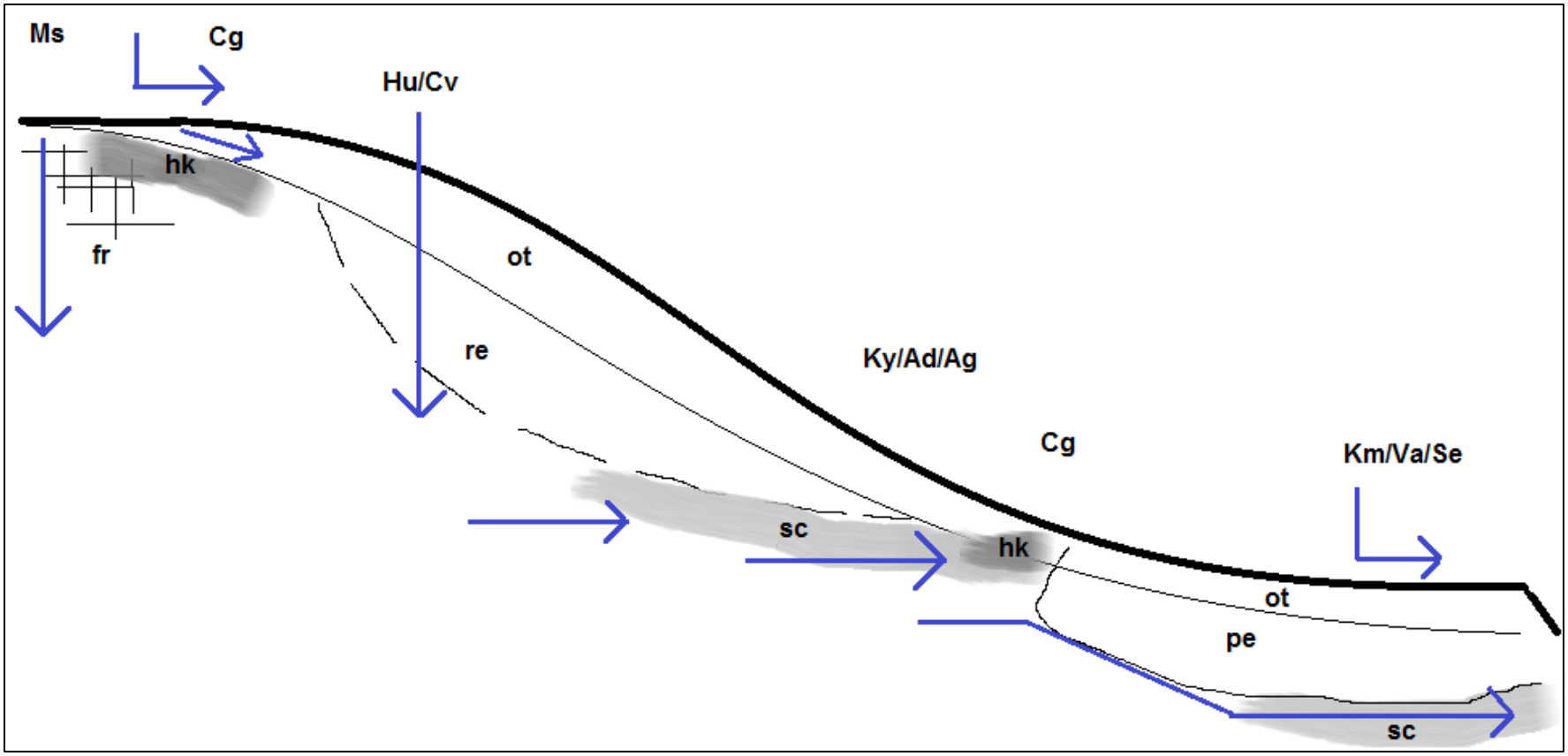

Figure 6. 19 CHRM of a soilscape of an arid region.

CHAPTER 7

HYDROLOGICAL PROPERTIES OF ARID SOILS

7.1 Results and Discussion

7.1.1 Site 1

Soil water characteristics of the horizons of soils representative of the site are reported (Table 7.1).

Table 7. 1 Hydrometric properties of the Kimberley, Addo, Hutton and Coega modal profiles P1 to P5

Profile	TMU	Diagnostic Horizon	Saturated hydraulic conductivity (mm h^{-1})	Macropore conducting flux (%)	DUL cm cm^{-3}	Water holding capacity (cm cm^{-3})	Bulk density
P1	4	ot	95	89.06	0.1315	0.3945	1.66
		re	193	92.02	-	-	-
		sl	117	79.89	0.0847	0.5353	1.67
		sc	27	79.27	0.0976	0.3514	1.62
		ob	25	93.76	0.0559	0.3086	1.50
P2	4	ot	84	61.92	0.1072	0.4403	1.59
		nc1	177	74.23	0.1409	0.4806	1.79
		nc2	142	69.34	0.1423	0.4723	1.72
		sl	30	72.44	0.1377	0.4652	1.70
		sc	58	32.49	0.1349	0.4896	1.74
P3	4	ot	84	45.67	0.0914	0.3930	1.54
		re	153	74.20	0.0965	0.4469	1.57
		sc	279	88.13	0.1254	0.4110	1.47
		on	92	42.95	0.1138	0.6572	1.54
P4	4	ot	159	97.44	0.1278	0.3907	1.60
		re1	112	94.10	0.1363	0.4593	1.61
		re/so	143	96.90	0.1027	0.4724	1.52
P5	1	ot	358	93.86	0.1322	0.4032	1.64
		hk	-	90.29	0.1449	0.4963	1.93

DUL – Drained upper limit.

7.1.1.1 Kimberley soils (P 1, P 3)

High saturated hydraulic conductivity (Ks) in all the horizons of the Kimberley soil supports fast vertical drainage and recharge of the underlying fractured rock (Table 7.1). Ks decreases down the profile and so does the contribution of macropore (MP) flow. This is an indication that biopores, more frequently generated closer to the surface, are the main contributions to Ks. With Ks values exceeding rainfall intensity, the topsoil and red apedal B horizon will rapidly discharge to the soft carbonate horizon, with increasing possibility of saturation on impermeable layers and resulting interflow. The high to extremely high Ks of the soft carbonate horizon indicates a permeable medium draining fast but overlying an impermeable layer resulting in lateral flow dependant on slope. The lime precipitate indicates slow flow of lime rich water.

The K_s of all the horizons are high (>25 mm h^{-1} to 358 mm h^{-1}) (Table 7.1). It is indicating good vertical internal drainage that meet interflow at the soil/rock transition. It is suggested that a slow rate (<3 mm h^{-1}) of interflow and longer duration of a phreatic water table in the soft carbonate B horizon may be responsible for capillary rise.

7.1.1.2. Hutton soil (P 4)

The Hutton soil has a very high saturated hydraulic conductivity (> 112 mm h^{-1}), supporting fast vertical recharge of the saprolite. Here water flow is reduced to induce ponding as result of extremely fast recharge, however is lost to underlying rock fast enough to not induce redox conditions (Table 7.1).

As in the Kimberley soils, Ks is high and almost exclusively controlled by the MPs (Table 7.1). Both Ks and MPs dip in the red apedal B1 horizon, with a slight increase in bulk density. Lack of carbonate precipitation in the saprolite, indicates rapid recharge of the lower lying fractured rock and by implication a flowpath in the fractured rock, not affecting the soil at this point.

7.1.1.3. Addo soil (P 2)

High Ks is observed, increasing from orthic A horizon to neocarbonate B2 horizon (Table 7.1). A drop in Ks to moderately high (30 mm h^{-1}) and drop in macropore flow is observed in the stoneline (Table 7.1). This drop in Ks is controlled by the slightly higher Ks (58 mm h^{-1}) of the soft carbonate horizon. A diffuse transition between neocarbonate B2, stone line and soft carbonate horizons indicates a relationship which may be linked to capillary rise.

Ks increase is associated with an increase in macropore flow (Table 7.1). Low Ks in the stone line (30 mm h^{-1}) with a high macropore flow (77%) may be due to the high coarse fraction (Appendix B). The inverse in macropore flow and saturated hydraulic conductivity ratio is observed in the soft carbonate horizon (Table 7.1). This may be due to the carbonate precipitating stabilizing pore channels and creating continuous pores.

The reduced Ks of the soft carbonate horizon and diffuse transition of the above-lying neocarbonate B2 horizon indicate a longer period of ponding lower in the profile. This, may result in some water flowing laterally and some return flow from the saprolite and fractured rock.

7.1.1.4. Coega soil (P 5)

The high macropore conducting flux and very high K_s (358 mm h^{-1}), with underlying hardpan carbonate horizon very low Ks (<1 mm h^{-1}) (Table 7.1), indicates the profile to have an A/C interflow, to accommodate such a high Ks.

7.1.2. Site 2

Soil water characteristics of the horizons of soils representative of the site are reported (Table 7.2).

Table 7. 2 Hydrometric properties of the Addo, Hutton, Coega and Clovelly modal profiles P6 to P11

Profile	TMU	Diagnostic Horizon	Saturated hydraulic conductivity (mm h^{-1})	Macropore conducting flux (%)	DUL cm cm^{-3}	Water holding capacity (cm cm^{-3})	Bulk density
P6	5	ot	244	73.94	0.0945	0.4491	1.57
		nc1	623	86.04	0.101	0.4328	1.54
		sc	255	87.59	0.1445	0.4286	1.39
P7	4	ot	273	90	0.1293	0.4483	1.39
		re1	2462	98.21	0.2105	0.4029	1.61
		re2	2431	-	-	-	-
		so	58		0.1227	0.4340	1.60
P8	5	ot	41	22.29	0.2024	0.7286	-
		hk	20	23.58	0.0853	0.4219	1.60
		hk2	116	93.58	0.1186	0.5571	1.43
P9	4	ot	255	47.23	0.0721	0.3652	-
		re	741	91.77	0.1122	0.4880	1.59
		nc	380	38.26	0.0782	0.4880	1.70
P10	3	ot	277	48.33	0.0591	0.4189	1.60
		re1	1593	99.60	0.0987	0.3836	1.60
		re2	-	-	-	-	
		yb	1003	93.41	0.0849	0.4057	1.64
P11	4	ot	268	94.15	0.0968	0.4618	1.51
		yb1	1228	90.00	0.1267	0.5001	1.60
		yb2	1151	98.98	0.1269	0.5001	-

DUL – Drained upper limit.

7.1.2.1. Addo soil (P 6)

Very high (244 mm h^{-1}) to extremely high Ks (623 mm h^{-1}) indicates a rapid recharge of the profile. Reduced macropore flow (180 mm h^{-1}) in the orthic A is due to bioturbation, followed by stable high macropore flow in the neocarbonate B1 and soft carbonate horizons.

A lower Ks (255 mm h^{-1}) in the soft carbonate horizon could promote some ponding. This may facilitate the diffuse transitions and carbonate precipitation as free lime and nodules, increasing with depth to soft carbonate horizon. Underlying hardpan carbonate horizon is

assumed to have a very low Ks, indicating this profile to have a lateral flowpath in the soft carbonate horizon to accommodate such a high Ks.

7.1.2.2. Coega soil (P 8)

The high Ks in the orthic A horizon (41 mm h^{-1}) and the moderately high Ks of the hardpan carbonate horizon (20 mm h^{-1}) are controlled by the meso and micro pores (Table 7.2). This is associated with a lower contribution in flow of MPs. The high (116 mm h^{-1}) Ks of the hardpan carbonate 2 horizon is controlled by macropore flow. This is an indication of vertical flow to facilitate such a high Ks.

Under high rainfall intensity this soil will react hydrologically responsive.

7.1.2.3. Hutton soils (P 7, P 9, P 10)

High Ks (255 to 277 mm h^{-1}) is observed in the orthic A horizons. Hutton soils with dominant overburdens orthic A horizons have a lower (47.23% (P9) 48.33% (P10)) MP contribution than lower-lying Hutton soils (P7) (90%) (Table 7.2). Very high Ks of B horizons indicate a rapid through-flow. Hutton soils have very high Ks at their transition to rock, with Ks increasing with increase in slope (Table 7.2, Chapter 5). These have a soil / rock interflow hydrological response. Hutton soil on flat topography show a reduced high Ks (58 mm h^{-1}) in saprolite horizon. These have a recharge hydrological response.

7.1.2.4. Clovelly soil (P 11)

High Ks (268 mmh^{-1}) increasing to very high Ks (1228 mmh^{-1}) vertically down the profile, indicates a dominant recharge hydrological response (Table 7.2). The high Ks at the yellow-brown apedal B2 horizon indicates Ks (1151 mmh^{-1}) to be facilitated by a lateral flowpath (Table 7.2) at the soil/rock transition.

7.1.3. Site 3

7.1.3.1. Namib soil (P 12)

Soil water characteristics of the horizons of soils representative of the site are reported (Table 7.3).

Table 7. 3 Hydrometric properties of the Namib modal profile P12

Profile	TMU	Diagnostic Horizon	Saturated hydraulic conductivity (mm h^{-1})	Macropore conducting flux (%)	DUL cm cm^{-3}	Water holding capacity (cm cm^{-3})	Bulk density
P12	3	ot	370	77.24	0.0616	0.4413	1.46
		rs1	14.58	3.877	0.0928	0.4413	1.48
		rs2	-	-	-		1.53

DUL – Drained upper limit.

Very high Ks indicates a rapid infiltration and drainage of the orthic A horizon. This reduces to moderately high Ks (14 mm h^{-1}) (Table 7.3). This indicates that some ponding will occur at this transition. A lateral flowpath exists to accommodate the high Ks of the orthic A horizon.

7.1.4. Site 4

Soil water characteristics of the horizons of soils representative of the site are reported (Table 7.4).

Table 7. 4 Hydrometric properties of the Valsrivier modal profile P13

Profile	TMU	Diagnostic Horizon	Saturated hydraulic conductivity (mm h^{-1})	Macropore conducting flux (%)	DUL cm cm^{-3}	Water holding capacity (cm cm^{-3})	Bulk density
P13	5	Ot	10	37.44	0.1518	0.6497	1.3
		pe1	3	20.96	0.2137	0.7142	1.28
		pe2	3	28.6	-	-	1.24

DUL – Drained upper limit.

7.1.4.1. Valsrivier soil (P 13)

The moderately low Ks in the orthic A horizon decrease to a low Ks in the pedocutanic B1 and 2 horizons, is ascribed to the increase in clay (Table 6.4, Table 7.4). The low Ks is controlled by the meso- and micro-pores (Table 7.4). Ks is lower than rainfall intensity and therefore will have a responsive hydrological response.

7.2. Predicting unsaturated hydraulic conductivity curves using water retention curve data

The unsaturated hydraulic conductivity ($K\vartheta$) curves predicted from the van Genuchten-Mualem (VGM) predictive model (Van Genuchten & Leij, 1991), are shown in Figures 7.1 - 7.4. Water content was expressed as 'degree of saturation' of the soil available porosity or '(s)' to facilitate hydropedological interpretations of the hydrology of the profiles (Van Huyssteen *et al*., 2005; Kuenene *et al*., 2011; Kuenene *et al*., 2015).

Most of these curves show that hydraulic conductivity is rapid in the profiles and very few horizons have a hydraulic conductivity at 0.7 of saturation (Figures 7.1 – 7.4). This is as a result of macropore contribution controlling Ks (Tables 7.1 to 7.4).

This confirms the dominant high and very high saturated hydraulic conductivities primarily controlled by macropore flow. Lower hydraulic conductivities are associated with meso and micro-pore flow dominating Ks. This is can be seen in orthic A horizon of the Coega soil form of site 2 (Figure 7.2 (d) and orthic A horizon of the Hutton profiles (P9) and (P10) (Figure 7.3 (b) and (c)) having a much higher hydraulic conductivity curve before hydraulic conductivity is negligible (<1 mm).

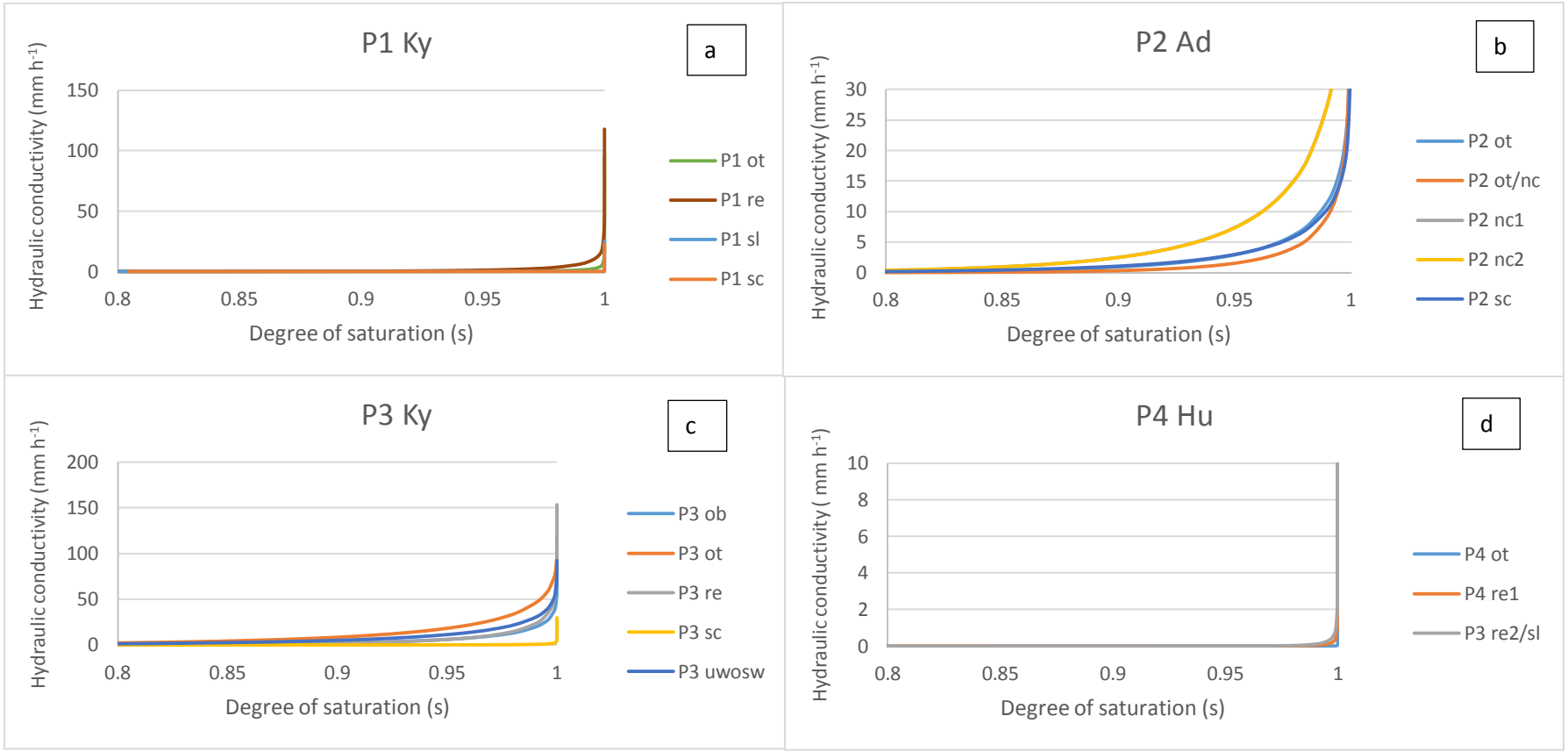

Figure 7. 1 The relationship of the hydraulic conductivity (mm hr^{-1}) versus the predicted water content relationship of the Kimberley (a), Addo (b), Kimberley (c) and Hutton (d) soil forms and their respective horizons.

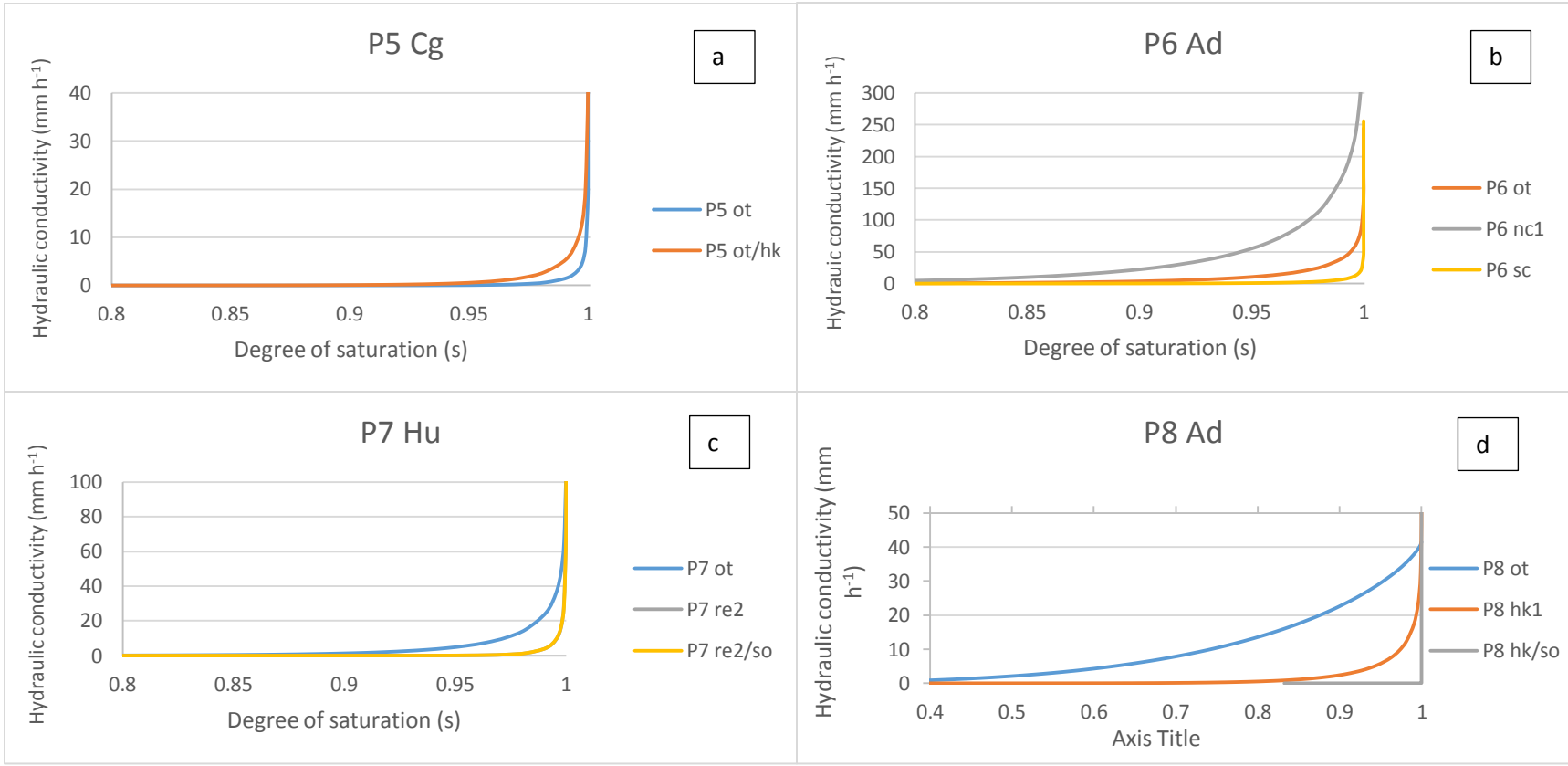

Figure 7. 2 The relationship of the hydraulic conductivity (mm hr^{-1}) versus the predicted water content relationship of the Coega (a), Addo (b), Hutton (c) and Addo (d) soil forms and their respective horizons.

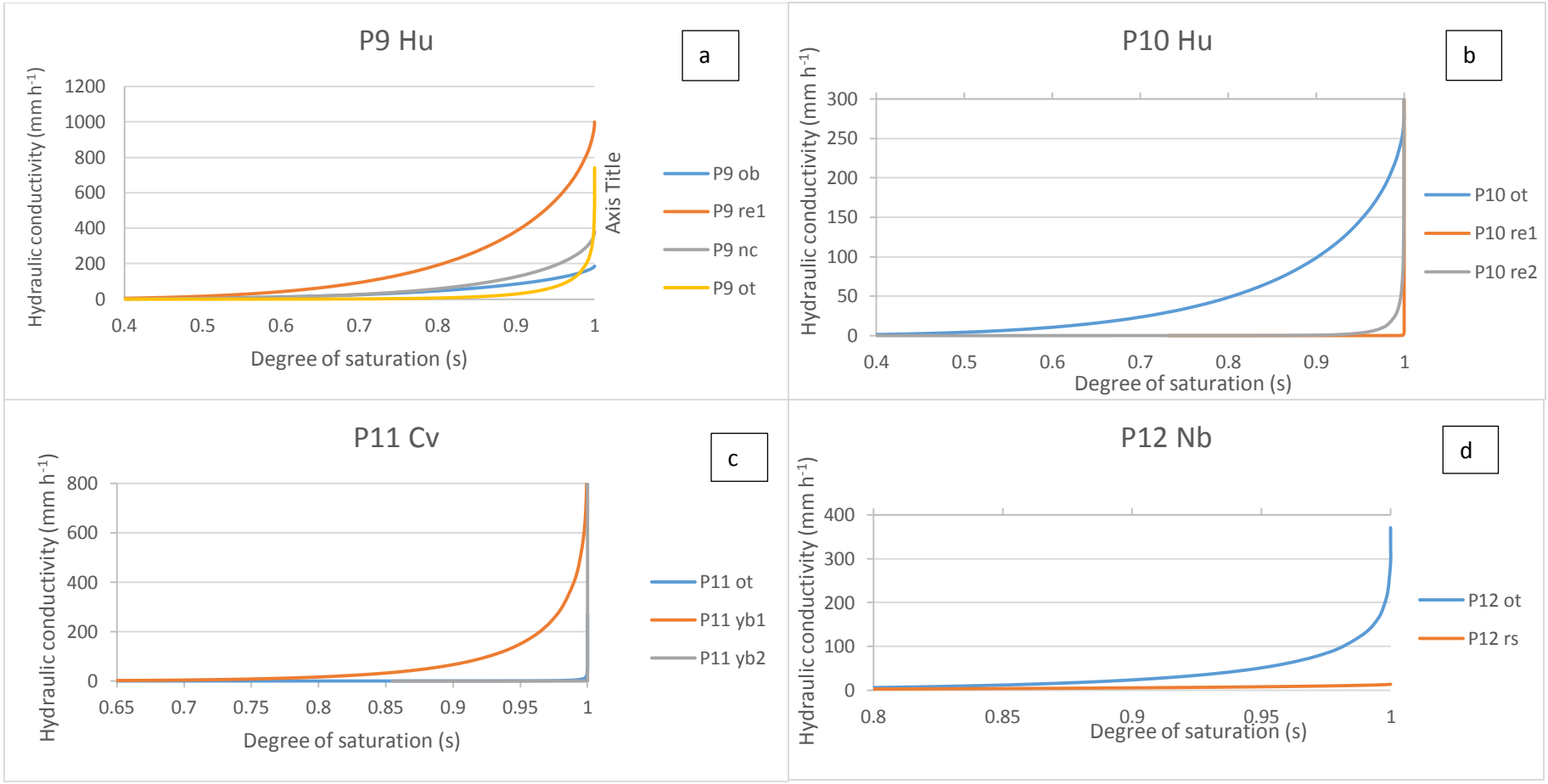

Figure 7. 3 The relationship of the hydraulic conductivity (mm hr^{-1}) versus the predicted water content relationship of the Hutton (a), Hutton (b), Clovelly (c) and Namib (d) soil forms and their respective horizons.

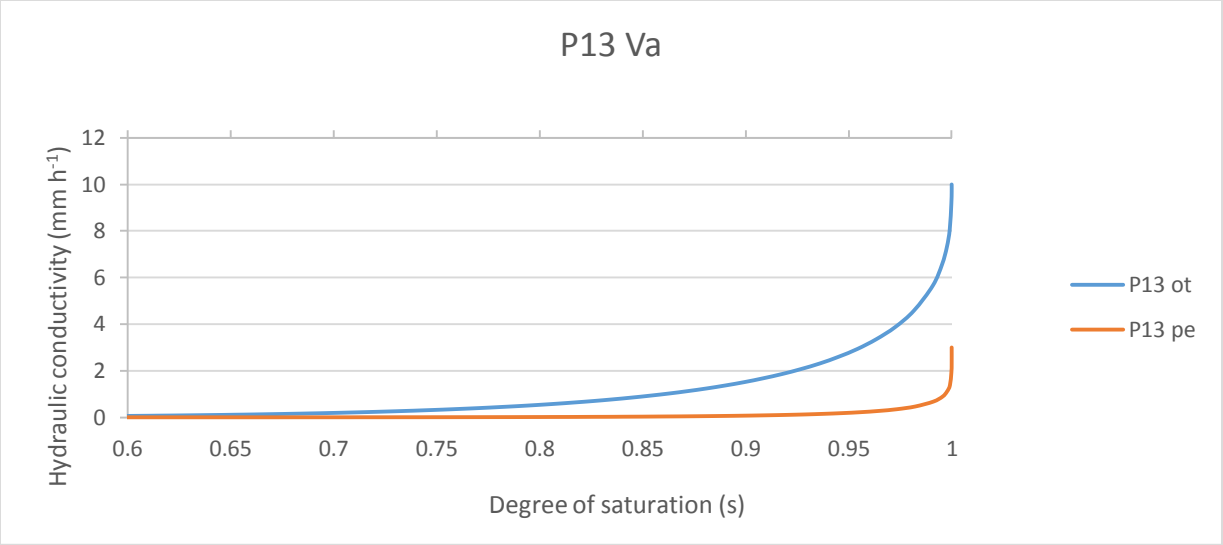

Figure 7. 4 The relationship of the hydraulic conductivity (mm hr^{-1}) versus the predicted water content relationship of the Addo soil form and its respective horizons.

These soils have poor water retention characteristics. Water retention characteristics are further presented in Appendix D.

7.3. Conclusion

Saturated hydraulic conductivity confirms conceptual hydrological response by means of morphological and chemical interpretation. High to very high saturated hydraulic conductivities for apedal soils dominate hydrological response of soils. Carbonate precipitation is an indicator of a lateral flowpath both towards and away from the zone of precipitation. Very high and high Ks rates observed at transitions to lower conductivity zones, such as hard rock, indicate a lateral flowpath facilitating high vertical Ks.

Hutton soils, depending on TMU position, have rapid vertical internal drainage. Type of underlying rock, as well as degree of weathering, facilitate profile hydrological response to be of soil / rock interflow or recharge.

Very high to high Ks rates are controlled by macropores. Low to moderately low Ks are observed to be controlled by meso- and micro-pores.

Boundary conditions to underlying material control hydrological response of these sandy apedal soils. This confirms a soil / rock interflow recharge to wetland conceptual hydrological response of these arid soils.

CHAPTER 8

CONCLUSIONS AND RECOMMENDATION

The morphology and chemistry of the arid soils of South Africa are matured and carry the signatures of interaction with water. The morphological properties are therefore good indicators of flowpaths. Chemical properties are one-sided, especially the high pH and base oversaturation and are less suitable for flowpath interpretation. The conceptual hydrological response predicted from the morphology is confirmed by hydrometrics. The binary origin of parent material in arid zones should be taken into account: for example the colour of aeolian sand of different river sources, but this does not prevent sound predictions.

All four sites have a large area with signatures of shallow lower vadose zone interflow. The homogeneous nature of the CHRMs is an indication that it is lithology related, in this case Dwyka tillite with the aeolian sand deposits now forming the majority of soils, is merely a water store and fast conduit that recharges the shallow lower vadose zone.

The CHRM can be classified as a class 1, soil/bedrock interflow to wetland with a shallow interflow zone dominating. It is supported by indicators of a fluctuating water table, as high chroma mottles occur localised under center pivots, indicating a periodic water table in the irrigation season. This occurs in combination with a shallow restrictive layers in the lower vadose zone of fractured rock.

Ks values of topsoils and a variety of apedal subsoils are high and exceed high rainfall intensities. Macropores in the apedal soils are dominated by biopores. Macropores primarily contribute more to Ks in the subsoil than in the topsoils. Indications are that event-driven vertical downward flowpath interacts with post-event interflow in the fractured rock, returning to the soil in different ways as indicated by the morphological variety of carbonate precipitates. Longer presence of water is probably responsible for capillary action and neocarbonate horizons. At the junction of event-driven and post-event driven interflow, the domination of flowpaths controls the formation of soft on hardpan and hardpan on soft carbonate horizons.

Flowpath indicators of carbonate are a product of hydropedology in arid climates, where the hydropedology can assist in the understanding their formation process.

Responsive areas on the floodplain are limited to shallow responsive soils with low permeability in the subsoil. Abrupt transitions from the orthic A horizon to the impermeable hardpan carbonate and low Ks pedocutanic B horizons is typical. Gypsum occurring in the pedocutanic B horizon and neo- and soft carbonate precipitates lower down the profile is in harmony with low Ks values and therefore a lack of vertical flow.

Eco-hydrology particularly, benefits from such CHRMs, as the understanding of the hydrological cycle is enriched with information of soil flowpaths and their connectivity in the landscape.

The CHRM is suitable for wide spread application in the arid zone with same and similar hydrological lithology.

REFERENCES

ANKENY, M. D., AHMED, M., KASPAR, T. C. & HORTON, R. (1991). Simple field method for determining unsaturated hydraulic conductivity. *Soil Sci. Soc. Am. J.* 55, 467 – 470.

AMOOZEGAR, A. (2002). Soil Science Society of North Carolina proceedings, Vol XLV.

ASANO, Y., UCHIDA, T. & OHTE, N., (2002). Residence times and flow paths of water in steep unchannelled catchments, Tanakami, Japan. J. Hydrol., 261, 173-192.

BAGARELLO, V., DI PIAZZA, G.V. & FERRO, V. (2004). Manual sampling and tank size effects on the calibration curve of plot sediment storage tanks. Transactions of the American Society of Agricultural Engineering 47, 1105-1112.

BIREKLAND, (1974). in Bhaskar, B. P., Baruah, U., Vadivelu, S., & Butte, P. S. (2005). Characterization of soils in the 'Bil'environs of Brahmaputra valley in Jorhat district, Assam for land use interpretation. *Journal of the Indian Society of Soil Science*, *53*(1), 3-10.

BEAR, F.E. (1964). Chemistry of the Soil, 2nd Ed. Reinhold Publishing Corporation. New York.

BEEH. (2003). Weatherly Database V1.0. School of Bioresources Engineering and Environmental Hydrology, University of Natal, Pietermaritzburg. BOUMA, J. (1989) Using soil survey data for quantitative land evaluation. *Adv. Soil Sci.* 9:177-213.

BEVEN, K. J., (2000). Uniqueness of place and the representation of hydrological processes. *Hydrology and Earth Science.* (4) 203-213.

BODHINAYAKA, W., SI, B. C & XIAO, C. (2004). New method for determining water-conducting macro and mesoporosity from tension infiltrometer. *Soil Sci. Soc. Am. J.* 68, 760 – 769.

BOHN, H. L., McNEAL, B. L. o'CONNOR, G.A. (1985): Soil chemistry.

BOHN, K., (2005). An intorduction into applied soil hydrology. Lecture notes. Catena Verlag GMBH, Reiskirchen, Germany.

BOUMA, J. (2004). Foreword. *In:* Pachepksy, Y. and Rawls W. J. (Eds), Development of pedotransfer functions in soil hydrology. Elsevier, Amsterdam.

BURNS, D. A., HOOPER, R. P., McDONNELL, J. J., FREER, J. E., KENDALL, C., & BEVEN, K. (1998). Base cation concentrations in subsurface flow from a forested hillslope: The role of flushing frequency. *Water Resources Research*, *34*(12), 3535-3544.

BOUWER, D. (2013). Developing hydrological response models for selected soilscapes in the Weatherley catchment, Eastern Cape Province. M.Sc. thesis, Department of Soil, Crop and Climate Sciences, University of the Free State, Bloemfontein.

BOUWER, D., LE ROUX, P.A.L., VAN TOL, J.J., & VAN HUYSSTEEN, C.W. (2015). Using ancient and recent soil properties to design a conceptual hydrological response model. *Geoderma*, *241*, 1-11.

BRADFIELD, R., (1942). *Soil Sci. Soc. Am. Proc.* 6, 8.

BRETZ, J. H., & HORBERG, L. (1949). Caliche in southeastern New Mexico. *The Journal of Geology*, 491-511.

BROOKS, R.H., and COREY, A.T. (1964). Hydraulic properties of porous media. Hydrol. Paper 3. Colorado State Univ., Fort Collins, CO, USA.

BUOL, S.W., HOLE, F.D., McCRACKEN, R.J. & SOUTHARD, R.J. (1997). Soil genesis and classification. 4th edition. Iowa State Univ. Press, Ames.

CAMEIRA, M.R., FERNANDO, R.M. and PEREIRA, L.S. (2003). Soil macropore dynamics affected by tillage and irrigation for a silty loam alluvial soil in southern Portugal. Soil & Till. Res. 70, 131-140.

CARROLL, D. (1962). Rainwater as a chemical agent of geologic processes: A Review. US Government Printing Office.

CARSEL, R. F., & PARRISH, R. S. (1988). Developing joint probability distributions of soil water retention characteristics. Water Resource Research, 24(5), 755-769.

CHANG, J. Y. (2010). Predictions of saturated hydraulic conductivity dynamics in a midwestern agricultural watershed, Iowa. Masters thesis, University Iowa. http://ir.uiowa.edu/etd/476.

CLOTHIER, B. E., GREEN, S. R. & DEURER, M. (2008). Preferential flow and transport in soil: progress and prognosis. European Journal of Soil Science 59, 2-13.

CORNELL, R. M., SCHWERTMANN, U. (1996). The Iron Oxides: Structure, Properties, Reactions, Occurrence and Uses. VCH : Weinheim; New York; Basel; Cambridge; Tokyo.

D'AMORE, D. V., STEWART, R.S. & HUDDELSTON , H.J. (2004). Saturation, reduction, and the formation of iron-manganese concreations in the Jackson-Fraizer wetland, Oregon. *Soil. Sci. Soc. Am. J.* 68, 1012-1022.

DAVIDSON, E. A., & LEFEBVRE, P. A. (1993). Estimating regional carbon stocks and spatially covarying edaphic factors using soil maps at three scales. Biogeochemistry, 22(2), 107-131.

DEXTER, A. R. (2004). Soil physical quality: Part I. theory, effects of soil texture, density, and organic matter, and effects on root growth. Geoderma, 120(3), 201-214.

DIRKSEN, C. (1999), in BAGARELLO, V. I., CASTELLINI, M. I., & IOVINO, M. A. (2007). Comparison of unconfined and confined unsaturated hydraulic conductivity. *Geoderma*, *137*(3), 394-400.

DIRKENSEN, C. (1999). Soil Physics Measurements*, pp.* 96–113*, Catena Verlag,* Reiskirchen, Germany.

DUNN, G. H., and PHILIPS, R. E. (1991). Macroporosity of a well drained soil under no-till and conventional tillage. Soil Sci. Soc. 55, 817-823.

DU TOIT, A. L. (1966). The geology of South Africa (3rd edition). London: Oliver & Boyd.

EVERSON, C.S., MOLEFE, G.L., & EVERSON, T.M. (1998). Monitoring and modelling components of the water balance in a grassland catchment in the summer rainfall area of South Africa. WRC Report No. 493/1/98. WRC, Pretoria.

EVERSON, C.S., MOODLEY, M., GUSH, M., JARMAN, C., GOVENDER, M. & DYE, P. (2006). Can effective management of riparian zone vegetation significantly reduce the cost of catchment management and enable greater productivity of land resources. WRC Report No, K5/1284, Water Research Commission, Pretoria.

ESSINGTON, M.E. (2004). Soil and Water Chemistry: An Intergrative Approach. CRC press.

FREEZE, R.A., & HARLAN, R.L. (1969). Blueprint for a physically-based, digitally- simulated hydrological response model. Journal of Hydrology, 9(3), 237-258.

FRITSCH, E., and FRITZPATRICK, R.W. (1994). Interpretation of soil features produced by ancient and modern processes in degraded landscapes: 1. A new Method for Constructing Conceptual Soil-Water-Landscape models. Australian Journal of Soil Research 32:889-907.

GALFI and KOVACS (1981), in SZABó, N. P., KORMOS, K., & DOBRóKA, M. (2015). Evaluation of hydraulic conductivity in shallow groundwater formations: a comparative study of the Csókás' and Kozeny–Carman model. *Acta Geodaetica et Geophysica*, 1-17.

GARDNER, R., and WHITNEY, R. S. (1943a). *Soil Sci.* 56 (63).

GARDNER, R., and WHITNEY, R. S. (1943b). *Soil Sci.* 55 (127).

GILE, L.H. (1961). A classification of ca horizons in soils of a desert, Dona-Ana County, New Mexico. *Soil Sci. Soc. Am. Proc*. 25: 52-61.

GILE, L.H., PETERSON, F.F., GROSSMAN. R.B. (1966). Morphological and genetic sequences of carbonate accumulation in desert soils. *Soil Sci*., 101:5, 347-360.

GOOGLE, Inc., Google Earth software, http://earth.google.com/.

GUPTA, R. K., BHUMBLA, D. K., and ABROL, I. P. (1984). EFFECT OF SODICITY, pH, ORGANIC MATTER, AND-CALCIUM CARBONATE ON THE DISPERSION BEHAVIOR OF SOILS. *Soil Science*, 137 (4), 245-251.

HAISE, H. R., DONNAN, J. T., PHELAN, L.F., & SHOCKLEY, D. G. (1956). The use of cylinder infiltrometers to determine the intake characteristics of irrigated soil. USDA-ARS and USDA SCS, ARS 41-7. Gov. Print. Office, Washington, DC.

HARMSE, H. J. van M. (1963). The sedimentary petrology of the aeolian sands in the North-Western Orange Free State. M.Sc. Thesis, P.U. for C.H.E., Potchefstroom.

HENSLEY, M., BOTH, J.J., ANDERSON, J.J., VAN STADEN, P.P., & DU TOIT, A. (2000). Optimizing Rainfall Use Efficiency for Developing Farmers with Limited Access to Irrigation Water. WRC Report No. 878/1/00. Water Research Commission, Pretoria.

HENSLEY, M., LE ROUX, P.A.L., DU PREEZ, C., VAN HUYSSTEEN, C.S., KOTZE,E. & VAN RENSBURG, L. (2012). SOILS: THE FREE STATE'S AGRICULTURAL BASE, South African Geographical Journal, 88:1, 11-21.

HILL, J.N.S., & SUMNER, M.E. (1967). Effect of bulk density on moisture characteristics of soil. Soil Science, 103(4), 234-238.

HILLEL, D., (1980 a). Fundamentals of soil physics. Academic press, New York.

HILLEL, D. (1980 b). Soil structure and aggregation. *Introduction to soil physics*, 40-52.

HOFFMAN, T. & TODD, S. (1999). The South African environment and land use. In land degradation in South Africa. Open Access, University of Cape Town.

HOLE, F. D. (1978). An approach to landscape analysis with emphasis on soils. Geoderma, 21(1), 1-23.

HUTSON, J.L. (1984). Estimation of hydrological properties of South African soils. University of Natal, Pietermaritzburg, Department of Soil Science and Agrometeorology.

JACOBS, M.P., WEST, L.T. & SHAW, J.N. (2002). Redoximorphic features as indicators of seasonal saturation, Lowndes County, Georgia. *Soil Sci. Soc. Am. J.* 66, 315-323.

JARVIS, N. J., LEEDS-HARRISON, P. B., & Dosser, J. M. (1987). The use of tension infiltrometers to assess routes and rates of infiltration in a clay soil. *Journal of soil science*, *38*(4), 633-640.

JARVIS, N. J., & MESSING, I. (1995). Near-saturated hydraulic conductivity in soils of contrasting texture measured by tension infiltrometers. Soil Science Society of America Journal, 59(1), 27-34.

JENNY, H. (1980). The Soil Resource: Origin and Behaviour, Ecological Studies No. 37. Springer, New York.

JURY, W., GARDENER, W.R., AND GARDNER, W.H. (1991). Soil Physics (5th Ed.). John Wiley & Sons, New York.

KING, L. C. (1963). South African Scenery (3rd edition). Oliver and Boyd. Edin.

KLUTE, A., & DIRKSEN, C. (1986). Hydraulic conductivity and diffusivity: Laboratory methods. P.687-734. In A. Klute (ed.) Methods of soil analysis. Part1. 2nd ed. Agron. Monogr. 9. ASA and SSSA Madison, WI.

KUENENE, B.T., Van HUYSSTEEN, C.W., LE ROUX, P.A., and HENSLEY, M. (2011). Facilitating interpretation of the Cathedral Peak VI catchment hydrograph using soil drainage curves. South African Journal of Geology 114:525-234.

KUENENE, B.T. (2013). Hillslope hydropedology of the Two Streams ctahcment in KwaZulu-Natal. PhD Dissertation, University of the Free State, Bloemfontein.

KUENENE, B.T., LE ROUX, P.A.L., EVERSON, C.S. and HENSLEY, M. (2013). Hydraulic conductivity and macroporosity of diagnostic horizons in the Two Streams first order catchment in Kwazulu-Natal. Under peer review in WATER SA Journal.

KUENENE, B, T., LE ROUX, P.A.L., EVERSON, C, S., and HENSLEY, M. (2014 a). Hillslope water flowpaths and storage for an Acacia mearnsii dominated catchment in Kwazulu-Natal. Paper under review in Southern African Forestry journal.

KUENENE, B. T., LE ROUX, P.A. L., EVERSON, C. S. & HENSLEY, M. (2014 b). The importance of *in situ* measurements of hydraulic conductivity in the quantification of hydrological processes. Paper under review in Water SA.

KUITLEK, M. & NIELSON, R. D. (1994). Soil hydrology. Catena Verlag. Cremlingen-Drestedt, Germany.

KUITLEK, M. (2004). Soil water in the system of hydropedology. Lecture and proceedings. EUROSOIL congress, Freiburg, Germany. 4-12 September 2004. CD.

LAND TYPE SURVEY STAFF. (1972-2006). Land type Soil and Terrain Inventories from Northern Cape, Free State, North West, Gauteng, Kwazulu-Natal and Eastern Cape provinces. Land type survey database of South Africa. *Mem*. *Agric.Nat.Resour*. *S. Afr*. ARC-ISCW, Pretoria.

LILI, M., BRALTS, V. F., YINGHUA, P., HAN, L. & TINGWU, L. (2008). Methods for measuring soil infiltration: State of the art, *Int J Agric & Biol Eng.* **1** (1), 22-30.

LIN, H. (2003). Linking Properties of Soil Formation and Flow Regimes. *Dept. of Crop and Soil Sciences, The Pennsylvania State Univ., University Park, PA 16802, USA.*

LIN, H., WHEELER, D., BELL, J., WILDING, L. (2005). Assessment of soil spatial variability at multiple scales. *Ecological Modelling* 182, 271-290.

LIN, H.S., KOGELMAN, W., WALKER, C. & BRUNS, M.A. (2006). Soil moisture patterns in a forested catchment: A hydropedological perspective. *Geoderma* 131, 345 – 368.

LIN, H. S. (2010). Earth's critical zone and hydropedology: concepts, characteristics and advances. *Hydrol.Earth Syst. Sci.,* 14. 25-45.

LIN, H. S. (Ed.) (2012). Hydropedology: Synergistic intergration of soil science and hydrology. Academic Press.

LECO*.* (*2004*). LECO ChromaTof Help Version 2.22*. Mönchengladbach, Germany: LECO Corporation.*

LE ROUX, P.A.L., J.J. VAN TOL, B.T. KUENENE, M. HENSLEY, S.A. LORENTZ, C.S. EVERSON, C.W. VAN HUYSSTEEN, E. KAPANGAZIWIRI, & E. RIDDELL. (2011). Hydropedological interpretations of the soil of selected catchments with the aim of improving the efficiency of hydrological models. WRC Report No.: 1748/1/10. WRC, Pretoria.

LE ROUX, P.A.L., M.J. DU PLESSIS, D.P. TURNER, J. VAN DER WAALS, & H.B. BOOYENS. (2013). FIELD BOOK For the classification of South African soils. SASSO. Reach Publishers. Wandsbeck.

LE ROUX, P.A.L., J.J., VAN TOL, G.M. VAN ZIJL, B.T. KUENENE, M. HENSLEY, S.A. LORENTZ, D. BOUWER, M. TINNEFELD, C.C. JACOBS, & C.S. FREEZE. (2015). HOSASH (Hydrology of South Arican Soils and Hillsopes). WRC Report No.: K5/2021. WRC, Pretoria.

LUXMOORE, R. J. (1981). Micro-, meso-, and macroporosity of soil. *Soil Sci. Soc. Am. J.* 45, 671 – 672.

MARSMAN, B.A., J. J. DE GUIJTER. (1986). Quality of soil maps, a comparison of soil survey methods in a study area. Soil Survey papers no. 15. Wageningen, Netherlands Soil Survey Institute.

MARSHALL, T. J. (1959). Relationship between water and soil.

MCDONNELL, J. J. (1990). A rational for old water discharge through macropores in a steep, humid catchment. *Water Resour. Res.* 26, 2821 – 2832.

McGUIRE, K.J. & MCDONNELL, J.J. (2006). A review and evaluation of catchment transit time modeling. *Journal of Hydrology*, *330*(3), 543-563.

MESSING, I. (1989). Estimation of the saturated hydraulic conductivity in clay soils from soil moisture retention data. Soil Science Society of America Journal, 53(3), 665-668.

MEYER, P.D., & GEE, G.W. (1999). Flux-based estimation of field capacity. *Journal of Geotechnical and Geoenvironmental Engineering*, 125(7), 595-599.

MORGAN, M. G., & HENRION, M. (1990). Uncertainty: A Guide to Dealing with Uncertainty in Quatntiative Risk and Policy Analysis. Cmabridge University Press, New York.

Munsell Color Company. (1980). Munsell book of color. Munsell Color, Baltimore.

National Water Act (Act 36 of 1998). (NWA), as per section 5(1).

PAIGET, J. E. H. (1963). Coarse fraction mineralogy and granilometry of selected soil of the Western O.F.S. D.Sc. Thesis, U.O.F.S., Bloemfontein.

PERROUX, K. M. & WHITE, I. (1988). Design for disc permeameters. *Soil Sci. Soc. Am. J.* 52, 1205 – 1212.

PIPUJOL, M.D. & BUURMAN, P. (1997). Dynamics of calcium carbonate and iron redistribution and palaeohydrology in the middle Eocene aeolian paleosols of the Southeast Ebro Basin Margin. (Catalonia, northeast Spain). *Palaeogeography, Palaeoclimatology, Palaeoecology* 134, 87-107.

PHILLIPS, I.R. and M. GREENWAY, (1998). Changes in water soluble and exchangeable ions, cation exchange capacity, and phosphorus$_{max}$ in soils under alternating waterlogged and drying conditions. Communication in Soil Science and Plant Analysis 29:51-65.

PUPISKY, H., and SHAINBERG, I. (1979). Salt effects on the hydraulic conductivity of a sandy soil. *Soil Science Society of America Journal*, *43*(3), 429-433.

RAWLS, W. J., AHUJA, L. R. and BRANENSIEK, D. L. (1992). Estimating soil hydraulic properties from soil data. In M. Th. Van Genuchten et al (ed.) indirect methods for estimating the hydraulic properties of unsaturated soils. Univ. of California, Riverside.

REYNOLDS, W. D., ELRICK, D. E., & TOPP, G. C. (1983). A re-examination of the constant head well permeameter method for measuring saturated hydraulic conductivity above the water table. Soil Sci.136, 4:250-268.

REYNOLDS, W.D. and ELRICK, D.E. (1991). Determination of hydraulic conductivity using a tension infiltrometer. Soil Sci. Soc. Am J, 55: 633-639

SCHULZE, R.E. (1995). Hydrology and Agrohydrology: A text to accompany the ACRU 3.00 Agrohydrological Modelling system. WRC Report No 63/2/84. WRC, Pretoria.

SCHWERTMANN, U. (1985). The effect of pedogenic environments on iron oxide minerals. *Advances in Soil Science* 1:171-200.

SCHOENBERGER, P.J., & WYSOCKI, D.A. (2005). Hydrology of soils and deep regolith: A nexus between soil geography, ecosystems and land management. Geoderma 126:117–128.

SEATZ, L. F. & PETERSON, H. B. (1964). Acid, Alkaline, Saline, and Sodic Soils. Department of Agronomy, University of Tennessee, Knoxville, and Department of Agronomy, Utah State University, Logan, USA. In BEAR (1964). Chemistry of the Soil. 2nd Ed. Reinhold Publishing Corporation, New York.

SIVAPALAN, M. (2003 a). Prediction in ungauged basins: a grand challenge for theoretical hydrology. Hydrol. Process., 17, 3163 – 3170.

SIVAPALAN, M., (2003 b). Process complexity at hillslope scale, process simplicity at the watershed scale: is there a connection? Hydrol. Process., 17, 1037 – 1041.

SIVAPALAN, M., TAKEUCHI, K., FRANKS, S.W., GUPTA, V.K., KARAMBIRI, H., LAKSHMI, V., LIANG, X., MCDONNELL, J.J., MENDIONDO, E. M., O'CONNELL, P.E., OKI, T., POMEROY, J.W., SCHERTZER, D., UHLENBROOK, S., & ZEHE, E., (2003). IAHS

decade on prediction in ungauged basins (PUB), 2003 – 2012: Shaping an exciting future for the hydrological sciences. Hydrol. Sci. J., 48, 857 – 880.

SMITH, K. & VAN HUYSSTEEN, C. W. (2011). The effect of degree and duration of water saturation on selected redox indicators: pe, Fe^{2+} and Mn^{2+}. South African Journal of Plant and Soil 28:2, 119-126.

SOIL CALSSIFICATION WORKING GROUP. (1991). Soil Classification – A taxonomic system for South Africa. *Mem .agric. Nat. Resour. S. Afr.* No. 15. Dept. Agric. Dev., Pretoria.

SOULSBY, C., TETZLFF, D., RODGERS, P., DUNN, S., & WALDRON, S. (2006). Runoff processes, stream water residence times and controlling landscape characteristics in a mesoscale catchment: An initial evaluation. *J. Hydrol.* 325, 197-221.

South African Weather Services (Data accessed 10 August 2014). www.saws.co.za/hopetown/northerncape.

SöHNGE, P. G., & VISSER, D. J. L. (1937). The Geology and Archeology of the Vaal River Basin. Geol. Sur. Mem. No. 35. Dept. of Mines, Union of S.A. I: 5-59. Govt. Printer, Pretoria.

STOCKTON, J.G., & WARRICK, A.W. (1971). Spatial variability of unsaturated hydraulic conductivity. Soil. Sci. Soc. Am. Proc. 35: 847:848.

TOMASELLA, J., PACHEPSKY, Y.A., CRESTANA, S., & RAWLS, W.J. (2003). Comparison of two techniques to develop pedotransfer functions for water retention. *Soil Science Society of America Journal*, *67*(4), 1085-1092.

TANI, M. (1997). Runoff generation processes estimated from hydrological observations on a steep forested hillslope with a thin soil layer. *Journal of Hydrology,* 200, 84-109.

THE NON-AFFILIATED SOIL ANALYSIS WORK COMMITTEE (1990). Handbook of standard soil testing methods for advisory purposes. *Soil Science Society of South Africa,* Pretoria.

THOMPSON, J.G. (1965). The soil of Rhodesia and their classification. Ph. D. Thesis, Univ. of Natal, Pietermaritzburg.

TICEHURST, J.L., CRESSWELL, H.P., McKENZIE, N.J., & CLOVER, M.R. (2007). Interpreting soil and topographic properties to conceptualise hillslope hydrology. *Geoderma* 137, 279-292.

TROMP-VAN MEERVELD, H.J., & McDonnell, J.J., (2006). Threshold relations in subsurface stormflow:2. The fill and spill hypothesis. Water Resources Research, 42(2).

TULLER, M., & OR, D. (2002). Unsaturated hydraulic conductivity of structured porous media. A review. Vadose Zone J. 1, 14-37.

TURNER, D.P. (1976). A study of water infiltration into soils. M.Sc. University of Natal.

TURNER, D.P. (1991). A procedure for describing soil profiles. ARC-ISCW report No. GB/A/91/67. ARC-ISCW, Pretoria.

UHLENBROOK, S., WENNINGER, J. & LORENTZ, S. (2005). What happens after the catchment caught storm? Hydrological processes at the small, semi-arid Weatherley catchment, South-Africa. Advances in Geosciences 2, 237 - 241.

VAN ALPHEN, B.J., BOOLTINK, H.W.G.M., & BOUMA, J. (2001). Combining pedotransfer functions with physical measurements to improve the estimation of soil hydraulic properties. Geoderma. 103, 133-147.

VAN BEERS, W. F. (1983). The auger hole method. A field measurements of the hydraulic conductivity of soil below the water table. International Institute for Land Reclamation and Improvement/ILRI, Wageningen, The Netherlands.

VAN DER MERWE, C.R. (1962). Soil Groups and Sub-Groups of South Africa. Bull. 231. Dept. Agric. Forestry, Pretoria (2nd edition).

VAN DER MERWE, C.R. (1954). Kalahari and Sahara sandy soils. Trans. 5th intern. Congr. Soil Sci. IV:117-122.

VAN DER SLUIJS, P., & DE GRUIJTER, J. J. (1985). Water table classes: a method to describe seasonal fluctuation and duration of water tables on Dutch soil maps. *Agricultural water management*, *10*(2), 109-125.

VAN GENUCHTEN, M. (1980): A closed-form equation for predicting the hydraulic conductivity of unsaturated soils. *Soil Sci. Soc. Am. J.* 44:892-898.

VAN GENUCHTEN, M.T., LEIJ, F.J., and YATES, S.R. (1991). The RETC code for quantifying the hydraulic functions of unsaturated soils. Rep. EPA/600/2-91/062. R.S. Kerr Environmental Research Laboratory, USEPA, Ada, OK.

VAN GENUCHTEN, M.T.H., & LEIJ, F.L. (1992). On estimating the hydraulic conductivity properties of unsaturated soils. In M. Th. van Genuchten, F.J. Leij, & L.J. Lund. Eds. Indirect methods for estimating the hydraulic properties of unsaturated soils. Proc. Int. Workshop. Riverside, California. 11-13 October, 1989. University of California.

VAN HUYSSTEEN, C.W. (1995). The relationship between subsoil colour and degree of wetness in a suite of soils in the Grabouw district, Western Cape. Characterization of colour-defined horizons. M.Sc. University of Stellenbosch, South Africa.

VAN HUYSSTEEN, C.W., and ELLIS, F. (1997). The relationship between subsoil colour and degree of wetness in a suite of soils in the Grabouw district, Western Cape. Characterization of colour-defined horizons. *South African Journal of Plant and Soil*, *14*(4), 149-153.

VAN HUYSSTEEN, C.W., HENSLEY, M., LE ROUX, P.A., ZERE, T.B., & DU PREEZ, C. C. (2005). The relationship between soil water regime and soil profile morphology in the Weatherley catchment, An afforestation area in the Eastern Cape. WRC Report 1317/1/05, Water Research Commission, Pretoria.

VAN HUYSSTEEN, C.W. (2008). A review of advances in hydropedology for application in South Africa: review article. *S. Afr. J. Plant & Soil*, *25*(4), 245-253.

VAN HUYSSTEEN, C.W., ZERE, T.B., Hensley, M. (2009a). Soil water variability in the Weatherly grassland catchment, South Africa: I. Evapotranspiration *S. Afr. J. Plant & Soil*, 26(3).

VAN HUYSSTEEN, C.W., ZERE, T.B., Hensley, M. (2009b). Soil water variability in the Weatherly grassland catchment, South Africa: II. Soil water content *S. Afr. J. Plant & Soil*, 26 (3).

VAN HUYSSTEEN, C.W., LE ROUX, P.A.L., HENSLEY, M., and LORENTZ, S.A. (2010). Soil-water relationships in the Weatherly catchment, South Africa. Water SA. 36: 521-530.

VAN HUYSSTEEN, C.W., P.A.L. LE ROUX, M. HENSLEY, & T.B.ZERE. (2013 a). Duration of water saturation in selected soils of Weatherly, South Africa. *S. Afr .J. Plant & Soil*, 24:3, 152-160.

VAN HUYSTEEN, C.W. (2013). Hydrological classification of orthic A horizons in Weatherly, South Africa. *S. Afr .J. Plant & Soil* 29(2)101-107.

VAN HUYSSTEEN, C.W., TURNER, D.P. & LE ROUX, P.A.L. (2013 b). Principles of soil classification and the future of the South African system. S*. Afr. J. Plant & Soil*, 30(1): 23–32.

VAN ROOYEN, T.H. (1971). Soil of the central Orange River Basin. D. Sc. Thesis, U.O.F.S., Bloemfontein.

VAN TOL, J.J., LE ROUX, P.A.L., & HENSLEY, M. (2010 a). Soil indicators of hillslope hydrology in Bedford catchment. *S. Afr .J. Plant & Soil 27(3)* 242-251.

VAN TOL, J.J., LE ROUX, P.A.L., HENSLEY, M., & LORENTZ, S.A. (2010 b). Soil as indicator of hillslope hydrological behaviour in the Weatherly Catchment, Eastern Cape, South Africa. *Water SA 36(5).*

VAN TOL, J.J., LE ROUX, P.A.L., & LORENTZ, S.A. (2011 a). From genetic soil horizons to hydropedological functional units. http://www.ru.ac.za/static/institutes/iwr/SANCIAHS/2012/documents/054_Van_Tol.pdf.

VAN TOL, J.J., LE ROUX P.A.L., & HENSLEY, M. (2011 b). Soil Indicators of Hillslope Hydrology, Principles, Application and Assessment in Soil Science, Dr. Burcu E. Ozkaraove Gungor (Ed.); 12 (209-240).

VAN TOL J.J., LE ROUX, P.A.L., & HENSLEY, M. (2012). Pedotransfer functions to determine water conducting macroporosity in South Africa. Water Science & Technology. 65.3, 550-557.

VAN TOL, J.J., LE ROUX, P.A.L., & HENSLEY, M. (2013 a). Pedological criteria for estimating the importance of subsurface lateral flow in E horizons in South African soils.

VAN TOL, J.J., LE ROUX, P.A.L., LORENTZ, S.A. & HENSLEY, M. (2013 b). Hydropedological classification of South African hillslopes. Vadose Zone J. 12 (4) DOI:10.2136/vzj2013.01.0007.

VAN ZIJL, G.M. (2013). Developing a digital soil mapping protocol for Southern Africa using case studies. PhD, UFS Dept. Soil, Crop and Climate Sciences.

VAN ZIJL, G.M., LE ROUX, P.A.L., & TURNER, D.P. (2013). Disaggregation of land types using terrain analysis, expert knowledge and GIS methods. South African Journal of Plant and Soil, 30:3, 123-129.

VAN ZIJL, G.M., and LE ROUX, P.A.L. (2014). Creating a conceptual hydrological soil response map for the Stevenson Hamilton Research Supersite, Kruger National Park, South Africa. *WaterSA* 40, 331 – 336.

VEREECKEN, H., DIELS, J., VAN ORSHOVEN, J., FEYEN, J., & BOUMA, J. (1992). Functional evaluation of pedotransfer functions for the estimation of soil hydraulic properties. *Soil Science Society of America Journal*, *56*(5), 1371-1378.

WAGENER T., SIVAPALAN M., TROCH P. & WOODS R. (2007). Catchment classification and hydrologic similarity. Geography Compass, 1, 901 – 931.

WATSON, K. W., & LUXMOORE, R. J. (1986) Estimating macroporosity in a forested watershed by use of a tension infiltrometer. Soil. Sci. Soc. Am. J. 50: 578-582.

WEBSTER, R. (2000). Is soil variation random? Geoderma 97, 149-163. Proposal Number: 1001948 Page 16 of 18.

WEBSTER, R., & BECKETT, P.H.T. (1968). Quality and usefulness of soil maps. *Nature*, *219*, 680-682.

WENNINGER, J., UHLENBROOK, S., LORENTZ, S. & LEIBUNDGUT, C., (2008). Identification of runoff generation processes using combined hydrometric, tracer and geophysical methods in a headwater catchment in South Africa. Journal des Sciences Hydrologiques 53, 65-80.

WEILER, M. and MCDONNELL, J., (2004). Virtual experiments: a new approach for improving process conceptualization in hillslope hydrology. *J. Hydrol.* 285, 3 – 18.

WEILER M., MCDONNELL J.J., TROMP-VAN MEERVELD I.L.J.A., & UCHIDA T. (2005). Subsurface Stormflow. Encyclopedia of Hydrological Sciences. John Wiley & Sons, Ltd.

WILLMOTT, C. J., ACKLESON, S. G., DAVIS, R. E., FEDDEMA, J. J., KLINK, K. M., LEGATES, D. R., ... & ROWE, C. M. (1985). Statistics for the evaluation and comparison of models. Journal of Geophysical Research: Oceans (1978–2012), 90(C5), 8995-9005.

WöSTEN, J. H. M., BOUMA, J., & STOFFELSEN, G. H. (1985). Use of soil survey data for regional soil water simulation models. *Soil Science Society of America Journal*, *49*(5), 1238-1244.

Appendix A

Land Types

LAND TYPE / *LANDTIPE* : **Ae15**

CLIMATE ZONE / *KLIMAATSONE* : S571S

Area / *Oppervlakte* : 322010 ha

Estimated area unavailable for agriculture
Beraamde oppervlakte onbeskikbaar vir landbou : 422000 ha

Occurrence (maps) and areas / *Voorkoms (kaarte) en oppervlakte* :
2824 Kimberley (168210 ha) 2922 Prieska (47090 ha)
2924 Koffiefontein (102500 ha)

Inventory by / *Inventaris deur* :
J F Eloff

Modal Profiles / *Modale profiele* :
P231 P232 P234
67 68 70

Terrain unit / *Terreineenheid*	1	3	4	5
% of land type / *% van landtipe*	10	9	82	5
Area / *Oppervlakte (ha)*	32201	28981	264048	16100
Slope / *Helling (%)*	1 - 4	0 - 40	0 - 2	0 - 2
Slope length / *Hellingslengte (m)*	0 - 300	150 - 600	0 - 2000	50 - 200
Slope shape / *Hellingsvorm*	Z	Y	Z	Z
MB0, MB1 (ha)	0	0	227081	7245
MB2 - MB4 (ha)	32201	28981	63372	8855

Soil series or land classes *Grondseries of landklasse*	**Depth** *Diepte* (mm)	MB	1 ha	1 %	3 ha	3 %	4 ha	4 %	5 ha	5 %	**Total** *Totaal* ha	**Total** *Totaal* %	**Clay content %** *Klei-inhoud %* A	E	B21	Hor	**Texture** *Tekstuur* Class / *Klas*	*Diepte-beperkende materiaal*
Soil-rock complex																		
Grond-rotskompleks:																		
Rock/Rots		4	28981	90	24634	85					53615	16.7						
Mispah Ms10, Mangano Hu33	100-250	3	1932	6	2898	10					4830	1.5	4-10		6-15	A	fiSa	R
Glendale Sd21, Bakklysdrift Ss13, Craven Va21	100-250	2	1288	4	1449	5					2737	0.9	8-15		35-45	B	fiSaCl	vr,pr
Mangano Hu33, Zwartfontein Hu34	700-1200+	0					203317	77			203317	63.1	4-10		6-15	B	fi/meSa-LmSa	R,ka
Kalkbank Ms22, Mangano Hu33	0-450	3					47529	18	8855	55	56384	17.5	4-10		6-15	A	fiSa-LmSa	ka
Annandale Cv33, Makuya Cv34, Blinkklip Cv36	600-1200+	0					13202	5			13202	4.1	4-12		6-20	B	fi/meSa-SaLm	R,ka
Lindley Va41, Nyoka Sw41	100-300	0					5281	2	4025	25	9306	2.9	8-20		60-65	B	fiSaCl	R
Craven Va21, Bakklysdrift Ss13, Broekspruit Sw21	100-300	3					7921	3			7921	2.5	8-15		56-75	B	fiSaCl	vr,pr
Mispah Ms10	100-450	3					7921	3			7921	2.5	4-10			A	fiSa	R
Shorrocks Hu36	600-1200	0					5281	2			5281	1.6	8-15		15-25	B	fiSaLm-SaClLm	R,ka
Dundee Du10, Killarney Ka20	450-900	0							3220	20	3220	1.0	15-40			A	fiSaLm-SaCl	R

Terrain type / *Terreintipe* : A3

For an explanation of this table consult LAND TYPE INVENTORY (table of contents)
Ter verduideliking van hierdie tabel kyk LANDTIPE - INVENTARIS (inhoudsopgawe)

Geology: Red to flesh-coloured wind-blown sand of Tertiary to Recent age, with dolerite outcrops.

Geologie: Rooi tot vleeskleurige waaisand van Tersiere tot Resente ouderdom, met doleriet dagsome.

10 November 2006 1

Figure Appendix 1 Land type data of Land Type Ae15.

LAND TYPE / *LANDTIPE* : **Ae277**

CLIMATE ZONE / *KLIMAATSONE* : 1309S

Area / Oppervlakte : 6610 ha

Estimated area unavailable for agriculture

Beraamde oppervlakte onbeskikbaar vir landbou : 25 ha

Occurrence (maps) and areas / *Voorkoms (kaarte) en oppervlakte :*

2922 Prieska (6610 ha)

Inventory by / *Inventaris deur :*

BC Geers & RW Bruce

Modal Profiles / *Modale profiele :*

None / Geen

Terrain unit / *Terreineenheid*	3	4	5
% of land type / *% van landtipe*	15	80	5
Area / *Oppervlakte (ha)*	992	5288	330
Slope / *Helling (%)*	3 - 4	0 - 2	1 - 2
Slope length / *Hellingslengte (m)*	300 - 1000	2000 - 4000	50 - 200
Slope shape / *Hellingsvorm*	Z	Z-X	Z-X
MB0, MB1 (ha)	228	3331	264
MB2 - MB4 (ha)	763	1957	66

Soil series or land classes *Grondseries of landklasse*	**Depth** *Diepte* (mm)	MB	ha	%	ha	%	ha	%	**Total** *Totaal* ha	%	**Clay content %** *Klei-inhoud %* A	E	B21	Hor	**Texture** *Tekstuur* Class / *Klas*	**Depth limiting material** *Diepte-beperkende materiaal*
Rock / Rots		4	188	19			13	4	202	3.1						
Mangano Hu33, Zwartfontein Hu34, Shorrocks Hu36	>600	0	198	20	3014	57	165	50	3378	51.1	5-10		6-20	B	Lmfi/meSa-SaLm	R
Mangano Hu33, Zwartfontein Hu34, Shorrocks Hu36	100-300	3	446	45	1110	21	33	10	1590	24.1	5-10		6-20	B	Lmfi/meSa-SaLm	R
Mispah Ms10, Kalkbank Ms22	50-200	3	129	13	846	16	20	6	995	15.1	3-10			A	fiSa-LmSa	R,ka
Annandale Cv33, Sunbury Cv30	>600	0	30	3	317	6	79	24	426	6.5	2-10		2-10	B	fiSa-LmSa	R,ka
Rockford Oa14, Leeufontein Oa16	>1200	0					20	6	20	0.3	5-10		10-20	B	LmmeSa-SaLm	R,ka

Terrain type / *Terreintipe* : A2

Terrain form sketch / *Terreinvormskets*

For an explanation of this table consult LAND TYPE INVENTORY (table of contents)

Ter verduideliking van hierdie tabel kyk LANDTIPE - INVENTARIS (inhoudsopgawe)

Geology: Alluvium, sand and calcrete deposits overlying andesite (Allanridge Formation) and also conglomerate and sandstone (Bothaville Formation), both Formations belonging to the Ventersdorp Supergroup.

Geologie: Alluvium, sand en kalkreetafsettings op andesiet (Formasie Allanridge) asook konglomeraat en sandsteen (Formasie Bothaville) albei van die Supergroep Ventersdorp.

10 November 2006

1

Figure Appendix 2 Land type data of Land Type Ae277.

LAND TYPE / *LANDTIPE* : **Ae276**

CLIMATE ZONE / *KLIMAATSONE* : 1168S

Area / *Oppervlakte* : 136740 ha

Estimated area unavailable for agriculture

Beraamde oppervlakte onbeskikbaar vir landbou : 550 ha

Occurrence (maps) and areas / *Voorkoms (kaarte) en oppervlakte* :

2922 Prieska (130200 ha) 2924 Koffiefontein (6540 ha)

Inventory by / *Inventaris deur* :

RW Bruce & BC Geers

Modal Profiles / *Modale profiele* :

P43

6139

Terrain unit / *Terreineenheid*	1	3	4	5
% of land type / *% van landtipe*	6	16	75	3
Area / *Oppervlakte (ha)*	8204	21878	102555	4102
Slope / *Helling (%)*	0 - 2	2 - 3	0 - 1	0 - 1
Slope length / *Hellingslengte (m)*	200 - 500	500 - 1000	1000 - 4000	50 - 500
Slope shape / *Hellingsvorm*	Y	Y-Z	Z-X	Z-X
MB0, MB1 (ha)	1231	7657	62559	2995
MB2 - MB4 (ha)	6974	14221	39996	1108

Soil series or land classes *Grondseries of landklasse*	**Depth** *Diepte* (mm)	MB	ha	%	ha	%	ha	%	ha	%	**Total** *Totaal* ha	%	**Clay content %** *Klei-inhoud %* A	E	B21	Hor	**Texture** *Tekstuur* Class / *Klas*	*Diepte-beperkende materiaal* **Depth limiting material**
Rock / Rots		4	820	10	1313	6					2133	1.6						
Mangano Hu33, Shorrocks Hu36	500-1000	0	1231	15	7657	35	57431	56	697	17	67016	49.0	5-10		6-20	B	fiSa-SaLm	R,ka
Mangano Hu33, Shorrocks Hu36	100-300	3	3446	42	6782	31	31792	31	410	10	42430	31.0	5-10		6-20	B	fiSa-SaLm	ka,db
Mispah Ms10, Loskop Ms12	10-200	3	2707	33	6126	28	8204	8	697	17	17735	13.0	6-10			A	LmfiSa	R,ka
Valsrivier Va40, Craven Va21, Malakata Sw40, Broekspruit Sw21	600-1200	0					4102	4	943	23	5046	3.7	15-30		30-45	B	SaClLm-ClLm	R,so,ca
Vaalbank Cv43, Dudfield Cv46	600-1200	0					1026	1			1026	0.8	6-10		10-20	B	LmfiSa-SaLm	ca,ka
Pans/Panne:																		
Killarney Ka20	500-1000	0							1354	33	1354	1.0	20-30		45-60	B	Cl	gc

Terrain type / *Terreintipe* : A2

Terrain form sketch / *Terreinvormskets*

For an explanation of this table consult LAND TYPE INVENTORY (table of contents)

Ter verduideliking van hierdie tabel kyk LANDTIPE - INVENTARIS (inhoudsopgawe)

Geology: Deposits of aeolian sand, alluvium and calcrete underlain by andesite (Allanridge Formation) and tillite and mudstone (Dwyka Formation). Outcrops of andesite and tillite occur in places.

Geologie: Afsettings van eoliese sand, alluvium en kalkreet onderlê deur andesiet (Formasie Allanridge) en tilliet en moddersteen (Formasie Dwyka). Dagsome van andesiet en tilliet kom plek-plek voor.

Figure Appendix 3 Land type data of Land Type Ae276.

LAND TYPE / *LANDTIPE* : **Ia4**

CLIMATE ZONE / *KLIMAATSONE* : 931S

Area / *Oppervlakte* : 11420 ha

Estimated area unavailable for agriculture
Beraamde oppervlakte onbeskikbaar vir landbou : 320 ha

Occurrence (maps) and areas / *Voorkoms (kaarte) en oppervlakte* :
2824 Kimberley (8650 ha) 2924 Koffiefontein (2770 ha)

Inventory by / *Inventaris deur* :
J F Eloff

Modal Profiles / *Modale profiele* :
None / Geen

Terrain unit / *Terreineenheid*	1	3	4	5
% of land type / *% van landtipe*	1	1	80	18
Area / *Oppervlakte (ha)*	114	114	9136	2056
Slope / *Helling (%)*	0 - 2	8 - 35	0 - 1	0 - 3
Slope length / *Hellingslengte (m)*	50 - 200	100 - 300	500 - 2000	100 - 400
Slope shape / *Hellingsvorm*	Z	Z-X	Z	Z-X
MB0, MB1 (ha)	0	0	7948	1747
MB2 - MB4 (ha)	114	114	1188	308

Soil series or land classes *Grondseries of landklasse*	**Depth** *Diepte* (mm)	MB	ha	%	ha	%	ha	%	ha	%	**Total** *Totaal* ha	%	**Clay content %** *Klei-inhoud %* A	E	B21	Hor	**Texture** *Tekstuur* Class / *Klas*	**Depth limiting material** *Diepte-beperkende materiaal*
Soil-rock complex																		
Grond-rotskompleks:																		
Rock/Rots		4	80	70	74	65					154	1.4						
Mispah Ms10, Mangano Hu33, Shorrocks Hu36	100-250	3	23	20	23	20					46	0.4	8-20		10-25	A	LmfiSa-SaClLm	R
Glendale Sd21, Rasheni Bo21, Glengazi Bo31, Skilderkrans Sw11	150-250	3	11	10	17	15					29	0.3	10-40		35-55	B	fiSaCl	R
Limpopo Oa46, Jozini Oa36, Mutale Oa47, Koedoesvlei Oa37	900-1200+	0					3198	35	576	28	3773	33.0	10-20		15-40	B	fiSaLm-SaClLm	R
Lindley Va41, Sheppardvale Va42	200-300	0					1553	17	206	10	1759	15.4	10-25		40-60	B	fiSaCl-Cl	vp
Leeufontein Oa16, Letaba Oa26	900-1200+	0					914	10	308	15	1222	10.7	10-20		15-30	B	fiSaLm-SaClLm	R
Swartland Sw31, Nyoka Sw41, Omdraai Sw42	150-250	3					731	8			731	6.4	10-25		40-60	B	fiSaCl-Cl	so
Arniston Va31	200-300	0					731	8			731	6.4	10-25		35-55	B	fiSaCl	vp
Dundee Du10	>1200	0							555	27	555	4.9	15-50			A	fiSaLm-Cl	R
Valsrivier Va40, Herschel Va30	200-300	0					365	4	103	5	468	4.1	8-20		25-35	B	fiSaClLm	vp
Loskop Ms12, Kalkbank Ms22	150-300	3					457	5			457	4.0	10-25			A	LmfiSa-SaClLm	R,ka
Sterkspruit Ss26	150-250	0					274	3			274	2.4	15-20		40-55	A	fiSaLm	pr
Craven Va21, Marienthal Va22	200-300	0					274	3			274	2.4	10-25		40-60	B	fiSaCl-Cl	vr
Stanford Ss23	150-250	0					183	2			183	1.6	8-15		35-50	A	LmfiSa	pr
Mangano Hu33, Maitengwe Hu43	600-1200+	0					183	2			183	1.6	6-12		8-15	B	fiSa-LmSa	R,ka
Shorrocks Hu36, Shigalo Hu46	450-900	0					183	2			183	1.6	10-18		15-25	B	fiSaLm-SaClLm	R,ka
Dudfield Cv46, Vaalbank Cv43	600-1200+	0					91	1			91	0.8	6-18		8-25	B	fiSa-LmSa	R,ka
Stream beds/Stroombeddings		4							308	15	308	2.7						

LAND TYPE /*LANDTIPE*..... : Ia4 Continued / *Vervolg*

Terrain type / *Terreintipe* : A2

Terrain form sketch /*Terreinvormskets*

For an explanation of this table consult LAND TYPE INVENTORY (table of contents)

Ter verduideliking van hierdie tabel kyk LANDTIPE - INVENTARIS (inhoudsopgawe)

Geology: Shale and mudstone of the Dwyka Formation and Ecca Group with dolerite intrusions. Andesitic to basaltic lavas of the Ventersdorp Supergroup also occur.

Geologie: Skalie en moddersteen van die Formasie Dwyka en Groep Ecca met dolerietindringings. Andesitiese tot basaltiese lawas van die Supergroep Ventersdorp kom ook voor.

10 November 2006 2

Figure Appendix 4 Land type data of Land Type Ia4.

Appendix B

Soil profile description forms

Profile P1: Kimberley (*Ky*) 1100 (Taung)

Physical and Chemical description

The profile was classed as an orthic A / red apedal B with stone line / soft carbonate C /rock (Mudstone) horizon. Orthic A horizon is an accumulation of aeolian deposits. Orthic A has very weak subangular blocky medium ped formation. Transition to *re* is irregular and wavy, but clear. Colour in the dry state ranges from 7.5YR brown to 5Y white (*sc*). In the wet state 5YR yellowish red (*ob* and *ot*), reddish brown (*re*), 7.5YR brown (*sl*) and 5Y pale yellow (*sc*). Overall textural class is dominated by the sand fraction with highest in the *sc* (92.8%) to lowest in the *ot* (85.1%). The textural class of *ob* and *re* horizons are classed as medium sand and *ot, sl* and *sc* as fine sand. The coarse fraction of the *sl* (52.8 % by weight of sample) and *sc* (47.1% by weight of sample) is also considered as parent material, as well as influencing the hydrology and chemistry of these horizons. Clay percentage increase from *ob* to *ot* (4.3 to 6.75%) and from *re* to *sl* (4.4 to 6.7%). Decrease in clay is observed from *ot* to *re* and from *sl* to *sc* (2.3%). Bulk density (Db) is higher (1.66, 1.74 and 1.67 g cm^{-3}) for horizons (*ob, ot and re*) with low coarse fraction (< 5%) and lower for *sl* and *sc* (1.62 and 1.50 g cm^{-3}) with high coarse fractions. Db of *ot* is very high and is interpreted as compacted, however shows many fine and few coarse roots and common fine cracks. Precipitation of carbonates in the *ot* (3.61% of sample by weight) as free lime and *sc* (9.84% of sample by weight) as precipitated lime, do not show a trend with Db.

PH increases with horizons showing accumulation of carbonates such as *ot* (6.65 *ob to* 7.23 *ot*) and *sc* (7.71 *sl* to 8.16 *sc*). The pH also increases with vertical depth. Low organic carbon (OC 0.203%) and nitrogen (N 0.032%) are observed in the *ob*/*ot* transition. Sum of cation exchange capacity described by the base saturation % (BS) is overall high, close to or above saturation (from 77.68 in *sl* to 303.57 in *sc*). An increase in BS is observed in the *ot* (101.66) from *ob* (98.48) and *sl* to *sc*, with a decrease from *ot* to *re* (97.19) to *sl*. Cation exchange capacity (CEC $cmol_c$ kg^{-1} soil) increases vertically down the profile from

ob to *re* (5.93, 7.20, 7.82), decreasing in the *sl* (4.56) and increasing again in the *sc* (7.84). The largest contribution to the S value (sum of exchangeable cations) is calcium and magnesium (*ob*), with sodium contributing the least. Sodium increases from 0.03 to 0.06 $cmol_c\ kg^{-1}$ soil (*ob* to *ot*), decreasing from *ot* to *sl* (0.06 to 0.008 $cmol_c\ kg^{-1}$ soil) and increasing again in the *sc* to 0.08 $cmol_c\ kg^{-1}$ soil.

Table Appendix 1 Profile description of Profile P1, Kimberley soil form

Map/photo:		Soil form and family:	Ky (Taung) 1100
Latitude/Longitude	29°32'22.92"S / 23°57'34.07"E	Surface rockiness:	None
Altitude (m) :	1132	Occurrence of flooding:	None
Terrain unit:	Lower Midslope	Wind erosion:	Slight
Slope:	3%	Water erosion:	None
Slope shape:	Convex/Convex	Vegetation/Land use:	Virgin (DS/DD, HE3)
Aspect:	NE	Water table:	None
Microrelief:	Y Anthills/earthworm mounds	Described by:	Martin Tinnefeld
Parent Material Solum:	Aeolian	Date described (20yymmdd):	140131
Underlying Material:	SC3 Dwyka Tillite/Mudstone	Weathering of underlying material:	Physical (moderate) Chemical (weak)
Weather conditions:	SU	Alteration of underlying material:	Y (mudstone : hk)
Soil Temperature regime:	IH	Former Weather conditions:	WC2
Moisture regime:	AR		

Horizon	Depth (mm)	Description	Diagnostic horizon
Ob	0-10	Moisture status: moist; dry colour: 7.5YR5/4; moist colour: 5YR5/6; Sand; loose, non-sticky, non-plastic; slight wind erosion; <2mm weak surface sealing, fine, medium and wide surface cracks; 4.72% surface gravel (2-5mm), no visible OM embedded.	Surface
A	0-200	Moisture status: moist; dry colour: 7.5YR4/4; moist colour: 5YR4/6; Sand; apedal; massive, very weak sub-angular blocky ped formation; non-sticky; non-plastic; common, fine cracks; common fine, few coarse roots; 4.47% coarse fragments (2-5mm); free lime; clear transition.	Orthic A
B	300-800	Moisture status: dry; dry colour: 7.5YR4/3; moist colour: 5YR5/3; Sand; apedal; massive; no cracks; few fine roots; clear, wavy transition.	Red-apedal B
Sl	800-900	Moisture status: dry; dry colour: 7.5YR4/6; moist colour: 7.5YR4/4; Sand; apedal; massive; few fine and medium cracks; 52.8% coarse fragments (2-5 mm 80%, 25-75 mm 20%); few, fine roots; free lime; abrupt, wavy transition.	Stone line
C	900-1300	Moisture status: dry; dry colour: 5Y8/1; moist colour: 5Y7/3; gravel; angular; moderate, continuous carbonate cementation; few fine, coarse roots; physically moderate weathered 47.1% coarse fragments (2-25 mm); clear transition; single stone line at transition to r (10 mm); free lime, angular concretions < 2-6 mm; abrupt transition.	Soft carbonate B
R	1300+	Moisture status: dry; mudstone; continuous massive; hard.	Rock

Y – Yellow, YR – Yellow-red (Munsel colour); SU – sunny/clear, IH - Isohyperthermic, AR - Aridic, DS – semi deciduous dwarf shrub, DD – deciduous dwarf shrub, HE3 – extensive grazing, ranching, WC2 – no rain in the last week (FAO, 2006); hk – hardpan carbonate horizon, Ky – Kimberley soil form (SCWG, 1991)

Table Appendix 2 Physical and Chemical properties of a Kimberley soil P1

	Overburden (undisturbed)	Orthic (A horizon)	Red apedal (B horizon)	Stone line	Soft carbonate C horizon
	0-10 (mm)	0-200 (mm)	200-800 (mm)	800-900 (mm)	(900-1300 mm)
Physical properties					
Coarse sand (0-0.5 mm)	4	4.5	2.2	9.6	11.4
Medium sand (0.5-0.25 mm)	26.4	25.8	43.7	24.1	19.7
Fine sand (0.25-0.106 mm)	50.4	41.8	38.8	41	42.7
Very fine sand (0.106-0.05 mm)	7.6	13	6.2	10.6	19
Sand fraction texture	Medium Sand (88.4)	Fine Sand (85.1)	Medium Sand (90.9)	Fine Sand (85.3)	Fine Sand (92.8)
Coarse silt (0.05-0.02 mm)	2.7	3.8	3.2	2.1	1.5
Fine silt (0.02-0.002 mm)	2.4	2	0.5	3.5	3.4
Clay (>0.002 mm)	4.3	6.75	4.4	6.7	2.3
Total texture fraction	97.8	97.65	99	97.6	100
Texture	Sand	Sand	Sand	Sand	Sand
CO_3^- (% of sample removed before texture analysis)	0	3.61	0	0	9.84
Coarse fraction % of weight (>2 mm)	4.72	4.47	0	52.8	47.1
Bulk density (g cm^{-3})	1.66	1.74	1.67	1.62	1.50
Chemical properties					
pH (H_2O)	6.65	7.23	6.88	7.71	8.16
pH (KCL)	6.42	7.06	6.53	7.63	7.62
OC% (MIR)	0.203	-	-	-	-
N% (MIR)	0.032	-	-	-	-
Mn (mg kg^{-1}) plant available	-	4.4	5.5	-	-
Fe (mg kg^{-1}) plant available	-	3.9	5.4	-	-
Exchangeable cations ($cmol_c kg^{-1}$ soil)					
Calcium	1.69	5.08	5.92	3.41	20.98
Magnesium	3.60	1.80	1.47	1.02	2.62
Potassium	0.52	0.38	0.19	0.12	0.12
Sodium	0.03	0.06	0.04	0.008	0.08
CEC	5.93	7.20	7.82	5.87	7.84
S Value	5.84	7.32	7.6	4.56	23.8
BS (%)	98.48	101.66	97.19	77.68	303.57

Figure Appendix 5 Profile P1, Kimberley soil form.

Profile P2: Addo (*Ad*) 1211 (Spekboom)

Physical and Chemical description

The profile was classed as an orthic A / neocarbonate B1 / neocarbonate B2 / stone line / soft carbonate C horizon. Orthic A and *nc* horizons are an accumulation of aeolian deposits, and illuvial subject to leaching from higher-lying elluvic soils. The profile itself is non-luvic. Colour in the dry state ranges from 2.5YR to 10YR including light reddish brown to reddish brown to pinkish grey to very pale brown to white. Colour in the wet state ranges from 10YR to 5YR including dark yellowish brown to brown to dark brown to grey. The soil surface has a characteristic <2mm moderate surface sealing, with non-visible lime accumulation. Water rill erosion is visible by surface vertical cracks being washed out and thus widened to 5 mm breadth. The *ot* tests negative for lime accumulation. It is apedal, massive with weak crumb, sub-angular blocky ped formation. The *nc* B1 is apedal massive with weak crumb, subangular blocky and has weak prism ped formation. The *nc* B2 is apedal massive with weak stratification of layers (25 mm) in multiple sequence. Clay % increase from 3.8 to 7.9 in the *ot* to *nc* B2 and 7.9 to 8.8 from *nc* B2 to *sl*, effects changes in texture class from sand to loamy sand and loamy sand to sandy loam, respectively. Change in sand fraction from fine sand to medium sand of below lying horizons influence change in the texture class with depth from sand, to sandy loam to loamy sand in the *ot*, *nc* B's, to *sl* and *sc*, respectively. Increase in coarse sand fraction is observed in the *nc* B1 and *sc* with 3.6-9.0% and 5.2-14%, respectively. Coarse fraction % by weight increases down the profile. Coarse fraction is of mixed origin (mudstone and dolerite) from surface to B2 and *sc*, to dolerite only in the *sl*. Size of coarse fraction varies from fine gravel in the *ot*/*nc* B1 horizons to fine, medium and coarse gravel with stone in the *nc* B1 to *sc*.

PH_{water} increases with depth from 7.43 (*ob*) to 8.29 (*sc*). Low organic carbon (OC 0.19%) and nitrogen (N 0.035%) are observed in the *ob*/*ot* transition. CEC increases from *ob* (5.07 $cmol_c\ kg^{-1}$ soil) to *nc*B2 (20.87 $cmol_c\ kg^{-1}$ soil) decreasing over *sl* (17.84 $cmol_c\ kg^{-1}$ soil) to 19.38 ($cmol_c\ kg^{-1}$ soil). BS peaks from 98.42% in the *ob* at 129.56 in the *nc*B2. *Sl*

and *sc* slightly decrease to 113.73% and 110.78%, respectively. The flocculating properties observed in the *ot* and *nc* B1 and B2 horizon can be ascribed to the increased values of Ca^{+2} of values contributing 68, 71 and 89% to the S-value, respectively. Exchangeable cations Ca^{+2}, Mg^{+2} and Na^{+} increase from *ob* to *nc*B2, with K^{+} (0.28 to 0.17 $cmol_c kg^{-1}$ soil) decreasing over the same vertical sequence. An overall drop of S value and CEC is observed, with Na^{+} increasing slightly from 0.06 (*nc*B2) to 0.09 (*sc*) $cmol_c kg^{-1}$ soil.

Table Appendix 3 Reference Profile description of the Addo soil form P2

Map/photo:		Soil form and family:	Ad (Spekboom) 1211
Latitude/Longitude	29°31'27.73"S23°57'4.72"E	Surface rockiness:	None
Altitude (m) :	1125	Occurrence of flooding:	None
Terrain unit:	Upper Midslope	Wind erosion:	Slight
Slope:	1%	Water erosion:	None
Slope shape:	Concave/straight	Vegetation/Land use:	Virgin (DS/DD, HE3)
Aspect:	NW	Water table:	None
Microrelief:	Y anthills/earthworms	Described by:	Martin Tinnefeld
Parent Material Solum:	Aeolian	Date described (20yymmdd):	140131
Underlying Material:	SC3 Dwyka Tillite/Mudstone	Weathering of underlying material:	Physical modaerate
Weather conditions:	SU	Alteration of underlying material:	Y (mudstone; hk)
Soil Temperature regime:	IH	Former Weather conditions:	WC1
Moisture regime:	AR		

Horizon	Depth (mm)	Description	Diagnostic horizon
Ob	0	Moisture status: moist; dry colour: 2.5YR/6/4; moist colour: 10YR4/4; Loose, slightly-sticky, non-plastic; slight water erosion; <2mm moderate surface sealing, fine, medium and wide surface cracks; < 15%Surface gravel (2-5mm), visible OM embedded.	Surface
A	0-250	Moisture status: moist; dry colour: 5YR5/4; moist colour: 7.5YR5/3; Sand; apedal; massive; weak crumb, sub-angular blocky ped formation; slightly sticky; slightly plastic; fine, medium, wide cracks; free lime; < 15% coarse fragments (2-5mm & 6-25mm); few roots; <2-6 mm angular lime nodules, free lime, clear wavey transition.	Orthic A
B1	250-600	Moisture status: dry; dry colour: 2.5YR6/2; moist colour: 7.5YR5/4; Sand; massive; apedal; weak crumb, sub-angular blocky & prism ped formation; slightly sticky, slightly plastic, fine, medium cracks; < 10% coarse fragments (2-5mm & 6-25mm); few fine & coarse roots; free lime; diffuse transition.	Neocarbonate B1
B2	600-1300	Moisture status: dry; dry colour: 7.5YR7/2; moist colour: 7.5YR3/4; Loamy Sand; apedal; massive; stratification of layers (25 mm), multiple; slightly sticky, slightly plastic; < 15% coarse fragments (2-5mm & 6-25mm), mixed origin; few <2-6 mm angular lime nodules, free lime; clear transition.	Neocarbonate B2
Sl	1300-1400	Moisture status: dry; dry colour: 10YR8/3; moist colour: 7.5YR5/2; Sandy Loam; apedal; slightly sticky, slightly plastic; massive; fine, medium and wide cracks; 60-90% coarse fragments (2-250 mm), single origin; common roots; clear transition; free lime; abrupt, wavy transition.	Stone line
C	1400-1500	Moisture status: dry; dry colour: 5YR8/1; moist colour: 5YR6/1; Sandy Loam; apedal; massive; fine, common roots; 60-90% coarse fragments (2-750 mm), mixed origin; clear transition; stone-line, single; free lime, powdery; clear transition.	Soft carbonate B with saprolitic character
R		Moisture status: dry; mudstone; continuous massive; hard; clear transition.	Rock

Y – Yellow, YR – Yellow-red (Munsel colour); SU – sunny/clear, IH - Isohyperthermic, AR - Aridic, DS – semi deciduous dwarf shrub, DD – deciduous dwarf shrub, HE3 – extensive grazing, ranching, WC2 – no rain in the last week (FAO, 2006); hk – hardpan carbonate horizon, Ky – Kimberley soil form (SCWG, 1991)

Table Appendix 4 Physical and Chemical properties of Profile 2 Addo soil form P2

	Overburden	Orthic (A horizon)	Neocarbonate (B horizon)	Neocarbonate (B2 horizon)	Stone line	Soft carbonate C horizon
	0 (mm)	0-250 (mm)	250-600 (mm)	600-1300 (mm)	1300-1400 (mm)	1400-1500 (mm)
Physical properties						
Coarse sand (0-0.5 mm)	2.6	3.6	9.0	4.8	5.2	14
Medium sand (0.5-0.25 mm)	26.2	26.8	31.4	27.2	22.6	22.8
Fine sand (0.25-0.106 mm)	45.7	45.6	44.2	40.8	38.3	28.8
Very fine sand (0.106-0.05 mm)	13.4	11.4	1.4	7.0	12	9.6
Texture	Fine Sand (87.9)	Fine Sand (87.4)	Medium Sand (86)	Fine Sand (79.8)	Fine Sand (78.1)	Medium Sand (75.2)
Coarse silt (0.05-0.02 mm)	5.6	5.6	5.4	2.7	4.7	5
Fine silt (0.02-0.002 mm)	1.3	2.0	3.2	4.1	6.2	8.7
Clay (>0.002 mm)	3.7	3.8	4.1	7.9	8.8	8.7
Total texture fraction	98.5	98.8	98.7	94.5	97.8	97.6
Texture	Sand	Sand	Sand	Loamy Sand	Sandy Loam	Sandy Loam
CO_3^- (% of sample removed before texture analysis)	1.03	0	0	1.15	0.87	0.33
Coarse fraction % of weight	3.86	4.71	6.07	7.60	18.86	49.91
Bulk density (g cm^{-3})		1.59	1.79	1.72	1.70	1.74
Chemical properties						
pH (H_2O)	7.43	7.46	7.75	8.25	8.3	8.29
pH (KCL)	7.24	7.37	7.57	8.22	8.24	8.14
OC%	0.190	-	-	-	-	-
N%	0.035	-	-	-	-	-
Mn (mg kg^{-1})	-	-	-	-	-	-
Fe (mg kg^{-1})	-	-	-	-	-	-
Exchangeable cations ($cmol_c kg^{-1}$ soil) exchangeable/soluble + exchangeable						
Calcium	3.64	3.57	3.92	24.06	18.34	18.89
Magnesium	1.04	1.41	1.43	2.75	1.69	2.31
Potassium	0.28	0.23	0.17	0.17	0.18	0.18
Sodium	0.03	0.05	0.04	0.06	0.08	0.09
CEC	5.07	5.34	5.78	20.87	17.84	19.38
S	4.99	5.26	5.56	27.04	20.29	21.47
BS (%)	98.42	98.5	96.19	129.56	113.73	110.78

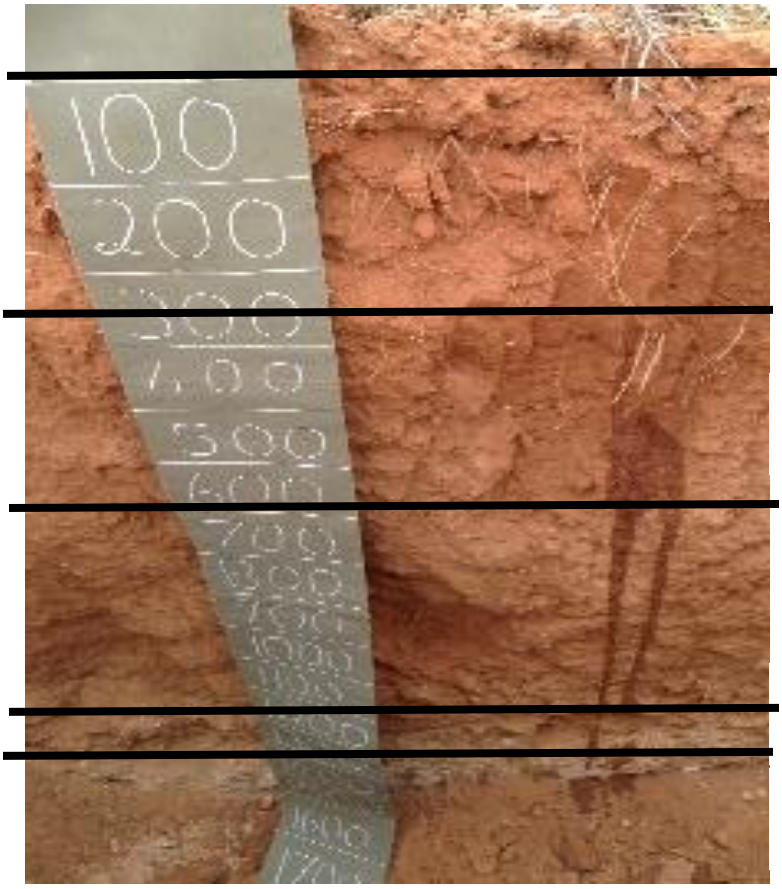

Figure Appendix 6 Figure Profile P2, Addo soil form.

Profile P3: Kimberley (*Ky*) 1100 (Taung)

Physical and chemical description

The profile was classed as an orthic A / red apedal B / soft carbonate C / unspecified without sign of wetness (uwosw) / rock (mudstone) horizon. Orthic A and *re* horizons are an accumulation of aeolian deposits. Colour in the dry state is 2.5YR reddish brown and 7.5YR strong brown (*uwosw*). Colour in the dry state ranges from 2.5YR to 7.5YR yellowish red to red to light brown down the profile.Coarse fractions are observed throughout the profile, ranging from 2-5 mm gravel in all horizons, and 6-25 mm on the surface, at the transition from *ot* to *re*, throughout the *sc* (2-750 mm) and *uwosw* (2-750 mm). Roots were observed throughout the *ot* (fine and common), *re* (fine and few) and *sl* (fine and coarse, common). The coarse fraction at the *ot*/*re* transition is partially impregnated with carbonate. Transition from *re* to *sc* is marked by an abrupt indurated, cracked layer of carbonates of 15 mm thickness. This is not sufficient to class the *sc* as *hk* as the induration does not extend further down the horizon and is cracked. Texture fraction classifies all horizons as sand, with sand fractions differing for *ob* and *ot* (medium sand) to *re, sc and uwosw* (coarse sand). Coarse sand fraction increases down the profile. Medium sand decreases down the profile, increasing again in the uwosw. Fine sand increases to the *re* (1.3% (*ob*) to 33.5% (*re*)) and decreases to the *uwosw* (2.0%). Very fine sand increases from 0.6% to 9% in the *re* and *sc*, decreasing again in the *uwosw* to 7.1%. Calcium carbonate comprises 0.78%, 3.54% and 1.26% of *re*, *sc* and *uwosw* by weight of sample, respectively. Db is stable around 1.54 g cm^{-3} with an increase to 1.57 and decrease to 1.47 g cm^{-3} from *ot* to *re* to *sc*.

The pH_{water} increases from 6.69 in the *ob* to 8.25 in the *ot*, remaining relatively stable with a sudden increase from 8.16 in the *sc* to 8.51 in the *uwosw*. Low organic carbon (OC 0.203) and nitrogen (N 0.032%) are observed in the *ob*/*ot* transition. CEC increases from 1.16 to 10.74 $cmol_c kg^{-1}$ soil *ob* to *sc*, decreasing to 1.2 $cmol_c kg^{-1}$ in the *uwosw*. Base saturation fluctuates: increases from 11.6% in the *ob* to 620% in the *ot*, decreasing again in the *re* to 89.92 and increasing again to 159.31% in the *sc*, decreasing again in the *uwosw* to 73.3%.

Table Appendix 5 Reference Profile description of the Kimberley soil form P3

Map/photo:		Soil form and family:	Kimberly (Taung) 1100
Latitude/Longitude	29°34'37.99"S 23°58'37.95"E	Surface rockiness:	None
Altitude (m) :	1129	Occurrence of flooding:	None
Terrain unit:	UMS	Wind erosion:	Slight
Slope:	1%	Water erosion:	None
Slope shape:	Convex/convex	Vegetation/Land use:	Virgin (DS/DD, HE3)
Aspect:	S	Water table:	None
Microrelief:	Y anthills	Described by:	Martin Tinnefeld
Parent Material Solum:	Aeolian	Date described (yymmdd):	140131
Underlying Material:	SC3 Dwyka Tillite/Mudstone	Weathering of underlying material:	Physical strong, Chemical weak
Weather conditions:	SU	Alteration of underlying material:	Y (mudstone; hk) calcified
Soil Temperature regime:	IH	Former Weather conditions:	WC2
Moisture regime:	AR		

Horizon	Depth (mm)	Description	Diagnostic horizon
Ob	0	Moisture status: moist; dry colour: 2.5YR4/8; moist colour: 2.5YR2.5/4; Sand; apedal; non-sticky; non-plastic; slight wind erosion; surface gravel and coarse gravel 2-10%, flat & round; <2mm moderate surface sealing, fine, medium, wide surface cracks; common roots; abrupt transition.	Overburden
A	0-175	Moisture status: moist; dry colour: 5YR4/6; moist colour: 2.5YR3/4; Sand; apedal; massive; non-sticky; non-plastic; slight wind erosion; fine, medium, wide cracks; few fine and coarse roots; clear, wavy transition; 15-20 mm stone line (20-28 mm), 53.32% coarse fraction, impregnated with carbonate, single origin.	Orthic A
B	175-550	Moisture status: dry; dry colour: 5YR4/6; moist colour: 2.5YR3/4; Coarse sand; massive; apedal; fine, medium cracks; 2-10% fine gravel, single origin; few, fine and coarse roots; clear transition; abrupt, wavy transition.	Red apedal B
C1	550-1600	Moisture status: dry; dry colour: 2.5YR4/6; moist colour: 2.5YR4/4; Coarse sand; apedal; massive; top 10 mm cemented by calcium carbonate, laminar, strong, wavey, continuous; gravel, sub-angular blocky, impregnated with carbonate; fine, medium and wide cracks; 60-90% coarse fragments (2-750 mm), single origin; Rocks at transition, single origin; few fine & coarse roots; clear transition; free lime, lime concretions <2-6 mm, mixed shapes; abrupt, wavy transition.	Soft carbonate B horizon
C2	1600-1700	Moisture status: dry; dry colour: 7.5YR6/3; moist colour: 7.5YR4/6; ; Coarse sand; brittle; fine, common fine & coarse roots; 60-90% coarse fragments (2-750 mm); clear transition; stone-line, single, single origin; free lime, angular concretions <2-6 mm.	Unspecified without signs of wetness/ Saprolite

Y – Yellow, YR – Yellow-red (Munsel colour); SU – sunny/clear, IH - Isohyperthermic, AR - Aridic, DS – semi deciduous dwarf shrub, DD – deciduous dwarf shrub, HE3 – extensive grazing, ranching, WC2 – no rain in the last week (FAO, 2006); hk – hardpan carbonate horizon, Ky – Kimberley soil form (SCWG, 1991)

Table Appendix 6 Physical and Chemical properties of a Kimberley soil form P3

	Overburden	Orthic (A horizon)	Red apedal (B horizon)	Soft carbonate C horizon	Unspecified without s.o.w./ saprolite

	0 (mm)	0-175 (mm)	175-550 (mm)	550-1600 (mm)	1600-1700 (mm)
Physical properties					
Coarse sand (0-0.5 mm)	5.6	6.2	22.3	21.0	27.5
Medium sand (0.5-0.25 mm)	82.6	74.7	22.9	25.1	49.6
Fine sand (0.25-0.106 mm)	1.3	8.1	33.5	28.9	2.0
Very fine sand (0.106-0.05 mm)	0.6	0.6	9	9.6	7.1
Sand fraction texture	Medium Sand (90.1)	Medium Sand (89.6)	Coarse Sand (87.7)	Coarse Sand (84.6)	Coarse Sand (86.2)
Coarse silt (0.05-0.02 mm)	1	1	2.1	3.3	3.3
Fine silt (0.02-0.002 mm)	0.8	1.6	4.1	5.3	4
Clay (>0.002 mm)	4.3	5.2	5.8	6.5	5.2
Texture	Sand	Sand	Sand	Sand	Sand
Total texture fraction	96.2	97.4	99.7	99.7	98.7
CO_3^- (% of sample removed before texture analysis)	0	0	0.78	3.54	1.26
Coarse fraction % of weight	0.976	2.421	1.63	1.465	62.21
Bulk density (g cm^{-3})	1.53	1.54	1.57	1.47	1.54
Chemical properties					
pH (H_2O)	6.69	8.25	8.27	8.16	8.51
pH (KCL)	5.81	7.14	7.92	7.79	7.85
OC%	0.203	-	-	-	-
N%	0.032	-	-	-	-
Mn (mg kg^{-1})	-	9.9	6.2	4.4	-
Fe (mg kg^{-1})	-	7.5	1	3.1	-
Exchangeable cations ($cmol_c kg^{-1}$ soil)					
Calcium	0.08	5.02	5.08	15.7	0.81
Magnesium	0.01	1.42	1.80	1.10	0.06
Potassium	0.01	0.34	0.38	0.29	0.01
Sodium	0.002	0.04	0.06	0.02	0.003
CEC	1.16	1.10	6.58	10.74	1.2
S	0.10	6.82	7.32	17.11	0.88
BS (%)	11.6	620	89.92	159.31	73.3

Figure Appendix 7 Profile P3, Kimberley soil form.

Profile P4: Hutton (*Hu*) 3100 (Stella)

Physical and chemical description

The profile was classed as an orthic A / red apedal B1 / red apedal B2 / stone line horizon which grades into solid rock. Orthic A and *re* horizons are an accumulation of aeolian deposits. Horizons have clear transitions. Soil colour in the dry state ranges from 10YR to 7.5YR brownish yellow, yellowish brown to brown. Soil colour in the wet state ranges from 7.5YR brown to 5YR reddish brown. *Re* B1 and B2 are also of aeolian deposits, yet have undergone pedogenesis, with massive apedal loose structure, and few fine cracks. The profile is eutrophic with an increase in clay percentage from *ot* to *re* B1 to *re* B2 horizon as 12/12/27%. Overall texture changes from sand in *ot* and *re* B1 to sandy clay loam in *re* B2. Bulk density decreases with a decrease in medium sand : increase in clay percentage from 1.60 to 1.61 to 1.52 g cm^{-3}. Coarse fraction as % of total sample weight, decreases from 1.2 (*ot*) to 0.08 (*re* B2), and increases to 0.56 (*re* B2).

The pH_{water} increases down the profile from 6.89 (*ot*) to 7.87 (*re* B2). Low organic carbon (OC 0.118) and nitrogen (N 0.038%) are observed in the *ot*. An increase in Mn (0.28 to 0.47 mg kg^{-1} plant extractable) and decrease in Fe (5.4 to 2.3 mg kg^{-1} plant extractable) is observed down the profile. Ca^{+2} and Na^{+} also increases down the profile from 2.85 to 8.53 $cmol_c$ kg^{-1} soil and 0.05 to 0.07 $cmol_c$ kg^{-1} soil, respectively. BS is observed to decrease from 87.03% in the *ot*, to 73.1% in the *re* B1 and increase again to 112.22% in the *re* B2. CEC increases vertically from *ot* to *re* B2 from 4.78 to 8.14 to 9.33 $cmol_c kg^{-1}$ soil, respectively.

Table Appendix 7 Modal Profile description of the Hutton soil form P4

Map/photo:		Soil form and family:	Hutton (Stella) 3100
Latitude/Longitude	29°33'9.72"S / 23°58'17.71"E	Surface rockiness:	None
Altitude (m) :	1131	Occurrence of flooding:	None
Terrain unit:	UMS/BS	Wind erosion:	Slight
Slope:	1%	Water erosion:	None
Slope shape:	Concave/Concave	Vegetation/Land use:	Virgin (DS/DD, HE3)
Aspect:	E	Water table:	None
Microrelief:	Y anthills, earthworm mounds	Described by:	Martin Tinnefeld
Parent Material Solum:	Aeolian	Date described (yymmdd):	140201
Underlying Material:	SC3 Dwyka Tillite/Mudstone	Weathering of underlying material:	Physical moderate, Chemical weak
Weather conditions:	SU	Alteration of underlying material:	Y (mudstone)
Soil Temperature regime:	IH	Former Weather conditions:	WC2
Moisture regime:	AR		

Horizon	Depth (mm)	Description	Diagnostic horizon
A	0-200	Moisture status: moist; dry colour: 10YR6/6; moist colour: 7.5YR5/4; Sand; apedal; massive; apedal; non-sticky; loose; non-plastic; slight wind erosion; fine, medium, wide cracks; common roots; clear transition.	Orthic A
B1	200-600	Moisture status: dry; dry colour: 10 YR5/4; moist colour: 7.5YR5/4; Sand; apedal; massive; non-sticky; loose; non-plastic; fine, medium cracks; many roots; clear transition.	Red apedal B1
B2	600-1200	Moisture status: dry; dry colour: 7.5YR5/4; moist colour: 5YR5/4; Sandy clay loam; apedal; massive; soft, non-sticky, non-plastic; fine, medium and wide cracks; 0.56% coarse fragments (2-250 mm); common roots; clear transition.	Red apedal B2
C	1200-1300	Moisture status: dry; dry colour: 7.5YR5/4; moist colour: 5YR4/3; Sandy clay loam; apedal; massive; slightly hard, sticky, slightly-plastic; fine, few roots; 60-90% coarse fragments (2-20 mm); clear transition; stone-line, single; sub-angular blocky.	Stone line

Y – Yellow, YR – Yellow-red (Munsel colour); SU – sunny/clear, IH - Isohyperthermic, AR - Aridic, DS – semi deciduous dwarf shrub, DD – deciduous dwarf shrub, HE3 – extensive grazing, ranching, WC2 – no rain in the last week (FAO, 2006); hk – hardpan carbonate horizon, Ky – Kimberley soil form (SCWG, 1991)

Table Appendix 8 Physical and Chemical properties of a Hutton soil form P4

	Orthic (A horizon)	Red apedal (B1 horizon)	Red apedal (B2 horizon)
	0-200 (mm)	200-600 (mm)	600-1200 (mm)
Physical properties			
Coarse sand (0-0.5 mm)	5.7	5.2	7.3
Medium sand (0.5-0.25 mm)	48	69	13
Fine sand (0.25-0.106 mm)	24	8.2	21
Very fine sand (0.106-0.05 mm)	8.3	1.6	17.7
Sand fraction texture	Medium Sand (86)	Medium Sand (84)	Fine Sand (59)
Coarse silt (0.05-0.02 mm)	0.31	2.0	6.3
Fine silt (0.02-0.002 mm)	1.69	1.7	7.6
Clay (>0.002 mm)	12	12.4	27
Texture	Sand	Sand	Sandy Clay Loam
Total texture fraction	100	97.4	99.9
Coarse fraction % of weight	1.2	0.08	0.56
Bulk density (g cm^{-3})	1.60	1.61	1.52
Chemical properties			
pH (H_2O)	6.89	6.53	7.87
pH (KCL)	6.2	6.1	7.56
OC%	0.118	-	-
N%	0.038	-	-
Mn (mg kg^{-1})	0.28	0.22	0.47
Fe (mg kg^{-1})	5.4	5.01	2.3
Exchangeable cations ($cmol_c kg^{-1}$ soil)			
Calcium	2.85	4.43	8.53
Magnesium	0.9	1.25	1.75
Potassium	0.36	0.21	0.12
Sodium	0.05	0.06	0.07
CEC	4.78	8.14	9.33
S	4.16	5.95	10.47
BS (%)	87.03	73.1	112.22

Figure Appendix 8 Profile P4, Hutton soil form.

Profile P5: Coega (*Cg*) 1000 (Nabies)

Physical and chemical description

The profile is classed as an orthic A / hardpan carbonate horizon. Orthic A horizon is an accumulation of aeolian deposits. Sand fraction is predominantly of medium sand at 84.7% of total texture fraction. Carbonate by weight is for the *ot* 0.15%, whereas for the hk 86%.

The pH_{water} changes from 6.15 *ot* to 8.84 in the *hk* horizon. Low organic carbon (OC 0.255) and nitrogen (N 0.041%) are observed in the *ot*. The CEC is 0.84 $cmol_c kg^{-1}$ soil and BS is at 378.57% for the *ot*.

Table Appendix 9 Modal profile description of the Coega soil form P5

Map/photo:		Soil form and family:	Coega (Nabies) 1000
Latitude/Longitude	29°34'23.05"S, 23°58'5.30"E	Surface rockiness:	None
Altitude (m) :	1132	Occurrence of flooding:	None
Terrain unit:	UP	Wind erosion:	Slight
Slope:	1%	Water erosion:	None
Slope shape:	Convex/Convex	Vegetation/Land use:	Virgin (DS/DD, HE3)
Aspect:	NW	Water table:	None
Microrelief:	Y Anthills/earthworm mounds	Described by:	Martin Tinnefeld
Parent Material Solum:	Aeolian	Date described (20yymmdd):	140201
Underlying Material:	SC3 Dwyka Tillite/Mudstone	Weathering of underlying material:	None
Weather conditions:	SU	Alteration of underlying material:	Y (mudstone : hk)
Soil Temperature regime:	IH	Former Weather conditions:	WC2
Moisture regime:	AR		

Horizon	Depth (mm)	Description	Diagnostic horizon
A	0-150	Moisture status: moist; dry colour:10YR7/4; moist colour:10YR5/6; Sand; apedal; massive; non-sticky; non-plastic; slight wind erosion; <2mm weak surface sealing, fine, medium and wide surface cracks; many roots; abrupt transition.	Orthic A
B	150 +	Underlying non-gravelly matrix, 100 mm depth; gravelly matrix; < 8 mm laminar coating of > 500 mm dolerite round boulders; < 1 mm cracks in dry state of laminar sheeting; very hard; weak inter-rock filling.	Hardpan carbonate C

Y – Yellow, YR – Yellow-red (Munsel colour); SU – sunny/clear, IH - Isohyperthermic, AR - Aridic, DS – semi deciduous dwarf shrub, DD – deciduous dwarf shrub, HE3 – extensive grazing, ranching, WC2 – no rain in the last week (FAO, 2006); hk – hardpan carbonate horizon, Ky – Kimberley soil form (SCWG, 1991)

Table Appendix 10 Physical and Chemical properties of a Coega soil form P5

	Orthic (A horizon)	Hardpan carbonate
	0-100 (mm)	100 mm +
Physical properties		
Coarse sand (0-0.5 mm)	4.2	-
Medium sand (0.5-0.25 mm)	84.7	-
Fine sand (0.25-0.106 mm)	1.7	-
Very fine sand (0.106-0.05 mm)	1.3	-
Sand fraction texture	Medium Sand (91.9)	-
Coarse silt (0.05-0.02 mm)	2.4	-
Fine silt (0.02-0.002 mm)	0.3	-
Clay (>0.002 mm)	5.4	-
Texture	Sand	-
Total texture fraction	100	
CO_3^- (% of sample removed before texture analysis)	0.15	86
Coarse fraction % of weight	0	100
Bulk density (g cm^{-3})	1.64	-
Chemical properties		
pH (H_2O)	6.15	8.84
pH (KCL)	5.04	7.96
OC%	0.255	-
N%	0.041	-
Mn (mg kg^{-1})	6.7	-
Fe (mg kg^{-1})	5.2	-
Exchangeable cations ($cmol_c kg^{-1}$ soil)		
Calcium	2.06	-
Magnesium	0.68	-
Potassium	0.4	-
Sodium	0.04	-
CEC	0.84	-
S	3.18	-
BS (%)	378.57	-

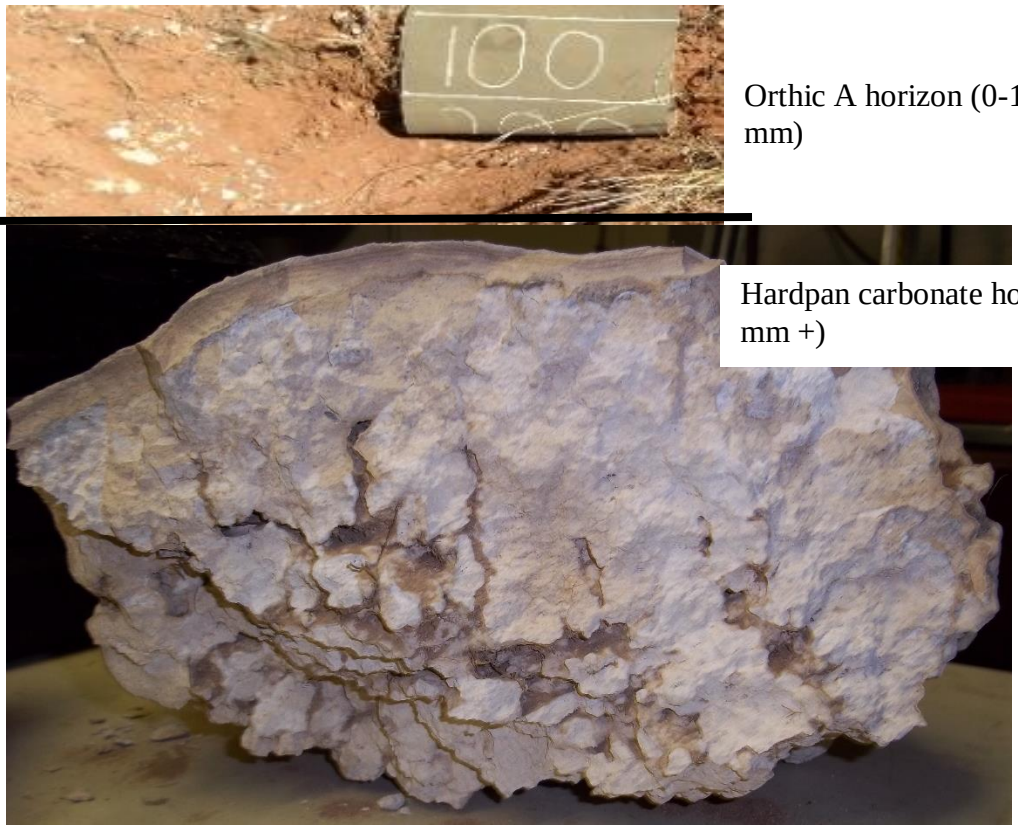

Figure Appendix 9 Profile P5, Coega soil form.

Profile P6: Addo (*Ad*) 1211 (Spekboom)

Physical and chemical description

The profile was classed as an orthic A / neocarbonate B /soft carbonate C / hardpan carbonate C2 horizon. Orthic A horizon and *nc* Bare an accumulation of aeolian deposits. The soil surface is characterized by a 20 mm overburden with a very weak <1 mm crust. Organic material is embedded with many fine roots within the *ob*. Colour in the dry state is 5YR yellowish red and 2.5YR red. Colour in the wet state ranges from 2.5YR dark reddish brown to 5YR reddish brown. Orthic A includes a coarse fraction of mixed round and subangular 2-25 mm gravel 0.62% by weight. Sand texture fraction is medium for *ob* and *ot*, fine sand for *nc B* and coarse sand for *sc*. Overall texture fraction analysis showed that *ob*, *ot* and *nc* are of sand and *sc* of sandy loam. An increase in coarse and medium sand is observed from *ob* to *ot* and from *nc* to *sc*. Clay fraction increases vertically, with clay percentage increasing gradually from 3.6% in the *ob* to 15.9% in the *sc*. Clay fraction increase from *nc* (6.7%) to *sc* (15.9%) horizon can also be ascribed to chemical weathering of underlying material, however not significant enough to show signs of wetness. Free lime is observed as from the *nc* and *sc* with 1.2 and 5.2% carbonate of total weight, respectively. The coarse fraction in the *sc* is impregnated with visible carbonate. The *nc* B has 5% <2-6 mm oval lime concretions. Db decreases down the profile from 1.57 g cm^{-3} (*ot*) to 1.54 g cm^{-3} (*nc*) to 1.39 g cm^{-3} (*sc*).

The pH_{water} increases from *ob* to *ot* by 1.6, decreasing again to 6.85 and increasing to 8.13 in the *sc*. Low organic carbon (OC 0.203) and nitrogen (N 0.032%) are observed in the *ot*. Exchangeable cations remain constant except an increase in the *sc*, where an increase in calcium from 1.98 to 16.08 $cmol_c kg^{-1}$ soil, magnesium from 1.75 to 3.11 $cmol_c kg^{-1}$ soil and sodium, where an increase from 0.02 to 0.05 $cmol_c kg^{-1}$ soil is observed. CEC increases with clay fraction from 3.9 $cmol_c kg^{-1}$ soil with clay of 3.6% in the *ob*, to 11.9 $cmol_c kg^{-1}$ soil with a clay of 15.9%. Base saturation increases from 2.36% to 93.42% from *ob* to *ot* and *nc* increases from 61.38% to 162.86% in the *sc*. Mn and Fe decrease down the profile from 7.9 to 1.0 and 5.5 to 2.2 mg kg^{-1}, respectively.

Table Appendix 11 Modal profile description of the Addo soil form P6

Map/photo:		Soil form and family:	Addo Spekboom (1211)
Latitude/Longitude	28°51'57.04"S / 24° 4'18.56"E	Surface rockiness:	None
Altitude (m) :	1031	Occurrence of flooding:	None
Terrain unit:	Toeslope	Wind erosion:	Slight
Slope:	1%	Water erosion:	Slight
Slope shape:	Straight /Concave	Vegetation/Land use:	Virgin (DS/DD, HE3)
Aspect:	SE	Water table:	None
Microrelief:	Y anthills/earthworms	Described by:	Martin Tinnefeld
Parent Material Solum:	Aeolian	Date described (yymmdd):	140202
Underlying Material:	SC3 Dwyka Tillite/Mudstone	Weathering of underlying material:	Physical modaerate
Weather conditions:	SU	Alteration of underlying material:	Y (mudstone; hk)
Soil Temperature regime:	IH	Former Weather conditions:	WC3
Moisture regime:	AR		

Horizon	Depth (mm)	Description	Diagnostic horizon
Ob	0-20	Moisture status: dry; dry colour: 5YR4/6; moist colour: 2.5YR3/4; Sand; slight water erosion; <1mm weak surface sealing, fine, medium and wide surface cracks; visible OM embedded (0.26% by weight); many fine, few coarse roots; smooth abrupt transition.	Overburden
A	20-300	Moisture status: moist; dry colour: 2.5YR5/8; moist colour: 2.5YR3/4; Sand; apedal; massive; slightly sticky; slightly plastic; fine, medium, cracks; few fine roots; 0.62% round and subangular 2-5 mm coarse fraction; stone line 2-5 mm single stoneline at transition 0.97%; diffuse transition.	Orthic A
B	300-600	Moisture status: dry; dry colour: 2.5YR4/6; moist colour: 2.5YR3/4; Sand; apedal; massive; slightly sticky, slightly plastic; fine, medium cracks; common fine, few coarse roots; Coarse fraction 0.73%; at 550 mm 43.25% (20% 25-75 mm and 80% 6-25 mm) subangular coarse fraction; free lime, 5% <2-6 mm calcium concretions; clear, broken transition.	Neocarbonate B
C1	600-800	Moisture status: dry; dry colour: 5YR4/6; moist colour: 5YR4/4; Sandy loam; apedal; massive; slightly sticky, slightly plastic; fine; 43.25% coarse fragments (2-25 mm); coarse fraction impregnated by carbonates, medium; clear transition; free lime; abrupt, wavy transition.	Soft carbonate C horizon
C2	800	Moisture status: dry; massive, very hard; few medium cracks; carbonate indurated.	Hardpan carbonate C2 horizon

Y – Yellow, YR – Yellow-red (Munsel colour); SU – sunny/clear, IH - Isohyperthermic, AR - Aridic DS – semi deciduous dwarf shrub, WD – deciduous woodland, HM – medium grassland, HE3 – extensive grazing, ranching, WC4 – no rain in the last 24 hours (FAO, 2006); hk – hardpan carbonate horizon, Ky – Kimberley soil form (SCWG, 1991)

Table Appendix 12 Physical and Chemical properties of an Addo soil form P6

	Overburden	Orthic (A horizon)	Neocarbonate (B horizon)	Soft carbonate (B horizon)
	0 (mm)	0-300 (mm)	300-600 (mm)	600-900 (mm)
Physical properties				
Coarse sand (0-0.5 mm)	7.0	10.2	6.4	31.2
Medium sand (0.5-0.25 mm)	46.2	68.5	29.6	21.8
Fine sand (0.25-0.106 mm)	35.4	12.8	52.0	22.6
Very fine sand (0.106-0.05 mm)	2.8	1.2	0.7	1.7
Sand fraction Texture	Medium Sand (91.4)	Medium Sand (92.7)	Fine Sand (88.7)	Coarse Sand (77.3)
Coarse silt (0.05-0.02 mm)	1.5	1.2	0.9	0.9
Fine silt (0.02-0.002 mm)	1.7	1.0	1.5	4.2
Clay (>0.002 mm)	3.6	4.5	6.7	15.9
Texture	Sand	Sand	Sand	Sandy Loam
Total texture fraction	98.2	99.4	97.8	98.3
CO_3^- (% of sample removed before texture analysis)	0	0	1.4	5.2
Coarse fraction % of weight	0.26	0.62	0.73	49.01
Bulk density (g cm^{-3})	-	1.57	1.54	1.39
Chemical properties				
pH (H_2O)	5.3	7.29	6.85	8.13
pH (KCL)	4.78	5.75	6.28	6.58
OC%	0.203	-	-	-
N%	0.032	-	-	-
Mn (mg kg^{-1})	-	7.9	4.6	1.0
Fe (mg kg^{-1})	-	5.0	4.8	2.2
Exchangeable cations ($cmol_c kg^{-1}$ soil)				
Calcium	0.07	2.3	1.98	16.08
Magnesium	0.01	1.45	1.75	3.11
Potassium	0.01	0.35	0.16	0.14
Sodium	0.002	0.02	0.02	0.05
CEC	3.9	4.41	6.37	11.9
S Value	0.092	4.12	3.91	19.38
BS (%)	2.36	93.42	61.38	162.86

Orthic A horizon (0-300 mm)

Neocarbonate B-horizon (300-700 mm)

Soft carbonate B horizon (700-900 mm)

Hardpan carbonate C horizon (900-1000 mm)

Figure Appendix 10 Depicted is a picture of a profile similar in morphology to Profile P6. Differences only in depth of horizons, as well as soft carbonate horizon at 700 - 900 mm missing is to be considered to the actual profile.

Profile P7: Hutton (*Hu*) 3100 (Stella)

Physical and chemical description

The profile was classed as an overburden / orthic A / red apedal B1 / Red apedal B2 / saprolite horizon. The overburden (*ob*), orthic A horizon (*ot*), red apedal B1 and B2 (*re* B1 and B2) are an accumulation of aeolian deposits. Overburden is observed to be loose and have little to no roots, with a thin very weak <1 mm surface crust. Colour in the dry state is 7.5YR brown, light brown and dark brown. In the wet state colour is 7.5YR dark brown, brown and strong brown. *Ot*, *re* B1 and *so* have a textural sand fraction of medium sand, whereas *re* B2 is classed as fine sand. Overall, horizons are classed according to their textural fractions as sand and *re* B2 sandy loam. *Re* B2 is marked by the highest textural silt and clay fraction, increasing from 0.4%, 1.6% and 4.1% (CoSi, FiSi, Cl) in the *ot*, to 0.4%, 0.4% and 3.9% in *re* B1 to 2.5%, 4.3% and 9.8% in *re* B2, and decreasing again to 1.4%, 1.2% and 4.4% in *so*. Calcium carbonate as percentage of weight for *re* B1, *re* B2 and *so* is 0.03, 0.1 and 0.9, respectively. This is not enough to show effervescing with 10% HCl. Mentionable coarse fraction of *so* is 70% of sample weight. Db is stable at around 1.6 g cm^{-3}.

The pH_{water} is high throughout the profile, at 8.04, 8.96, 8.19 and 8.89 for the sequencing of *ot*, *re* B1, *re* B2 and *so*, respectively. Low organic carbon (OC 0.197%) and nitrogen (N 0.035%) are observed in the *ot*. Exchangeable cations in $cmol_c$ kg^{-1} soil for calcium (Ca^{+2}) is around 1.05 (*re* B2) to 1.8 (*re* B1), magnesium (Mg^{+2}) increases from 0.8 (*ot*) to 1.51 (*so*), potassium (K^{+}) decreases from 0.3 (*ot*) to 0.15 (*so*) and for sodium (Na^{+}) increases from 0.02 (*ot*) to 0.045 (*so*). CEC decreases from 1.8 $cmol_c kg^{-1}$ soil in the *ot* to 1.45 $cmol_c kg^{-1}$ soil in the *re* B1, increasing again to 1.87 and 2.2 $cmol_c kg^{-1}$ soil in the *re* B2 andso horizon. Base saturation increases with depth from 123.33% in the *ot* to 242.76% in the *re* B1 and decreases to 148.13% and 145.91% in the *re* B2 and *so*, respectively. Manganese decreases from 9.7 to 2.0 mg kg^{-1} soil and iron slightly from 4.7 to 4.3 mg kg^{-1} soil from *ot* to *so*.

Table Appendix 13 Modal profile description of the Hutton soil form P7

Map/photo:		Soil form and family:	Hutton (Stella) 3100
Latitude/Longitude	28°51'29.40"S 24° 3'57.00"E	Surface rockiness:	None
Altitude (m) :	1030	Occurrence of flooding:	None
Terrain unit:	Upper footslope	Wind erosion:	Slight
Slope:	1%	Water erosion:	None
Slope shape:	Concave/flat	Vegetation/Land use:	Virgin (WD, HE3, HM)
Aspect:	S	Water table:	None
Microrelief:	Y Anthills/Windblown depressions	Described by:	Martin Tinnefeld
Parent Material Solum:	Aeolian	Date described (20yymmdd):	140202
Underlying Material:	SC3 Dwyka Tillite/Mudstone	Weathering of underlying material:	NA
Weather conditions:	SU	Alteration of underlying material:	Y (mudstone/dolerite)
Soil Temperature regime:	IH	Former Weather conditions:	WC3
Moisture regime:	AR		

Horizon	Depth (mm)	Description	Diagnostic horizon
Ob	0-20	Moisture status: dry; apedal, loose, non-sticky, non-platic; slight wind erosion; organic matter embedded; <1mm weak surface sealing.	Overburden
A	20-300	Moisture status: dry; dry colour: 7.5YR5/4; moist colour: 7.5YR3/4; Sand; apedal; massive; non-sticky; non-plastic; fine, medium and wide cracks; many fine roots; 0.98% 2-6 mm fine gravel; few manganese concretions at transition; clear transition.	Orthic A
B1	300-1400	Moisture status: dry; dry colour: 7.5YR5/4; moist colour: 7.5YR4/3; Sand; apedal; massive; fine, medium cracks; many roots; 0.02% 2-6 mm fine gravel; clear transition; diffuse smooth transition.	Red-apedal B1
B2	1400-2000	Moisture status: dry; dry colour: 7.5YR6/4; moist colour: 7.5YR5/3; Sand; apedal; massive; 0.004% 2-6 mm fine gravel; clear transition; diffuse smooth transition; few, fine, medium cracks; few fine roots; free lime at transition; abrupt transition; clear transition.	Red-apedal B2
C	2000-2100	Moisture status: dry; dry colour: 7.5YR5/6; moist colour: 7.5YR4/6; Sand; apedal; massive; fine, medium and wide cracks; 70.0% coarse fragments (2-50 mm); free lime.	Saprolite

Y – Yellow, YR – Yellow-red (Munsel colour); SU – sunny/clear, IH - Isohyperthermic, AR - Aridic, DS – semi deciduous dwarf shrub, WD – deciduous woodland, HM – medium grassland, HE3 – extensive grazing, ranching, WC3 – no rain in the last 24 hours (FAO, 2006); hk – hardpan carbonate horizon, Ky – Kimberley soil form (SCWG, 1991)

Table Appendix 14 Physical and Chemical properties of a Hutton soil form P7

	Orthic (A horizon)	Red apedal (B1 horizon)	Red apedal (B2 horizon)	Saprolite
	0-300 (mm)	300-1400 (mm)	1400-2000 (mm)	2000-2100 (mm)
Physical properties				
Coarse sand (0-0.5 mm)	6.6	4.4	9.2	5.9
Medium sand (0.5-0.25 mm)	42.9	76.6	18.2	56.3
Fine sand (0.25-0.106 mm)	15.2	12.4	40.8	26.0
Very fine sand (0.106-0.05 mm)	27.3	1.0	14.1	4.9
Sand fraction texture	Medium Sand (92)	Medium Sand (94.4)	Fine Sand (82.3)	Medium Sand (93.1)
Coarse silt (0.05-0.02 mm)	0.4	0.4	2.5	1.4
Fine silt (0.02-0.002 mm)	1.6	0.4	4.3	1.2
Clay (>0.002 mm)	4.1	3.9	9.8	4.4
Texture	Sand	Sand	Sandy Loam	Sand
Total texture fraction	98.1	99.1	98.9	100.1
CO_3^- (% of sample removed before texture analysis)	0	0.03	0.10	0.19
Coarse fraction % of weight	0.18	0.02	0.004	70.0
Bulk density (g cm^{-3})	1.61	-	1.60	-
Chemical properties				
pH (H_2O)	8.04	8.96	8.19	8.89
pH (KCL)	7.61	8.01	8.01	8.39
OC%	0.197	-	-	-
N%	0.035	-	-	-
Mn (mg kg^{-1})	-	9.7	4.0	2.0
Fe (mg kg^{-1})	-	4.7	4.3	4.3
Exchangeable cations $cmol_c kg^{-1}$ soil				
Calcium	1.10	1.80	01.05	1.5
Magnesium	0.8	1.48	1.5	1.51
Potassium	0.3	0.21	0.18	0.15
Sodium	0.02	0.03	0.04	0.045
CEC	1.8	1.45	1.87	2.2
S Value	2.22	3.52	2.77	3.21
BS (%)	123.33	242.76	148.13	145.91

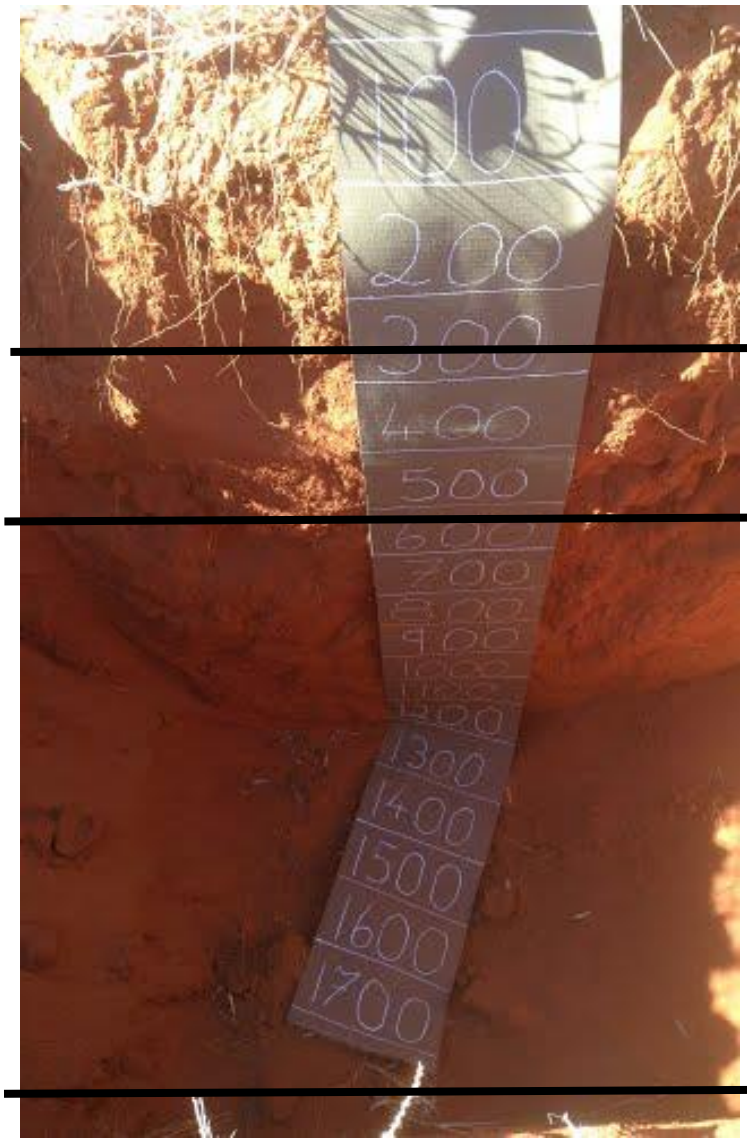

Orthic A horizon (0-300 mm)

Red apedal B1 (300-600 mm)

Red apedal B2 (600-1380 mm)

Saprolite (1380-2000+ mm)

Figure Appendix 11 Profile P7, Hutton soil form.

Profile P8: Coega (*Cg*) 2000 (Marydale)

Physical and chemical description

The profile was classed as an orthic A / hardpan carbonate C1 / hardpan carbonate C2 horizon. The *ot* is an accumulation of aeolian deposits. Orthic A horizon is observed to be compact but friable with a strong < 2mm bleached crust. Soil has washed in between carbonate aggregates in the hardpan carbaonte C1 horizon. Colour in the dry state is 5YR reddish brown to 7.5YR brown and light brown. Colour in the wet state is 5YR dark reddish brown and 7.5YR dark brown and brown. Texture analysis showed that the sand fraction is classed as fine sand for *ob* and *ot*, whereas the *hk* is classed coarse sand. Total texture class is sand for *ot*, *hk1* and *hk2*. The silt / clay fraction is relatively homogenous, differing only slightly. Texturally, besides the difference in fine sand to coarse sand, the profile is very homogenous. Carbonate removed during texture analysis showed no carbonate in the overburden, 3.05% and 1.06% carbonate by weight of the soil in the *ot* and *hk1*, respectively. Coarse fraction is subangular and 5-30 mm in diameter. Difference in coarse fraction is observed that the hk includes indurated laminar carbonate aggregates, cemented together by carbonate. The semi brittle hard carbonates, with washed in aeolian sand of the *hk1* extends for 600 mm to 700 mm depth. Cracks filled with aeolian sand are <5 mm in diameter. Db decreases significantly from 1.69 g cm^{-3} in the *ot* to 1.43 g cm^{-3} in the *hk2*.

The pH_{water} average of the profile (8.45) is almost homogenous throughout. Low organic carbon (OC 0.284%) and nitrogen (N 0.044%) are observed in the *ot*. Exchangeable cations increase with depth, with calcium and magnesium showing differences of 0.10 and 0.25 $cmol_c$ kg^{-1} soil between the *ot* and *hk1*, respectively. A large increase of Ca^{+2} (18.69 $cmol_c$ kg^{-3} soil) is observed in the *hk2*. Sodium is comparatively to other profiles described high in the *hk2* at 0.06 $cmol_c$ kg^{-1} soil. Na^{+} in the *ot* and *hk1* is at 0.01 $cmol_c$ kg^{-1} soil. CEC decreases from 2.88 to 1.89 and increasing again to 19.27 for *ot*, *hk1* and *hk2* respectively. Base saturation peaks at 185.94% for *hk1*, with *ot* at 106.94% and *hk2* at 114.32%.

Table Appendix 15 Modal profile description of Profile P8, Coega soil form

Map/photo:		Soil form and family:	Coega (Marydale) 2000
Latitude/Longitude	28°50'50.44"S / 24° 2'39.00"E	Surface rockiness:	Yes
Altitude (m) :	1025	Occurrence of flooding:	None
Terrain unit:	Footslope	Wind erosion:	Slight
Slope:	0%	Water erosion:	None
Slope shape:	Straight/Straight	Vegetation/Land use:	Virgin (WD, HE3)
Aspect:	Flat	Water table:	None
Microrelief:	Y Anthills	Described by:	Martin Tinnefeld
Parent Material Solum:	Aeolian	Date described (20yymmdd):	140203
Underlying Material:	SC3 Dwyka Tillite/Mudstone	Weathering of underlying material:	Physical
Weather conditions:	SU	Alteration of underlying material:	Y (mudstone/calcarious)
Soil Temperature regime:	IH	Former Weather conditions:	WC3
Moisture regime:	AR		

Horizon	Depth (mm)	Description	Diagnostic horizon
Ob	0	Moisture status: moist; dry colour: 5YR5/3; moist colour: 5YR3/4; Sand; apedal; massive; apedal; non-sticky; non-plastic; slight wind erosion; <2mm weak surface sealing, fine, medium and wide surface cracks; common, fine roots; 22.43% coarse fraction; clear transition.	Overburden
A	0-150	Moisture status: dry; dry colour: 7.5YR5/4; moist colour: 7.5YR3/3; Sand; apedal; massive; apedal; fine, medium cracks; common, fine roots; 47.86% coarse fraction; abrupt, broken transition.	Orthic A
C1	150-600	Moisture status: dry; dry colour: 7.5YR6/3; moist colour: 7.5YR5/4; Sand; apedal; massive; fine, medium and wide cracks; 80% coarse fragments (2-250 mm); few, fine roots; free lime; coarse fragments partially impregnated and cemented by carbonates (<250 mm).	Hardpan carbonate C
C2	600-750	Moisture status: dry; dry colour: 7.5YR6/3; moist colour: 7.5YR5/4; Sand; apedal; massive; fine, medium and wide cracks; 80% coarse fragments (2-250 mm); few, fine roots; free lime; coarse fragments impregnated and cemented by carbonates (<750 mm).	Hardpan carbonate C

Y – Yellow, YR – Yellow-red (Munsel colour); SU – sunny/clear, IH - Isohyperthermic, AR - Aridic, DS – semi deciduous dwarf shrub, DD – deciduous dwarf shrub, HE3 – extensive grazing, ranching, WC3 – no rain in the last 24 hours (FAO, 2006); hk – hardpan carbonate horizon, Ky – Kimberley soil form (SCWG, 1991)

Table Appendix 16 Physical and Chemical properties of a Coega soil form P8

	Orthic (A horizon)	Hardpan Carbonate 1 (C horizon)	Hardpan Carbonate 2 (C horizon)
	0-150 (mm)	150-600 (mm)	600-750 (mm)
Physical properties			
Coarse sand (0-0.5 mm)	11.8	13.1	36.9
Medium sand (0.5-0.25 mm)	12.7	11.6	14.1
Fine sand (0.25-0.106 mm)	52	45.7	24.1
Very fine sand (0.106-0.05 mm)	11.8	16.3	12.8
Sand fraction texture	Fine Sand (88.3)	Fine Sand (86.7)	Coarse Sand (87.9)
Coarse silt (0.05-0.02 mm)	3.6	3.4	3.8
Fine silt (0.02-0.002 mm)	2.7	4	3.4
Clay (>0.002 mm)	5.3	4.6	4.4
Texture	Sand	Sand	Sand
Total texture fraction	99.9	98.7	99.5
CO_3^- (% of sample removed before texture analysis)	0	3.05	1.06
Coarse fraction % of weight	22.43	47.86	80
Bulk density (g cm^{-3})	1.69	1.60	1.43
Chemical properties			
pH (H_2O)	8.48	8.44	8.49
pH (KCL)	8.01	7.92	8.13
OC%	0.284	-	-
N%	0.044	-	-
Mn (mg kg^{-1})	2.20	1.90	1.30
Fe (mg kg^{-1})	2.20	2.70	2.40
Exchangeable cation ($cmol_c$ kg^{-1} soil)			
Calcium	1.68	1.78	18.69
Magnesium	1.09	1.34	2.98
Potassium	0.3	0.37	0.3
Sodium	0.01	0.01	0.06
CEC	2.88	1.89	19.27
S – value	3.08	3.5	22.03
BS (%)	106.94	185.19	114.32

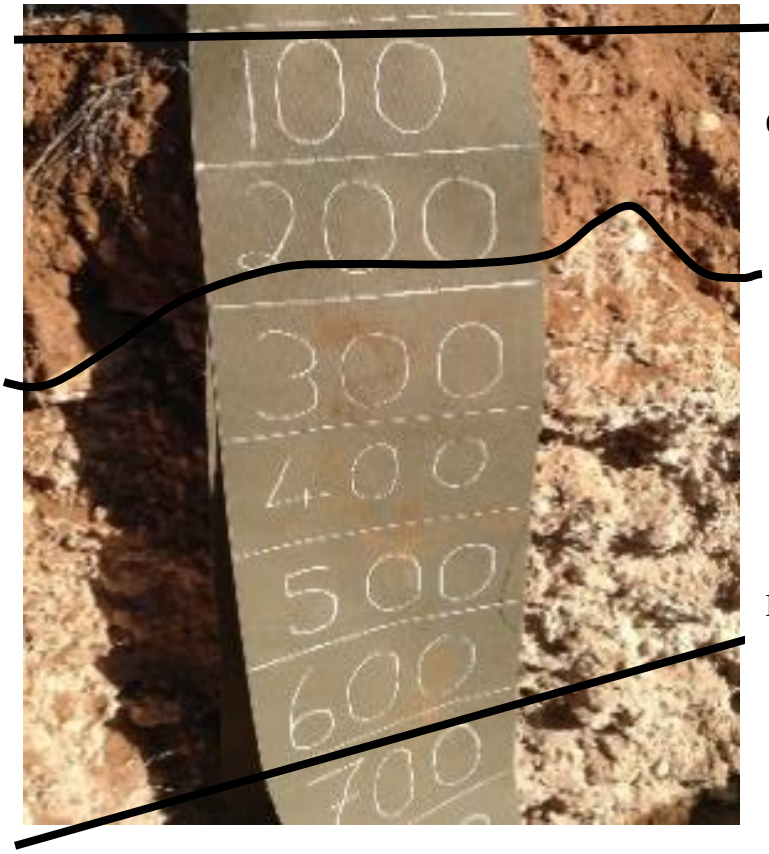

Overburden (0 mm)

Orthic A horizon (0-150 mm)

Hardpan carbonate C1 horizon (150-600 mm)

Hardpan carbonate C2 horizon (600-750 mm)

Figure Appendix 12 Profile P8, Coega soil form.

Profile P9: Hutton (*Hu*) 3100 (Stella)

Physical and chemical description

The profile was classed as an overburden, orthic A / red apedal B1 / red apedal B2 / neocarbonate B3 horizon. The *ob*, *ot*, *re* and *nc* are an accumulation of aeolian deposits. Colour in the dry state is 5YR yellowish red and in the wet state 5YR dark reddish brown and 2.5YR dark reddish brown and reddish brown. The *ob* and *ot* are slightly bleached. Sand texture fraction analysis shows *ot* and *re* B1 and 2 being classed as medium sand and *nc* B3 as fine sand. Overall texture fraction for all horizons is sand. Medium sand fraction increases from 36 to 76%, decreasing to 21% for *ot*, *re* B1 and B2 and *nc* B3, respectively. *Re* B1 and B2 have a very low (4.1 & 0.7%) fine and very fine sand fractions. Coarse silt decreases from *ot* at 2.3% to 0.6% (*re*) and 0.2% (*nc*). Clay % increases gradually from *ot* at 4.9% to 5.9% (*re*) and 6.4% (*nc*). Db increases from *ot* at 1.59 g cm^{-3} to 1.7 g cm^{-3} in the *re* B1 and 2 and decreases to 1.60 in the *nc* B3.

The pH_{water} increases slightly in the *re* horizons, and decreasing again slightly in the *nc* horizon with values of 6.59 (*ot*), 6.92 (re) and 6.7 (*nc*). Low organic carbon (OC 0.19%) and nitrogen (N 0.031%) are observed in the *ot*. Exchangeable cations calcium (2.11 (*ot*) to 15.47 (*nc*) $cmol_c kg^{-1}$ soil) and magnesium (1.16 (*ot*) to 3.98 (*nc*) $cmol_c kg^{-1}$ soil) increase with depth, and sodium increases from 0.02 (*ot*) and 0.01 (*re*) to 0.13 (*nc*) $cmol_c kg^{-1}$ soil. CEC decreases from 4.9 (*ot*) to 3.6 (*re*) $cmol_c kg^{-1}$ soil and increases again to 7.2 $cmol_c kg^{-1}$ soil in the *nc*. Base saturation increases from 78.8% (*ot*) to 118.61 (*re*) to 273.47% (*nc*).

Table Appendix 17 Modal profile description of Profile P9, Hutton soil form

Map/photo:		Soil form and family:	Hutton (Stella) 3100
Latitude/Longitude	28°50'57.64"S 24° 1'56.43"E	Surface rockiness:	None
Altitude (m) :	1022	Occurrence of flooding:	None
Terrain unit:	Upper midslope	Wind erosion:	Slight
Slope:	6%	Water erosion:	None
Slope shape:	Concave/Concave	Vegetation/Land use:	Virgin (WD, HE3)
Aspect:	NW	Water table:	None
Microrelief:	Y Anthills	Described by:	Martin Tinnefeld
Parent Material Solum:	Aeolian	Date described (20yymmdd):	140203
Underlying Material:	SC3 Dwyka Tillite/Mudstone	Weathering of underlying material:	NA
Weather conditions:	SU	Alteration of underlying material:	Y (mudstone/dolerite)
Soil Temperature regime:	IH	Former Weather conditions:	WC3
Moisture regime:	AR		

Horizon	Depth (mm)	Description	Diagnostic horizon
Ob	0-10	Moisture status: moist; dry colour: 5YR4/6; moist colour: 5YR3/4; slightly bleached; sand; apedal; losse; non-sticky; non-plastic; slight wind erosion; <2mm moderate surface sealing, fine, medium and wide surface cracks; few roots; organic matter imbedded, 0.51% by weight; clear transition.	Overburden
A	10-200	Moisture status: moist; dry colour: 5YR4/6; moist colour: 5YR3/4; slightly bleached; sand; apedal; loose; non-sticky; non-plastic; fine, medium and wide cracks; few roots; organic matter imbedded, 0.04% by weight; clear transition.	Orthic A
B1	200-600	Moisture status: dry; dry colour: 5YR4/6; moist colour: 2.5YR3/4; Sand; apedal; massive; fine, few, medium cracks; few fine roots; organic matter imbedded, 0.04% by weight; diffuse transition.	Red-apedal B1
B2	600-100	Moisture status: dry; dry colour: 5YR4/6; moist colour: 2.5YR3/4; Sand; apedal; massive; fine, few, medium cracks; few fine roots; organic matter imbedded, 0.04% by weight; diffuse transition.	Red-apedal B2
B2	1000-1380+	Moisture status: dry; dry colour: 5YR4/6; moist colour: 5YR4/4; Sand; apedal; massive; fine wide cracks; 2.31% coarse fragments (2-6 mm); few fine roots; clear transition; <10% lime nodules, 1-3 mm; clear transition.	Neocarbonate B2

Y – Yellow, YR – Yellow-red (Munsel colour); SU – sunny/clear, IH - Isohyperthermic, AR - Aridic, DS – semi deciduous dwarf shrub, WD – deciduous woodland, HM – medium grassland, HE3 – extensive grazing, ranching, WC3 – no rain in the last 24 hours (FAO, 2006); hk – hardpan carbonate horizon, Ky – Kimberley soil form (SCWG, 1991)

Table Appendix 18 Physical and Chemical properties of the Hutton soil form P9

	Orthic (A horizon)	Red apedal (B1 + 2 horizon)	Neocarbonate (B3 horizon)
	10-200 (mm)	200-1380 (mm)	1380-2000 (mm)
Physical properties			
Coarse sand (0-0.5 mm)	11.3	11.1	27.9
Medium sand (0.5-0.25 mm)	36.4	76.9	21.7
Fine sand (0.25-0.106 mm)	39.5	4.1	30.9
Very fine sand (0.106-0.05 mm)	3.73	0.7	9.3
Sand fraction texture	Medium Sand (90.9)	Medium Sand (92.8)	Fine Sand (89.8)
Coarse silt (0.05-0.02 mm)	2.3	0.6	0.2
Fine silt (0.02-0.002 mm)	0.9	0.6	2.1
Clay (>0.002 mm)	4.9	5.9	6.4
Texture	Sand	Sand	Sand
Total texture fraction	99	99.9	98
CO_3^- (% of sample removed before texture analysis)	0	0	0.66
Coarse fraction % of weight	0.51	0.04	2.31
Bulk density (g cm^{-3})	1.59	1.70	1.60
Chemical properties			
pH (H_2O)	6.59	6.92	6.7
pH (KCL)	5.86	6.05	5.89
OC%	0.19	-	-
N%	0.031	-	-
Mn (mg kg^{-1})	3.5	2.3	6.4
Fe (mg kg^{-1})	4.0	4.0	1.2
Exchangeable cations $cmol_c kg^{-1}$ soil			
Calcium	2.11	2.47	15.47
Magnesium	1.16	1.49	3.98
Potassium	0.57	0.30	0.11
Sodium	0.02	0.01	0.13
CEC	4.9	3.6	7.2
S Value	3.86	4.27	19.69
BS (%)	78.8	118.61	273.47

Figure Appendix 13 Profile P9, Hutton soil form.

Profile P10: Hutton (*Hu*) 3100 (Stella)

Physical and chemical description

The profile was classed as an overburden / orthic A / red apedal B1 / red apedal B2 / yellow-brown apedal B3 horizon. All horizons are an accumulation of aeolian deposition. Colour hue in the dry state decreases with depth from 7.5YR (overburden) to 2.5YR (B3). Colour in the dry state is 7.5YR strong brown 5YR red and yellowish red. Colour in the wet state is 5YR reddish brown to 2.5YR dark red and reddish brown. Textural composition includes the sand fraction being classed as medium sand and overall composition as sand. Coarse sand fraction is evenly distributed and is low (4.3% – 5.7%), medium sand decreases from 87.1% to 53%, fine sand increases with depth from 1.9% to 33.7% and very fine sand being evenly distributed at 1.2, 2.2, 0.1 and 1% respectively down the profile. Fine silt increases from 1.0% to 2.1%, with coarse silt doubling from *ob* to *ot* and decreasing to 0.6% in *yb* B3. Clay percentage increases from *ob* (2.8%) to *re* B1 and B2 (6.0%) and decreases again to 2.4% in *yb* B3. Db is stable at 1.6 g cm^{-3} (*ot*) and 1.64 g cm^{-3} (*re's*) and decreasing to 1.51 g cm^{-3} in the *yb* B3.

The pH_{water} increases to a maximum of 8.34 in the *re* B2 from 6.06 (*ob*) to 7.04 (*ot*), with a value of 7.62 in *yb* B3. Low organic carbon (OC 0.521%) and nitrogen (N 0.04%) are observed in the *ot*. Exchangeable cations of calcium remain constant (0.47 to 1.67 $cmol_c$ kg^{-1} soil), magnesium increasing in the B horizons' (from 1.69 to 2.49 $cmol_c$ kg^{-1} soil), potassium decreasing from an initial value of 0.09 $cmol_c$ kg^{-1} soil to 0.013 $cmol_c$ kg^{-1} soil, and soidium decreasing gradually from 0.11 $cmol_c$ kg^{-1} soil to 0.01 $cmol_c$ kg^{-1} soil vertically down the profile. CEC increases from 3.5 $cmol_c$ kg^{-1} soil (*ob*) to 9.4 $cmol_c$ kg^{-1} soil (*re* B1 and B2) and decreasing again to 6.2 $cmol_c$ kg^{-1} soil (*yb* B3). Base saturation decreases significantly from 55.43% (*ob*) to 64.75% and 45% (*re* B1 and B2) to increases again to 144.89% (*yb* B3).

Table Appendix 19 Modal profile description of Profile P10, Hutton soil form

Map/photo:		Soil form and family:	Hutton (Stella) 3100
Latitude/Longitude	28°52'22.33" / S 24° 2'26.58"E	Surface rockiness:	None
Altitude (m) :	1052	Occurrence of flooding:	None
Terrain unit:	Upper midslope	Wind erosion:	Slight
Slope:	6%	Water erosion:	None
Slope shape:	Convex/Convex	Vegetation/Land use:	Virgin (WD, HE3)
Aspect:	N	Water table:	None
Microrelief:	Y Terraces	Described by:	Martin Tinnefeld
Parent Material Solum:	Aeolian	Date described (20yymmdd):	140203
Underlying Material:	SC3 Dwyka Tillite/Mudstone	Weathering of underlying material:	NA
Weather conditions:	SU	Alteration of underlying material:	Y (mudstone/dolerite)
Soil Temperature regime:	IH	Former Weather conditions:	WC3
Moisture regime:	AR		

Horizon	Depth (mm)	Description	Diagnostic horizon
Ob	0-100	Moisture status: dry; Sand, apedal; loose, non-sticky; non-plastic; slight wind erosion; <0.5 mm weak surface sealing; medium and wide surface cracks.	Overburden
A	100-300	Moisture status: dry; dry colour: 7.5YR5/6; moist colour: 5YR3/4; Sand; apedal; massive; apedal; non-sticky; non-plastic; slight wind erosion; <2mm weak surface sealing; fine, cracks; few fine and coarse roots 20 mm above transition; coarse fraction 2-5 mm round, single source, 0.06% by weight; clear transition.	Orthic A
B1	300-600	Moisture status: dry; dry colour: 5YR4/6; moist colour: 5YR4/4; Sand; apedal; massive; many fine and coarse roots, 0.06% by weight, mainly along transition; clear, smooth transition.	Red-apedal B1
B2	600-1000	Moisture status: dry; dry colour: 2.5YR4/6; moist colour: 2.5YR3/6; Sand; apedal; massive; common fine and coarse roots, 0.07% by weight; clear transition; clear, slightly wavy transition.	Red-apedal B2
B3	1000-1400+	Moisture status: dry; dry colour: 5YR4/6; moist colour: 2.5YR4/4; Sand; apedal, massive; 0.06% coarse fragments (2-6 mm); common roots; lime nodules <5% <2-6 mm round.	Yellow-brown apedal B3

Y – Yellow, YR – Yellow-red (Munsel colour); SU – sunny/clear, IH - Isohyperthermic, AR - Aridic, DS – semi deciduous dwarf shrub, WD – deciduous woodland, HM – medium grassland, HE3 – extensive grazing, ranching, WC3 – no rain in the last 24 hours (FAO, 2006); hk – hardpan carbonate horizon, Ky – Kimberley soil form (SCWG, 1991)

Table Appendix 20 Physical and Chemical properties of a Hutton soil P10

	Orthic (A horizon)	Red apedal (B1 horizon)	Red apedal (B2 horizon)	Yellow-brown apedal (B3 horizon)
	0-300 (mm)	300-600 (mm)	600-1000 (mm)	1000-1400+ (mm)
Physical properties				
Coarse sand (0-0.5 mm)	4.3	5.7	4.3	5.1
Medium sand (0.5-0.25 mm)	87.1	44.9	57.8	53
Fine sand (0.25-0.106 mm)	1.9	37.7	29.4	33.7
Very fine sand (0.106-0.05 mm)	1.2	2.2	0.1	1.0
Sand fraction texture	Medium Sand (94.5)	Medium Sand (90.5)	Medium Sand (91.6)	Medium Sand (92.8)
Coarse silt (0.05-0.02 mm)	1	1.1	0.6	2.1
Fine silt (0.02-0.002 mm)	0.8	2.6	1.1	0.6
Clay (>0.002 mm)	2.8	5.5	6.0	2.4
Texture	Sand	Sand	Sand	Sand
Total texture fraction	99.1	99.7	99.3	97.9
CO_3^- (% of sample removed before texture analysis)	0	0	0	0
Coarse fraction % of weight	0.06	0.06	0.07	0.06
Bulk density (g cm^{-3})	1.60	-	1.64	1.51
Chemical properties				
pH (H_2O)	6.06	7.04	8.34	7.62
pH (KCL)	5.21	6.05	7.29	6.33
OC%	0.521	-	-	-
N%	0.04	-	-	-
Mn (mg kg^{-1})	-	-	-	-
Fe (mg kg^{-1})	-	-	-	-
Exchangeable cations ($cmol_c$ kg^{-1} soil)				
Calcium	1.05	0.99	1.67	0.47
Magnesium	1.69	1.48	2.49	5.61
Potassium	0.09	0.09	0.017	0.013
Sodium	0.11	0.03	0.05	0.01
CEC	3.5	4.0	9.4	4.21
S Value	1.94	2.59	4.23	6.10
BS (%)	55.43	64.75	45.0	144.89

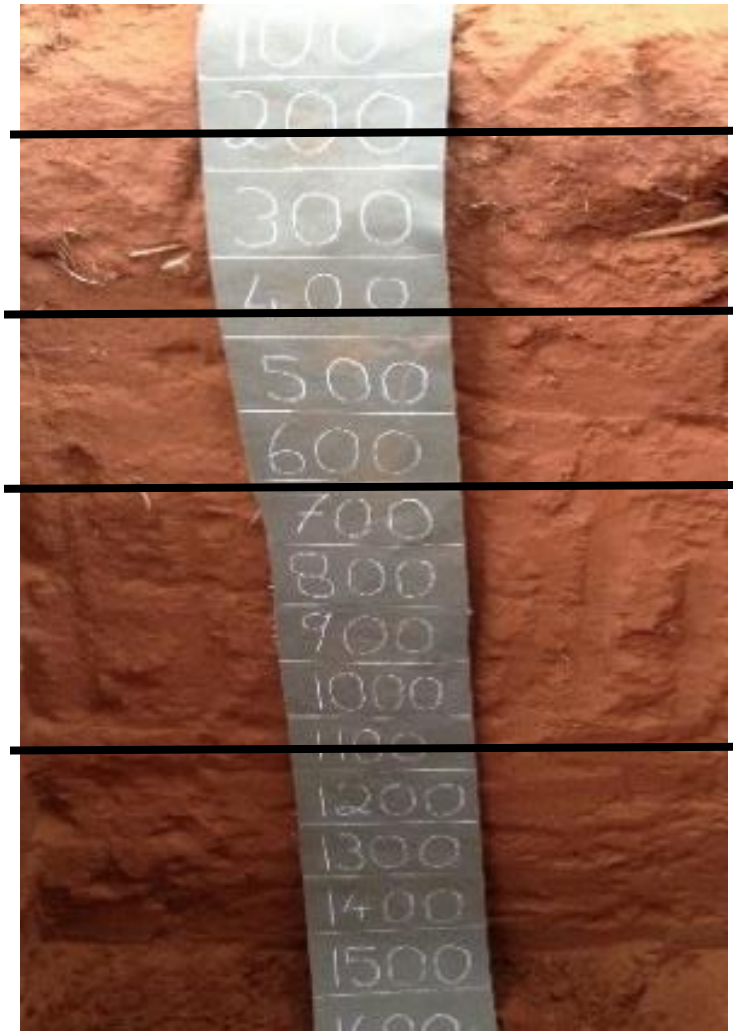

Figure Appendix 14 Profile P10, Hutton soil form.

Profile P11: Clovelly (*Cv*) 3100 (Setlagole)

Physical and chemical description

The profile was classed as an overburden / orthic A / yellow-brown apedal B1 / yellow-brown apedal B2 horizon. Parent material of the profile is aeolian deposits. Overburden and *ot* are lighter in hue, showing marked yellowing in the dry state. Colour in the dry state is 7.5YR strong brown and in the wet state 5YR dark brown 7.5YR brown and strong brown. Texture analysis shows overall sand fraction is of medium sand and overall texture is of pure sand for the *ot* and sand for the *yb* B's. Significant texture variations are observed from top to bottom in the medium sand and coarse sand fractions, which increase and decrease with depth from 48.1% to 81.4% and 44.9% to 7.1%, respectively. Coarse and fine silt values remain relatively stable with clay increasing from 2.3% to 5.8%. Coarse fraction percentages increase slightly in the *yb* B1 horizon from 0.06% to 0.21% and drop again to 0.08%, in the *yb* B2 horizon. Db decreases with depth from 1.6 g cm^{-3} in the *ot* to 1.56 g cm^{-3} in the *yb* B2.

The pH_{water} increases from 7.3 to 8.01 from *ot* to *yb* B2 horizons. Low organic carbon (OC 0.091%) and nitrogen (N 0.018%) are observed in the *ot*. Exchangeable cations of calcium increase from 1.27 $cmol_c$ kg^{-1} soil to 1.67 $cmol_c$ kg^{-1} soil, magnesium increases from 0.84 $cmol_c$ kg^{-1} soil to 2.43 $cmol_c$ kg^{-1} soil, potassium remains stable around 0.19 $cmol_c$ kg^{-1} soil and for sodium increases from 0.02 to 0.1 $cmol_c$ kg^{-1} soil. CEC fluctuates from 4.7 to 3.3 to 5.4 $cmol_c$ kg^{-1} soil. Base saturation follows trend in fluctuation with 49.57, 116.36 and 80.74%.

Table Appendix 21 Modal profile description of profile P11, Clovelly soil form

Map/photo:		Soil form and family:	Clovelly (Setlagole) 3100
Latitude/Longitude	28°51'58.56"S / 24° 2'15.07"E	Surface rockiness:	None
Altitude (m) :	1025	Occurrence of flooding:	None
Terrain unit:	Lower midslope	Wind erosion:	Slight
Slope:	1%	Water erosion:	None
Slope shape:	Concave/straight	Vegetation/Land use:	Virgin (HM, DS, WD, HE3)
Aspect:	NW	Water table:	None
Microrelief:	Y Anthills	Described by:	Martin Tinnefeld
Parent Material Solum:	Aeolian	Date described (20yymmdd):	140204
Underlying Material:	SC3 Dwyka Tillite/Mudstone	Weathering of underlying material:	Physical (moderate) Chemical (weak)
Weather conditions:	SU	Alteration of underlying material:	Y (mudstone : hk)
Soil Temperature regime:	IH	Former Weather conditions:	WC3
Moisture regime:	AR		

Horizon	Depth (mm)	Description	Diagnostic horizon
Ob	0-100	Moisture status: dry; Sand, apedal; loose, non-sticky; non-plastic; slight wind erosion; <1 mm weak surface sealing; fine surface cracks; embedded organic material.	Overburden
A	100-300	Moisture status: dry; dry colour: 7.5YR5/6; moist colour: 5YR3/4; Pure sand; apedal; massive; non-sticky; non-plastic; common roots; organic material embedded, 0.06% by weight; clear transition.	Orthic A
B1	300-850	Moisture status: dry; dry colour: 7.5YR5/6; moist colour: 7.5YR4/4; Sand; apedal; massive; few, fine cracks; many fine roots 0.21% by weight; coarse fraction include few manganese concretions <5 mm; clear transition.	Yellow-brown apedal B1
B2	850-1400+	Moisture status: dry; dry colour: 7.5YR5/6; moist colour: 7.5YR4/6; Sand; apedal; massive; fine, medium and wide cracks; 0.08% coarse fragments, sub-angular blocky (2-20 mm); common fine roots; coarse fragments impregnated with carbonate; gradual transition.	Yellow-brown apedal B2

Y – Yellow, YR – Yellow-red (Munsel colour); SU – sunny/clear, IH - Isohyperthermic, AR - Aridic, DS – semi deciduous dwarf shrub, WD – deciduous woodland, HM – medium grassland, HE3 – extensive grazing, ranching, WC3 – no rain in the last 24 hours (FAO, 2006); hk – hardpan carbonate horizon, Ky – Kimberley soil form (SCWG, 1991)

Table Appendix 22 Physical and Chemical properties of the Clovelly soil form P11

	Orthic (A horizon)	Yellow-brown apedal (B1 horizon)	Yellow-brown apedal (B2 horizon)
	0-300 (mm)	300-850 (mm)	850-1400+ (mm)
Physical properties			
Coarse sand (0-0.5 mm)	2.8	3.3	3
Medium sand (0.5-0.25 mm)	48.1	53.2	81.4
Fine sand (0.25-0.106 mm)	44.9	37.0	7.1
Very fine sand (0.106-0.05 mm)	0.2	0.2	0.9
Sand fraction texture	Medium Sand (96)	Medium Sand (94)	Medium Sand (93)
Coarse silt (0.05-0.02 mm)	0.2	0.4	0.7
Fine silt (0.02-0.002 mm)	0.7	0.7	0.4
Clay (>0.002 mm)	2.3	4.12	5.8
Texture	Pure sand	Sand	Sand
Total texture fraction	99.2	99.22	99.9
CO_3^- (% of sample removed before texture analysis)	0	0	0
Coarse fraction % of weight	0.06	0.21	0.08
Bulk density (g cm^{-3})	1.60	-	1.56
Chemical properties			
pH (H_2O)	7.3	7.5	8.01
pH (KCL)	6.58	5.91	6.41
OC%	0.091	-	-
N%	0.018	-	-
Mn (mg kg^{-1})	2.10	4.20	-
Fe (mg kg^{-1})	1.10	2.80	-
Exchangeable cations ($cmol_c$ kg^{-1} soil)			
Calcium	1.27	1.74	1.67
Magnesium	0.84	1.87	2.43
Potassium	0.20	0.19	0.16
Sodium	0.02	0.04	0.10
CEC	4.7	3.3	5.4
S Value	2.33	3.84	4.36
BS (%)	49.57	116.36	80.74

Overburden (0-100 mm)

Orthic A horizon (100-300 mm)

Yellow-brown apedal B (300-850

Yellow-brown apedal B horizon (850-1400+

Figure Appendix 15 Profile P11, Clovelly soil form.

Profile P12: Namib (*Nb*) 1200 (Beachwood)

Physical and chemical description

The profile was classed as an overburden / orthic A / regic sand B1 / regic sand B2 horizon on rock. Parent material of the profile is aeolian deposits. Colour in the dry state is 7.5YR brown and strong brown. Colour in the wet state is 7.5YR dark brown. Overburden and *ot* are lighter in hue, showing marked yellowing in the dry state. Texture analysis showed an overall sand fraction classed as medium sand for *ob* and *ot* and coarse sand for *rs* B1 and *rs* B2 horizons. Overall texture is of pure sand, for the *ob* and *ot*, and sand for the *rs* B1 and B2 horizons. Significant texture variations are observed from top to bottom in the fine (36.1%-29.10%-13.1%), medium (46.65%-25.65%-37.65%) and coarse (1.98%-27.80%-35.23%) sand fractions. Coarse, fine silt and clay values remain relatively stable. Slight aggregation around root hairs is observed in the *ot*. Bulk density increases down the profile from 1.46 g cm^{-3} in the *ot*, to 1.53 g cm^{-3} in the *rs* B2.

The pH_{water} fluctuates from 8.24 to 7.48 (*rs* B1) to 7.95 (*rs* B2). Low organic carbon (OC 0.061%) and nitrogen (N 0.08%) are observed in the *ob*. Exchangeable cations of calcium increase from 9.30 $cmol_c$ kg^{-1} soil to 13.28 $cmol_c$ kg^{-1} soil, sodium remains stable at 0.08 $cmol_c$ kg^{-1} soil from *ot* to *rs* B1 and increases to 0.13 $cmol_c$ kg^{-1} in the *rs* B2 horizon. CEC decreases from 2.8 to 2.11 2.34 $cmol_c$ kg^{-1} soil down the profile. Base saturation increases from 442.14 to 585.31 to 735.47% for *ot*, *rs* B1 and *rs* B2 horizons, respectively.

Table Appendix 23 Modal profile description form of Profile P12, Namib soil form

Map/photo:		Soil form and family:	Namib (Beachwood) 1200
Latitude/Longitude	29° 8'40.41"S / 23°45'2.31"E	Surface rockiness:	None
Altitude (m) :	1045	Occurrence of flooding:	None
Terrain unit:	Lower midslope	Wind erosion:	Slight
Slope:	5%	Water erosion:	None
Slope shape:	Concave/straight	Vegetation/Land use:	Virgin (DS, HM, WD, HE3)
Aspect:	W	Water table:	None
Microrelief:	Y Anthills	Described by:	Martin Tinnefeld
Parent Material Solum:	Aeolian	Date described (20yymmdd):	140214
Underlying Material:	Dolerite	Weathering of underlying material:	Physical (moderate) Chemical (weak)
Weather conditions:	SU	Alteration of underlying material:	N
Soil Temperature regime:	IH	Former Weather conditions:	WC3
Moisture regime:	AR		

Horizon	Depth (mm)	Description	Diagnostic horizon
Ob	0-20	Moisture status: dry; dry colour: 7.5YR4/4; moist colour: 7.5YR3/2; Pure sand, apedal; loose, non-sticky; non-plastic; slight wind erosion; <1 mm weak surface sealing; fine surface cracks; embedded organic material.	Overburden
A	20-120	Moisture status: dry; dry colour: 7.5YR4/6; moist colour: 7.5YR3/3; Pure sand; apedal; massive; non-sticky; non-plastic; common roots; organic material embedded, 0.08% by weight; clear transition.	Orthic A
B1	120-1150	Moisture status: dry; dry colour: 7.5YR4/6; moist colour: 7.5YR3/4; Pure sand; apedal; massive; non-sticky; non-plastic; 20 mm thick layers of aeolian stratification; common roots; 0.02% by weight; clear transition.	Regic sand B1
B2	1150-2000	Moisture status: dry; dry colour: 7.5YR4/2; moist colour: 7.5YR3/3; Pure sand; apedal; massive; non-sticky; non-plastic; 20 mm thick layers of aeolian stratification; common fine roots; 0.04% by weight; clear transition.	Regic sand B2
C/R	2000+	Boulders and other coarse fragments form the boundary between the rock and soil.	

Y – Yellow, YR – Yellow-red (Munsel colour); SU – sunny/clear, IH - Isohyperthermic, AR - Aridic, DS – semi deciduous dwarf shrub, WD – deciduous woodland, HM – medium grassland, HE3 – extensive grazing, ranching, WC3 – no rain in the last 24 hours (FAO, 2006); hk – hardpan carbonate horizon, Ky – Kimberley soil form (SCWG, 1991)

Table Appendix 24 Physical and Chemical properties of a Namib soil form P12

	Orthic (A horizon)	Regic sand (B1 horizon)	Regic sand (B2 horizon)
	20-200 (mm)	200-1150 (mm)	1150-2000 (mm)
Physical properties			
Coarse sand (0-0.5 mm)	1.98	27.80	35.23
Medium sand (0.5-0.25 mm)	46.65	25.65	37.65
Fine sand (0.25-0.106 mm)	36.10	29.10	13.10
Very fine sand (0.106-0.05 mm)	8.39	8.37	5.68
Sand fraction texture	Medium Sand (93)	Coarse Sand (91)	Coarse Sand (92)
Coarse silt (0.05-0.02 mm)	1.31	1.34	2.06
Fine silt (0.02-0.002 mm)	1.23	1.13	1.11
Clay (>0.002 mm)	3.40	3.69	4.52
Texture	Pure Sand	Pure Sand	Pure Sand
Total texture fraction	98.94	97.16	99.69
CO_3^- (% of sample removed before texture analysis)	0.09	0.22	0.45
Coarse fraction % of weight	0.08	0.02	0.04
Bulk density (g cm^{-3})	1.46	1.48	1.53
pH (H_2O)	8.24	7.48	7.95
pH (KCL)	7.36	6.67	7.01
OC%	0.061	-	-
N%	0.014	-	-
Mn (mg kg^{-1})	-	-	-
Fe (mg kg^{-1})	-	-	-
Calcium	9.30	8.99	13.28
Magnesium	3.27	3.18	3.66
Potassium	0.18	0.10	0.14
Sodium	0.08	0.08	0.13
CEC	2.8	2.11	2.34
S Value	12.83	12.35	17.21
BS (%)	442.14	585.31	735.47

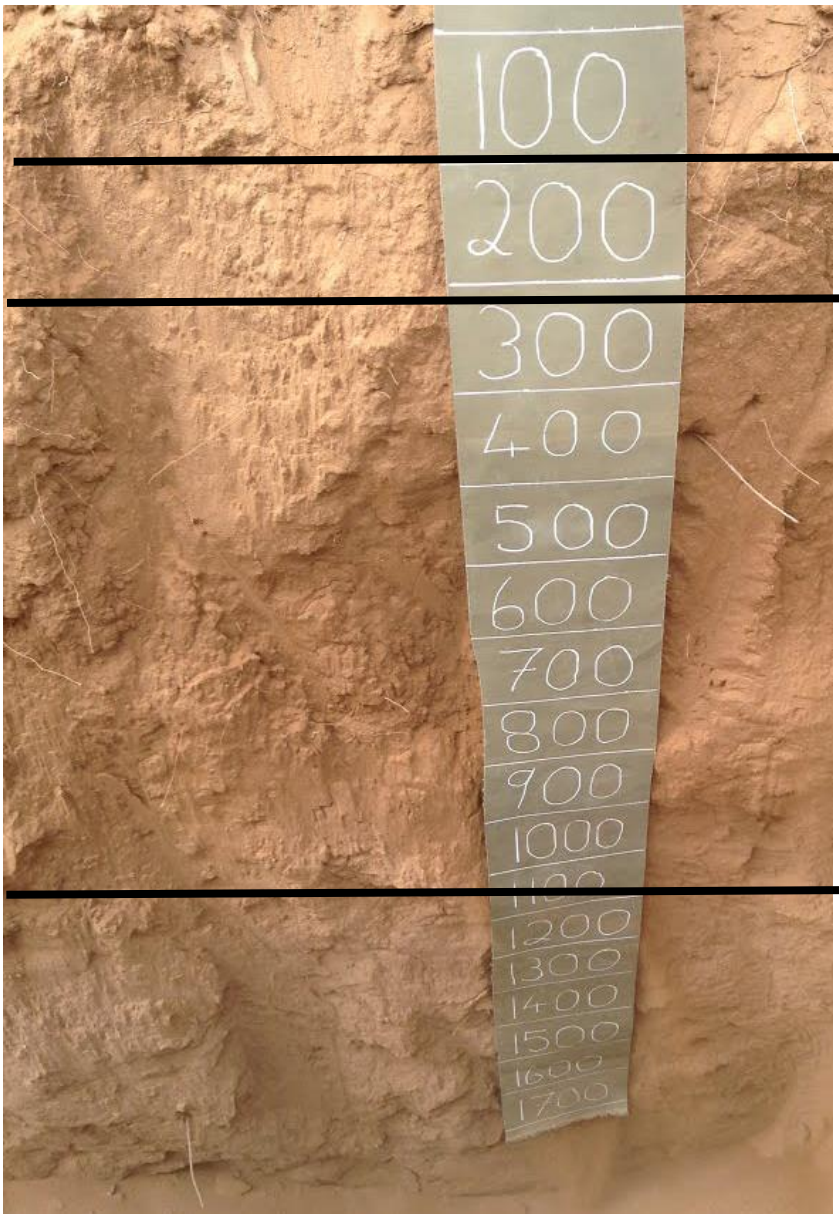

Overburden (0-20 mm)

Orthic A horizon (20-120 mm)

Regic sandB1 (120-1150 mm)

Regic sandB2 (1150-2000 mm)

Figure Appendix 16 Profile P12, Namib soil form.

Profile P13: Valsrivier (*Va*) 1112 (Luckhoff)

Physical and chemical description

The profile was classed as an orthic A / pedocutanic B1 / pedocutanic B2 / rock (Mudstone). Orthic A horizon is an accumulation of colluvial and aeolian deposits. The surface has a thin <2 mm hard surface crust with fine moderately wide spaced cracks. Colour in the dry stat is 10YR very pale brown, pale brown, yellowish brown to brown. Colour in the wet state is 2.5Y light yellowish brown, light olive brown, to 10YR dark brown to very dark greyish brown. Orthic A has moderate subangular blocky ped formation. It is bleached throughout with no transition between ped face and ped interior. Transition to *pe* B1 is clear. Pedocutanic B1 horizon has a medium sub-angular blocky structure. It has an abrupt transition to underlying *pe* B2. The *pe* B2 has a medium to hard sub-angular blocky structure. A change in hue from light to dark is observed at the *pe* B1/B2 transition. The textural class of *ot* changes from silt loam to clay loam in the *pe* B1 and *pe* B2. Sand fraction decreases from 48% (*ot*) *to* 15 % (*pe* B2) and clay/silt fraction increase from 30/22% (*ot*) to 31/40% (*pe* B1) to 47/38% (*pe* B2). Bulk density decreases from 1.3 g cm^{-3} in the *ot* to 1.24 g cm^{-3} in *pe* B2.

The pH_{water} increases down the profile from 6.65 (*ot*) to 8.05 (*pe* B2). Exchangeable K^{+} decreases down the profile, with Ca^{+2}, Mg^{+2} and Na^{+2} increasing resulting in S-value increasing from 8.89 to 35.4 $cmol_c kg^{-1}$. Sodium values increase from 0.34 to 9.48 $cmol_c kg^{-1}$ soil. CEC increases from 8.8 to 13.29 $cmol_c kg^{-1}$ and BS increases from 101.02% to 266.37%.

Table Appendix 25 Modal profile description of Profile P13, Valsrivier soil form

Map/photo:		Soil form and family:	Va (Luckhoff) 1112
Latitude/Longitude	29°32'22.92"S / 23°57'34.73"E	Surface rockiness:	None
Altitude (m) :	1036	Occurrence of flooding:	None
Terrain unit:	Toeslope	Wind erosion:	Slight
Slope:	0%	Water erosion:	None
Slope shape:	Flat	Vegetation/Land use:	Virgin (DS/DD, HE3)
Aspect:	NW	Water table:	None
Microrelief:	Y Anthills	Described by:	Martin Tinnefeld
Parent Material Solum:	Colluvial	Date described (20yymmdd):	140214
Underlying Material:	SC3 Dwyka Tillite/Mudstone	Weathering of underlying material:	Physical (moderate) Chemical (weak)
Weather conditions:	SU	Alteration of underlying material:	Y (mudstone : hk)
Soil Temperature regime:	IH	Former Weather conditions:	WC2
Moisture regime:	AR		

Horizon	Depth (mm)	Description	Diagnostic horizon
surface	0	Moisture status: dry; dry colour: 10YR7/3; moist colour: 2.5Y6/4; dominant surface bleaching; Silt Loam; moderate, sub-angular blocky; slightly-sticky, slightly-plastic; thin <2 mm, hard surface crust; fine moderately widely spaced; common fine roots; no visible OM embedded.	Surface
A	0-350	Moisture status: dry; dry colour: 10YR6/3; moist colour: 2.5Y5/6; dominant bleaching; Silt Loam; moderate, sub-angular blocky; slightly-sticky, slightly-plastic; common fine roots; no visible OM embedded; clear transition.	Orthic A
B	350-700	Moisture status: dry; dry colour: 10YR5/4; moist colour: 10YR3/3; high bleaching; Clay Loam; moderate, sub-angular blocky; slightly-sticky, slightly-plastic; common fine roots; abrupt transition.	Pedocutanic B1
	700-1800	Moisture status: dry; dry colour: 10YR4/3; moist colour: 10YR3/2; Clay Loam; moderate to strong, medium, sub-angular blocky; very hard, slightly-sticky, slightly-plastic; common fine roots; few fine and medium cracks; few, fine roots; 20 mm stratifications; continuous distinct clay coating of the pedsurfaces; free lime; gypsum crystals in between peds; no transition observed.	Pedocutanic B2

Y – Yellow, YR – Yellow-red (Munsel colour); SU – sunny/clear, IH - Isohyperthermic, AR - Aridic, DS – semi deciduous dwarf shrub, DD – deciduous dwarf shrub, HE3 – extensive grazing, ranching, WC2 – no rain in the last week (FAO, 2006); hk – hardpan carbonate horizon, Ky – Kimberley soil form (SCWG, 1991)

Table Appendix 26 Physical and Chemical properties of Valsrivier soil form P13

	Orthic (A horizon)	Pedocuatnic (B1 horizon)	Pedocutanic (B2 horizon)
	0-350 (mm)	350-700 (mm)	700-1800 (mm)
Physical properties			
Coarse sand (0-0.5 mm)	6.2	5.1	3.6
Medium sand (0.5-0.25 mm)	29.3	3.8	5.1
Fine sand (0.25-0.106 mm)	11.7	9.4	0.6
Very fine sand (0.106-0.05 mm)	0.8	10.7	5.7
Sand fraction texture	Medium Sand (48)	Very fine Sand (29)	Very fine Sand (15)
Coarse silt (0.05-0.02 mm)	26.5	18.8	23.3
Fine silt (0.02-0.002 mm)	3.4	11.1	21.7
Clay (>0.002 mm)	21.2	40	38
Texture	Silt Loam	Clay Loam	Clay Loam
Total texture fraction	99.1	98.9	98
CO_3^- (% of sample removed before texture analysis)	0	3.61	4.96
Coarse fraction % of weight	4.72	4.47	0
Bulk density (g cm^{-3})	1.3	1.28	1.24
Chemical properties			
pH (H_2O)	6.65	7.23	8.05
pH (KCL)	6.3	7.5	7.9
OC%	0.298	-	-
N%	0.047	-	-
Mn (mg kg^{-1})	11.5	7.2	3.9
Fe (mg kg^{-1})	10.5	10.3	2.4
Exchangeable cations ($cmol_c kg^{-1}$ soil)			
Calcium	4.34	4.34	16.1
Magnesium	3.68	3.93	9.65
Potassium	0.52	0.12	0.22
Sodium	0.34	5.17	9.48
CEC	8.8	13.56	13.29
S Value	8.89	22.4	35.4
BS (%)	101.02	165.19	266.37

Orthic A horizon (0-350 mm)

Pedocutanic B1 horizon (350-700 mm)

Pedocutanic B2 horizon (700-1800 mm)

Figure Appendix 17 Profile P13, Valsrivier soil form.

Appendix C

Soil observation distribution maps

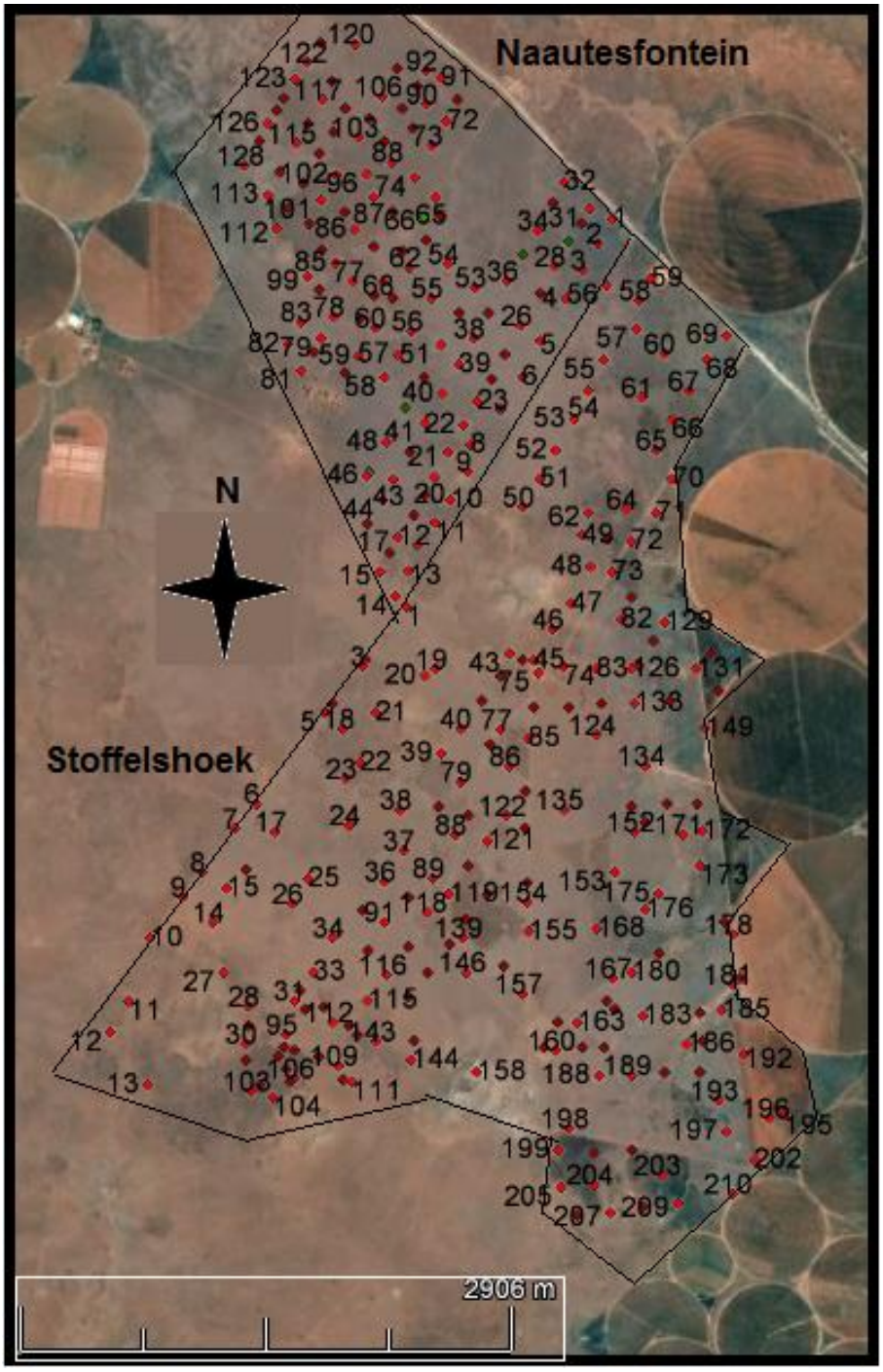

Figure Appendix 18 Profile distribution on Naautesfontein and Stoffelshoek, collectively site 1.

Figure Appendix 19 Profile distribution on Eldorein, site 2.

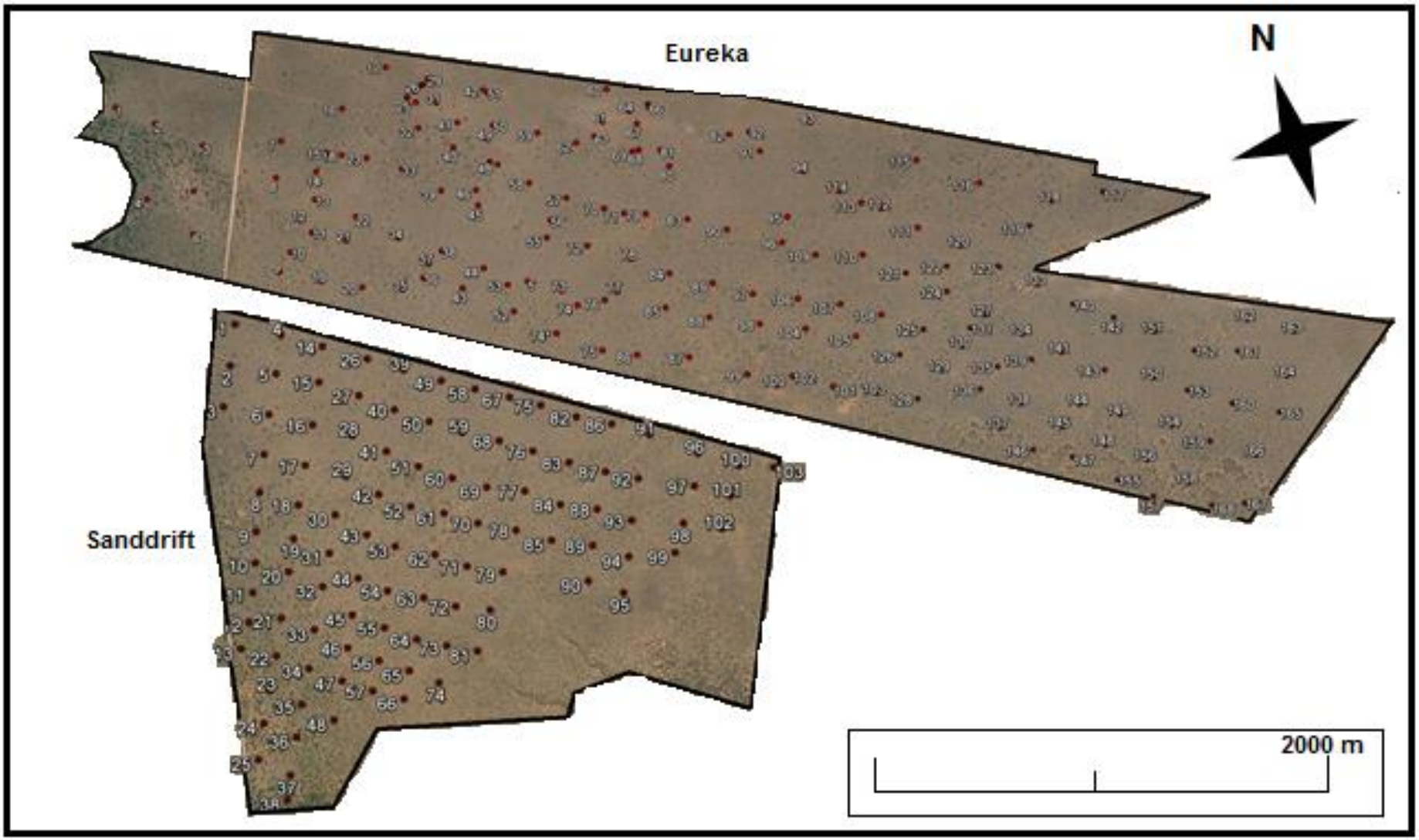

Figure Appendix 20 Profile distribution on Eureka (top) and Sanddrift (bottom), collectively site 3.

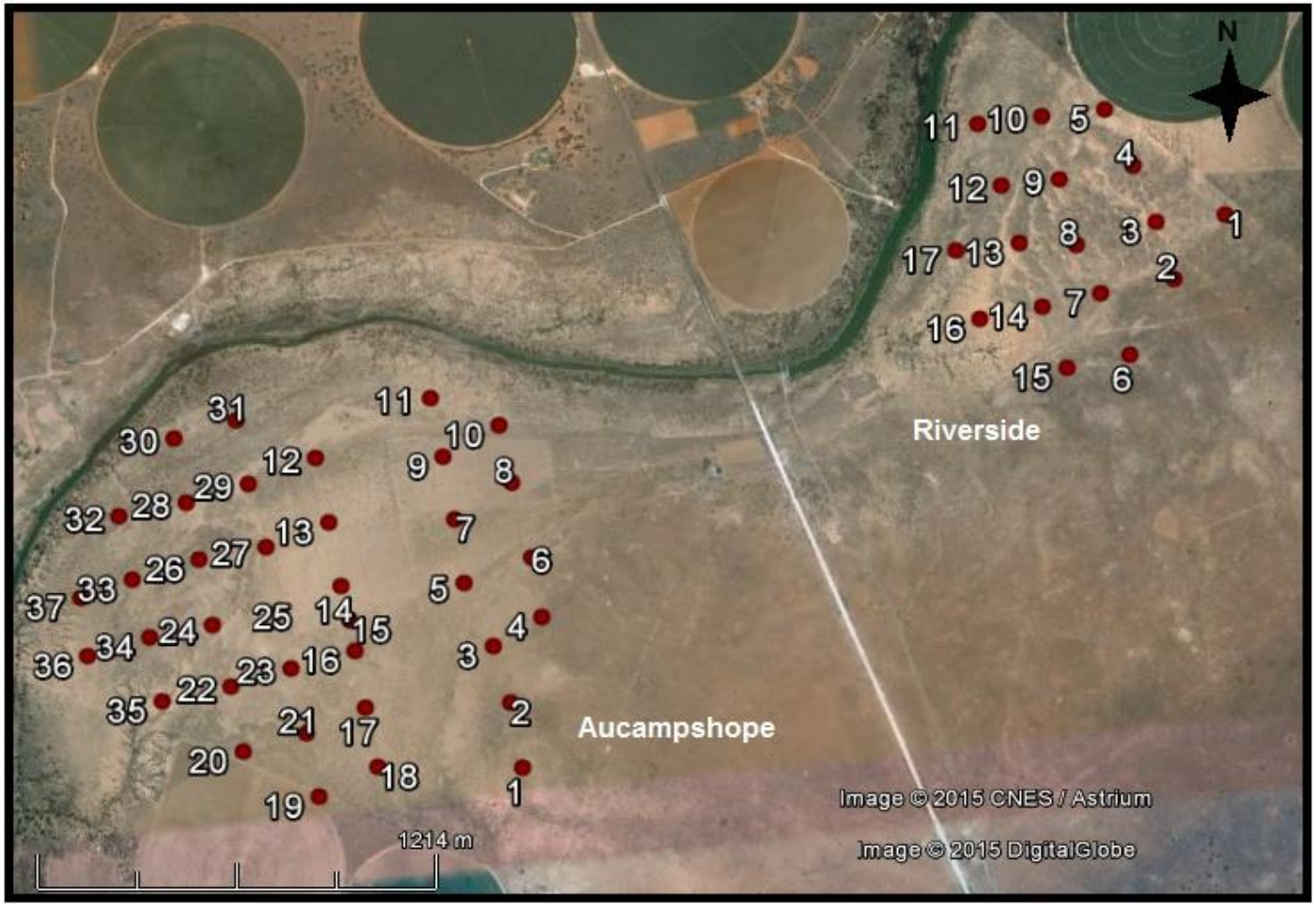

Figure Appendix 21 Profile distribution on Riverside and Aucampshope, collectively site 4.

Appendix D

Hydraulic properties of select arid soils

Table Appendix 27 Porosities and bulk densities of diagnostic horizons in sequence of master profiles on different sites

Profile and soil from	TMU	DH	Cl (%)	Lower depth (mm)	Porosity (cm^3 cm^{-3})	Db (mg m^{-3})
Site 1						
P1	3	otd	5	300	0.58	1.66
Kimberley soil form		re1	7	1100	0.55	1.74
		re2	4	1250	0.57	1.67
		sl	8	1350	0.59	1.62
		sc	-	1500	0.94	1.50
P2	4	ot	5	250	0.55	1.59
Addo soil form		nc	10	1000	0.58	1.79
		sl	9	1100	0.57	1.70
		sc	27	1300	0.64	1.50
P3	3	otd	6	250	0.63	1.53
Kimberley soil form		ot-re	6	500	0.62	1.54
		re	6	800	0.61	1.57
		sl	8	1300	0.65	1.47
		sc	6	1500	0.62	1.54
		uwsow	10	1550	0.55	1.74
P4	4	otd	6	200	0.59	1.60
Hutton soil form		ot/re	12	400	0.60	1.61
		re	12	850	0.63	1.53
P5	3	ot		150	0.58	1.64
Coega soil form		re		650	0.51	1.87
Site 2						
P6	5	ot	4	300	0.59	1.57
Addo soil form		nc1	8	700	0.58	1.54
		sc	17	900	0.69	1.39
P7	4	ot	5	300	0.62	1.61
Hutton soil form		re	10	1400	0.63	1.61
P8	5	ot	5	150	0.56	1.69
Coega soil form		hk1	5	300	0.60	1.60
		hk2	5	700	0.67	1.43
P9	4	ot	5	200	0.61	1.59
Hutton soil form		re	4	600	0.65	1.49
		re		1000	0.56	1.70
		nc	6	1400	0.60	1.60
P10	3	ot	3	300	0.60	1.60
Hutton soil form		re1		700		1.62
		re2	3	1400	0.62	1.51
P11	4	ot	2	300	0.59	1.60
Clovelly soil form		yb1		700		1.56
		yb2	6	900	0.60	1.56
Site 3						
P12	3	ot		200	0.44	1.46
Namib soil form		rs	4	500	0.44	1.48
Site 4						
P13	5	ot	48	350	0.65	1.30
Valsrivier soil form		pe1	29	700	0.71	1.28
		pe2	15	1800	-	1.24

DH – diagnostic horizon, Db – bulk density, ot – Orthic A horizon, otd – distrurbed orthic A horizon, otud – undisturbed orthic A horizon, re – red apedal B horizon, re1 – red apedal B1 horizon, re2 – red apedal B2 horizon, yb – yellowbrown apedal B horizon, yb1 - yellowbrown apedal B1 horizon, yb2 - yellowbrown apedal B2 horizon, pe – pedocutanic B horizon, pe1 – pedocutanic B1 horizon, pe2 – pedocutanic B2 horizon, nc – neocarbonate B horizon, - nc1 – neocarbonate B1 horizon, nc2 – neocarbonate B2 horizon, sc – soft carbonate horizon, hk – hardpan carbonate horizon.

Table Appendix 28 Soil hydraulic conductivity (K_s), total effective porosity (θ_m) and percent contribution of different pores to the total saturated water flux (ϕ_i).This is analyzed as the difference between each set of consecutive water tensions on different diagnostic horizons

Profile	Horizons	K (cm s^{-1})			Macropores		Meso & Micropores	
		0 cm	- 3 cm	K_m	$\theta_{m\ -0\ to\ -3}$ (%)	$\phi_{-0\ to\ -3}$ (%)	$\theta_{mm\ -3\ to\ -15000}$(%)	$\phi_{-3\ to\ -15000}$(%)
P1	otd	0.002654	0.00029	0.002364	0.0000208	89.07	99.99	10.93
Kimberley	re1	0.005363	0.000428	0.004935	0.0000421	92.02	99.99	7.98
	re2	0.003269	0.000657	0.002611	0.0000257	79.89	99.99	20.11
	sl	0.000769	0.00016	0.00061	0.00000604	79.27	99.99	20.73
	sc	0.0007	0.0000436	0.000656	0.0000055	93.77	99.99	6.23
P2	ot	0.002347	0.000894	0.001453	0.0000184	61.92	99.99	38.08
Addo	nc	0.004929	0.00127	0.003659	0.0000387	74.24	99.99	25.76
	sl	0.000836	0.00023	0.000606	0.00000657	72.44	99.99	27.56
	sc	0.001614	0.001089	0.000524	0.0000127	32.49	99.99	67.51
P3	otd	0.002347	0.00151	0.000837	0.0000184	35.67	99.99	64.33
Kimberley	ot/re	0.003332	0.00181	0.001522	0.0000262	45.67	99.99	54.33
	re	0.004265	0.0014	0.002865	0.0000335	67.17	99.99	32.83
	re	0.000829	0.000214	0.000615	0.0000651	74.20	99.99	25.8
	sc	0.007754	0.000921	0.006833	0.0000609	88.13	99.99	11.87
	uwosw	0.002562	0.001462	0.001101	0.0000201	42.95	99.99	57.05
P4	otd	0.002509	0.00004.89	0.00246	0.0000197	98.05	99.99	1.95
Hutton	ot/re	0.004423	0.000113	0.004309	0.0000347	97.44	99.99	2.56
	re	0.003124	0.000184	0.00294	0.0000245	94.10	99.99	5.9
	sl	0.00398	0.000123	0.003857	0.0000313	96.90	99.99	3.1
	so	0.000658	0.000104	0.000553	0.00000516	84.14	99.99	15.86
P5	otud	0.009951	0.000611	0.00934	0.0000782	93.86	99.99	6.14
Coega	otd	0.007616	0.000739	0.006876	0.0000598	90.29	99.99	9.71
P6	ot	0.006785	0.001768	0.005017	0.0000533	73.94	99.99	26.06
Addo	nc1	0.017306	0.002417	0.014889	0.000136	86.04	99.99	13.96
	sc	0.007108	0.000882	0.006226	0.0000558	87.59	99.99	12.41
P7	ot	0.00759	0.000759	0.00683	0.0000596	89.99	99.99	10.01
Hutton	re 2	0.068413	0.001226	0.067187	0.000537	98.21	99.99	1.79
P8	ot	0.00115	0.00089	0.000257	0.00000904	22.29	99.99	77.71
Coega	hk1	0.00056	0.000428	0.000132	0.000044	23.58	99.99	76.42
	hk2	0.003227	0.000198	0.003029	0.000025	93.85	99.99	6.15
P9	ot	0.007108	0.003751	0.003357	0.0000558	47.23	99.99	52.77
Hutton	re	0.020588	0.001694	0.018894	0.000162	91.77	99.99	8.23
	re	0.02777	0.008345	0.019425	0.000218	69.95	99.99	30.05
	nc	0.010567	0.006525	0.004043	0.000083	38.26	99.99	61.74
P10	ot	0.007721	0.003989	0.003731	0.0000606	48.33	99.99	51.67
Hutton	re1	0.044227	0.000176	0.04405	0.000347	99.60	99.99	0.4
	re2	0.027863	0.001835	0.026027	0.000219	93.41	99.99	6.59
P11	ot	0.007463	0.000436	0.007027	0.0000586	94.15	99.99	5.85
Clovelly	yb1	0.034118	0.003411	0.030707	0.000268	90.00	99.99	10
	yb2	0.031985	0.000327	0.031658	0.000251	98.98	99.99	1.02
P12	ot	0.010294	0.002342	0.007952	0.0000808	77.25	99.99	22.75
Namib	rs	0.000388	0.000373	0.000015	0.0000031	3.877	99.99	96.123
P13	ot	0.000280	0.000175	0.000104	0.0000022	37.44	99.99	62.56
Valsrivier	pe1	0.000091	0.000072	0.000019	0.0000007	20.96	99.99	79.04

DH – diagnostic horizon, Db – bulk density, ot – Orthic A horizon, otd – distrurbed orthic A horizon, otud – undisturbed orthic A horizon, re – red apedal B horizon, re1 – red apedal B1 horizon, re2 – red apedal B2 horizon, yb – yellowbrown apedal B horizon, yb1 - yellowbrown apedal B1 horizon, yb2 - yellowbrown apedal B2 horizon, pe – pedocutanic B horizon, pe1 – pedocutanic B1 horizon, pe2 – pedocutanic B2 horizon, nc – neocarbonate B horizon, - nc1 – neocarbonate B1 horizon, nc2 – neocarbonate B2 horizon, sc – soft carbonate horizon, hk – hardpan carbonate horizon.

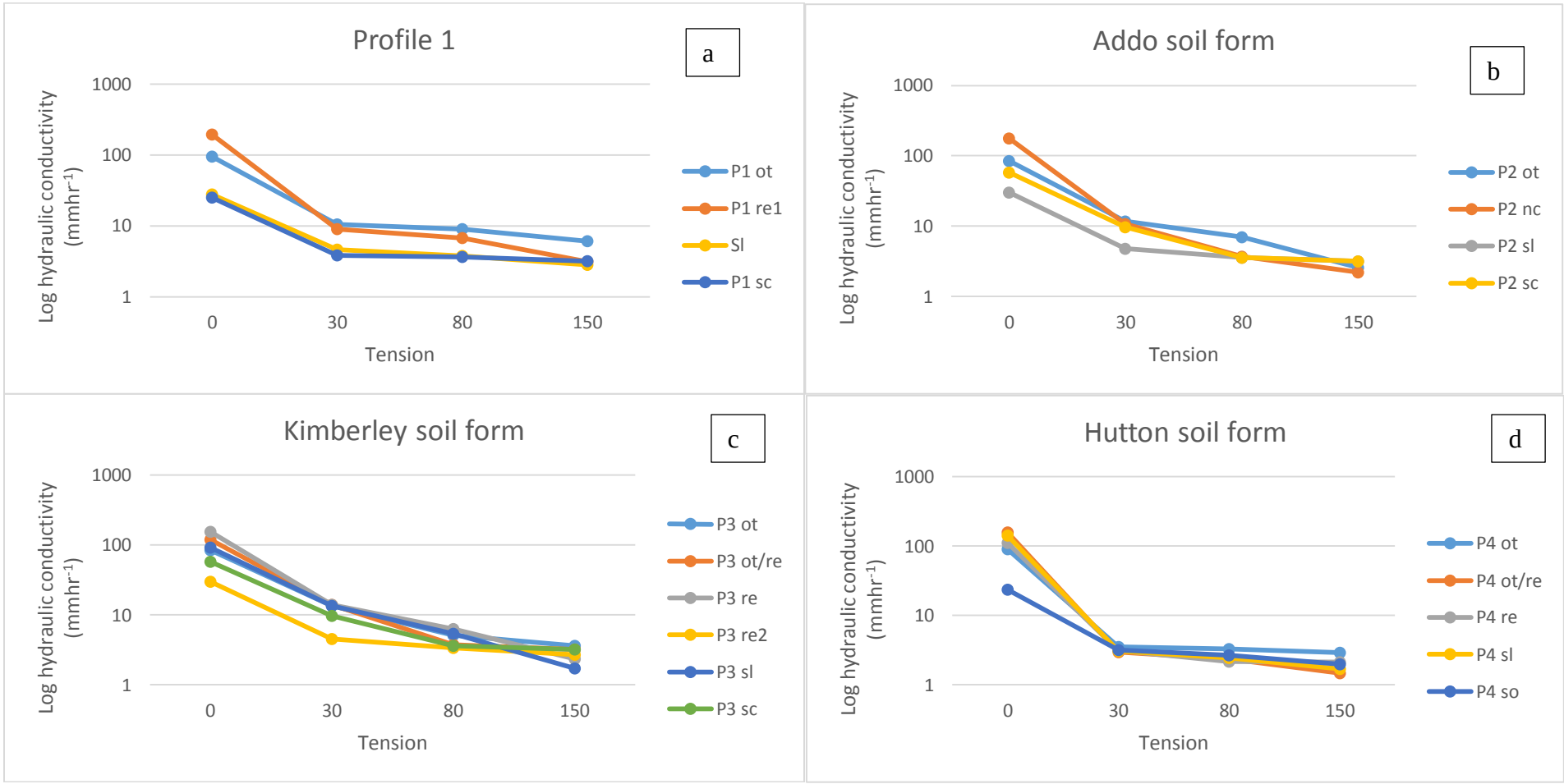

Figure Appendix 22 The relationship of the hydraulic conductivity (mm hr^{-1}) versus the in-situ tension relationship of the Kimberley (a), Addo (b), Kimberley (c) and Hutton (d) soil forms and their respective horizons.

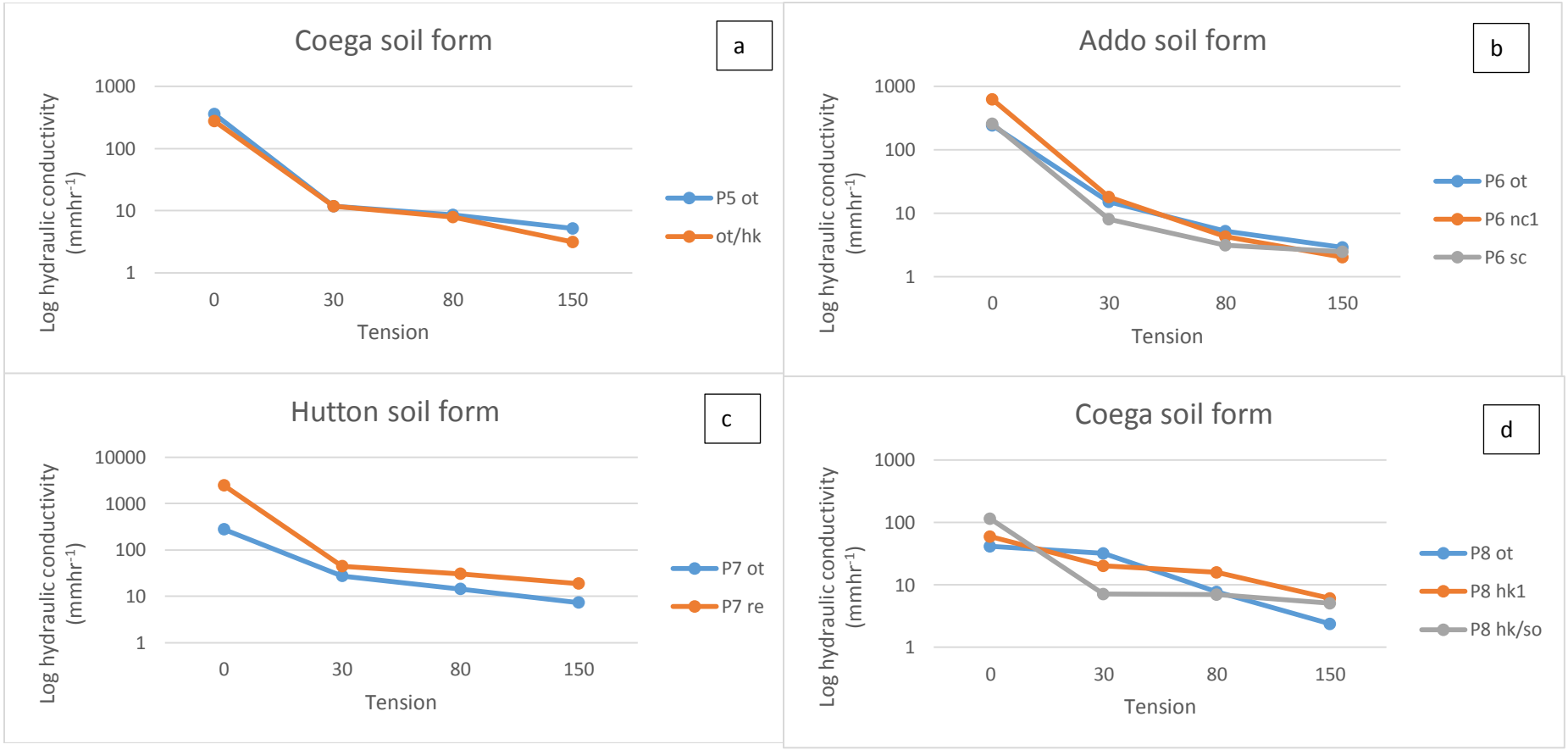

Figure Appendix 23 The relationship of the hydraulic conductivity (mm hr^{-1}) versus the in-situ tension relationship of the Coega (a), Addo (b), Hutton (c) and Coega (d) soil forms, and their respective horizons.

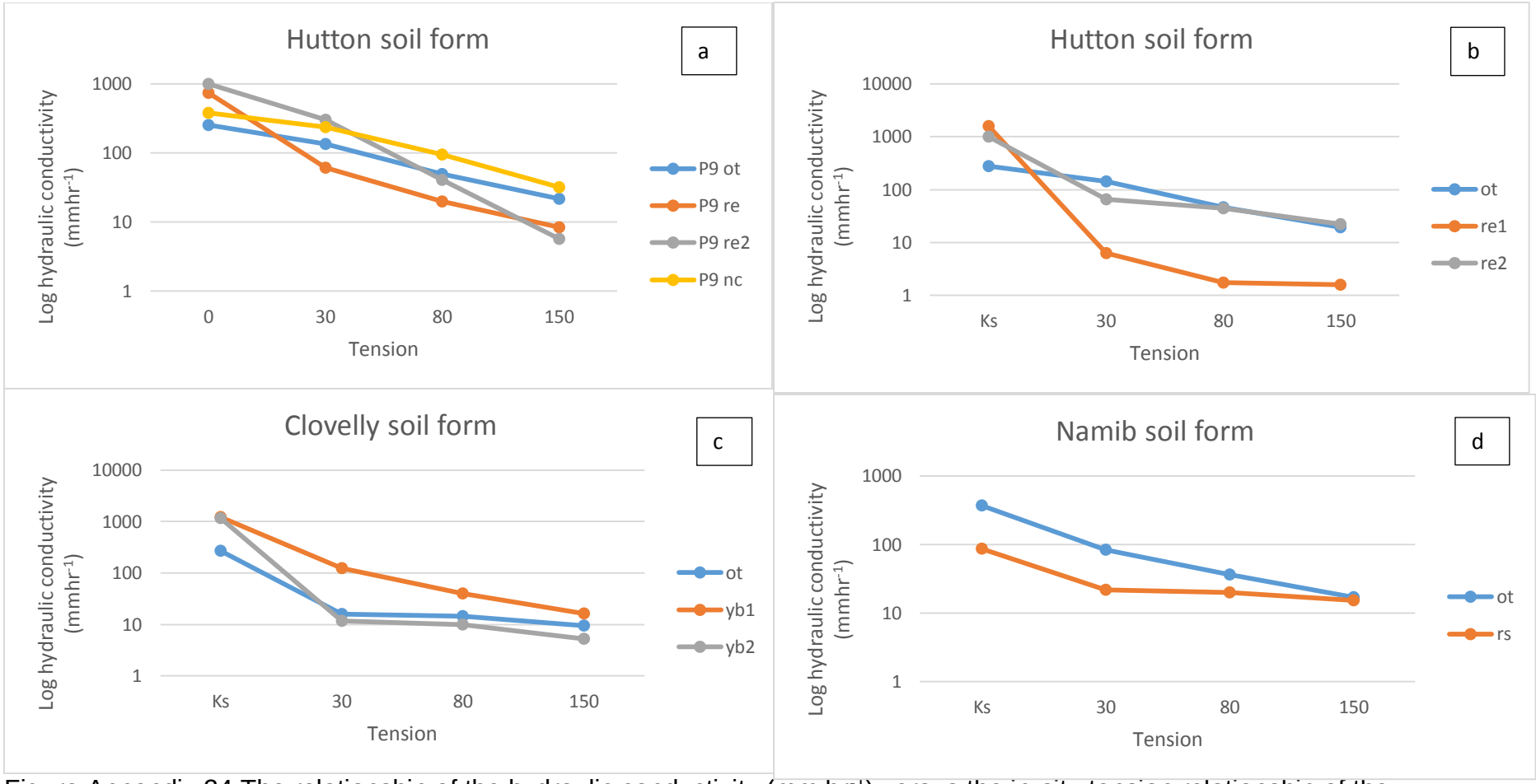

Figure Appendix 24 The relationship of the hydraulic conductivity (mm hr^{-1}) versus the in-situ tension relationship of the Hutton (a), Hutton (b), Clovelly (c) and Namib soil froms, and their respective horizons.

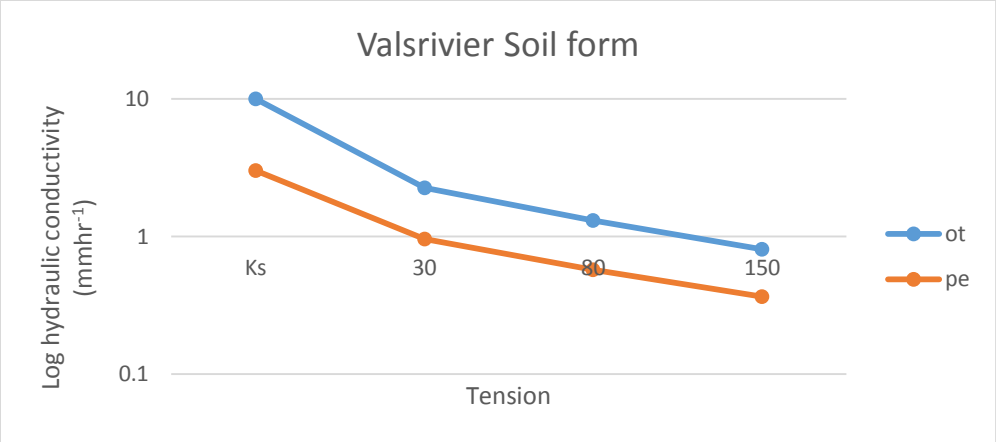

Figure Appendix 25 The relationship of the hydraulic conductivity (mm hr^{-1}) versus the in-situ tension relationship of the Valsrivier soil form and its respective horizons.

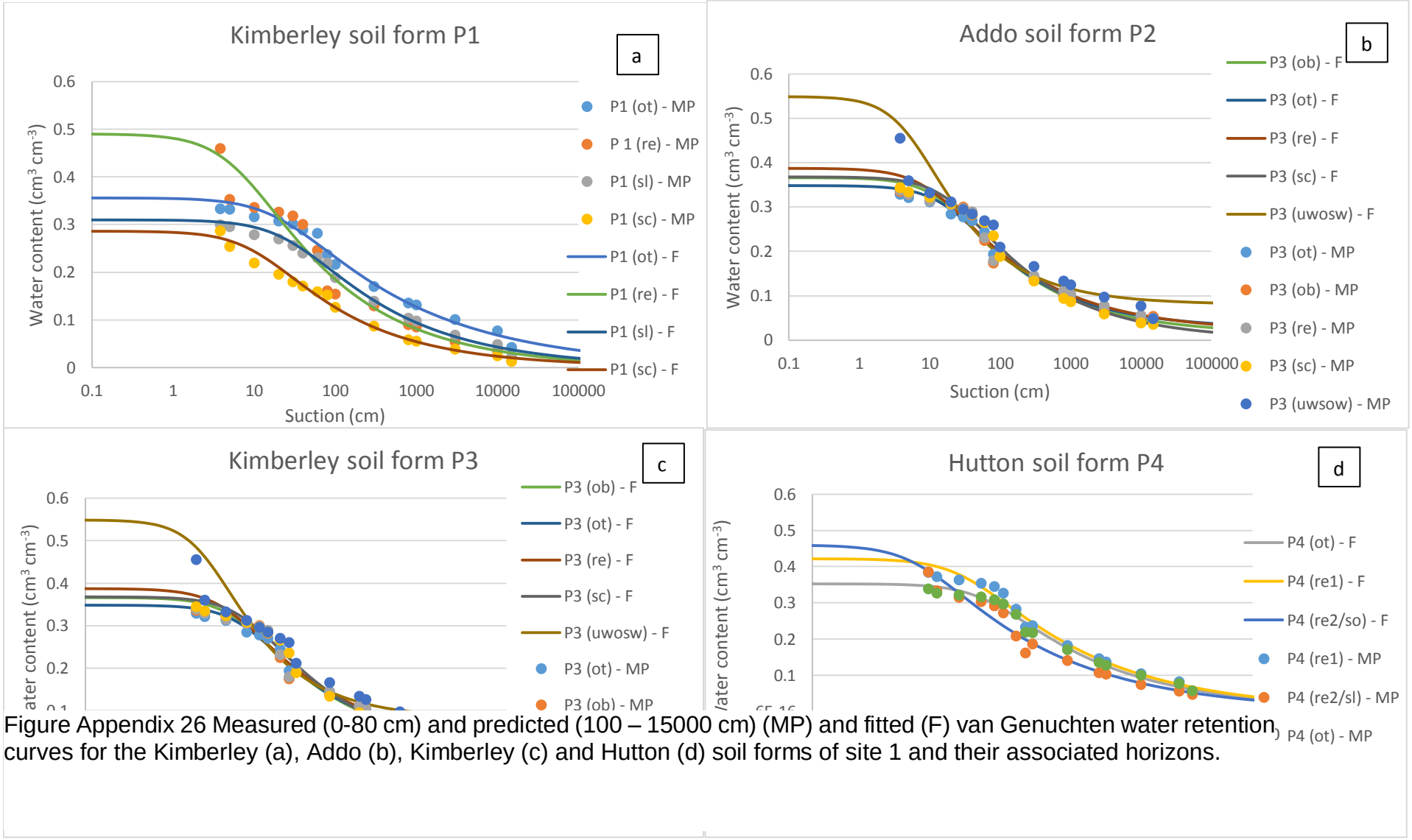

Figure Appendix 26 Measured (0-80 cm) and predicted (100 – 15000 cm) (MP) and fitted (F) van Genuchten water retention curves for the Kimberley (a), Addo (b), Kimberley (c) and Hutton (d) soil forms of site 1 and their associated horizons.

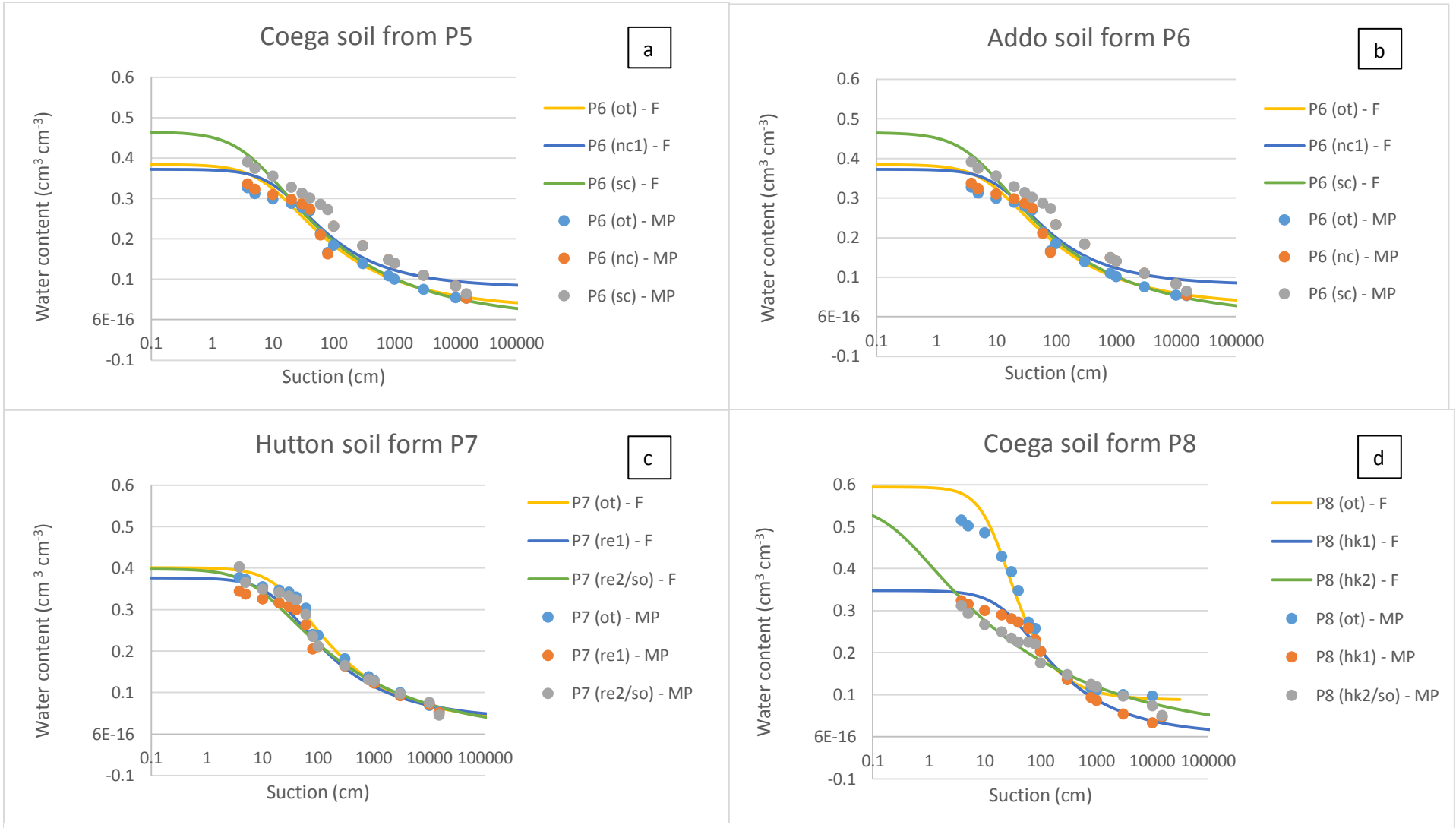

Figure Appendix 27 Measured (0-80 cm) and predicted (100 – 15000 cm) (MP) and fitted (F) van Genuchten water retention curves for the Coega (a) soil form of site 1, and Addo (b), Hutton (c) and Coega (d) soil forms of site 2, and their associated horizons.

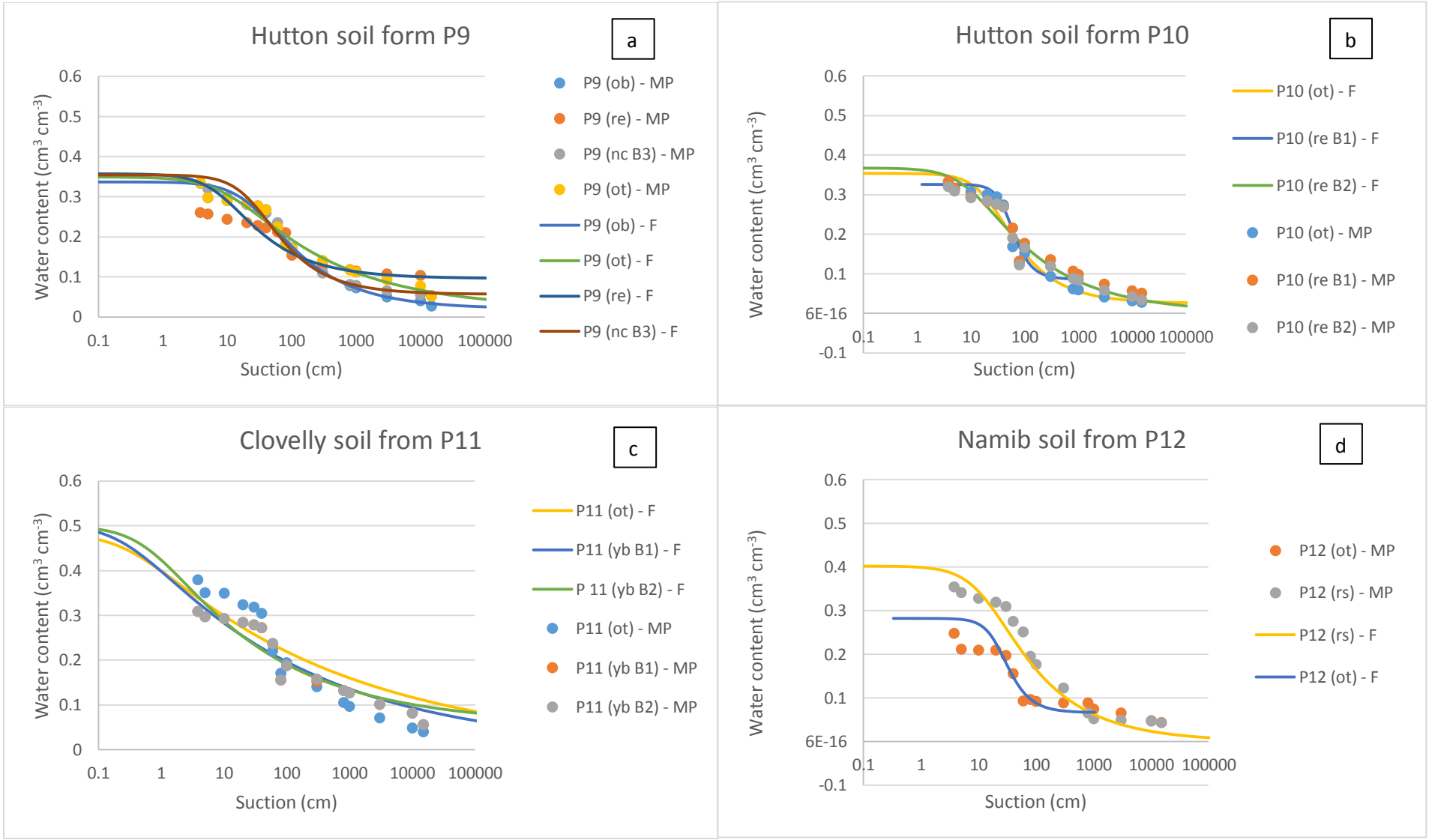

Figure Appendix 28 Measured (0-80 cm) and predicted (100 – 15000 cm) (MP) and fitted (F) van Genuchten water retention curves for the Hutton (a), Hutton (b), Clovelly (c) soil forms of site 2 and Namib (d) soil form of site 3, and their associated horizons.

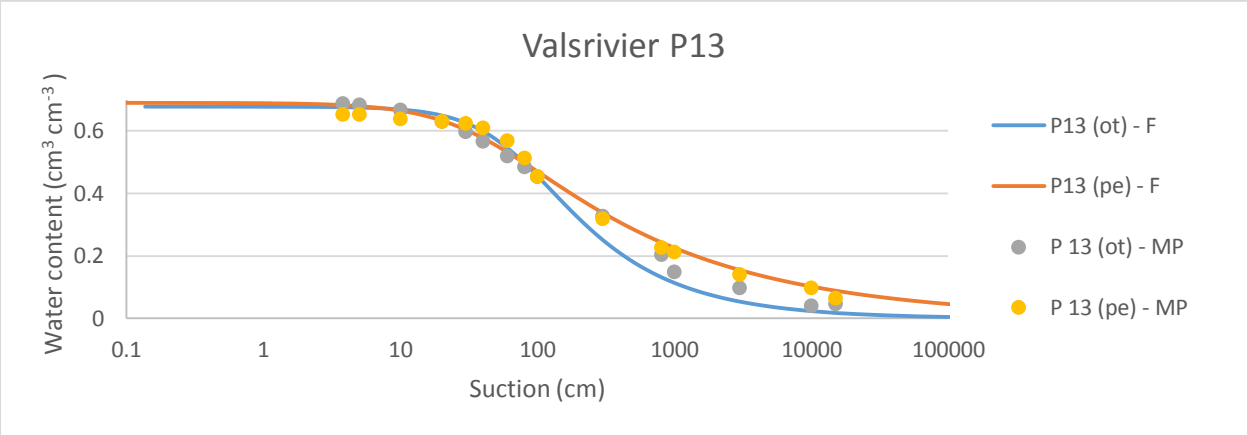

Figure Appendix 29 Measured van Genuchten water retention curves for the orthic A hroizon and pedocutanic B1 horizon of a Valsrivier profile on site 4.

Table Appendix 29 Parameters of the RETention Curve Program of the Van Genuchten model and the results of the Willmott statistical test to describe the extent to which the model fitted the measured data.

Soil form	Horizon	Lower depth (mm)	Θ_s cm^3 cm^{-3}	Θ_r cm^3 cm^{-3}	A	n	R^2	D-index	RMSE	RMSEu/RMSE
Kimberley	ot	200	0.39	0.05	0.004	1.92	0.961	1.0	0.02	1.05
	re	800	0.54	0.05	0.003	2.55	0.952	1.0	0.03	1.02
	sl	900	0.35	0.05	0.003	2.06	0.971	1.0	0.02	1.09
	sc	1300	0.31	0.05	0.003	3.13	0.982	1.0	0.01	1.05
Addo	ob	10	0.44	0.05	0.004	2.43	0.958	1.0	0.03	1.06
	ot	250	0.41	0.05	0.004	2.34	0.960	1.0	0.02	1.13
	nc1	600	0.48	0.04	0.004	2.03	0.949	1.0	0.03	1.06
	nc2	1300	0.47	0.04	0.004	1.61	0.956	1.0	0.03	1.05
	sl	1400	0.47	0.04	0.004	1.57	0.954	1.0	0.03	1.07
	sc	1500	0.49	0.04	0.004	1.47	0.962	1.0	0.03	1.05
Kimberley	ob	0	0.39	0.05	0.003	2.88	0.960	1.0	0.02	1.10
	ot	175	0.39	0.05	0.003	2.60	0.969	1.0	0.02	1.16
	re	550	0.38	0.05	0.004	2.22	0.956	1.0	0.03	1.22
	re	550	0.45	0.05	0.004	2.02	0.956	1.0	0.03	1.22
	sc	1600	0.41	0.05	0.004	2.02	0.942	1.0	0.03	1.10
	uwsow	1700	0.65	0.05	0.004	2.28	0.974	1.0	0.03	1.05
Hutton	ot	200	0.39	0.06	0.003	1.89	0.969	1.0	0.02	1.10
	re1	600	0.46	0.06	0.003	1.82	0.962	1.0	0.03	1.05
	re/so	1200	0.47	0.069	0.002	1.33	0.955	1.0	0.03	1.12
Coega	ot	150	0.40	0.052	0.003	2.66	0.942	1.0	0.03	1.02
	ot/hk	150+	0.49	0.052	0.003	2.66	0.943	1.0	0.05	1.28
Addo	ot	300	0.45	0.054	0.003	2.91	0.937	1.0	0.03	1.03
	nc	600	0.43	0.054	0.003	2.46	0.917	1.0	0.04	1.13
	sc	800	0.43	0.064	0.003	1.60	0.970	1.0	0.03	1.46
Hutton	ot	300	0.45	0.053	0.003	2.92	0.965	1.0	0.03	1.13
	re1	1400	0.40	0.054	0.003	3.14	0.965	1.0	0.02	1.03
	re2	2000	0.43	0.051	0.003	1.81	0.948	1.0	0.03	1.04
Coega	ot	150	0.73	0.047	0.004	2.23	0.940	1.0	0.08	1.27
	hk1	400	0.42	0.047	0.004	2.31	0.926	1.0	0.04	1.14
	hk/so	700	0.56	0.049	0.004	2.33	0.977	1.0	0.02	1.06
Hutton	ot	200	0.37	0.053	0.003	2.63	0.974	1.0	0.02	1.10
	re1	600	0.49	0.053	0.003	2.63	0.877	1.0	0.04	1.05
	re2	1000	0.49	0.052	0.003	2.63	0.955	1.0	0.02	1.05
	nc3	1380	0.42	0.052	0.003	2.52	0.945	1.0	0.04	1.20
Hutton	ot	300	0.38	0.053	0.003	3.25	0.958	1.0	0.03	1.05
	re1	600	0.41	0.051	0.003	2.52	0.934	1.0	0.05	1.30
	re2	1000	0.41	0.053	0.003	2.57	0.939	1.0	0.03	1.03
Clovelly	ot	300	0.46	0.053	0.003	3.53	0.955	1.0	0.03	1.04
	yb1	850	0.50	0.054	0.003	3.07	0.937	1.0	0.03	1.08
	yb2	1400	0.50	0.056	0.003	2.89	0.938	1.0	0.03	1.08
Namib	ot	120	0.44	0.054	0.003	3.19	0.956	1.0	0.03	1.10
	rs	1150	0.44	0.055	0.003	2.85	0.951	1.0	0.02	1.04
Valsrivier	ot	350	0.65	0.067	0.001	1.47	0.991	1.0	0.06	3.35
	pe	700	0.71	0.0943	0.015	1.38	0.978	1.0	0.04	1.27

Appendix E

Figures explained in detail

Total hillslope on x-y axis with vertical bars indicating location of site

Location of this master profile on this hillslope

Hillslope section hemispherical orientation i.e. the left of the site in this case is West and right East

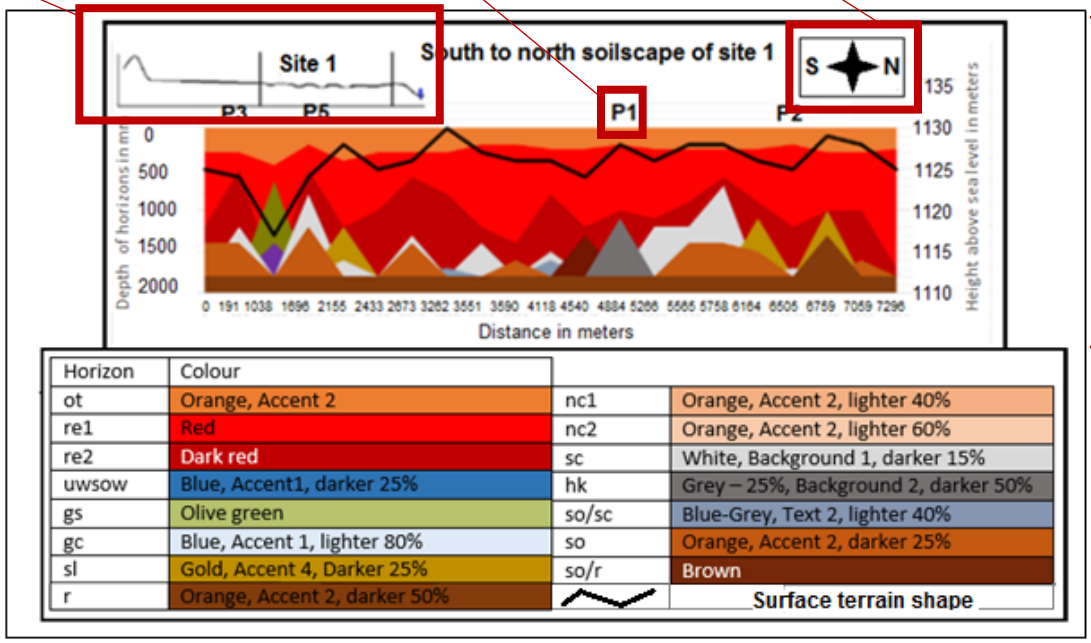

Graph depicting landscape morphological attributes (right y-axis and black line), horizon depth and variation (left y-axis and colours in graph).

Legend indicating colour coded soil horizons and surface terrain slope of the selected hillslope.

Figure Appendix 30 Description of complex diagram of Chapter 5.

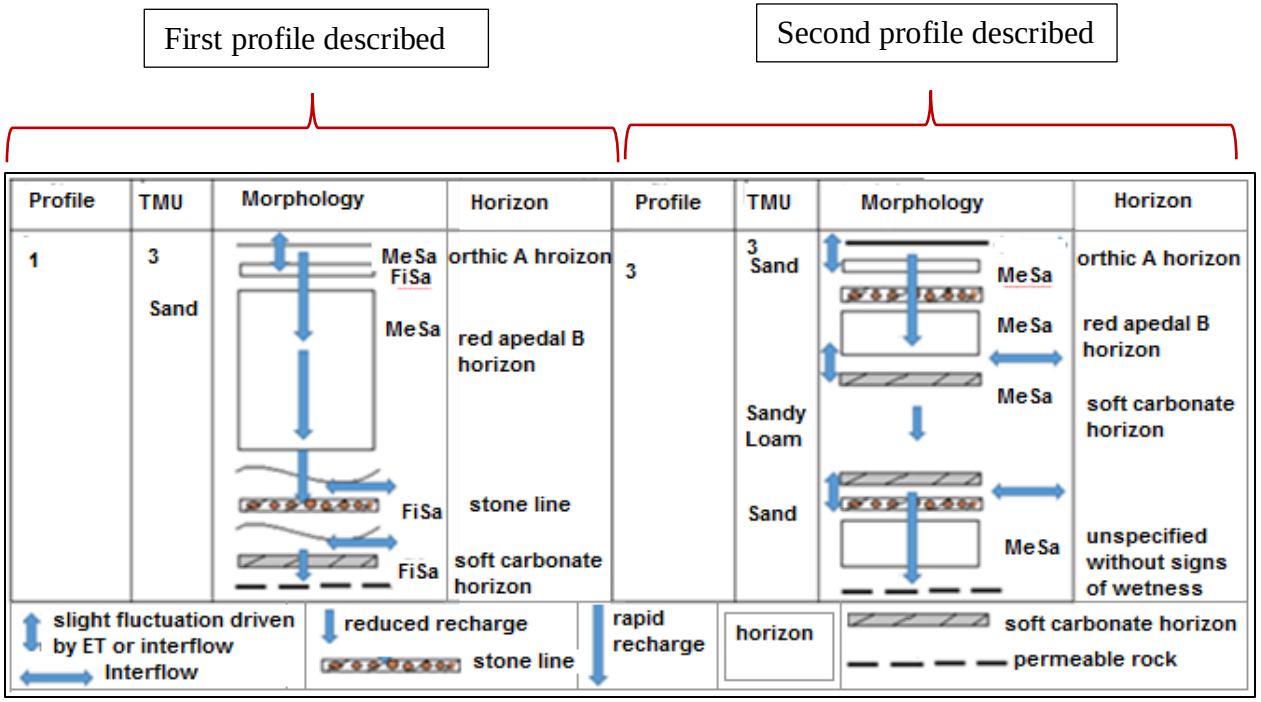

Figure Appendix 31 Description of complex diagram of Chapter 6.